Analytical solutions of orientation aggregation models, multiple solutions and path following with the Adomian decomposition method

A Thesis submitted for the degree of Doctor of Philosophy

by

Alex Clive Seymoore McKee

Department of Mathematical Sciences, School of Information Systems, Computing and Mathematics, Brunel University, London.

August 2011

To the faithful; who keep striving...

Acknowledgements

With certainty we often make plans neglecting the thought that we never know what the future holds and whether our plans will come to fruition.

Both biblical texts and classic writings such as works by Grotius, Anacreon, Euripides, Menander, Seneca and Horace, offer wise counsel and beautiful expressions regarding the folly of forming plans as if the future was granted to us. For example, in the book of James 4:14 we read:

"Whereas you don't know what your life will be like tomorrow. For what is your life? For you are a vapour, that appears for a little time, and then vanishes away."

Given such a reality I am grateful to the Creator that I have seen the day when the great effort put into the development of this thesis has finally come to fruition; for health and strength and a measure of ability that enabled me to undertake this thesis and to strive to live up to the spirit of the wise words

"Whatever your hand finds to do, do it with all your might" (Ecclesiastes 9:10).

We are also blessed to find fellowmen possessed with talent and ability who ably assist us in our endeavours. In this regard I am especially grateful to my thesis supervisor Dr. Jacques Furter for all his guidance and fine instruction. Dr. Furter who has a warm disposition and a profound mathematical capability has always been able to effectively advise on how best to overcome obstacles encountered during my research. He has a self sacrificing spirit and always makes himself available. He patiently and clearly explains difficult subject matters; all hallmarks of a good educator.

I am also grateful for both of my examiners Dr. Fatima Fahr and Dr. Mike Warby for their keen observations and helpful suggestions for improvements to the quality of this text.

Abstract

In this work we apply the Adomian decomposition method to an orientation aggregation problem modelling the time distribution of filaments. We find analytical solutions under certain specific criteria and programmatically implement the Adomian method to two variants of the orientation aggregation model. We extend the utility of the Adomian decomposition method beyond its original capability to enable it to converge to more than one solution of a nonlinear problem and further to be used as a corrector in path following bifurcation problems.

Contents

List of Figures

List of Tables

Chapter 1

Introduction

The interaction of elements to form a collective entity is a behaviour that can be universally observed. Such systems make up the physical world, biological processes and national economies to note a few. And in all such instances nonlinear behaviour, where the output, final result is not linearly related to input can also be found [9]. In seeking to understand the surrounding world, mathematical models designed to capture the behaviour of the system under consideration are constructed. The resulting equations are studied, then the results are interpreted with respect to the original system. A fundamental decision is whether the model should be linear or nonlinear. While linear models have proven very useful, nonlinear models are more realistic [9]. The difficulty facing Mathematicians is that nonlinearity is very difficult to handle mathematically. Both theory and techniques are limited and nonlinearity presents many challenges that have proven persistently difficult to surmount.

> "The Retreat to Linearity: On the one hand, their analytical methods were not powerful enough to deal with the problem of nonlinearity; on the other hand, purely numerical techniques were not far advanced nor were they feasible from the stand points of economics and engineering. Taking the only possible way out, they changed the problem, tailoring it to fit their modest mathematical means. Specifically, they "linearized" the equations... " - Philip Duncan Thomas [9].

> " A tremendous body of knowledge exists about linear systems, linear equations, and linear operator theory, but only some ad hoc techniques are available for nonlinear operators" - George Adomian [9].

One consequence of this is that many real world systems, physical systems, biological systems are not adequately modelled by their linear proxies.

> "...since the basic equations of physics are nonlinear, all of mathematical physics will have to be done over again..." Albert Einstein [9].

If the benefits that come with understanding the real world are to be sustained then nonlinearity must be understood.

> "The necessity of a theory of stochastic processes for the description of physical phenomena in conceptually, analytically, and computationally tractable form is by now understood and accepted and the steady trend in theories from linear deterministic to nonlinear and stochastic must be regarded as the primary goal of future research efforts." - Richard Bellman [9].

1.1 The Adomian Decomposition Method

This thesis is mainly concerned with a constructive method introduced by the American physicist George Adomian (1923-1996). The **Adomian decomposition method (ADM)** is a quantitative method for solving analytically nonlinear equations of any kind by means of series. In mathematical terms, the nonlinear problems we have in mind are equations

$$f(u) = 0 \tag{1.1}$$

where f is a nonlinear function of variable u belonging to some subset of a Banach space. An alternative form of (1.1), preferred when using constructive methods, is a fixed point problem

$$u = g(u), \tag{1.2}$$

where g is a nonlinear map, because a solution of (1.2) can be found using the iterative scheme

$$u_{n+1} = g(u_n)$$

from some starting point u_0. If the sequence $\{u_n\}_{n=1}^{\infty}$ converges and g is continuous,

$$\bar{u} = \lim_{n\to\infty} u_n$$

is a solution of (1.2). Convergence can be ascertained, for instance, if g is a contraction (see Appendix B), that will also ensure the continuity of g.

1.1.1 Formulation of the ADM

We shall construct series solutions of the functional equations of the general form

$$u = c + N(u) \tag{1.3}$$

where $u \in X$, a Banach space, $N : X \to X$ is a nonlinear analytic map in a neighbourhood of $c \in X$. Although (1.2) does not require that u is in a linear space, use of the ADM requires the summation of infinite series, a concept well defined in Banach spaces. Note also that, when X is a linear space, the solution set of equations (1.1) and (1.2) are identical by choosing

$$N(u) = f(u) + u - c \quad \text{or} \quad f(u) = N(u) - u + c.$$

We shall discuss this point further in Chapter 3. Another reason to choose (1.3) as the standard form is that it fits nicely with the abstract formulation of semi-linear dynamical systems, PDEs or ODEs. Suppose such equations can be written as

$$Lu + F(u) = g$$

where u is the unknown state variable (or function), L an (easily) invertible linear operator and F contains the nonlinear as well as 'awkward' linear terms. Then, inverting L, we get

$$u = g - L^{-1}F(u)$$

where the inhomogeneous term g contains information about the boundary or initial values. This is an equation of the type (1.2). Such a shape will become useful in our analysis of the equations depicting the **orientation aggregation problems (OAP)** in Chapters 5 and 6.

Clearly a solution of (1.3) can be found if N is a contraction on X using the iterative scheme

$$v_{n+1} = N(v_n) + c \tag{1.4}$$

for any v_0. A problematic issue with that scheme is that $N(v_n)$ can be difficult to evaluate in practice. The Adomian scheme tries to avoid such practical issues. Looking for a constructive method, we are seeking solutions u of (1.3) as a convergent series

$$u = \sum_{n=0}^{\infty} u_n, \tag{1.5}$$

where the u_n's need to be determined. To circumvent the difficulty of evaluating N, we assume that $N(u)$ can be itself written as a series

$$N(u) = \sum_{n=0}^{\infty} A_n(u) \tag{1.6}$$

where A_n depends only on the first $n+1$ terms of the series in (1.5), that is,

$$A_n(u) = A_n(u_0, \ldots, u_n), \qquad n \geq 0,$$

whenever u is a convergent series. The A_n are the Adomian polynomials of N at u_0. Replacing u and $N(u)$ in (1.3), we get the following decomposition scheme linking u_{n+1} with A_n:

$$u_0 = c, \quad u_{n+1} = A_n(c, u_1, \ldots, u_n),\ n \geq 0. \tag{1.7}$$

If convergence is assured, the scheme (1.7) will converge to a root of (1.3). Its two main ingredients are that the Adomian polynomials $A_n(u)$ are easier to evaluate than the full nonlinear term $N(u_n)$ and, provided we can evaluate $A_n(u)$, the scheme has a wide range of applicability. Nevertheless, the issue of convergence is in general non trivial. In a nutshell, the ADM involves rearrangements of convergent series to achieve simpler, better summation processes. In that context, it is not really geared towards existence proofs (unlike the CMT), nor are the Adomian polynomials unique. There are several possible rearrangements mentioned in the literature.

1.1.2 A need for the ADM

The mathematical modelling of many real world systems leads to nonlinear functional equations such as ODEs, PDEs, algebraic, integral or integro-differential equations. Notable examples are the Duffing's equation depicting a dynamical system with chaotic behaviour; the Navier-Stokes equation modelling fluid motion; advection problems modelling the transport of a substance through a fluid medium; Volterra-Fredholm equations modelling the spatio-temporal development of an epidemic; integro-differential equations with time periodic coefficients modelling the charged particle motion for certain configurations of oscillating magnetic fields; OAPs describing the change in relative position of elongated objects and the density of their clustering.

The need therefore arises to effectively analyse and solve mathematical models which may be strongly nonlinear in space and time. It is common for frequently used analytic procedures to linearise the system or assume the insignificance of these nonlinearities. The drawback to such procedures is that in trying to make the problem tractable by the conventional method there results a mathematical problem that remains distinct to the real world problem. The physical problem remains disconnected from the mathematical one for which the solution is more readily available with the result that the obtained solution might not adequately represent the behaviour of the physical problem ([67]). Further, since generally, nonlinear dynamic systems exhibit some delicate structures in very small time and space intervals, numerical methods in particular, those based on discretisation techniques such as Runge-Kutta methods which calculate the approximate solution for some values of time and space variables may not detect important phenomena such as bifurcation or chaos in very small time and space intervals. Perturbation is only reasonable when nonlinear effects are small and furthermore numerical methods need a substantial amount of computational resources but yield limited information ([67]).

1.1.3 Perspective, the development of the ADM

The ADM developed out of a push towards a generalised theory for dealing with stochastic systems. From around the turn of the 20th century, notable mathematicians including Einstein, Smoluchowsky and Langevin, subsequently Wiener, Itô, Moyal and Spacek, had studied random equations. The results were based on special situations involving special processes, restrictive conditions and, in general, where the system inputs were stochastic, the operators were deterministic. By the 1950s a general theoretical framework for dealing with stochastic equations was still lacking. In 1953 Zadeh had suggested the idea of a stochastic operator but very little of the existing literature ever dealt with an operator approach. An engineering dissertation by Rosenbloom ([88]) considered the analysis of randomly time varying linear systems and indicated many of the difficulties associated with an operator approach to stochastic systems. Reports by Samuels and Eringen ([89]) further indicated the difficulties associated with treating such an operator and, in particular, considered the mean square stability of systems of second and higher order involving one purely random parameter. The Prague School of probability under Spacek initiated a systematic study using probabilistic operator equations as models for various systems ([84]), but their work did not contribute to the explicit solution of physical problems ([9]). In 1956 Adomian and DuBois ([14]) investigated the behaviour of a radar system involving random parameters in the signal processing. In 1959 Bellman and Kalaba produced important work on wave propagation in stochastic media ([25, 26]).

In 1960 Adomian was concerned with the case of a differential equation involving stochastic process coefficients or a stochastic (input-output) dynamical system in which both the system parameters and the inputs were stochastic processes ([9]). In his dissertation, Adomian ([5]) explored the concept of a stochastic operator and applications and provided answers to basic questions relating to the nature of the solution of a stochastic operator equation or **stochastic differential equation (SDE)**. This work was substantially different from other works in this area at this time as it sought to develop a generalised theory for SDEs useful to engineers and physicists which would avoid assumptions that would limit practical applicability. It explored concepts such as stochastic filters, stochastic systems, stochastic Green's function and statistical measures of solutions of SDEs. It drew upon probability theory, stochastic processes and linear systems analysis and made specific application to solving a first-order SDEs. Tikhonov ([94]) had similar ideas at this time and work by Balakrishnan ([24]) and by Bergen ([28, 29]) on stochastic transformation of a stochastic process involving the random sampling at random times of a random process also appeared.

Between 1962-1965 much work was produced in this field on modelling and finding solutions to SDEs. Notable among this was Bershad's dissertation ([30]), Caughey and Dienes ([37]) on solutions of an n^{th}-order SDE, Chernov ([39]), Tatarski ([95]) on scattering by inhomogeneities, Bogdanoff and Kozin ([32]) on random harmonic oscillators, Kraichnan et al. ([69, 87]) on the closure or truncation connected with the hierarchy method for turbulence theory. At this time, emerging ideas from Adomian's work and others encouraged the development and teaching of courses in SDEs for physicists, engineers and applied mathematicians. In 1964 Bharucha and Reid ([31]) pooled many of the existing ideas on how to deal with stochastic operators and Adomian published ([15]) on stochastic Green's function. In this paper Adomian suggested a new procedure for approximating the solution of linear SDEs, called the iterative method or the stochastic Green's function method, latter the decomposition method. The approach taken was to make practical application of much of the theoretical developments, in particular in probability theory, and relate them to solutions of equations. Subsequent papers taking a similar approach appeared; Astrom ([20]) on first order SDEs, Sibul's dissertation ([93]) on stochastic operators, Elrod's dissertation ([54]) on SDEs and Malakian ([17]) on hierarchy methods for SDEs.

Adomian generalised his ideas on differential equations and the decomposition method to nonlinear SDEs in 1976 and, from 1976 to 1980, broadened the application to a wide class of nonlinearities. Adomian took the view of linearity as an included special case of nonlinearity and a deterministic case to be an included special case of nonlinearity where stochasticity vanishes. Adomian's approach could treat cases where stochasticity exists in the initial or boundary conditions - in the input to a dynamical system being modelled - or in the coefficients of the differential operator - the stochastic operator. Adomian implemented his method for many scientific and frontier physics problems and subsequent publications in the early eighties formally in more detail introduced and developed the decomposition method with applications ([3, 4, 6, 7, 8, 11, 12, 13, 16, 65, 101]).

1.2 Main contributions and structure of the thesis

The main contributions of this thesis are twofold. On the one hand for the first time the ADM is applied to OAPs on the unit circle S^1. These problems describe the collective distribution of elongated objects (filaments) with respect to time. The key result from this application is the discovery of exact analytical solutions to some forms of the OAP. The specific criteria for their existence is stipulated and a formula which gives the exact analytical solution of the equation for a class of initial conditions is presented. These result also confirm the ADM's utility as an effective tool for dealing with OAPs. Further the software Maple 15 is programmed to implement the ADM for two variants of the OAP and many analytical solutions and graphs thereof along with plots of the solution parameters are generated and presented. These programs are also provided as part of the thesis as useful time saving tools for studying the solutions of the OAP. On the other hand for the first time, since the ADM in its original development did not address any procedure for obtaining more than one solution to a nonlinear problem a main contribution has been the extension of the method's utility to enable it to converge to more than one solution of a nonlinear problem. What's more, an extension of the method's utility is developed and introduced to enable it to handle bifurcation problems through path following and extended systems for higher singularities. The new mathematical theoretical framework that allows such applications is also developed and introduced in this thesis. A more detailed mathematical outline of the eight chapters comprising this thesis follows.

After the introduction of preliminary and general ideas on the formulation and the development of the ADM, Chapter 2 discusses its formulation in more mathematical detail. Herein a scheme for its practical implementation is provided and proof of the convergence of the method is presented in detail. Methods for calculating the requisite Adomian polynomials are discussed as are the limitations and key advantages of the method. These ideas set the groundwork for the application of the method in subsequent chapters and provides perspective on where the thesis fits within the current body of mathematical knowledge.

The ADM represents a significant step forward in treating nonlinearity in diverse nonlinear systems ([10]). A fundamental characteristic of nonlinear problems is that they often have multiple solutions. Being iterative, the method generates only one solution in the form of a series. All of Chapters 3 and 4 detail original contributions of the thesis. It is shown how to implement the ADM to obtain more than one solution to nonlinear problems and how the ADM can be used in path following techniques for bifurcation problem. First the theoretical framework is developed and introduced to facilitate such applications and consequently the utility of the ADM is extended beyond its original capability to enable it to converge to more than one solution when applied to nonlinear equations. The aim is to find the solutions to equations of the form

$$f(u) = 0 \tag{1.8}$$

using the ADM. A simple idea is to write (1.8) as a fixed point problem

$$u = F(u) \tag{1.9}$$

whose solutions are exactly the zeroes of f. The fixed point problem can be solved by successive iterations. This technique works well when F is a contraction. By influencing whether the

contraction holds, the ADM can be made to converge to the desired root of the equation. Lemmas 3.1 and 3.2 set up criteria for making F a contraction.

The theoretical framework is applied to a one dimensional example of the form

$$f(u) = e^u - u - a, \quad a > 1. \tag{1.10}$$

Being one dimensional, (1.9) uses $F(u) = u + \alpha f(u)$ where α is a free constant. Using the freedom we have on α and the initial condition u_0, we set-up and discuss criteria for ensuring that a contraction holds at both roots, one positive, one negative. A straight application when $\alpha = 1$ of the ADM results in a solution giving the negative root of the equation but by adjusting the locality of the contraction through an adjustment of the values of α and u_0, the ADM is made to converge to the positive root. To enable the quick solution of (1.10) for varying starting values of u_0, a program was developed (and provided as part of the thesis) using Maple 15 software. It returns the sum of the first seven terms of the ADM solution; it also checks that a contraction holds for specified values of α and plots the value of the resulting Adomian solution against a plot of (1.10) for comparison purposes. The manner in which the ADM switches between the roots of (1.10) is documented, presented graphically and discussed in detail. A detailed comparison is undertaken of the manner of convergence for select values of α. The results demonstrate the importance of selecting an α value so as to optimise the convergence of the method to the positive root since the α value influences the strength of the contraction which in turn influences the manner of convergence to multiple roots.

Within the theoretical framework developed and introduced in this chapter the utility of the restarted ADM (a technique for accelerating the convergence of the ADM originally presented in [22] and detailed for convenience in this chapter) as an effective technique for accelerating the convergence of the method to the desired root of a nonlinear problem is demonstrated using (1.10). The use of the restarted method in this particular way i.e. for accelerating the convergence of the ADM to multiple solutions of a nonlinear problem is in itself a contribution of the thesis. In one instance the restarted method is implemented using the sum of the seven terms of the Adomian series solution and a comparison is made to when the restarted method is made 'light in application' by using only three terms of the ADM series solution instead. The specific data points detailing the convergence path taken to the positive solution of (1.10) by the ADM is tabulated and graphically documented for both the restarted method and the straightforward application of the ADM.

Next the theoretical framework for utilising the ADM as a corrector in conjunction with the Euler predictor in path following applications is developed, introduced and exemplified. Within this theoretical framework the ADM is utilised in path following the known solution branches of a bifurcation problem example of the form

$$f(u, \gamma) = \gamma u^2 - u + 2 = 0. \tag{1.11}$$

The manner in which the ADM path follows the solution branches of the bifurcation problem is documented in detail graphically and solutions are also tabulated. It is demonstrated that the ADM constitutes an effective and accurate corrector for path following bifurcation problems. In order to quickly solve (1.11) a program was developed using Maple 15 and this program is provided as part of the thesis. It checks that the requisite contraction holds for the α and γ

values which must be specified and returns the sum of the first seven terms of the ADM solution. The theory in this chapter greatly extends the utility of the ADM for application to nonlinear problems in general and increases the scope of mathematical technique that can be applied to solving nonlinear problems. It also makes the solutions of these equations and the understanding of the system behaviour they depict more accessible.

In Chapter 5, orientation aggregation models are introduced in general. These multifaceted nonlinear equations model important biological systems. Their general applicability and origins are explored. Notable examples modelling swarms of elongated cells ([52]), fibroblasts and collagen and chemicals on the surface of a spherical tumour are cited ([44]). Then the relevant forms of the OAP pertaining to the modelling of a dynamical system of filaments under the influence of actin binding proteins are specified. Much of the existing ideas on ways to solve these OAP models and the behaviour of their solutions are extensively pooled together. Key ideas are drawn from [60] and [56]. Some specific mathematical detail as to how these problems are traditionally solved numerically along with what the common types of solutions such as peak solutions, bifurcation solutions; how they are found; under what conditions they arise and what these solutions mean to the system dynamics (the transitional stages of filament bundling such as uni or bidirectional bundling or network formation) are chronicled. This is so as to provide a comprehensive background as to the current state of knowledge about OAPs and their solutions before venturing to the new implementation of the ADM to the OAP in the successive chapter.

The relevant form of the equation is

$$c_t(\theta,t) = -c(\theta,t)\int_{S^1} W[c](\theta,\psi,\Lambda)\mathrm{d}\psi + \int_{S^1} W[c](\psi,\theta,\Lambda)c(\psi,t)\mathrm{d}\psi, \tag{1.12}$$

where the kernel $W[c](\theta,\psi,\Lambda)$ represents the turning rate, the probability of filaments jumping from orientation θ to ψ given the distribution c. The first term respectively the second term accumulates all the filaments jumping away from, onto, orientation θ.

Explicitly, W is given by

$$W[c](\theta,\psi,\Lambda) = \int_{S^1} K(\theta-\psi,\theta-\phi,c(\phi,t),\Lambda)\mathrm{d}\phi. \tag{1.13}$$

A typical form for K is

$$K(x,y,c) = h_\rho(y)w(x,y)p_\beta(c). \tag{1.14}$$

The term $h_\rho(y) : S^1 \to \mathbb{R}_+$ is the **frequency function**. This is the rate per unit time of interaction between two filaments with a difference of direction y.

The term $w(x,y)$ is the **turning probability function**. This is the probability of a filament turning by angle x as a result of interaction with filaments with a difference of direction of y.

In practice, w is often taken of the form

$$w(x,y) = g_\sigma(x - v_{k,\mu}(y)). \tag{1.15}$$

The turning function $v_{k,\mu}$ represents the average angle of turning as a function of the interaction angle and the **attractivity coefficient** $0 \leq k \leq 1$.g_σ is a periodic **Gaussian distribution**.

The term ρ_β is a measure of the **nonlinear interaction** with parameter β.

For more details regarding the description of terms comprising the model refer to chapter 5.

It is of interest to note the connections of this equation to a similar equation developed by Lee Segel (1932-2005). These equations modelling dynamical systems of slime mold and insect colonies are considered early prototypes for what are now commonly termed emergent systems ([66],[70]).

In the next Chapter 6 concern is focused on applying the ADM to the OAP for the first time. The entire chapter details original contributions. The specific forms treated herein are

$$\begin{aligned} c_t(\theta,t) &= \frac{1}{2\pi}\int_{-\pi}^{\pi}\int_{-\pi}^{\pi} p_\beta(c(\phi,t))\left[g_\sigma(\psi-\theta)\,c(\psi,t)-g_\sigma(\theta-\psi)\,c(\theta,t)\right]\,\mathrm{d}\phi\mathrm{d}\psi \\ &= \frac{1}{2\pi}\left(\int_{-\pi}^{\pi} p_\beta(c(\phi,t))\,\mathrm{d}\phi\right)\left[\left(\int_{-\pi}^{\pi} g_\sigma(\psi-\theta)\,c(\psi,t)\,\mathrm{d}\psi\right)-c(\theta,t)\right], \qquad (1.16) \\ c(\theta,0) &= \frac{1}{2\pi}+Q\cos k\theta, \qquad (1.17) \end{aligned}$$

where

$$p_\beta(c)=c \quad \text{or} \quad p_\beta(c)=\frac{c^2}{1+\beta^2c^2}$$

and the periodic Gaussian distribution is

$$g_\sigma(x)=\frac{1}{\sigma\sqrt{2\pi}}\sum_{n\in\mathbb{Z}} e^{-\frac{1}{2}(\frac{x+2\pi n}{\sigma})^2}.$$

A general formulation of the ADM for application to the OAP is developed. Specifically (1.16) is transformed into an integral equation of the Volterra type

$$c(\theta,t)=c(\theta,0)+\int_0^t F(c)(\theta,s)\,\mathrm{d}s. \qquad (1.18)$$

To apply the ADM to (1.18), c is decomposed into an infinite series of components

$$c(\theta,t)=\sum_{n=0}^{\infty} c_n(\theta,t),$$

and the nonlinear terms in (1.18) are basically represented from the integration of the Adomian polynomials obtained from p_β.

For particular initial conditions, the OAP is solved using the ADM giving exact solutions. What's more, for a general class of initial conditions, a general formula giving the solution of the equation is presented. More specifically it is established that when h_ρ is a constant, the

turning function $v_{k,\mu}$ is zero, the variation function g_σ is a periodic Gaussian and the nonlinear interaction is the quadratic case $p_\beta(c) = c$, the solution is

$$c(\theta, t) = \frac{1}{2\pi} + \sum_{k=1}^{\infty} e^{\frac{(e^{-\frac{1}{2}k^2\sigma^2}-1)t}{2\pi}} \left(\hat{a}_k \cos k\theta + \hat{b}_k \sin k\theta\right), \tag{1.19}$$

where the initial distribution is $c(\theta, 0) = \dfrac{1}{2\pi} + \displaystyle\sum_{k=1}^{\infty} \left(\hat{a}_k \cos k\theta + \hat{b}_k \sin k\theta\right)$.

Chapter 7 details the results of implementing the ADM programmatically in order to solve the OAP. Two programs have been developed using Maple 15 for solving two variants of the OAP. The programs return a solution which is the sum of the first four terms of the Adomian solution. From these four solution terms patterns in the generated series solution could be seen and a closed form solution verified. The programs are able to handle initial conditions of the form $\frac{1}{2\pi} + Q\cos k\theta + P\cos m\theta$ and $\frac{1}{2\pi} + Q\sin k\theta + P\sin m\theta$. Both programs are provided as time saving tools in generating solutions to the OAP and studying its behaviour. The chapter details the algorithms the programs follow to implement the ADM. Further, results of using the program to solve the OAP are presented. Many closed form solutions are presented as are plots of solutions and solution parameters. These provide insight to the functioning of the solutions. Through extensive utilisation of the program, patterns observed in the outputted solutions led to the discovery of (1.19).

Finally in the last chapter a general summary is presented along with a discussion of the results in this thesis. More suggestions and potential problems for further study and investigation that could be used to extend the current work are provided.

1.3 Terminology and a list of notations

We end this chapter listing some important notations used in this thesis. The symbols $\mathbb{N}, \mathbb{Z}, \mathbb{R}$ and $\mathbb{C}$ represent the sets of natural, integer, real or complex numbers, respectively. Other notations and their meaning are shown in the following list:

$\mathbb{R}^n$	the real n-dimensional vector space,
$\mathbb{N}_0$	the set of non negative integers,
$C(A, B)$	the set of continuous functions $f : A \to B$,
$C^n(A, B)$	the set of n-times continuously differentiable functions $f : A \to B$,
$\mathrm{re}(z)$	the real part of the complex number z,
$\mathrm{im}(z)$	the imaginary part of the complex number z,
$\|x\|$	the norm of the vector x in a Banach space.

1.3.1 About Banach spaces

In this section we recall some important notions, definitions and notations about Banach spaces and their convergent series (see [50, 64]). In Appendix B we deal with nonlinear analysis in

Banach spaces. Let X be a Banach space with norm $\| \ \|$. Let $x_0 \in X$ and $r \in (0, +\infty)$. We denote by $B_{x_0}(r)$ the **open ball** of **centre** $x_0 \in X$ and **radius** r, that is,

$$B_{x_0}(r) = \{ x \in X : \|x - x_0\| < r \}.$$

Similarly, $B_{x_0}[r]$ denotes the **closed ball** of centre $x_0 \in X$ and radius r, that is,

$$B_{x_0}[r] = \{ x \in X : \|x - x_0\| \leq r \}.$$

Unconditionally convergent series

For convenience with other notations, the series in X will start with index $k = 0$. Recall that in a Banach space, if a series $\sum_{k=0}^{\infty} x_k$ is absolutely convergent (if $\sum_{\boldsymbol{k=0}}^{\boldsymbol{\infty}} \|\boldsymbol{x_k}\| < \boldsymbol{\infty}$) then it is convergent. If a series is convergent, but not absolutely convergent, it is called **conditionally convergent**. There is an intermediate stage between absolutely convergent and conditionally convergent series, the idea of an unconditionally convergent series. A series is **unconditionally convergent** if it converges for any permutation of its indices. In that case, it is shown that the limit is independent of the permutation ([64]). In finite dimension, unconditional and absolute convergence are the same but not in infinite dimensions. Indeed, in every infinite dimensional Banach space, there exists an unconditional sequence that is not absolutely convergent ([51]).

Proposition 1.1 *The set $C(X)$ of convergent series in X is a normed vector space with the* **sup-norm**

$$\| \sum_{k=0}^{\infty} x_k \|_{\infty} = \sup\{ \ \|x_k\| : \ k \in \mathbb{N}_0 \ \}.$$

Proof.

First we show that the sup-norm of a series as defined above exists for any convergent series. We need to calculate the sup of an infinite set of norms $\|x_k\|$. To be sure that an infinite set of real numbers has a sup, we need to show that it is bounded (then it is an axiom of the real numbers that such a set always has a sup). Now, convergent series have elements x_k that converge to 0 in a norm (otherwise it is a well-known result that the series cannot converge). The sup-norm of a series is well defined because $\lim_{k \to \infty} \|x_k\| = 0$. So that means that the tail of the sequence $\|x_k\|$ is bounded. The terms outside the tail are finite, so the whole sequence is bounded and so the sup-norm is well defined on convergent sequences. What remains now is to show that the axioms of a norm are satisfied.

The sup-norm satisfies the axioms of a norm because, for any $0 \leq k < \infty$,

$$\|x_k + y_k\| \leq \|x_k\| + \|y_k\| \leq \| \sum_{k=0}^{\infty} x_k \|_{\infty} + \| \sum_{k=0}^{\infty} y_k \|_{\infty}.$$

□

1.3.2 Computer algebra package

We use the computer algebra package Maple version 15.

Chapter 2

The Adomian Decomposition Method

The ADM belongs to the class of decomposition theories defined in Gabet [55], an abstract framework useful to understand the main issues, in particular, about convergence.

2.1 Basic concepts of decomposition theory

Let X be a Banach space of norm $\| \ \|$. It could be finite dimensional or a function space like $C^k(U)$ or $L^2(U)$, equipped with the relevant norms, or even the cartesian product of such spaces. A **decomposition series** is a series $\sum_{k=0}^{\infty} C_k$ where each $C_k : X^{k+1} \to X$ is an X-valued function of the $(k+1)$ variables: $(x_0, \ldots, x_k)$. It is **weakly convergent** if the series

$$\sum_{k=0}^{\infty} C_k(x_0, \ldots, x_k)$$

converges in X for each convergent series $\sum_{k=0}^{\infty} x_k$ in X. The **sum** S of a weakly convergent decomposition series is a map $S : C(X) \to X$ defined by

$$S\left(\sum_{k=0}^{\infty} x_k\right) = \sum_{k=0}^{\infty} C_k(x_0, \ldots, x_k).$$

To ensure the independence of the sum with respect to the re-ordering of series, we say that a decomposition series is **strongly convergent** if it is weakly convergent and if its sum S depends only on the sum of the series in X, that is, if $\sum_{k=0}^{\infty} x_k = \sum_{k=0}^{\infty} y_k$ then

$$S\left(\sum_{k=0}^{\infty} x_k\right) = S\left(\sum_{k=0}^{\infty} y_k\right).$$

Because one can add and multiply strongly convergent decomposition series, the set of the strongly convergent decomposition series in X is a vector space ([55]).

With strongly convergent decomposition series we can define a new operator $S^* : X \to X$, the **degenerated sum of a strongly convergent decomposition series**, of value $S^*(x) = S\left(\sum_{k=0}^{\infty} x_k\right)$ for any convergent series $\sum_{k=0}^{\infty} x_k$ of sum x. Note that S^* is defined for every $x \in X$ because we can evaluate $S\left(\sum_{k=0}^{\infty} x_k\right)$ for the series $x + \sum_{k=1}^{\infty} 0$.

The **decomposition scheme (associated with a strongly convergent decomposition series $\sum_{k=0}^{\infty} C_k$)** is the recurrent scheme

$$x_0, \quad x_{k+1} = C_k(x_0, \ldots, x_k)$$

which constructs a series $\sum_{k=0}^{\infty} x_k$ in X. Such a series can be constructed because each C_n is a function of $x_0, \ldots, x_k$ but not of the following terms. The **decomposition method** is the method consisting of constructing the solution of an equation with a decomposition scheme.

2.1.1 The Fundamental Convergence Theorem

We cannot obtain the convergence of the scheme by adding the equalities defining x_k:

$$x_0, \quad x_{k+1} = C_k(x_0, \ldots, x_k), \ k \geq 0,$$

because we do not know if the series $\sum_{k=0}^{\infty} C_k(x_0, \ldots, x_k)$ converges. We only know that the decomposition scheme $\sum_{k=0}^{\infty} C_k$ strongly converges, that is, $\sum_{k=0}^{\infty} C_k(x_0, \ldots, x_k)$ converges when $\sum_{k=0}^{\infty} x_k$ converges and that is exactly what we want to prove.

Theorem 2.1 (Convergence of the decomposition scheme, [55]) *Let X be a Banach space and $\sum_{k=0}^{\infty} C_k$ be a strongly convergent decomposition series of degenerated sum $S^* : X \to X$. When S^* is a contraction, every decomposition scheme gives a convergent series whose sum verifies the fixed point equation $x = x_0 + S^*(x)$.*

Proof. Because S^* is a contraction, there is a unique fixed point $\bar{x}$ for the equation

$$\bar{x} = x_0 + S^*(\bar{x}).$$

Given any series $\sum_{k=0}^{\infty} x_k$, we define $X_n = \sum_{k=0}^{n} x_k$. Define $S_n : C(X) \to X$ by

$$S_n\left(\sum_{k=0}^{\infty} x_k\right) = \sum_{k=0}^{n} C_k(x_0, \ldots, x_k).$$

Thus, considering X_n as a degenerate infinite series (completing with zeroes),

$$S_n(X_n) = \sum_{k=0}^{n} C_k(x_0, \ldots, x_k) = \sum_{k=0}^{n} x_{k+1} = X_{n+1} - x_0.$$

and so, $X_{n+1} = S_n(X_n) + x_0$. We claim that the sequence $\{X_n\}_{n=0}^{\infty}$ converges to $\bar{x}$. Note that $S_n(X_n) = S_n(X_{n+1})$ because S_n depends only on $(x_0, \ldots, x_n)$. We have

$$\begin{aligned} X_n - \bar{x} &= S_{n-1}(X_{n-1}) + x_0 - (x_0 + S^*(\bar{x})) = S_{n-1}(X_{n-1}) - S^*(\bar{x}) \\ &= S_{n-1}(X_n) - S^*(\bar{x}) = S_{n-1}(X_n) - S^*(X_n) + S^*(X_n) - S^*(\bar{x}). \end{aligned} \tag{2.1}$$

Because S^* is a strongly convergent decomposition series, for any ϵ there exists $N_1(\epsilon)$ such that $\|S_{n-1}(X_n) - S^*(X_n)\| < \epsilon$ for all $n > N_1(\epsilon)$. Therefore (2.1) becomes

$$\|X_n - \bar{x}\| \leq \epsilon + k\,\|X_n - \bar{x}\|,$$

where $0 < k < 1$ is a contraction constant for S^*. Hence, $\|X_n - \bar{x}\| \leq \dfrac{\epsilon}{1-k}$, showing that $\lim_{n\to\infty} X_n = \bar{x}$. □

2.2 The ADM

The practical problem is to solve an equation $x = G(x)$ where G is a given operator. Using Theorem 2.1 with a strongly convergent decomposition series of degenerated sum G, the solution x is obtained by applying the decomposition scheme associated with this series.

2.2.1 The Adomian decomposition series

Let $F : X \to X$ be an analytic function on a Banach space X and $\sum_{n=0}^{\infty} x_n$ be a convergent series in X of sum x. The **Adomian polynomials** A_n **of** F **at** x_0, $n \geq 0$, are defined by

$$A_n[F, x_0](x) = \frac{1}{n!}\left(\frac{d^n}{d\lambda^n}|_{\lambda=0} F\big(\sum_{k=0}^{n} x_k \lambda^k\big)\right). \tag{2.2}$$

Define $\bar{x} = \sum_{n=0}^{\infty} x_n$ and $x^+(\lambda) = \sum_{n=0}^{\infty} x_n \lambda^n$, a power series converging when $\lambda = 1$. We know that the sum of a power series, whose convergence radius is ρ, is analytic over $B_0(\rho)$ (B_{x_0} is abbreviated to B_0), thus x^+ is analytic over $B_0(\rho)$. Because F is analytic, from the composition theorem ([35]), $F(x^+)$ is analytic over $B_0(\rho)$, that is, there are A_n's so that $F(x^+)(\lambda) = \sum_{n=0}^{\infty} A_n \lambda^n$ and these A_n verify (2.2). We do not need to assume that the convergence radius is greater than 1. If $\rho = 1$, as $x^+(1)$ converges and its sum is $\bar{x}$, then Abel's theorem [85] leads to $\lim_{\lambda\to 1^-} x^+(\lambda) = \bar{x}$ (λ being a real number) and so $\lim_{\lambda\to 1^-} (F \circ x^+)(\lambda) = F(\bar{x})$.

Theorem 2.2 (Convergence of the Adomian decomposition series, [55]) *The Adomian polynomials $\{A_n[F, .]\}_{n=0}^{\infty}$ associated with the analytical function F define a strongly convergent decomposition series whose degenerated sum is F.*

2.2.2 Generalised formulation of the ADM

To demonstrate the flexibility of the ADM with respect to infinite series expansions, let

$$x = N(x) + c \tag{2.3}$$

where N is analytic at c_0 and $c = \sum_{k=0}^{\infty} c_k$ is an absolutely convergent series ([65]). The ADM takes the following form.

Proposition 2.3 *A solution of (2.3) is the series $\sum_{n=0}^{\infty} x_n$ given by*

$$x_0 = c_0, \quad x_{n+1} = A_n[N, c_0](x) + c_{n+1},\ n \geq 0. \tag{2.4}$$

Proof. Write (2.3) in the form

$$x = \lambda N(x) + \sum_{n=0}^{\infty} c_n \lambda^n \tag{2.5}$$

where λ is a parameter. Seeking a solution in a series form, (2.5) can be written as

$$\sum_{n=0}^{\infty} x_n \lambda^n = c_0 + \sum_{n=0}^{\infty} \left(A_n[N, c_0](x) + c_{n+1} \right) \lambda^{n+1},$$

leading to the ADM scheme given by (2.4) by equating coefficients of λ^n. □

2.2.3 What can the ADM be used for?

The ADM can be straightforwardly applied to all kinds of nonlinear or linear, homogenous or inhomogeneous functional equations such as ODEs, PDEs, algebraic equations, integral equations and systems thereof. It is a significant method with wide application for deriving rapidly convergent series solutions ([53, 10]).

With regard to the rapid convergence of the ADM many practical examples of applications of the ADM to PDEs and integral equations have been presented that show that closed form solutions could be identified (and in numerical applications the greater accuracy of the ADM series solution was found) from the first few iterates of the method (three or four terms) ([101], [100]). When the ADM is applied to ODEs and PDEs it was established that the value of successive series terms obtained by Adomian's method approach zero as $\frac{1}{(mn)!}$ if m is the order of the highest linear differential operator (n is the number of a given term in the series solution) and that the limit of the n^{th} order approximant at infinity approaches the exact solution ([79]). It was suggested that in general the rapid convergence of the method might be due to the definition of the $A_n s$ having a factor of $\frac{1}{n!}$ ([40]).

The ADM has been used to overcome difficulties in finding solutions to differential equations with discontinuities, like equations with singular coefficients such as Legendre's, Bessel's or Hermite's equations ([82]). Adopting a suitable definition of the operator and utilising a transformation formula while implementing the ADM, the difficulty associated with singular points in the Lane-Emden equations was overcome ([92, 98]). A general approach using the ADM to solve ODEs with discontinuities has been introduced in [36].

In [72], a series solution was found for a class of integro-differential equations which describe the charged particle motion for oscillating magnetic fields where it was found that the terms of the solution were related to distinct sequences of prime numbers. In [73], the use of the ADM for mixed nonlinear Volterra-Fredholm integral equations was demonstrated. In [21] the application of the ADM was extended in order to solve Volterra's problem related to population dynamics and a problem from polymer rheology where a solution for the equation modelling the elongation of a filamentous polyethylene which was stretched and released was studied.

Other applications include finding solutions to predator-prey models and to a system of linear ODEs, reduced approximations of a transport equation ([53, 96]). The ADM is particularly useful in applications to modelling where parameters have to be identified from experimental data.

In such instances the ADM can be associated to an optimization technique and may be applied to optimal control problems arising, for instance in biomedicine. It allows the transformation of an optimal control problem into a classical optimization problem ([1]).

2.3 Convergence of the ADM

We use the ADM to solve equations of the general functional form

$$x = N(x) + c, \tag{2.6}$$

where N is a nonlinear analytic operator from a Banach space X into itself and where $c \in X$ is given. In the absence of a unique solution, the ADM will give a solution among other possible solutions. When the Adomian series does not yield a closed form solution, a truncated series can be used if a numerical approximation is desired. The first few terms of the truncated series usually provide the higher accuracy level of the approximate solution ([101]). The analysis of the convergence of the ADM is difficult because of the following potential circular argument: the decomposition scheme converges when the series of the Adomian polynomials converges, and this is true when the decomposition scheme converges (because of the weak convergence of the decomposition series). The following result is fundamental to analyse the convergence of the composition of convergent power series.

Proposition 2.4 *Given a sequence $\{m_n\}_{n=0}^{\infty}$ of multilinear operators on X^n, consider the series $G(x) = \sum_{n=0}^{\infty} m_n x^n$ with radius of convergence r. Let $x(\lambda) = \sum_{n=0}^{\infty} b_n \lambda^n$, $b_n \in X$, be a convergent series. Suppose there exist $M, \epsilon > 0$ such that $\|b_n\| \leq \dfrac{M}{(1+\epsilon)^n}$, $n \geq 0$, and, in addition when $r < \infty$, $M < \dfrac{\epsilon r}{1+\epsilon}$, then the resulting power series $G(x(\lambda))$ in λ has a radius of convergence greater than 1.*

Proof. Because of the rules of convergence of the composition of convergent series, it is enough to show that $\|x(\lambda)\| \leq \sum_{n=0}^{\infty} \|b_n\| \cdot |\lambda|^n < r$ when $|\lambda| = 1$. From the estimate on the b_n's, we get

$$\sum_{n=0}^{\infty} \|b_n\| \cdot |\lambda|^n \leq \sum_{n=0}^{\infty} M \left(\frac{|\lambda|}{1+\epsilon} \right)^n = \frac{M}{1 - \frac{|\lambda|}{1+\epsilon}}$$

when $|\lambda| < 1 + \epsilon$. And so, when $r = \infty$, we have convergence when $|\lambda| \leq 1$. When $r < \infty$, from the condition on ϵ,

$$\sum_{n=0}^{\infty} \|b_n\| \leq \frac{M}{1 - \frac{1}{1+\epsilon}} < \frac{1+\epsilon}{\epsilon} \cdot \frac{\epsilon r}{1+\epsilon} = r,$$

and so $G(x(1))$ converges. □

Because our functions are analytic, the first sets of results estimate the norms of the Adomian polynomials from the estimates of the derivatives of the analytic function N. We consider two cases (see the examples in Section B.1.1). Let $x_0 \in X$ and $0 < r \leq \infty$. An analytic function $N : B_{x_0}(r) \subset X \to X$ with radius of convergence r satisfies hypotheses

(H1) when there exist $M, \alpha > 0$ such that $\|N^{(n)}(x_0)\| \leq M\alpha^n$, $n \geq 0$, $(r = \infty)$,

(H2) when there exist $M, \alpha > 0$ such that $\|N^{(n)}(x_0)\| \leq (n!)M\alpha^n$, $n \geq 0$, $(r \geq 1/\alpha)$.

Proposition 2.5 (Adomian polynomial estimates, [65]) *Let $N : B_{x_0}(r) \subset X \to X$ be analytic at $x_0 \in X$ with radius of convergence r. If N satisfies (H1), then*

$$\|A_n[N, x_0]\| \leq \frac{(n+1)^n}{(n+1)!} M^{n+1}\alpha^n, \tag{2.7}$$

or, if N satisfies (H2), then

$$\|A_n[N, x_0]\| \leq \frac{(2n)!}{(n+1)! \cdot n!} M^{n+1}\alpha^n. \tag{2.8}$$

Clearly, if N satisfies (H1), it satisfies (H2), and so, from (2.8), we check that it satisfies (2.7)

$$\|A_n[N, x_0]\| \leq \frac{(n+1)^n}{(n+1)!} M^{n+1}\alpha^n \leq \frac{(2n)!}{(n+1)! \cdot n!} M^{n+1}\alpha^n.$$

Following this estimate of the norm of the Adomian polynomial we obtain a general convergence result for the ADM.

Theorem 2.6 (Convergence estimates of the ADM, [65]) *Let $N : B_{c_0}(r) \subset X \to X$ be analytic at $c_0 \in X$ with radius of convergence r. If N satisfies (H1) and $eM\alpha < 1$, then the ADM converges for (2.6). If N satisfies (H2) and $4M\alpha < 1$, when $r = \infty$, or if $5M\alpha < 1$, when $r < \infty$, then the ADM converges for (2.6).*

Those results can be viewed as special cases of the corresponding results for the generalised ADM (2.3,2.4). We shall state and prove those results now.

2.3.1 Convergence of the generalised ADM

In the context of the generalised formulation of the ADM (2.4) we get the following generalisation of Proposition 2.5. We say that the problem (2.3) satisfies the hypotheses (H1g) if N satisfies (H1) and if there exist $M_1, \alpha_1 \geq 0$ such that $\|c_{n+1}\| \leq M_1\alpha_1^n$, $n \geq 0$, with $M_1 < M$ and $\alpha_1 < M\alpha$. In case N satisfies (H2), with all the other conditions being identical, we say that the problem satisfies (H2g). With (H1g) or (H2g), define the constant $\beta = (1 - \frac{M_1}{M})^{-1}(1 - \frac{\alpha_1}{M\alpha})^{-1}$.

Proposition 2.7 ([65]) *Suppose that the problem (2.3) satisfies the hypotheses (H1g), then the terms of the series (2.4) satisfy*

$$\|x_{n+1}\| \leq \frac{(n+1)^n}{(n+1)!} M^{n+1}\beta\alpha^n.$$

If (2.3) satisfies the hypotheses (H2g), then the terms of the series (2.4) satisfy

$$\|x_{n+1}\| \leq \frac{(2n)!}{(n+1)! \cdot n!} M^{n+1}\beta\alpha^n.$$

We see that if $c_n = 0$, $n \geq 1$, the results of Proposition 2.7 reduce to Proposition 2.5. As a consequence we get the following result for convergence of the generalised ADM.

Theorem 2.8 (Convergence estimates of the generalised ADM, [65]) *Let $N : B_{c_0}(r) \subset X \to X$ be analytic at $c_0 \in X$ with radius of convergence r. If N satisfies (H1g) and if $eM\alpha < 1$, then the generalised ADM converges. If N satisfies (H2g) and $4M\alpha \leq 1$, when $r = \infty$, or if $0 < 4M\alpha \leq 1 - \alpha\beta$, when $r < \infty$, then the generalised ADM converges.*

As before, we see that if $c_n = 0$, $n \geq 1$, we get $\beta = 1$ and so the results of Theorem 2.8 reduce to Theorem 2.6.

2.4 Time evolution problem

Let $X \subset Y$ be Banach spaces, with norms $\| \ \|_X$, $\| \ \|_Y$, respectively. A typical nonlinear evolution problem can be cast into the general form

$$u_t = Lu + F(u) \tag{2.9}$$

where $u(t) \in X$, $L : X \to Y$ is a linear operator and $F : X \to X$ is a nonlinear operator. Typically, $Y \neq X$ is necessary when L is a differential operator. A **solution of (2.9)** is a continuously differentiable function $u : I \to X$ where $I \subset \mathbb{R}$ is an interval.

2.4.1 Analytical solutions of evolution problems

We now establish sufficient conditions for the solution u of (2.9) to be analytic in time. For that it is convenient to transform (2.9) into a Volterra integral problem. For ODEs, this is the extension of the method of variation of constants. There is an extension to Banach spaces, called **Duhamel's principle** ([2]). It is based on $L : X \to Y$ defining a continuous semigroup $E(t) : X \to X$ such that $u(t) = E(t)u_0$ is a solution of the linear problem $u_t = Lu$ with $u(0) = u_0$ and the existence of a constant $C > 0$, independent of $u \in X$, such that

$$\|E(t)c_0\|_X \leq C \|c_0\|_X, \quad \forall c_0 \in X, \quad \forall t \in \mathbb{R}_+. \tag{2.10}$$

When L is independent of time, $E(t) = e^{tL}$ for $t \geq 0$. Moreover, let $F : X \to X$ be analytic near $u = u_0$ and X be a Banach algebra with the property

$$\|uv\|_X \leq \|u\|_X \|v\|_X, \quad \forall u, v \in X. \tag{2.11}$$

The initial-value problem (2.9) can be reformulated as an integral equation

$$u(t) = E(t)u_0 + \int_0^t E(t-s)\, F(u(s))\, ds, \quad t > 0. \tag{2.12}$$

If F is analytic near u_0, it satisfies a local Lipschitz condition in the ball $B_{u_0}(\delta)$. Therefore the CMT, Theorem ([50]) can be applied to (2.12) for small time intervals to find unique solutions of the integral equation, hence of the ODE (2.9). The precise statement follows.

Theorem 2.9 (Picard-Kato, [2]) *Let X, Y, L and F satisfy the previous conditions near $u_0 \in X$. There exists a $T > 0$ and a unique solution $u \in C([0,T],X) \cap C^1([0,T],Y)$ of the initial-value problem (2.9) on $[0,T]$ such that $u(0) = u_0$. Moreover, the solution u depends continuously on the initial data u_0.*

When F is analytic near u_0, we expect the unique solution u to be analytic in time. This is done in the following result.

Theorem 2.10 (Cauchy-Kowalevskaya, [2]) *Under the previous assumptions on (2.9) with $X = Y$. Let u be the unique solution of (2.9) in $C^1([0,T),X)$ such that $u(0) = u_0$ where $T > 0$ is the maximal existence time of u. If F is analytic around u_0, there exists $\tau \in (0,T)$ such that $u : [0,\tau] \to X$ is a real analytic function.*

2.4.2 Convergence of the ADM method for time evolution problems

To set up the ADM, we define the non linear operator

$$N(u) = \int_0^t E(t-s)\, F(u(s))\, ds$$

which is analytic when F is analytic. We write the solution $u(t)$ of (2.9) with initial condition $f \in X$ as the series

$$u(t) = u_0(t) + \sum_{n=1}^{\infty} u_n(t). \tag{2.13}$$

In that case, the ADM gives us $u_0(t) = E(t)f$ and

$$u_{n+1}(t) = \int_0^t E(t-s)\, A_n[F,f](u_1(s),\ldots,u_n(s))\, ds, \quad n \geq 0, \tag{2.14}$$

where the quantities $A_n[F,f]$ are the Adomian polynomials of F at $u = f$.

For Volterra integral equations like (2.12), a small time step allows us to control the size of the nonlinear operator, so we can apply the previous convergence theory, while preserving the analyticity of the nonlinear terms. A theorem by Re'paci [86] showed that the ADM can be safely applied when a fixed point theorem holds and that it may be used as an algorithm for the approximation of the dynamical response in a sequence of time intervals $[0,t_1],[t_1,t_2],\cdots,[t_{n-1},T]$ such that the condition at t_p is taken as the initial condition in the interval $[t_p,t_{p+1}]$ which follows ([86]). With the hypotheses (H1) and (H2), we get estimates similar to Proposition 2.5 and convergence results similar to Theorem 2.6.

Proposition 2.11 ([65]) *Let $F : B_f(r) \subset X \to X$ be analytic at $f \in X$ with radius of convergence R. If F satisfies (H1), then*

$$\|A_n[N,f]\| \leq M^{n+1}\alpha^n \frac{|t|^{n+1}}{n+1}, \tag{2.15}$$

or, if F satisfies (H2), then

$$\|A_n[N,f]\| \leq \frac{(2n)!}{(n+1)!\cdot n!\, 2^n}\, M^{n+1}\alpha^n \frac{|t|^{n+1}}{n+1}. \tag{2.16}$$

As a consequence we have the following convergence results.

Theorem 2.12 ([65]) *Let $F : B_f(r) \subset X \to X$ be analytic at $f \in X$ with radius of convergence r. If F satisfies (H1) and $M\alpha|t| < 1$, then the ADM converges for (2.12). If F satisfies (H2) and $4M\alpha|t| < 1$, when $r = \infty$, or if $5M\alpha|t| < 2$, when $r < \infty$, then the ADM converges for (2.12).*

2.5 Comments on the ADM

2.5.1 Limitations to the ADM

In some instances a direct computation method for solving an integral equation will be easier to implement when the resulting algebraic equations are easily dealt with. But in cases where the specific nonlinear expression $F(u)$ appearing in the integral equation are of a form such that algebraic equations of higher degree arise such as when $F(u) = u^n$, the ADM will be easier to use for $n \geq 2$. Similarly if the u_0 term selected from the integral equation is an exponential or trigonometric function, then the ADM is likely to work better than say the method of successive substitutions ([100]). What's more, if the nonhomogeneous part, forcing term $f(x)$ being used as the initial approximation $u_0(x)$ is not a polynomial of a few terms the ADM encounters computational difficulties. The modified decomposition method where upon splitting the forcing term $f(x) = f_1(x) + f_2(x)$ the first term $f_1(x)$ is assigned to u_0 with the remaining term $f_2(x)$ being assigned to the formula of the next term often reduces the volume of calculations.

Although the decomposition method is powerful, usually easier to use and is able to provide the solution to equations with strong nonlinearity it does not establish the existence and the uniqueness of the solution of the problem. The method produces at most one solution though for example, in the case of integral equations by using a direct computation method multiple solutions may be found. The fact that the method gives only one solution is not indicative of the uniqueness of the solution. A unique solution may however be determined under specific conditions ([100]). At the time of writing there is currently no procedure other than that presented here in Chapter 3 for getting the ADM to give more than one solution ([101]).

The series solution generated by the ADM often coincides with the Taylor expansion of the true solution at point $x = 0$ in the initial value case. This solution given by the ADM is usually rapidly convergent in a particular region. For instance, around the initial condition $x = 0$, but it might have a very slow convergence rate in a wider region with the result that a truncated Adomian series solution may be inaccurate or get progressively worse as an approximation in the wider region. This restricts the application area of the method ([67, 68, 74]). However, this shortcoming has been mitigated in the case of nonlinear oscillatory systems by modifying the series solution provided by the ADM so that it is periodic and using Laplace transforms and Padé approximants to deal with the truncated series solution obtained ([67, 97]). In general for ordinary and partial differential equations with initial conditions modifying the ADM solution with Padé approximant (taking the Padé approximant of the truncated series) can improve the accuracy in a wider range and the convergence rate of Adomian's series. Further in this way more information about the mathematical behaviour of the solution is obtained ([23, 67]).

Implementing the ADM for boundary value problems on an infinite or semi-infinite domain requires further adjustment after the method has been implemented. Power series are not useful for large values of x ([101]). Also a power series on its own has limited use in the handling of boundary value problems because of the possibility that the radius of convergence might not be sufficiently large to contain the boundaries of the domain ([33]). However an effective approach for utilising the ADM with boundary value problems is to derive the Adomian series solution on an unbounded domain of validity, form the diagonal Padé approximant as the most efficient and accurate approximation and then evaluate the limit as $x \mapsto \infty$.

In a particular instance regarding the handling of multispecies Lotka-Volterra predator-prey models, the ADM was used to give approximate solutions to coupled first order nonlinear differential equations subject to certain parameter choices. It was stated that the cost of implementing the ADM with regard to algebraic manipulation was greater than that of a direct implementation of a fourth order Runge Kutta method ([53]). However, a globally convergent solution utilising the ADM was not pursued. Instead implementation of the ADM involved a concatenation of Adomian polynomials over successive sub intervals i.e. the presented Adomian solution was a composite of ADM solutions over smaller intervals. Further the implementation of the Runge Kutta method was based on an earlier stability analysis where parameterisation had already been done but the ADM does not require parameterisation. Authors ([53]) neglected to consider comparative results if the coupled first order nonlinear ODEs were considered as a perturbation of the multispecies Lotka-Volterra predator-prey model and an Adomian-type perturbation of the series solution to the Lotka Volterra model had been developed. In ([78]) it was demonstrated that the ADM was a powerful tool in finding the solution of some predator-prey model equations and that it compared favourably with alternative analytic and numerical approximate methods.

In specific instances a comparison between the use of the ADM and a Taylor series perturbation method showed that the terms arising from the implementation of the ADM were more difficult to integrate but the Taylor series expansion avoided the occurrence of these complicated terms needing evaluating. However, on the whole in such instances the solutions afforded by the ADM were judged to perform reasonably well ([101]).

For numerical purposes it has been stated that when using software to compute the terms of the ADM series solution as the number of terms in the series solution increases, the number of terms in the formula for A_n also increases leading to propagation of round off errors ([22]). But the factor $\frac{1}{k!}$ in (2.2) makes it very small so that its contribution to the solution u is negligible and accordingly the first few terms of the series solution determine the accuracy of the approximate solution ([22]). Overall, errors can be significantly reduced by computing additional terms of the series. Furthermore algorithm (Restarted Adomian Decomposition Method, [RADM]) to improve the accuracy dramatically by modifying the equation of the form $u = N(u) + c$ so that the first term of the series solution is a better starting point with regard to convergence to the exact solution has been developed ([22]).

A common problem in the physical sciences is to obtain the solution of a partial differential equation which satisfies a set of functional values on a rectangular boundary. For example, a problem of the form

$$\frac{\partial^2 u}{\partial x^2} + \frac{\partial^2 u}{\partial y^2} - b\frac{\partial u^u}{\partial x} = \rho(x, y), \tag{2.17}$$

with the following boundary conditions defined on a rectangle

$$u(x = 0) = f_1(y), \quad u(x = x_1) = f_2(y), \quad u(y = -y_1) = g_1(x), \quad u(y = y_1) = g_2(x).$$

One of the most interesting consequences of applying the ADM to a problem like this is that in the general case the partial solutions (the solutions obtained by integrating in the x direction and the y direction) are equal ([101]). Thus, one of the two sets of boundary functions f_1, f_2 or g_1, g_2 is redundant, and u is in any case the solution. This implies that a PDE with boundary conditions on a rectangle cannot have arbitrary boundary conditions on the borders, since the conditions at $x = x_1, x = x_2$ must be consistent with those imposed at $y = y_1$ and $y = y_2$([79]). But many PDEs such as elliptic PDEs have solutions that are highly sensitive to the imposed boundary function when only two sides are used. This could restrict the application of the ADM from problems formulated as Von Neumann or Dirichlet problems on a closed contour ([79]). However, practical methods for finding the boundary functions that are compatible with any lateral set of conditions imposed have been suggested. This makes it possible to find the analytical solutions of PDE boundary problems on a closed rectangle with required accuracy thus facilitating the solution to a wide range of problems that the ADM would not otherwise be able to address ([79]).

2.5.2 Advantages of the ADM

Nonlinearity can be computationally difficult to handle mathematically. Furthermore questions relating to the uniqueness and stability of solutions present additional difficulties. Adequate theory for dealing with nonlinear equations is being developed and existing theory for linear equations such as the superposition principle do not relate to nonlinear equations. Therefore, in practice when modelling nonlinear processes numerical solutions are often sought and deterministic proxies are often utilised. Many specialised methods for treating linear and nonlinear functional equations such as a PDE exist and it is known that Newton's method combined with a finite difference or finite element method gives a general technique to get numerical solutions for many problems but traditionally there is no general method for analytically solving nonlinear differential (ordinary and partial) or integral equations. Depending on the nature of the equation, the given conditions and other factors, a method is chosen or several methods are used. An equation may be converted from one form to another, such as when a PDE is converted to an ODE or a system thereof.

However the ADM constitutes a general method that can be used in a straightforward manner for all types of functional equations such as ODEs, PDEs and integral equations. The application of the ADM can be organised in a similar manner for huge classes of linear and nonlinear problems, even stochastic problems. A key advantage of the ADM lies in its computational convenience and the rapid convergence of the series solution. The method provides the solution to any style equation (functional equations) homogenous, inhomogeneous, linear, nonlinear. There is no need to transform inhomogeneous conditions into homogenous conditions. The analytic method does

not require linearisation or perturbation. It is continuous without regard to discretisation and reduces the massive computation which may arise in the use of discretisation methods ([67]). The method can be implemented in a straightforward manner without the need for any restrictive assumptions or transformation formula that may change the physical behaviour of the model under consideration. The Adomian polynomials can be calculated for all kinds of nonlinearities and the method incorporates a formal algorithm to establish a proper representation for all forms of nonlinear terms ([101]). Because the method effectively handles all kinds of nonlinearities the analytical solutions to a large class of nonlinear equations become accessible.

The reliability, accuracy and effectiveness has been established for wide applications in both analytic and numerical purposes ([101]). For example, few numerical methods are known for mixed Volterra-Fredholm equations but, when compared to methods used such as Euler Nyström, trapezoidal Nyström, continuous time collocation, time discretisation collocation methods, the ADM was straightforward and offered significant improvement in accuracy ([73]). With regard to application to integral equations it has been noted that in general if the kernel is degenerate consisting of a polynomial of one or two terms then the ADM will most likely be the best method as it minimizes the volume of calculations when compared to a method of successive approximations or Neumann method ([100]).

In numerical applications the solution obtained by evaluating few terms of the series gives an approximation of a high degree of accuracy comparable with other numerical techniques ([27, 46, 47, 83, 99, 101]). The rate of convergence in many instances is faster than existing numerical methods ([101]). A comparison between the ADM and the perturbation method for nonlinear random differential equations showed that in general the ADM was more efficient and reliable in that it reduced the size of calculations ([27]). Similar results were obtained when compared with Picard's method for differential equations ([83]). It was found that the ADM was computationally easier to use in order to get the terms of the solution at different stages of calculation ([99]). Another comparative study for nonlinear ODEs showed that the ADM broadly required less computational work than the Taylor series method. Comparison with other methods such as finite difference and other series solution methods have shown that the ADM compares favourably well ([46, 47, 48, 49, 73]).

With regard to solving integral equations in the linear case each term in the series is an integral of one more transformation of the last term in the series. In the nonlinear case only the integral of another A_n is added making the ADM simpler computationally and more accurate ([9]). A comparison which holds true in general as the approach of applying the inverse differential operator as done when implementing the ADM often leads in practice to easier computations ([100, 101]).

With regard to applications to PDEs such as (2.17) one advantage of the ADM is that due to the equality of partial solutions and the convergence of the ADM to this one solution, a solution can therefore be sought in the direction that is most convenient computationally ([101]).

2.6 Examples

2.6.1 Simple nonlinear integral equation

Consider

$$u(x) = e^x - \frac{1}{3}xe^{3x} + \frac{1}{3}x + \int_0^x xu^3(t)\mathrm{d}t,$$

where in keeping with the formulation in equation (2.6), $u = N(u) + c$, the solution $u(x)$ is represented by a sum of infinite terms and the nonlinear expression $N(u)$ is accounted for by the Adomian polynomials.

$$u(x) = \sum_{k=0}^{\infty} u_k(x) \quad \text{and} \quad N(u) = \int_0^x xu^3(t)\mathrm{d}t.$$

Applying the modified ADM wherein the forcing term c is split between the first two terms of the series solution and consequently

$$c = c_0 + c_1, \quad c_0 = \mathrm{e}^x, \quad c_1 = \frac{x}{3}(1 - \mathrm{e}^{3x}),$$

then

$$u_0 = c_0 = e^x$$

and

$$A_0[N, c_0] = N(u_0) = e^{3t}.$$

This yields

$$u_1(x) = c_1 + A_0[N, c_0] = 0$$
$$u_1(x) = \frac{1}{3}x\left(1 - e^{3x}\right) + x\int_0^x e^{3t}\mathrm{d}t = 0$$

and it follows that $A_1[N, c_0] = 0$ and the other terms of the series solution are therefore calculated as $u_k = 0$, $k \geq 1$. The exact solution is therefore

$$u(x) = u_0 + u_1 + u_2 + \cdots = u_0$$

$$u(x) = e^x.$$

2.6.2 A nonlinear advection problem.

Consider

$$u_t + \frac{1}{2}(u^2)_x = x, \qquad u(x,0) = 2, \tag{2.18}$$

where

$$F(u) = \frac{1}{2}(u^2)_x \quad \text{and} \quad A_n[F,u_0] = \frac{1}{n!}\frac{\mathrm{d}^n}{\mathrm{d}\lambda^n} F\left(\sum_{k=0}^{n} u_k \lambda^k\right)\Bigg|_{\lambda=0}.$$

Define

$$L_x = \frac{\partial}{\partial x} \quad \text{and} \quad L_t^{-1}(.) = \int_0^t (.)\mathrm{d}t.$$

Operating with L_t^{-1} gives

$$u(x,t) = 2 + xt - \frac{1}{2}L_t^{-1}L_x(u^2). \tag{2.19}$$

Substituting $u(x,t) = \sum_{n=0}^{\infty} u_n(x,t)$ and $u^2(x,t) = \sum_{n=0}^{\infty} A_n$, into (2.19), gives

$$\sum_{n=0}^{\infty} u_n(x,t) = 2 + xt - \frac{1}{2}L_t^{-1}L_x\left(\sum_{n=0}^{\infty} A_n\right).$$

Whereupon,

$$\begin{aligned} u_0(x,t) &= 2 + xt, \\ u_{k+1}(x,t) &= -\frac{1}{2}L_t^{-1}L_x(A_k), \quad k \geq 0. \end{aligned} \tag{2.20}$$

The Adomian polynomials for the nonlinearity u^2 are

$$A_0 = F(u_0) = u_0^2, \tag{2.21}$$

$$A_1 = u_1 F^{'}(u_0) = 2u_0u_1, \tag{2.22}$$

$$A_2 = u_2 F^{'}(u_0) + \frac{1}{2!}u_1^2 F^{''}(u_0) = 2u_0u_2 + u_1^2. \tag{2.23}$$

Using (2.20) gives

$$\begin{aligned} u_1(x,t) &= -\frac{1}{2}L_t^{-1}L_x(A_0) = -t^2 - \frac{1}{3}xt^3, \\ u_2(x,t) &= -\frac{1}{2}L_t^{-1}L_x(A_1) = \frac{5}{12}t^4 + \frac{2}{15}xt^5, \\ u_3(x,t) &= -\frac{1}{2}L_t^{-1}L_x(A_2) = -\frac{61}{360}t^6 - \frac{17}{315}xt^7, \end{aligned}$$

and after rewriting the solution terms

$$u(x,t) = 2(1 - \frac{1}{2}t^2 + \frac{5}{24}t^4 - \frac{61}{720}t^6 + \cdots) + x\left(t - \frac{1}{3}t^3 + \frac{2}{15}t^5 - \frac{17}{315}t^7 + \cdots\right).$$

The exact solution can be deduced as

$$u(x,t) = 2\text{sech}\, t + x \tanh t. \tag{2.24}$$

Which can be justified by substitution of (2.24) into (2.18).

Alternatively given the form of (2.18) a solution of the form

$$u(x,t) = f(t) + xg(t) \tag{2.25}$$

can be sought. With (2.25), $u_t = f' + xg'(t)$, $u_x = g$ and $u(x,0) = f(0) + xg(0) = 2$ hence $f(0) = 2$ and $g(0) = 0$. Replacing u_t and u_x into (2.18) gives

$$f' + xg'(t) + (f + xg)g = (f' + fg) + x(g' + g^2) = x.$$

Hence

$$f' + fg = 0, \quad f(0) = 2, \tag{2.26}$$

$$g' + g^2 = 1, \quad g(0) = 0. \tag{2.27}$$

(2.27) can be solved using separation of variables to give

$$g(t) = \frac{\sinh(t)}{\cosh(t)} = \tanh(t)$$

and (2.26) can be solved using an integrating factor to give

$$f(t) = \frac{2}{\cosh(t)} = 2\text{sech}(t)$$

leading to (2.24).

2.6.3 The nonlinear Sine-Gordon equation

Let

$$u_{tt} - u_{xx} = \sin u, \qquad u(x,0) = \frac{\pi}{2}, \qquad u_t(x,0) = 0.$$

Here $F(u) = \sin u$.

Setting

$$\begin{aligned} u_0(x,t) &= \frac{\pi}{2}, \\ u_{k+1}(x,t) &= L_t^{-1}(u_{k_{xx}}(x,t)) + L_t^{-1}(A_k), \;\; k \geq 0, \end{aligned} \tag{2.28}$$

gives

$$\begin{aligned} A_0 &= \sin u_0, \\ A_1 &= u_1 \cos u_0, \\ A_2 &= u_2 \cos u_0 - \frac{1}{2!} u_1^2 \sin u_0, \\ A_3 &= u_3 \cos u_0 - u_2 u_1 \sin u_0 - \frac{1}{3!} u_1^3 \cos u_0. \end{aligned}$$

Using (2.28), we get

$$\begin{aligned} u_1(x,t) &= \frac{1}{2} t^2, \\ u_2(x,t) &= 0, \\ u_3(x,t) &= -\frac{1}{240} t^6, \\ u_4(x,t) &= 0, \\ u_5(x,t) &= \frac{1}{172800} t^{10}, \end{aligned}$$

and the series solution may be written as

$$u(x,t) = \frac{\pi}{2} + \frac{1}{2} t^2 - \frac{1}{240} t^6 + \frac{1}{172800} t^{10} + \cdots$$

Chapter 3

Multiple solutions of nonlinear problems with the ADM

To begin with consider the following definitions of the derivative and analytic functions.

Let X and Y be two Banach spaces, $U \subset X$ be a neighbourhood of $x_0 \in X$, the derivative $f'(x_0)$ at x_0 of a differentiable map $f : X \to Y$ is often calculated in practical terms using the **directional derivative**: for every $v \in X$, the value $f'(x_0)v \in Y$ is given by

$$f'(x_0)v = \lim_{t\to 0} \frac{f(x_0 + tv) - f(x_0)}{t} = \frac{\mathrm{d}}{\mathrm{d}t} f(x_0 + tv)\bigg|_{t=0}. \tag{3.1}$$

To apply the ADM, we need to deal with analytic functions. A map $f : U \subset X \to Y$ is **analytic at** $u_0 \in U$ if there exists $m_0 \in Y$ and a family of bounded k-multilinear symmetric maps $\{m_k\}_{k=1}^{\infty}$ with

$$f(x) = \sum_{k=0}^{\infty} m_k (x - x_0)^k$$

for every $x \in U$ such that $\|x - x_0\| < r$ is small enough and there exists $M, r > 0$ such that $\|m_k\| \leq \dfrac{M}{r^k}$ (or $\limsup_{k\to\infty} r^k \|m_k\| = M < \infty$). The map f is **analytic on** U if it is analytic at every point $x \in U$ (cf. Appendix B).

Let X, Y be two Banach spaces and $f : U \subset X \to Y$ be a nonlinear map, supposed analytic on U. The aim is to find the solutions of

$$f(u) = 0 \tag{3.2}$$

using the ADM. In particular we shall concentrate on getting multiple solutions for such nonlinear equations using that iterative method. Although multiple, we assume that each solution $\bar{u} \in U$ is isolated. A solution $\bar{u}$ of (3.2) is **isolated** if there exists a neighbourhood $\bar{u} \in V$ such that $f'(u) \neq 0$, $\forall u \in V$. Note that a sufficient condition to be an isolated zero of f is that $f'(\bar{u})$ is invertible. This is a direct consequence of the Inverse Mapping Theorem (B.4). From now on, we assume that the zeroes we seek are isolated roots of (3.2).

3.1 Isolated zeroes of maps

A simple idea is to write (3.2) as a fixed point problem

$$u = F(u) \tag{3.3}$$

whose solutions are exactly the zeroes of f. A simple candidate is $F(u) = u + f(u)$, but there are other possibilities, for instance (3.5). The fixed point problem (3.3) can be solved by successive iterations $u_{n+1} = F(u_n)$, $u_0 \in V$. This technique works well when F is a contraction, when

$$\|F'(u)\| \leq k < 1$$

for all $u \in U$. When f has multiple zeroes, that is, when F has multiple fixed points, we work locally, around each fixed point. Let $\bar{u}$ be such fixed point, we would like that $\|F'(\bar{u})\| < 1$. When this is not the case we should modify F. The following lemma gives more precise details.

Lemma 3.1 *Given $u_0 \in U$. Let $K : Y \to X$ be an injective linear operator, $\bar{u}$ is a solution of $f(u) = 0$ if and only if $\bar{u}$ is a fixed point of the equation*

$$u = u_0 + F(u) \tag{3.4}$$

where

$$F(u) = u - u_0 + Kf(u). \tag{3.5}$$

Proof. If $\bar{u} = u_0 + F(\bar{u})$, $Kf(\bar{u}) = 0$ and so $f(\bar{u}) = 0$ because K is injective. Conversely, if $f(\bar{u}) = 0$, $F(\bar{u}) = \bar{u} - u_0$. □

The issue now is to see how to determine K such that F is a contraction near the root we would like to approximate using the ADM. The following lemma gives some conditions and information we can use (see also Appendix C).

Lemma 3.2

1. *Let K such that $\|I + Kf'(\bar{u})\| < 1$, then F is a contraction in a neighbourhood of $\bar{u}$.*
2. *Suppose that $\lambda \in \mathbb{C}^*$ is an eigenvalue of an operator M and $\lambda \in \mathbb{R}$, then $1 + \alpha\lambda$ is an eigenvalue of $I + \alpha M$ of norm less than 1 if α has the same sign as $-\mathrm{re}(\lambda)$ and $|\alpha| < \dfrac{2\mathrm{re}(\lambda)}{|\lambda|^2}$. The minimum value of $|1 + \alpha\lambda|$ is achieved for $\alpha = \dfrac{-\mathrm{re}(\lambda)}{|\lambda|^2}$ and is equal to $\dfrac{|\mathrm{im}(\lambda)|}{|\lambda|}$.*

Proof.

1. At any point u, we get $F'(u) = I + Kf'(u)$. The conclusion follows from Appendix B.
2. When λ is real, it is a straightforward calculation (see the example thereafter) and the minimum is indeed 0 for $\alpha = -1/\lambda$. Let $\lambda = a + ib$, then $1 + \alpha\lambda = (1 + \alpha a) + ib$, and so

$$|1 + \alpha\lambda|^2 = 1 + 2a\alpha + \alpha^2(a^2 + b^2). \tag{3.6}$$

Hence, $0 \leq |1+\alpha\lambda|^2 < 1$ if and only if $\alpha\left(\alpha(a^2+b^2)^2+2a\right) < 0$, that is, α must be of the sign of $-a = -\mathrm{re}(\lambda)$ and $|\alpha| < \dfrac{2\mathrm{re}(\lambda)}{|\lambda|^2}$. The minimum in α of the quadratic polynomial (3.6) is achieved for $\alpha = \dfrac{-\mathrm{re}(\lambda)}{|\lambda|^2}$, of value $\dfrac{(\mathrm{im}(\lambda))^2}{|\lambda|^2}$, hence the conclusion.

□

Let $\sum_{n=0}^{\infty} u_n$ be an uniformly convergent series in U and define $u(\lambda) = \sum_{n=0}^{\infty} u_n \lambda^n$.

Proposition 3.3 *1. The Adomian polynomials for F in (3.5) near u_0 are given by*

$$A_n[F,u_0](u) = \begin{cases} KA_n[f,u_0], & n \neq 1; \\ (I + Kf'(u_0))\, u_1, & n = 1. \end{cases} \tag{3.7}$$

2. Let $f : U \subset X \to Y$ be an analytic map on U and $\bar{u} \in U$ be an isolated root of $f(u) = 0$. Suppose there exists $K : Y \to X$ as in lemma 3.1 so that F as in equation (3.4) is a contraction on some neighbourhood $V \subset U$. Then, if $u_0 \in V$ the following decomposition scheme converges to the solution $\bar{u}$:

$$u_{n+1} = A_n[F,u_0](u), \quad n \geq 0, \tag{3.8}$$

where $A_n(F,u_0)$ is given in (3.7).

Proof.

1. Because K is a linear operator, this is essentially an immediate calculation using the definition of the Adomian polynomials.
2. From theorem 2.2, the Adomian polynomials $\{A_n[F,.]\}_{n=0}^{\infty}$ of F define a strongly convergent decomposition series of degenerated sum F. From theorem 2.1, if the degenerated sum F is a contraction, every decomposition series verifies the fixed point equation (3.4) and so converges to it.

□

3.1.1 Example

As an example, suppose $F'(\bar{u})$ has four eigenvalues, $\lambda_+ > 0$, $\lambda_- < 0$ and $\lambda_*, \overline{\lambda_*} \in \mathbb{C} \setminus \mathbb{R}$, with respective eigenvectors v_+, v_- and $v_*, \overline{v_*}$. That is to say

$$F'(\bar{u})v_* = \lambda_* v_*, \quad v_* = \mathrm{re}(v) + i\,\mathrm{im}(v), \quad \lambda_* = \mathrm{re}(\lambda) + i\,\mathrm{im}(\lambda).$$

Equating real and imaginary parts give

$$F'(\bar{u})\mathrm{re}(v) = \mathrm{re}(\lambda)\mathrm{re}(v) - \mathrm{im}(\lambda)\mathrm{im}(v),$$

$$F'(\bar{u})\mathrm{im}(v) = \mathrm{re}(\lambda)\mathrm{im}(v) + \mathrm{im}(\lambda)\mathrm{re}(v).$$

To simplify we assume that $X = \mathbb{R}^4$, so $\{v_+, v_-, \mathrm{re}(v_*), \mathrm{im}(v_*)\}$ forms a basis of $\mathbb{R}^4$. Using that basis, $F'(\bar{u})$ is represented by the matrix

$$\begin{pmatrix} \lambda_+ & 0 & 0 & 0 \\ 0 & \lambda_- & 0 & 0 \\ 0 & 0 & \mathrm{re}(\lambda_*) & \mathrm{im}(\lambda_*) \\ 0 & 0 & -\mathrm{im}(\lambda_*) & \mathrm{re}(\lambda_*) \end{pmatrix}.$$

We can define $K : \mathbb{R}^4 \to \mathbb{R}^4$ as

$$Kv_+ = \alpha_+ v_+, \quad Kv_- = \alpha_- v_-, \quad K\left(\mathrm{re}(v_*)\right) = \alpha_1 \mathrm{re}(v_*) \quad \text{and} \quad K\left(\mathrm{im}(v_*)\right) = \alpha_2 \mathrm{im}(v_*).$$

Then we can choose the α's such that each eigenvalue $1 + \alpha\lambda$ is inside the unit disk. From the previous results, the optimal values are

$$\alpha_+ = -1/\lambda_+ < 0, \quad \alpha_- = -1/\lambda_- > 0, \quad \alpha_1 = -\mathrm{re}(\lambda_*)/|\lambda_*|^2 \quad \text{and} \quad \alpha_2 = -\mathrm{re}(\lambda_*)/|\lambda_*|^2.$$

With that last choice, the spectral radius of $I + KF'(\bar{u})$ is equal to $|\mathrm{im}(\lambda_*)|/|\lambda_*|$. With this choice of K there is no contraction when $|\mathrm{im}(\lambda_*)| = |\lambda_*|$.

3.2 One dimensional example

We examine more carefully an explicit example in this section. Let $f : \mathbb{R} \to \mathbb{R}$ be given by

$$f(u) = e^u - u - a, \quad a > 1.$$

The function f has two roots. At the positive root, the hypotheses of the CMT are not satisfied, but they are satisfied at the negative root.

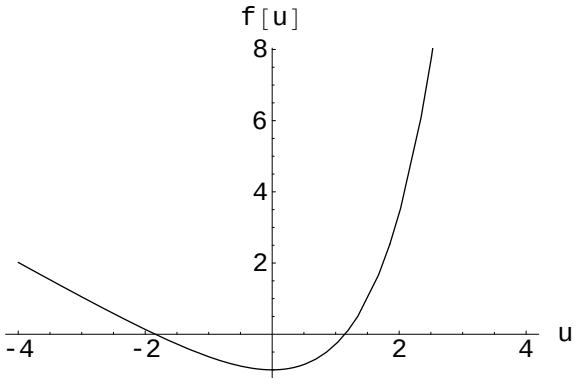

Figure 3.1: Graph of $f(u) = 0$ when $a = 2$.

Applying the previous ideas we get the following. Define

$$F(u) = u - u_0 + \alpha(e^u - u - a), \tag{3.9}$$

where α is a non-zero real number that can be determined ($Ku = \alpha u$, here). To find the positive root of f, we can use the following result.

Proposition 3.4 *1. F is a contraction on $[\epsilon, u^*]$ for any $0 < \epsilon < u^*$ such that $\frac{-2}{e^{u^*} - 1} < \alpha < 0$.*

2. Let $0 < \epsilon < \bar{u} < u^*$ where $\bar{u}$ is the positive root of f, then the ADM applied to (3.4) converges to $\bar{u}$ for any $u_0 \in [\epsilon, u^*]$.

Proof.

1. We need $-1 < k_- \leq F'(u) \leq k_+ < 1$, that is, to make sure that the extrema of the following expression satisfy
$$-1 < 1 + \alpha(e^u - 1) < 1.$$

2. Choosing ϵ and u^* such that the positive fixed point is inside the interval $[\epsilon, u^*]$ where F is a contraction means that the ADM will converge to that fixed point by using part 2 of proposition 3.3.

□

Another view of the problem as a fixed point iteration.

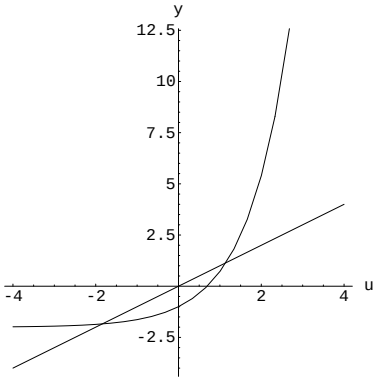

Figure 3.2: Graph of $u = e^u - 2$.

3.2.1 The two roots of f

With $a = 2$ and $\alpha = 1$ in (3.9), (3.1) may be written as

$$u = e^u - 2. \tag{3.10}$$

The two roots of this equation as given by Maple 15 are presented in Table 3.1 below.

Negative root	Positive root
-1.841405660437	1.146193220621

Table 3.1: The two roots of (3.10).

Maple has been programmed to solve (3.10) by calculating and summing the first seven terms of the ADM series solution. The Adomian polynomials are calculated using formulae in Appendix A. The program is included on the enclosed disc. To use the program the user will need to specify the starting value for the ADM, the u_0 along with the value of α. The program indicates whether a contraction holds for the specified value of α and also plots the location of the ADM solution in relation to (3.10).

3.2.2 Convergence to the negative root

When applied in the usual straightforward manner, the ADM strongly converges to the negative root but does not converge to the positive root. Figure 3.3 shows the manner in which the ADM approaches the negative root for varying values of u_0.

The graph shows that the ADM strongly converges to the negative root under the hypothesis that the CMT holds at the negative root but does not hold at the positive root. As a result the ADM rapidly diverges away from the positive root. Table F.1 contains the specific values.

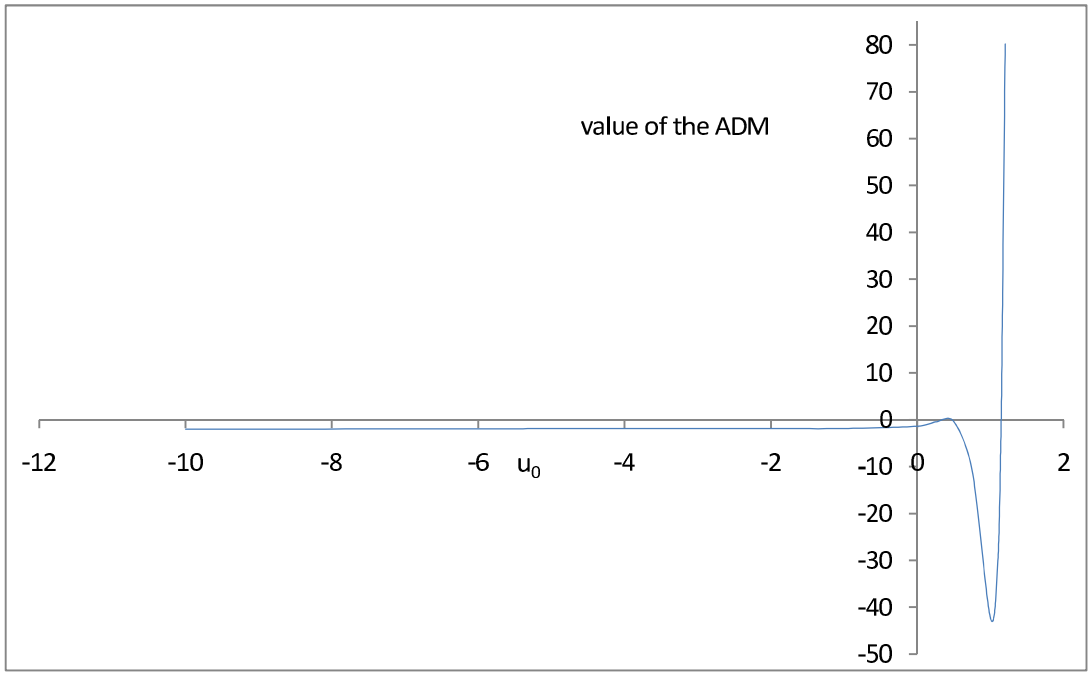

Figure 3.3: Sum of the first 7 terms of the ADM series for varying values of u_0 when $\alpha = 1$.

3.2.3 Convergence to the positive root

By changing the value of α in line with Proposition 3.4, a contraction can be created at the positive root thus enabling the ADM to converge to the other solution of (3.10).

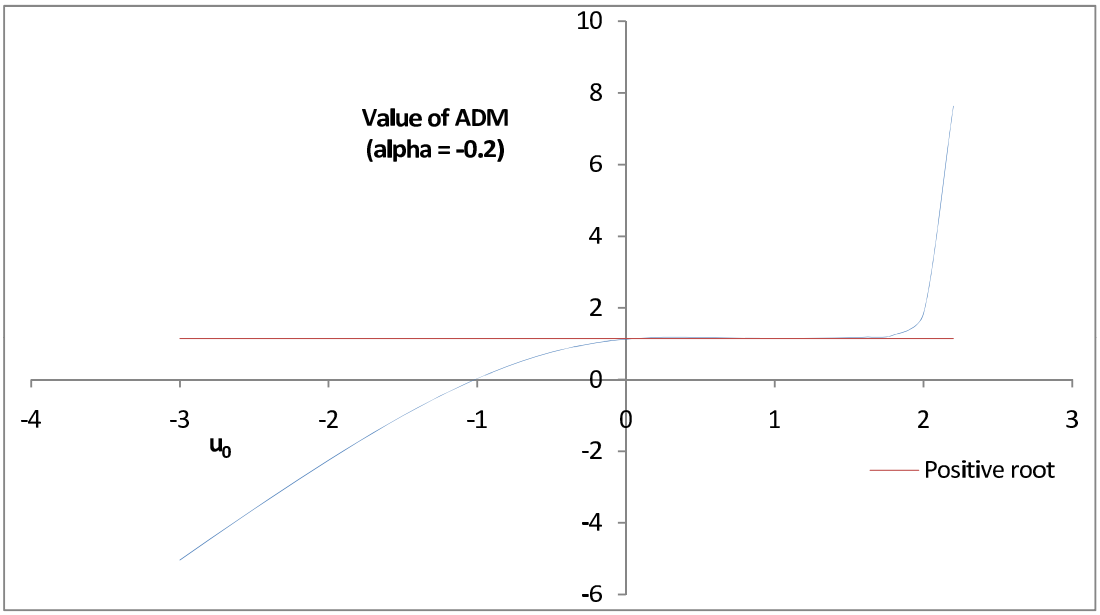

Figure 3.4: Sum of the first 7 terms of the ADM series for varying values of u_0 when $\alpha = -0.2$.

The graphs in Figures F.1, 3.4, F.2 and F.3 show the manner in which the ADM converges to

the positive root of (3.10) for selected values of α that satisfy proposition 3.4. Table F.1 shows the values given by seven terms of the ADM series solution for the different values of α. Figure 3.5 shows a comparison of the manner in which the ADM converges to the positive root for the selected values of α.

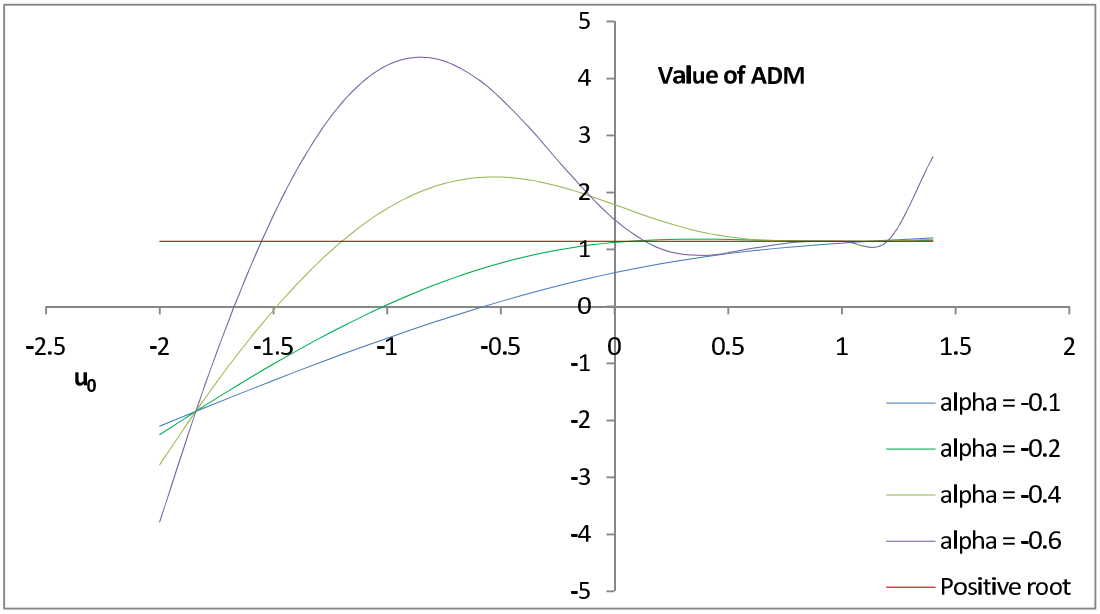

Figure 3.5: Sum of the first 7 terms of the ADM series for varying u_0 when α is varied.

See Section 3.2.5 for a discussion on the choice of α.

3.2.4 Restarted ADM for multiple solutions of a nonlinear problem

Introduced in [22], the **restarted ADM (RADM)** is an algorithm for accelerating the speed of convergence of the ADM. The method takes the result of applying the ADM with a few terms as the starting value in the next application of the ADM. It is detailed in the following algorithm.

RADM algorithm ([22])

Choose small positive number ϵ and small natural number m.
For $i = 0, 1, 2, \ldots$, do
(step 1)
$u_0 = c_i$
$u_1 = A_0$, $u_2 = A_1$, $\ldots$, $u_m = A_{m-1}$
(step 2)
$u^{(i)} = c_{i+1} = u_0 + u_1 + \cdots + u_m$,
if $|c_{i+1} - c_i| < \epsilon$ stop,
(step 3)
$F_{new} = F_0 - (c_{i+1} - c_0)$,
end(for).

The approach to implementing the RADM for this example was as follows. Starting at the negative u axis a value was chosen as the starting u_0 for implementing the RADM. If the result of implementing the ADM with this u_0 was closer to the positive root then that result was utilised as the next starting value for the subsequent implementation of the ADM and so on. If the result of implementing the ADM with the first u_0 diverged from the positive root then this result was noted but instead a value incrementally closer to the positive root was selected as the starting value for the initial implementation of the RADM.

Table F.2 shows the values given by the sum of the first seven terms for the RADM when $\alpha = -0.1$. For each u_0 in the table the value given by the ADM can be seen in the column to the right. The value in the column to the right can also then be located in the left column (or a value close to it) to determine the corresponding value of the ADM (again in the right column) when that particular value is used as the starting value in the ADM. For example, in the 17th row of Table F.2 the value of 0.981376983 was used as the starting value for the RADM. This resulted in an approximation to the positive root of 1.104734561. When the value of 1.104734561 was in turn used as the starting value of the ADM (row 18) this resulted in an approximation to the positive root of 1.136314962. Not all values are shown. When it is clear that the RADM would converge to the positive root it was not necessary to present all the resulting values as new starting values in the ADM. For example, if a starting value of -0.5 led to a succession of values that converged to the positive root it was not necessary to tabulate all the successive values from a starting value of -0.6 to the positive root once the result of using -0.6 as the starting value had increased above -0.5.

Similar results are presented for $\alpha = -0.2$, -0.4, and -0.6 in Tables F.3 to F.5. Looking down through the values in the table it is clear that the RADM accelerates the speed of convergence to the positive root since the result of the first implementation of the method - the first approximation to the positive root - becomes the subsequent starting point of the next approximation to the root using the ADM. Successive approximations are closer than the previous approximations provided the initial starting value of the ADM is suitably close to the desired root. Evidently the RADM will generate a succession of values that go to the positive root provided the first choice of u_0 was close enough to the positive root. Otherwise the effect of the RADM would be to accelerate the divergence of the method away from the desired root. This can be seen for example with a starting value of -3 or 3 in Table F.3.

While the RADM accelerates the speed of convergence of the ADM, it does not affect the strength of the convergence. Charts F.1 to F.3 show the same strength of convergence for a straight application of the ADM as for that of the RADM indicated in Charts F.4 to F.7. Proposition 3.4 and use of the RADM are both effective tools for enabling the ADM to access multiple solutions of nonlinear problems. An intended advantage of the RADM is computational ease. The more terms of the Adomian series that are calculated, the more accurate the Adomian solution becomes. However, calculating successive terms of the Adomian series becomes computationally more demanding because the formulae for successive Adomian polynomials (Appendix A) become more complex. The RADM can be applied with a smaller number of Adomian polynomials; 2, 3 or 4 with the value of these polynomials being recalculated for each successive starting value of the method. For comparison, Tables F.6 to F.9 show the sum of the first 3 terms of the solution given by the RADM. Compared to an approximation using 7 terms of the ADM in Table F.1, the RADM to 3 terms is not as accurate in successive approximations.

When mathematical software is used to calculate the Adomian polynomials, the computational demand of adding 7 terms as compared to adding 3 terms becomes less of a concern.

3.2.5 The choice of alpha

Observations

As can be seen in Figure 3.5, the choice of the value of α will influence the strength of the contraction and consequently the strength and manner of the convergence to multiple solutions of a nonlinear problem. When $\alpha = -0.1$, the method steadily and gradually but weakly converges to the positive root. For $\alpha = -0.2$, the convergence **appears** to be much stronger. For values of $\alpha = -0.4$ and $\alpha = -0.6$, the convergence does not **appear** to be as precise as $\alpha = -0.2$. In general, with limited terms of the Adomian series solution, in this case 7 terms, the u_0 would need to be suitably close to the positive root in order for the 7 terms of the ADM to return a good approximation. For values of $\alpha = -0.1$, $\alpha = -0.4$ and $\alpha = -0.6$, it **appears** the u_0 would need to be closer to the positive root than for $\alpha = -0.2$ in order for a good approximation to be returned. The same observations hold for the RADM. Again the strength of the contraction as influenced by the value of α will influence the strength of convergence to the positive root.

The manner in which the first seven terms of the RADM solution approaches the positive root is depicted in Charts F.4 to F.7. For each α the behaviour is broadly similar to that depicted in Charts F.1 to F.3. The strongest convergence **appears** to be for $\alpha = -0.2$.

A closer look at the α values

The parameter α can be selected in such a manner as to optimise the convergence. The absolute value of the derivative is a measure of the contraction's strength and the effect of α on the absolute value of the derivative can be examined at the positive root. It is desirable for the absolute value of the derivative to be close to 0. In this example

$$F(u) = u - u_0 + \alpha(e^u - u - 2), \tag{3.11}$$

$$F'(\bar{u}) = 1 + \alpha(e^{\bar{u}} - 1), \tag{3.12}$$

so $F'(\bar{u}) = 0$ when $\alpha \simeq -0.47$. This means that very close to the zero, the convergence for $\alpha = -0.4$ or $\alpha = -0.6$ should be better than for $\alpha = -0.2$. Comparison of the same value of u_0 close to the positive root for different values of α in Table F.1 indicates this to be the case. However, the **appearance** of better convergence when α is small in Figure 3.5 is due to there being better convergence for the ADM for **a larger range of values of** u_0. The contraction constant for F is equal to $F'(u_0)$ when $-0.47 < \alpha < 0$, so it is higher when α takes on smaller negative values for the same starting value u_0. This would mean that for values such as -0.6 and -0.4 there is a stronger contraction over the range of u_0 and the expectation is that the convergence should be better for such values. Further investigation into why this is not the case would be required. Note that with $\alpha = -0.6$ although a direct application of the ADM with seven terms of the ADM solution does not result in good estimates in the middle range, the estimates further away, when u_0 is negative are more reasonable. More terms of the ADM

solution would be needed to test if there is convergence there. The difference in behaviour due to different values of α is also relevant because in practical application it is often required to take limited terms of the series solution.

The range of convergence for the RADM and other interesting phenomenon

For all the approaches above the ADM will converge to the positive root provided the starting u_0 is close enough to the positive root. This suggests that for a limited number of terms of the solution series there is an effective range of values for u_0 for which the ADM will converge. This range of values will also depend on the value of α. These values of u_0 for which the method effectively converges to the positive root can be obtained from the tables and charts in Appendix F but are extracted here for convenience.

Table 3.2: Effective range of u_0 for convergence of the ADM using 7 terms to the positive root of (3.10).

α	Minimum	Maximum	Range
-0.1	1	1.2	0.2
-0.2	0	1.6	1.6
-0.4	0.6	1.4	0.8
-0.6	0.8	1.2	0.4

Table 3.3: Effective range of u_0 for convergence of the RADM using 7 terms of the ADM solution to the positive root of (3.10).

α	Minimum	Maximum	Range
-0.1	-1.8	2.5	4.3
-0.2	-1.8	2	3.8
-0.4	0.2	1.5	1.3
-0.6	0.1	1.3	1.2

Table 3.4: Effective range of u_0 for convergence of the RADM (3 terms) to the positive root of (3.10).

α	Minimum	Maximum	Range
-0.1	-1.8	3	4.8
-0.2	-1.8	2.3	4.1
-0.4	-1.8	1.7	3.1
-0.6	-1.8	1.4	3.2

It is noticeable in Table 3.2 that the range obtained experimentally when $\alpha = -0.1$ is narrow. The reason for this would require further investigation. Given that limited terms of the ADM solution are utilised the difference in the range of values in Table 3.2 to Table 3.3 might be due to the different manner in which the methods are implemented. In Table 3.2, for a given u_0, the result of applying the ADM gives the final outcome but the range in Table 3.3 occurs through a reapplication of the method each time bringing the result closer to the solution. So a value

further away from the positive root used as a u_0 in the restarted method would be brought closer to the positive root provided the starting u_0 is close enough for this to occur. As to why the range of values is broader when the restarted method is utilised with three terms than it is when it is applied with seven terms would require a further investigation of the behaviour of the convergence for a range of values of u_0. Local behaviour, near the fixed point is well studied, but the behaviour further away from the fixed point is not as well understood. An intuitive observation has been that if the starting u_0 is close to the edge of the 'radius' for which the restarted method would diverge then taking seven terms of the Adomian solution places the next value outside of this radius but taking three terms results in a smaller next value closer to the positive root and so on. It would be necessary to take more terms of the ADM solution in order to more carefully investigate these differing behaviours. It is of interest to note also that when $\alpha = 1$, for decreasingly smaller values of u_0, the first seven terms of the ADM solution returns a limiting value of -2 (Table F.1) as the exponential terms appearing in the Adomian polynomials are raised to increasingly higher negative powers.

3.2.6 Summary

The key objective in this chapter has been to implement the ADM in such a way as to enable it to find multiple solutions of nonlinear problems. The theory presented herein sets up the basis for making such an application which has been demonstrated with the one dimensional example. When the CMT holds, the ADM will converge to a particular solution. By influencing where the contraction holds, the particular solution to which the ADM converges can be determined. Further, by utilising a technique such as the RADM, the speed of convergence to any of the particular solutions can be greatly accelerated. In demonstrating the one dimensional example interesting behaviour warranting further investigation has been observed.

Chapter 4

Bifurcation problems

In this chapter we adapt the previous result of Chapter 3 to **bifurcation problems**

$$f(u, \gamma) = 0, \tag{4.1}$$

where $f : X \times \mathbb{R} \to Y$, using path following methods as described in Appendix D. The Adomian polynomial of the derivative is given by the following formula. Recall that the derivative is a linear operator.

Lemma 4.1 *Let $F : \mathcal{U} \subset X \to Y$ be analytic around $u_0 \in \mathcal{U}$, then*

$$A_n[F', u_0](u)v = \frac{d}{du_0} \left(A_n[F, u_0](u) \right) v.$$

Proof. This follows from the definitions. □

Explicitly, we get

$$\begin{aligned}
A_0[F', u_0](u)v &= F'(u_0)v, \\
A_1[F', u_0](u)v &= F''(u_0)u_1 v, \\
A_2[F', u_0](u)v &= \frac{1}{2}F'''(u_0)u_1^2 v + F''(u_0)u_2 v, \\
A_3[F', u_0](u)v &= \frac{1}{6}F^{(4)}(u_0)u_1^3 v + F'''(u_0)u_2 u_1 + F''(u_0)u_3 v.
\end{aligned}$$

4.1 Path following with the Euler predictor

In this section we implement the path following using the Euler predictor (see Section D.2.1 for more background details). An algorithm along a simple branch, is as follows. The branch is constituted of a sequence of points $(u^{(k)}, \gamma^{(k)})$ for $0 \leq k \leq n$. The increment in γ along the branch is given by $\Delta\gamma$.

1. For $k = 0$, initialise the branch. Determine $(u^{(0)}, \gamma^{(0)})$ from solving $f(u, \gamma^{(0)}) = 0$.

2. For $1 \leq k \leq n$,

   (a) create the prediction at the next step. Set $\gamma^{(k)} = \gamma^{(k-1)} + \Delta\gamma$. The predicted value of u can be determined from

$$\hat{u}^{(k)} = u^{(k-1)} + \Delta\gamma \cdot \Delta u^{(k-1)}, \tag{4.2}$$

   where the increment $\Delta u^{(k-1)}$ is given by the solution of the following equation

$$f_u(u^{(k-1)}, \gamma^{(k-1)})\Delta u^{(k-1)} + f_\gamma(u^{(k-1)}, \gamma^{(k-1)}) = 0. \tag{4.3}$$

   If the solution of (4.3) is not readily available, we can use the ADM.

   Proposition 4.2 *The solution of (4.3) is given by*

$$\Delta u^{(k-1)} = \sum_{j=0}^{\infty} v_j \tag{4.4}$$

   where the v_j's are the solutions of the linear equations and $u_0 = \hat{u}^{(k-1)}$.

$$\begin{aligned}
f_u(u_0, \gamma^{(k-1)})v_0 + f_\gamma(u_0, \gamma^{(k-1)}) &= 0, && (4.5)\\
f_u(u_0, \gamma^{(k-1)})v_1 + A_1[f_u, (u_0, \gamma^{(k-1)})](u^{(k-1)})v_0 & \\
+A_1[f_\gamma, (u_0, \gamma^{(k-1)})](u^{(k-1)}) &= 0, && (4.6)\\
&\vdots & &\\
f_u(u_0, \gamma^{(k-1)})v_n + \sum_{j=0}^{n-1} A_{n-j}[f_u(u_0, \gamma^{(k-1)})](u^{(k-1)})v_j & \\
+A_n[f_\gamma, (u_0, \gamma^{(k-1)})](u^{(k-1)}) &= 0, && (4.7)
\end{aligned}$$

   Proof. The idea is to expand $f_u(u^{(k-1)}\gamma^{(k-1)})\Delta u^{(k-1)}$ and $f_\gamma(u^{(k-1)}, \gamma^{(k-1)})$ using their Adomian series decomposition and collect the terms of the same degree. In terms of the Adomian decomposition

$$\begin{aligned}
f_u\left(u^{(k-1)}, \gamma^{(k-1)}\right) &= \sum_{m=0}^{\infty} A_m\left[f_u, (u_0, \gamma^{(k-1)})\right]\left(u^{(k-1)}\right)\lambda^m\\
f_\gamma\left(u^{(k-1)}, \gamma^{(k-1)}\right) &= \sum_{n=0}^{\infty} A_n\left[f_\gamma, (u_0, \gamma^{(k-1)})\right]\left(u^{(k-1)}\right)\lambda^n.
\end{aligned}$$

   The using (4.3) and (4.4) we get

$$\begin{aligned}
\sum_{m,j=0}^{\infty} A_m\left[f_u, (u_0, \gamma^{(k-1)})\right]\left(u^{(k-1)}\right)v_j\lambda^{m+j} & \\
+\sum_{n=0}^{\infty} A_n\left[f_\gamma, \left(u_0, \gamma^{(k-1)}\right)\right]\left(u^{(k-1)}\right)\lambda^n &= 0.
\end{aligned}$$

Collecting the terms of degree n gives

$$\sum_{m+j=n}^{\infty} A_m \left[f_u, (u_0, \gamma^{(k-1)}) \right] \left(u^{(k-1)} \right) v_j + A_n \left[f_\gamma, \left(u_0, \gamma^{(k-1)} \right) \right] \left(u^{(k-1)} \right) = 0.$$

Taking the terms $j = n$ out the sum and rewriting the equation, we find (4.7).

□

(b) Create the next point. Use the prediction $\hat{u}^{(k)}$ in (4.2) as the initial condition to solve $f(u, \gamma^{(k)}) = 0$ using the ADM. We follow Lemma 3.1 with

$$F(u) = u - u_0 + Kf(u, \gamma^{(k)}), \tag{4.8}$$

for a well chosen invertible operator K. The prediction $\hat{u}^{(k)}$ is the u_0 in (3.4). Then the ADM applied to (3.4) creates a series form for $u^{(k)} = \hat{u}^{(k)} + u_1 + \ldots$.

4.1.1 Example

The bifurcation problem

$$f(u, \gamma) = \gamma u^2 - u + 2 = 0 \tag{4.9}$$

has two branches

$$u_\pm(\gamma) = \frac{1 \pm \sqrt{1 - 8\gamma}}{2\gamma}, \tag{4.10}$$

for $\gamma \in (-\infty, 1/8]$, joining in a turning point at $(\bar{u}, \bar{\gamma}) = (4, 1/8)$. The branch $u_- : (-\infty, 1/8]$ is monotonically increasing from 0 to 4, infinitely differentiable through $\gamma = 0$, with $u_-(0) = 2$. The branch u_+ has two pieces, each monotonically decreasing, the first one from $(-\infty, 0)$ with range $(-\infty, 0)$, the second one from $(0, 1/8]$ with range $[4, \infty)$. The turning point is represented in the following Figure 4.1.

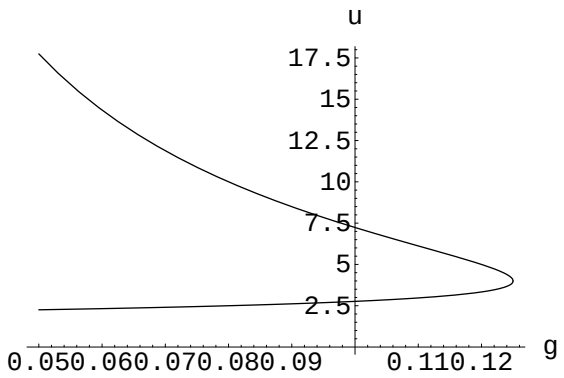

Figure 4.1: Graph of $f(u, \gamma) = 0$ for $\gamma \in [0.05, 1/8]$.

Applying the general algorithm of Section 4.1, we get the following. From (4.9), we have

$$f_u(u,\gamma) = 2\gamma u - 1, \tag{4.11}$$
$$f_\gamma(u,\gamma) = u^2. \tag{4.12}$$

1. For $k = 0$, initialise the branch. To simplify the determination of the branch, we see from (4.9) that $f = 0$ has an easy solution for $\gamma^{(0)} = 0$, namely $u^{(0)} = 2$.

2. For $1 \leq k \leq n$,

   (a) create the prediction at the next step. We choose $\Delta\gamma < 0$ to go into the negative γ-axis, for instance -1 or -0.1 (it seems that -1 is too big, -0.1 or -0.2 are to be preferred). To follow up the positive axis, which can only be done until $1/8 = 0.125$, we choose a small $\Delta\gamma > 0$, say 0.02 for 6 points up to the maximum positive value of γ. Set $\gamma^{(k)} = \gamma^{(k-1)} + \Delta\gamma$. The predicted value of u is determined from

   $$\hat{u}^{(k)} = u^{(k-1)} + \Delta\gamma \cdot \Delta u^{(k-1)}, \tag{4.13}$$

   where the increment $\Delta u^{(k-1)}$ is given by the solution of (4.14), that is,

   $$\left(2\gamma^{(k-1)}u^{(k-1)} - 1\right)\Delta u^{(k-1)} + (u^{(k-1)})^2 = 0. \tag{4.14}$$

   (b) Create the next point. Use the prediction $u_0 = \hat{u}^{(k)}$ in (4.13) as the initial condition u_0 to solve $f(u, \gamma^{(k)}) = 0$ using the ADM. We follow Lemma 3.1 with

   $$F(u) = u - u_0 + \alpha f(u, \gamma^{(k)}),$$

   for a well chosen non zero value α so that F is a local contraction around its fixed point. The prediction is the u_0 in (3.4). Then the ADM applied to (3.4) creates a series form for $u^{(k)} = \hat{u}^{(k)} + u_1 + \ldots$.

To path follow the two pieces of the branch u_+, we need another starting point on each piece on that branch and repeat the same algorithm. To get the turning point we need to move to the slightly more complicated augmented system for turning point.

4.2 Extended systems for bifurcation problems

From Appendix D.3, an extended system (D.3) near the turning point $(\bar{u}, \bar{\gamma})$ can be defined as

$$G(u,\gamma,\beta) = \begin{pmatrix} f(u,\gamma) \\ < \psi, (u - \bar{u}, \gamma - \bar{\gamma}) > -\beta \end{pmatrix} = 0, \tag{4.15}$$

where $\psi \in \ker(f_{(u,\gamma)}(\bar{u}, \bar{\gamma}))$. Then, path following in β, the solutions (u, γ) of $G(u, \gamma, \beta) = 0$ determine the points along the branch near the turning point.

4.2.1 Example

We say that (x_0, γ_0) is a **regular point** if the total derivative $DF(x_0, \gamma_0)$ of F at (x_0, γ_0) is of maximal rank (cf. Section D.1).

Lemma 4.3 *In one dimension, $\psi = (1, 0)$ at a regular turning point.*

Proof. The kernel of the linearisation is generated by $\psi = (1, 0)$ because $\psi = (\psi_1, \psi_2)$ satisfies

$$f_u(\bar{u}, \bar{\gamma})\psi_1 + f_\gamma(\bar{u}, \bar{\gamma})\psi_2 = 0. \tag{4.16}$$

At a regular turning point $(\bar{u}, \bar{\gamma})$, $f_u(\bar{u}, \bar{\gamma}) = 0$ and $f_\gamma(\bar{u}, \bar{\gamma}) \neq 0$. And so $\psi = (1, 0)$ is the generator of the solutions of (4.16). □

On the previous example, near the turning point $(\bar{u}, \bar{\gamma}) = (4, 1/8)$, the extended system is

$$G(u, \gamma, \beta) = \begin{pmatrix} f(u, \gamma) \\ u - \bar{u} - \beta \end{pmatrix} = 0. \tag{4.17}$$

Now, we often do not know values for the turning points. So, when we suspect a turning point, we could switch the path following to the extended system (4.17). We detail the algorithm in the following. Recall that we would like to determine the path $(u^{(k)}, \gamma^{(k)}, \beta^{(k)})$, $0 \leq k \leq n$, of solutions of (4.17). Note that we are really only interested in the first two components $(u^{(k)}, \gamma^{(k)})$.

1. For $k = 0$, initialise the branch. This time we suppose that we have reached a point $(u^{(N)}, \gamma^{(N)})$ using the path following for regular points. We initialise the path with $u^{(0)} = u^{(N)}$, $\gamma^{(0)} = \gamma^{(N)}$ and so $\beta^{(0)} = 0$. If we do not know the value of the turning point, the extended system we shall follow is

$$G(u, \gamma, \beta) = \begin{pmatrix} f(u, \gamma) \\ u - u^{(N)} - \beta \end{pmatrix} = 0. \tag{4.18}$$

2. For $1 \leq k \leq n$,

   (a) create the prediction at the next step. Depending where the turning point is, we choose a value for the increment in β. Here, when we come along the lower branch towards the turning point, we choose for $\Delta\beta$ a small enough positive value. Set $\beta^{(k)} = \beta^{(k-1)} + \Delta\beta$. The predicted values for u and γ come from

$$\hat{u}^{(k)} = u^{(k-1)} + \Delta\beta, \tag{4.19}$$
$$\hat{\gamma}^{(k)} = \gamma^{(k-1)} + \Delta\beta \cdot \Delta\gamma^{(k-1)}, \tag{4.20}$$

   determined from

$$f_u(u^{(k-1)}, \gamma^{(k-1)}, \beta^{(k-1)}) + f_\gamma(u^{(k-1)}, \gamma^{(k-1)}, \beta^{(k-1)})\Delta\gamma^{(k-1)} = 0. \tag{4.21}$$

   Here,

$$\left(2\gamma^{(k-1)}u^{(k-1)} - 1\right) + \Delta\gamma^{(k-1)} \cdot (u^{(k-1)})^2 = 0. \tag{4.22}$$

   It looks like we follow along the u-axis as the parameter axis and γ as the variable.

(b) Create the next point. We need to solve the equation

$$G(u, \gamma, \beta^{(k)}) = 0,$$

using the ADM with initial values $(\hat{u}^{(k)}, \hat{\gamma}^{(k)})$. As before we create the equations

$$u = \hat{u}^{(k)} + H_1(u, \gamma), \tag{4.23}$$
$$\gamma = \hat{\gamma}^{(k)} + H_2(u, \gamma), \tag{4.24}$$

where

$$H_1(u, \gamma) = u - \hat{u}^{(k)} + \alpha_1 f(u, \gamma), \tag{4.25}$$
$$H_2(u, \gamma) = \gamma - \hat{\gamma}^{(k)} + \alpha_2(u - u^{(0)} - \beta^{(k)}). \tag{4.26}$$

The parameters α_1 and α_2 can be adapted so that H is a contraction. Note that (4.24) is a linear equation. We now use the prediction $(\hat{u}^{(k)}, \hat{\gamma}^{(k)})$ in (4.22) as the initial condition to solve the system (4.23,4.24) using the ADM. This will give us the set of values $(\hat{u}^{(k)}, \hat{\gamma}^{(k)}, \beta^{(k)})$.

Here, everything gets simpler because of the shape (4.9) of f. Let us examine the corrector step. Equation (4.26) is linear and so the ADM is equivalent to solving it directly, hence

$$u^{(k)} = u^{(0)} + \beta^{(k)}. \tag{4.27}$$

Then, we can replace $u = u^{(k)}$ in (4.25). Then we can find directly the next value of γ,

$$\gamma^{(k)} = \frac{u^{(k)} - 2}{(u^{(k)})^2}. \tag{4.28}$$

This indicates that for this example the best way is to really use u as the parameter. To summarise, when we have reached $(u^{(N)}, \gamma^{(N)})$ using the path following for regular points, and want to switch to the extended system for turning points, we choose some Δu for the step size, in u because it plays the role of the parameter. Then, for $1 \leq k \leq n$, the next points are

$$u^{(k)} = u^{(k-1)} + \Delta u, \tag{4.29}$$
$$\gamma^{(k)} = \frac{u^{(k)} - 2}{(u^{(k)})^2}. \tag{4.30}$$

Then, we switch back to the regular system when we have passed across the turning point. The decision to switch into the extended system is when $f_u(u^{(k)}, \gamma^{(k)})$ becomes small, and the decision to switch back is when $f_u(u^{(k)}, \gamma^{(k)})$ increases again. With (4.8,4.9), (3.4) can be written as

$$f(u, \gamma) = u_0 + (u - u_0 + \alpha(\gamma u^2 - u + 2)) = 0. \tag{4.31}$$

Maple software version 15 has been programmed to solve (4.31) by calculating and summing the first seven terms of the Adomian solution using the formulae in Appendix A. The program is included on the enclosed disc. To use the program the user will need to specify the starting value for the ADM, the u_0 along with the values of α and γ. The program indicates whether a contraction holds for the specified value of α and also returns the solution to (4.9) by calculating (4.10). The latter is useful for making a comparison to the ADM solution. The following details the outcome of path following (4.31) with the ADM.

4.2.2 Path following along the lower branch in the direction of γ_-

Figure 4.2 shows a very close approximation to $u_{\pm}(\gamma)$ given by the ADM. In the plot the exact solution values cannot be distinguished from the values given by the ADM approximation.

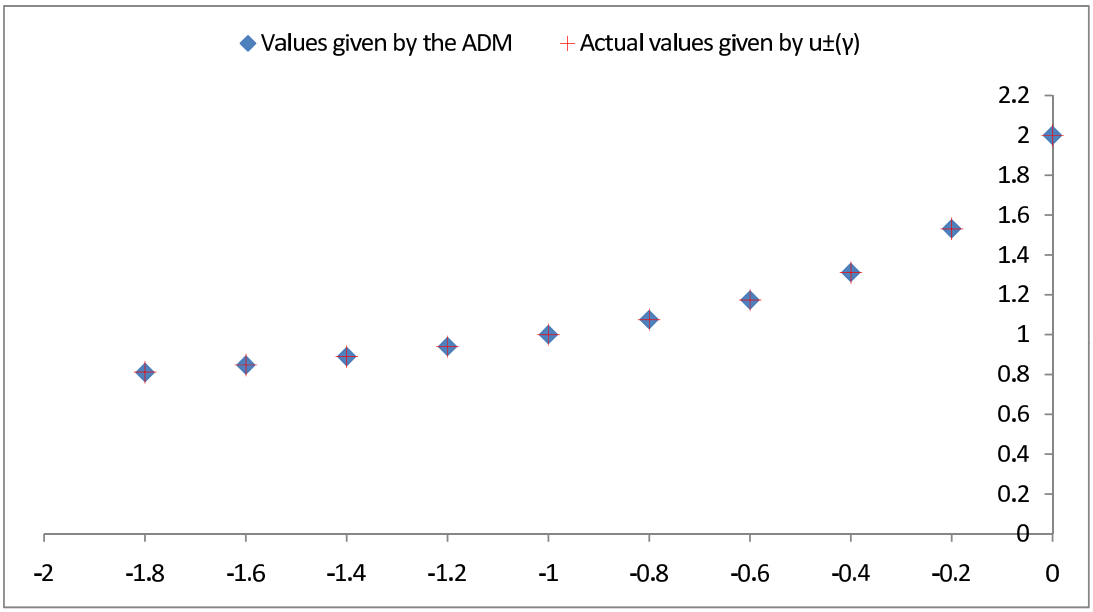

Figure 4.2: Path following along the lower branch in the negative direction $\Delta\gamma = -0.2$.

Figure 4.3 illustrates the outcome when $\Delta\gamma = -1$ is used. Care must be taken to choose a suitable step size in order to minimise errors. Here, with a negative predictor step, the ADM converged to the bottom branch of (4.31) where the contraction was strongest. With a successive predictor being closer to the upper branch the ADM then converged to the upper branch.

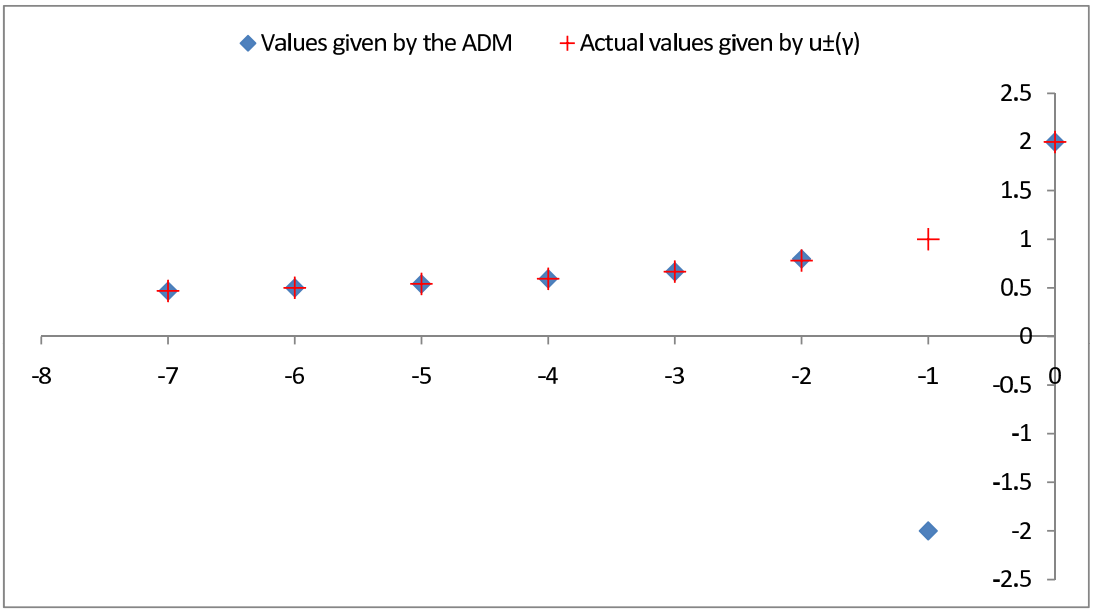

Figure 4.3: Path following along the lower branch in the negative direction $\Delta\gamma = -1$.

Specific values for $u^{(k)}$ and $\gamma^{(k)}$ are given in Tables 4.1 and 4.4.

Table 4.1: Path following along the lower branch in the negative direction $\Delta\gamma = -1$. Seven terms of the ADM solution are used in the corrector stage.

γ	$\Delta\gamma$	Pred.	Corr./$u_{\pm}(\gamma)$	Actual $u_{\pm}(\gamma)$	Diff1	Diff2
0			2			-2
-1	-1	-2	-2	1	3	3
-2	-1	-0.666666667	0.797186319	0.780776406	1.447443	-0.016410
-3	-1	0.645468804	0.666387370	0.666666667	0.021198	0.000279
-4	-1	0.577543168	0.593006205	0.593070331	0.015527	0.000064
-5	-1	0.531785223	0.540301210	0.540312424	0.008527	0.000011
-6	-1	0.494709324	0.499998300	0.5	0.005291	0.000002
-7	-1	0.464284153	0.467845237	0.467845317	0.003561	0.000000

4.2.3 Path following along the lower branch in the direction of γ_+

Given the turning point of 0.125 a step size of 1 would be too big to path follow the lower branch of the solution in the direction of positive γ. An erroneous value of $6.263635000 \cdot 10^5$ is returned by the ADM.

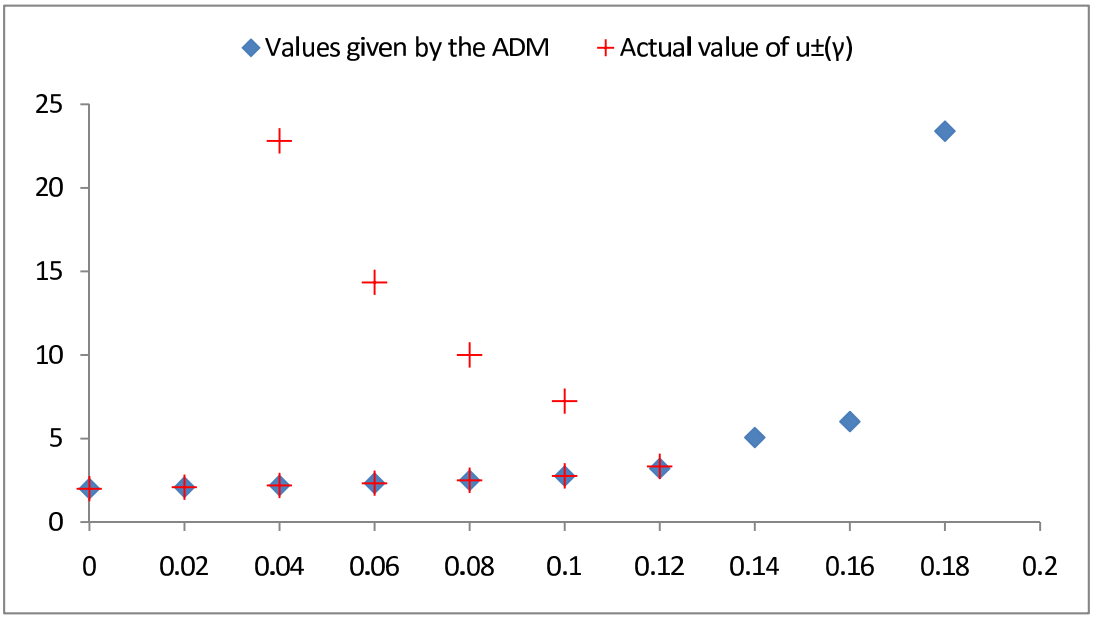

Figure 4.4: Path following along the lower branch in the positive direction $\Delta\gamma = 0.02$.

In Figure 4.4 it can be seen that path following for regular points fails to change branches at the turning point. Values that are largely different to those given by $u_{\pm}(\gamma)$ are given by the ADM if the path following for regular points continues to be implemented beyond the turning point of 0.125. Similar behaviour is observed if the upper branch is followed in the direction of

γ_+ using path following for regular points.

4.2.4 Path following along the upper branch in the direction of γ_+

The upper branch is initialised at $\gamma^{(0)} = 0.1$, $u^{(0)} = 7.23606798$.

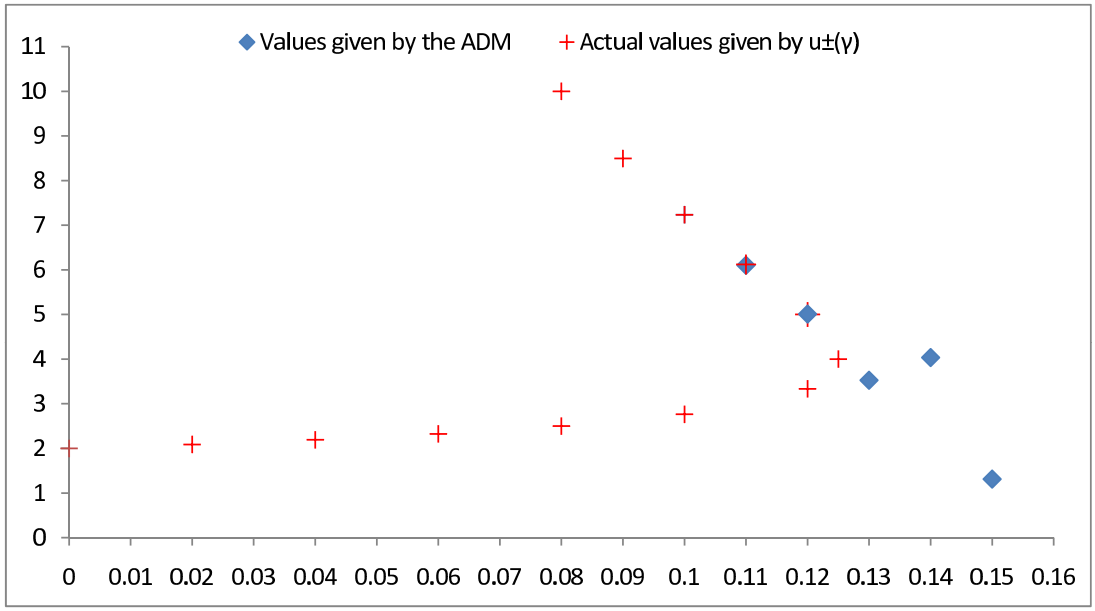

Figure 4.5: Path following along the upper branch in the direction of γ_+; $\Delta\gamma = 0.01$.

Figure 4.5 displays the outcome of path following this branch of the solution and the specific values for $u^{(k)}$ and $\gamma^{(k)}$ are given in Table 4.2.

Table 4.2: Path following along the upper branch in the direction of γ_+.

γ	Value given by the ADM	$u_\pm(\gamma)$
0.1		7.23606798
0.11	6.102361717	6.12004619
0.12	5.00802127	5
0.13	3.524708457	
0.14	4.033621932	
0.15	1.31184175	

Both Figures 4.4 and 4.5 illustrate the potential for generating erroneous results if the extended system for turning points is not switched to at the appropriate stage. What's more the examples herein have indicated that care must be taken to choose a suitable step size in order to ensure desired results are obtained. This thesis does not propose any systematic method for obtaining a step size needed to ensure convergence and with all the examples presented in this chapter there has not been much need to experiment to find a suitable step size to ensure convergence.

4.2.5 Implementing the extended system for turning points

In path following along the lower branch in the direction of γ_+ when the magnitude of the derivative gets small, in this case 0.2, the extended system for turning points is switched to with $\Delta\gamma = 0.5$. The magnitude of the derivative is monitored and Figure 4.6 shows a plot of $|f_u(u,\gamma)|$ against the value of $u(\gamma)$ as given by the ADM. As the magnitude of the derivative begins to increase again, in this case when it returns to a value of 0.2, a switch is made to path following for regular points on the upper branch in the direction of γ_+ with $\Delta\gamma = -0.02$.

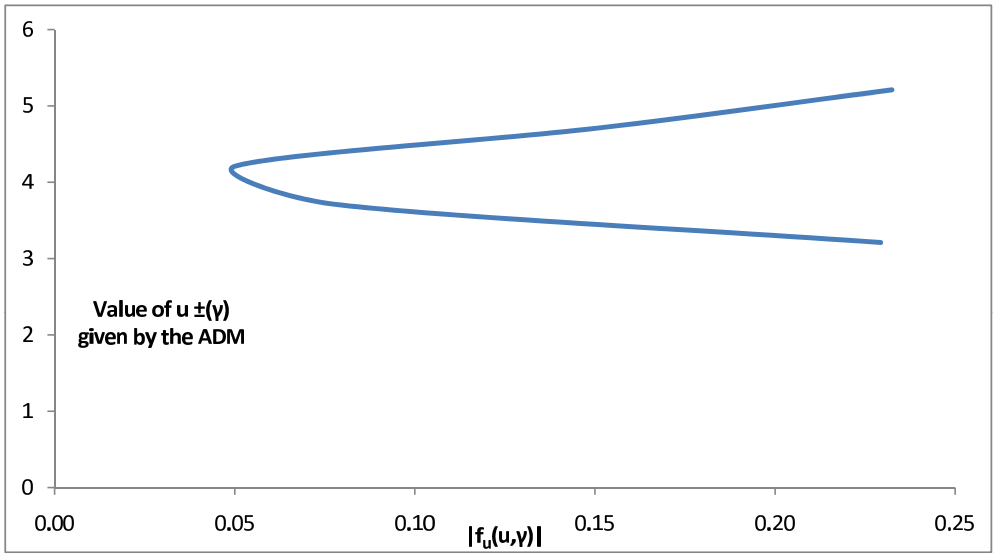

Figure 4.6: $|f_u(u,\gamma)|$ against $u(\gamma)$.

Figure 4.7 illustrates the outcome of path following the lower branch of the solution having initialised the path at $u^{(0)} = 2$, $\gamma^{(0)} = 0$ and moving in the direction of γ_+ and then around the turning point. It shows that the ADM very closely approximates the solution to (4.9).

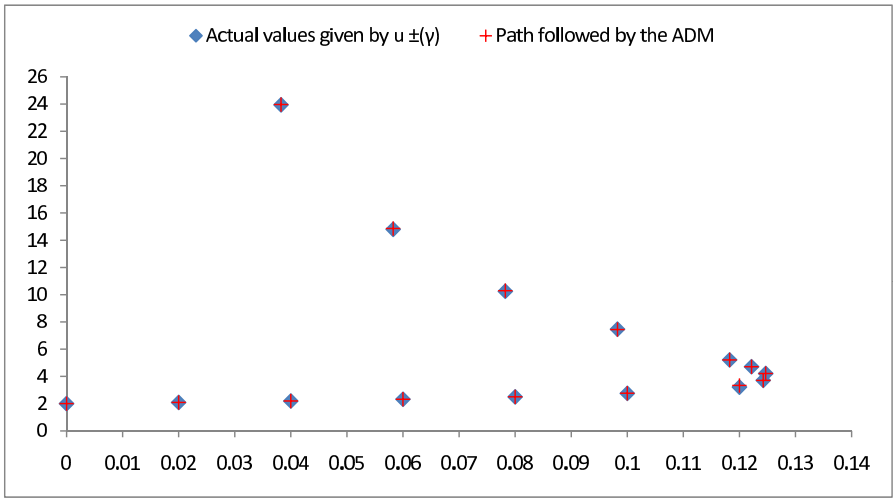

Figure 4.7: Path following along the lower branch, the turning point and the upper branch.

The bifurcation example above demonstrates that the ADM is an effective tool for path following nonlinear solutions. At each stage the ADM effectively corrects the predictor by bringing it substantially closer to the actual solution. Broadly speaking, differences between the value of the corrector and the actual solution occur in the third or fourth decimal place. By using more terms of the Adomian series solution and fine tuning step sizes the accuracy of the predictor corrector method could be improved. Notwithstanding Figure 4.8 shows a very close approximation to the actual solution given by the ADM when used as a corrector.

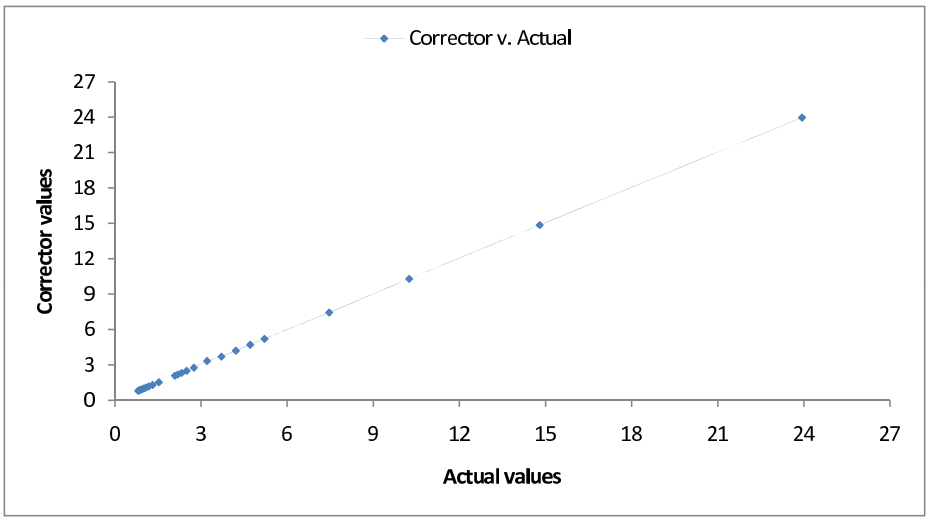

Figure 4.8: Corrector values against actual values.

With Lemmas 3.1 and 3.2 the ADM can be effectively implemented so as to allow the method to converge to more than one solution of a nonlinear problem. This approach to finding multiple solutions has been illustrated in the case of the one dimensional example and in the case of path following with the bifurcation problem above.

Table 4.4 shows the results of following the entire path of solutions of (4.9) using the ADM along with the actual solutions for the equation given by (4.10). The differences between both the predictor and the corrector from the actual solution are also shown. Initially the path of the lower branch in the direction of γ_- is followed; then the path is followed in the direction of γ_+; then using the extended system around the turning point; finally switching to path following for regular points having gone around the turning point. Table 4.3 will be useful when considering the information in Table 4.4 that follows.

Table 4.3: Key to the direction of the path followed and codes used.

LPN	lower path negative gamma axis
LPP	lower path positive gamma axis
ES	extended system around the turning point
UPN	upper path negative direction
Diff1	the difference between the actual solution and the value given at the predictor stage
Diff2	the difference between the actual solution and the value given at the corrector stage

Table 4.4: Path following $f(u, \gamma) = 0$.

Direction	$f_u(u,\gamma)$	γ	$\Delta\gamma$	Predictor	$u_\pm(\gamma)$;Corrector	$u_\pm(\gamma)$ given by formula (4.10)	Diff1	Diff2
	-1	0			2			0.000000
	-1.613	-0.2	-0.2	1.2	1.531482237	1.531128875	0.331129	-0.000353
	-2.049	-0.4	-0.2	1.240591976	1.311723836	1.311737691	0.071146	0.000014
	-2.408	-0.6	-0.2	1.143807666	1.173607877	1.173599096	0.029791	-0.000009
LPN	-2.72	-0.8	-0.2	1.059225233	1.075193471	1.075183814	0.015959	-0.000010
	-2.91	-1	-0.2	0.990200129	0.999928451	1	0.009800	0.000072
	-3.255	-1.2	-0.2	0.933268152	0.939613888	0.939901716	0.006634	0.000288
	-3.491	-1.4	-0.2	0.885367844	0.889612695	0.890303514	0.004936	0.000691
	-3.71	-1.6	-0.2	0.844271538	0.846989554	0.848385976	0.004114	0.001396
	-3.914	-1.8	-0.2	0.808319989	0.809561644	0.812300938	0.003981	0.002739
	-1	0			2			0.000000
	-0.917	0.02	0.02	2.08	2.086941294	2.087121525	0.007122	0.000180
LPP	-0.825	0.04	0.02	2.181981507	2.191812603	2.192235936	0.010254	0.000423
	-0.721	0.06	0.02	2.308322963	2.323001332	2.324081208	0.015758	0.001080
	-0.601	0.08	0.02	2.472641851	2.49677693	2.5	0.027358	0.003223
	-0.41	0.1	0.02	2.704394987	2.750964663	2.763932022	0.059537	0.012967
	-0.229	0.12	0.02	3.087455889	3.211165716	3.333333334	0.245877	0.122168
ES	-0.078	0.124242842	0.5		3.711165716	3.711165804		
	0.05	0.124685694	0.5		4.211165716	4.211166		
	0.151	0.12215164	0.5		4.711165716	4.711166		
	0.232	0.118247768	0.5		5.211165716	5.211166		
	0.172	0.098247768	-0.02	7.548017021	7.464911435	7.443531130	-0.104486	-0.021380
	0.243	0.078247768	-0.02	9.852328074	10.24930863	10.297865580	0.445538	0.048557
UPN	0.242	0.058247768	-0.02	13.72789686	14.7977826	14.856923400	1.129027	0.059141
	0.176	0.038247768	-0.02	20.847837856	23.93539247	23.963193630	3.115356	0.027801

Chapter 5

Orientational aggregation models

Change in both individual and group position is important to the dynamics of an aggregate of similarly sized elongated objects ([60]). For example, orienting into distinctive patterns is a noticeable feature of the behaviour of a school of fish. Where it is desirable to study the dynamics of positioning and grouping of such elongated objects, orientational aggregation models have been developed. Such models describe the change in relative position of the individual objects as well as the density of the way the objects come together and position en masse - the density of the clustering ([56]). Actin binding proteins perform important roles in certain cellular biological processes. Actin is a filamentous protein which forms one of the main components of the cytoskeleton. It gives the cell mechanical stability, connectivity, and motility ([18]). The required dynamic spatio-angular organisation of the actin filaments is regulated by a large number of actin binding proteins ([43, 56]). Angular structure develops when filaments interact by means of actin binding protein and reorient. In two dimensions, the **state space** representing the spatial orientation of the filaments is the circle $S^1 = [-\pi, \pi]$. The time dependent angular distribution c, called the **density of the filaments** is a function $c : S^1 \times [0, \infty) \to [0, 1]$. The time, space and orientation-dependent density of a large number of filaments was originally modelled by a linear partial integro-differential equation derived from a stochastic velocity jump process with interaction ([80]). In particular,

$$\frac{\partial(nu)}{\partial t} + \nabla . \int pv \mathrm{d}v = \lambda \iint W(v, v')vp(x, v', t)\mathrm{d}v'dv - \lambda nu + knur(n).$$

where

- $n(x, t) = \int p(x, v, t)\ \mathrm{d}v$ is the number density of filaments.
- $p(x, v, t)$ is the density function for individuals in a $2n$-dimensional phase space with coordinates (x, v), where $x \in \mathbb{R}^n$ is the position of a filament and $v \in \mathbb{R}^n$ is its velocity. Then $\int p(x, v, t)\ \mathrm{d}x\ \mathrm{d}v$ is the number density of filaments with position between x and $x + \mathrm{d}x$ and velocity between v and $v + \mathrm{d}v$.
- $u(x, t)$ is the average velocity of filaments.
- The kernel $W(v, v')$ gives the probability of a change in velocity from v' to v, given that a reorientation occurs, and therefore $T(v, v')$ is non-negative and normalised so that

$\int T(v,v')\mathrm{d}v = 1$ expressing the fact that no individuals are lost during the process of changing velocity.

- k is a constant. Random velocity changes are assumed the result of a Poisson process of intensity λ, where λ may depend upon other variables.
- $r(n)$ is a process that generates random velocity changes; $\frac{\partial p}{\partial t}.\frac{1}{kp} = r(n)$.

The equation becomes non-linear through the change in filament orientation depending on the density of the filaments but it is still interpreted as the expected value of a directional jump process with interaction. In [66] a linear turning rate equation was suggested to study the distribution of dominance in insect colonies. Under the hypothesis that anonymous organisms possess an attribute x called dominance $0 \leq x \leq 1$, a stochastic model based on a random variable $X(t)$ that takes a value x at any time t, from the dominance space $[0,1]$ was assumed. The idea of dominance, a character which changes according to certain rules as a result of encounters between pairs of organisms is important in the study of animal behaviour. This equation models the dynamics and the distribution of the characteristic of dominance.

$$\begin{aligned} \partial f \frac{(x,t|u,0)}{\partial t} &= -f(x,t|u,0)\int_0^1 \eta(x,y)f(y,t)\mathrm{d}y \\ &+ \int_0^1\int_0^1 \eta(v,y)f(y,t)\psi(v,y,x)f(v,t|u,0)\mathrm{d}y\mathrm{d}v \end{aligned} \tag{5.1}$$

where

- $f(u,t+dt|x,t)\ \mathrm{d}u$ denotes the probability that an individual with dominance x at time t will have its dominance in $(u,u+\mathrm{d}u)$ at time $t+\mathrm{d}t$.
- $\eta(x,y)\ \mathrm{d}t$ denotes the probability that a pair of individuals with dominance x and y, respectively, will have an encounter in the time interval of duration $\mathrm{d}t$ where $\mathrm{d}t \ll 1$.
- $\psi(x,y,u)\ \mathrm{d}u$ denotes the probability that after an encounter between two individuals with dominance x and y, respectively, the x individual will end up with its dominance in the interval $(u,u+\mathrm{d}u)$, irrespective of the y individual's change in dominance.

The periodic version of the equation in [66] was applied to the dynamics of actin filaments in [57] in order to grasp the action of actin binding proteins on actin filaments. If filament translocation velocity is small compared to the time scale of reorientations; if the filaments spatial interaction radius is large for example, long and stiff filaments with many interaction sites and if interactions between filaments do not depend on spatial position rather on their relative orientations then the partial differential equation can be averaged over space, arriving at an 'ordinary' integro-differential equation ([56]). The resulting integro-differential equation for the density of oriented filaments contains the action of actin binding proteins via the functional form of the interaction rate and of the turning rate. This model of filament dynamics which is similar to that which will be explored herein has been found useful in explaining the bundling and network formation of actin filaments.

The underlying directional jump process describes the change with respect to time of the orientation of spatially fixed or homogeneously distributed filaments. Rotational symmetry is derived from the mean-field approximation and averaging over space while the symmetry breaking follows from left-right differences during the aggregation process. Equations of this kind have

been used to analyse the influence of filament behaviour on swarm dynamics ([63, 81]). Other actin dynamics models use partial integro-differential equations where the partial derivative is orientational diffusion and the integrals describe jumping and binding to filaments in relatively favourable orientations ([42]). The model in [42] depicts the formation of actin cytoskeleton, bundles and orthogonal networks, via activation or inactivation of different types of actin binding proteins. Specifically the system of equations is given as

$$\frac{\partial L}{\partial t}(\theta,t) = \mu\frac{\partial^2 L}{\partial\theta^2} - \gamma L + \alpha A(t)L + \sigma B - \beta\rho L(K*B) - \beta\rho L(K*L), \tag{5.2}$$

$$\frac{\partial B}{\partial t}(\theta,t) = -\gamma B + \alpha A(t)B - \sigma B + \beta\rho B(K*L) + \beta\rho L(K*L), \tag{5.3}$$

where

- $A(t)$ denotes the density of actin monomers at time t
- $-\pi \leq \theta \leq \pi$ an angle with respect to some arbitrary fixed direction
- $L(\theta,t)$ the concentration of free actin filaments at orientation θ at time t. $K*L = \int_{-\pi}^{\pi} K(\theta-\theta')L(\theta',t)\mathrm{d}\theta'$
- $B(\theta,t)$ the concentration of bound actin filaments at orientation θ at time t
- $K(\phi)$ the probability that a filament contacting another filament at a relative angle ϕ binds to it in the presence of actin binding proteins.
- $L(K*B)$ represents the rate at which the free filaments, oriented at θ, bind to bound filaments at arbitrary orientation.
- $L(K*L)$ denotes the rate at which filaments, oriented at θ, bind to free filaments at arbitrary orientation.
- $B(K*L)$ denotes the rate at which free filaments oriented at arbitrary orientation bind to bound filaments oriented at θ.
- μ denotes the rotational diffusion constant of F-actin.
- $\rho(t)$ denotes the actin binding protein concentration.
- β denotes the affinity of binding.

Still other orientational aggregation models, based on systems of partial integro-differential equations, have been applied to swarms of elongated cells, fibroblasts and collagen and chemicals on the surface of a spherical tumour ([38, 44, 52]). In particular in [44] authors presented the following mathematical model for fibroblast and collagen orientation

$$\frac{\partial f}{\partial t} = \frac{\partial}{\partial\theta}\left(D\frac{\partial f}{\partial\theta} - f\frac{\partial}{\partial\theta}(W_1*c)\right) \text{ for } \theta\in[0,2\pi], \tag{5.4}$$

$$\frac{\partial c}{\partial t} = -\alpha\frac{\partial}{\partial\theta}\left(c(\theta)(W_2*f)(\theta)\frac{\partial}{\partial\theta}(W_3*f)(\theta)\right) \text{ for } \theta\in[0,\pi], \tag{5.5}$$

where

- where $f(t,\theta)$ and $c(t,\theta)$ denote the densities of fibroblasts and collagen fibres respectively at time t oriented at an angle θ with respect to an arbitrary reference direction.

- the kernel W_1 is determined by the way the orientation of the fibroblasts is changed due to collagen and W_2 and W_3 are determined by how the fibroblasts reorient the collagen.
- D is a dimensionless parameter obtained from experimental data which reflects the angular diffusion coefficient of the cells and α is a parameter also obtained from experimental data which reflects the rate at which collagen is realigned by the cells.

In [38] a reaction-diffusion system was presented to model the spatio-temporal pattern formation in reaction-diffusion systems on the surface of the unit sphere in 3D (cancer tumours).

$$u_t = D\triangle_* u + f(u)$$

where

- $u = u(x,t) = (u_1, \cdots u_s)^T \in \mathbb{R}^s$ on the space-time domain $(x,t) \in S \times [0,\infty]$, is a vector of (any number of) chemical concentrations or growth factors.
- $D = \text{diag}\{d_1, \cdots, d_s\}$ is a diagonal matrix of positive diffusion coefficients.
- $\triangle_*$ is the Laplace-Beltrami operator

$$\triangle_* u = \frac{1}{\sin\theta}\left\{\frac{\partial}{\partial\theta}\left(\sin\theta\frac{\partial u}{\partial\theta}\right) + \frac{1}{\sin\theta}\frac{\partial^2 u}{\partial\phi^2}\right\}$$

- $f : \mathbb{R}^s \to \mathbb{R}^s$ is a (nonlinear) vector-valued function representing the reaction kinetics. It is assumed that $f(u)(x,t) = f(u(x,t))$, $(x,t) \in S \times [0,\infty)$.

In [52] the model

$$\frac{\partial C}{\partial t}(\theta,t) = \beta C(\theta,t)\int_{-\pi}^{\pi} K(\theta-\theta')C(\theta',t)\mathrm{d}\theta'$$

which gives the net effect $C(\theta,t)$ on the entire density of cells at angle θ was presented. This model is a counterpart to and precedes the model treated in this thesis in development. $K(\theta)$ is the probability that a cell contacting a neighbour at relative angle θ aligns with it and sticks.

5.1 Formulation of the OAP

The model to be considered in this thesis is described as follows. The density of the filaments c satisfies the time dependent equation

$$c_t(\theta,t) = -c(\theta,t)\int_{S^1} W[c](\theta,\psi,\Lambda)\mathrm{d}\psi + \int_{S^1} W[c](\psi,\theta,\Lambda)c(\psi,t)\mathrm{d}\psi \tag{5.6}$$

where Λ represents the parameters of the problem. The notation $W[c]$ indicates that W is a functional of c. The trivial solution for (5.6) is the normalised constant solution $c(\theta,t) = \frac{1}{2\pi}$. The kernel $W[c](\theta,\psi,\Lambda)$ represents the **turning rate**, the probability of filaments jumping from location θ to location ψ given the distribution c. $W[c](\theta,\psi,\Lambda)$ is a functional, mapping functions on S^1 to square integrable functions on $S^1 \times S^1$. The first term accumulates all the filaments

jumping away from orientation θ and the second those jumping onto orientation θ. Explicitly, W is given by

$$W[c](\theta, \psi, \Lambda) = \int_{S^1} K(\theta - \psi, \theta - \phi, c(\phi, t), \Lambda) \mathrm{d}\phi, \tag{5.7}$$

where K is a function that is 2π periodic in its first two arguments. Because the material is assumed isotropic, the value of K depends on the differences of positions between filaments. A typical form for K is

$$K(x, y, c) = h_\rho(y) w(x, y) p_\beta(c), \tag{5.8}$$

where the different components of K satisfy the following hypotheses.

Frequency function

The term $h_\rho(y) : S^1 \to \mathbb{R}_+$ is the **frequency function**, $h_\rho(y) \in \mathbb{L}^{\infty,+}$. This is the rate per unit time of interaction between two filaments with a difference of direction y. The interaction rate also depends on the relative interaction angle $\phi - \theta$. Examples are the **uniform distribution** $h_\rho(x) = \dfrac{1}{2\pi}$, or $h_\rho(x) = g_\rho(x)$ where ρ is the effective range at which filaments interact, or

$$h_\rho(x) = \frac{1}{2}\left[g_\rho\left(x - \frac{\pi}{2}\right) + g_\rho\left(x + \frac{\pi}{2}\right)\right],$$

where the frequency of turning is greater at orthogonal angles and smaller for parallel directions. With regard to actin filaments, $h_\rho(y)$ represents the binding rate of proteins to actin.

Turning probability function

The term $w(x, y)$ is the **turning probability function**. This is the probability of a filament turning by angle x as a result of interaction with filaments with a difference of direction of y. Note that $\int_{S^1} w(x, y) \mathrm{d}x = 1$. In practice, w is often taken of the form

$$w(x, y) = g_\sigma(x - v_{k,\mu}(y)), \tag{5.9}$$

where $v_{k,\mu}$ is the **turning function** with parameters k and μ and g_σ the variation function $g_\sigma : S^1 \to \mathbb{R}_+$ is an even and bounded probability distribution, $g_\sigma \in \mathbb{L}^{\infty,+}$ (the set of non-negative bounded functions) and $\int g_\sigma = 1$ with parameter $\sigma > 0$. With these examples, (5.9) means that, with highest probability, a filament turns by angle $x - v_{k,\mu}(y)$ as a result of the interaction with a filament with angular difference of direction of x. The parameter σ is called the **uncertainty of turning** and, the smaller the value of σ, the stricter the alignment. For actin filaments, w is the turning mechanism eg. favouring parallel alignment or orthogonal configuration. Specific examples for g_σ are the **periodic Gaussian**

$$g_\sigma(\theta) = \frac{1}{\sigma\sqrt{(2\pi)}} \sum_{n \in \mathbb{Z}} e^{(-\frac{1}{2}(\frac{\theta + 2\pi n}{\sigma})^2)}$$

or the normalised step-function for $\sigma \leq \pi$ given by $g_\sigma(\theta) = \dfrac{1}{2\sigma}\chi_{[-\sigma,\sigma]}$. With regard to actin filaments g_σ models random deviations from the optimal resultant angle. The turning function

$v_{k,\mu}$ represents the average angle of turning as a function of the interaction angle and the **attractivity coefficient** $0 \leq k \leq 1$. If $0 < v_k(\theta) < \theta$ for $\theta \in [0, \pi]$, for instance if

$$v_k(\theta) = k \sin\theta \quad \text{or} \quad k\theta,$$

then there is an attracting interaction. When

$$v_k(\theta) = \frac{1}{2} k \sin(2\theta) \quad \text{or} \quad -\frac{1}{2} k \sin(2\theta),$$

there are mixed attracting-repulsing interactions depending on the size of the difference of directions. The dependence of v on the symmetry coefficient μ is linked with the reflection symmetry. It is assumed that h_ρ and g_σ are even functions as $v_{k,\mu} : S^1 \to S^1$ is an odd measurable function that shall break the symmetry, that is $v_{k,\mu}(\theta)$ is not odd if $\mu \neq 0$. $v_{k,\mu}$ being odd follows from the assumption that filaments do not distinguish between left and right but only take into account angular differences. Since the turning mechanism is invariant to rotations the new orientation

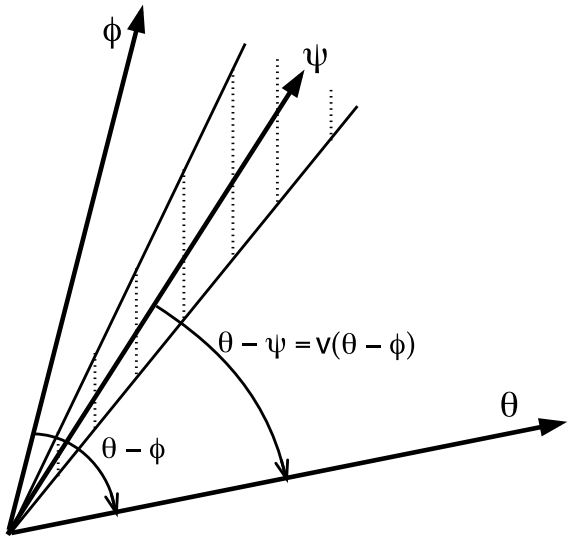

Figure 5.1: Geometrical interpretation of the turning rate W ([56]).

ψ occurs relative to the locations of the interaction partners θ, ψ. The preferred value of ψ is given by the optimal reorientation angle $v(\phi - \theta)$ depending on the relative interaction angle $\phi - \theta$ and the inaccuracy of the movement is measured by σ where small σ means high accuracy.

Nonlinear interaction

Finally, the term ρ_β is a measure of the nonlinear interaction with parameter β. Examples are

$$\rho_\beta(c) = c$$

where the interaction is proportional to the concentration c, or

$$\rho_\beta(c) = \frac{c^2}{1 + \beta c^2}, \tag{5.10}$$

a typical sigmoid function where a single filament interacts with two at low densities and is indifferent to the filament distribution at high densities.

5.1.1 Elementary Dynamics

Note that time can be re-scaled in (5.6)-(5.8). This is used to normalise h_ρ to $\int_{S^1} h_\rho(y)\mathrm{d}y = 1$. If $h \in L^2(S^1)$ and v is measurable then there exists unique square-integrable solutions to (5.6) ([58]). Given a non-negative initial distribution, the solution is strictly positive for all times $t > 0$ because the deviation $g_\sigma > 0$ distributes filaments to any orientation ([60]). Since the integro-differential equation (5.6) conserves mass, both stationary and time dependent solutions can be normalised to $\int_{S^1} c(\theta, t)\mathrm{d}\theta = 1$.

Lemma 5.1 *Let c be a solution of* (5.6)*, then $\int_{S^1} c(\theta, t)\mathrm{d}\theta$ is a constant of time.*

The equation is also equivariant with respect to the action of $\mathbb{SO}(2)$ as a shift on the angle in c. Solutions are invariant to rotations. The special orthogonal group $\mathbb{SO}(2)$ consists of all planar rotations about a fixed point. It is isomorphic to the multiplicative group of complex numbers of norm 1.

If K is an even function of the first two (angle) variables, then there is an additional angle reversal action of $\mathbb{Z}_2$ which is the multiplicative group $\{1, -1\}$. Together with the action of $\mathbb{SO}(2)$, it corresponds to an action of $\mathbb{O}(2)$, the symmetry group of the circle.

The $\mathbb{SO}(2)$-symmetry breaking will occur if the filament aggregation process discerns between left and right when $\mu \neq 0$. The two processes of choosing an interaction partner h and turning g_σ, v are independent. The symmetries of interaction rate, optimal turning and probability density correspond to the assumption of no chirality.

5.2 How the OAP has been solved to date

Analysis of the orientation aggregation system is informed by the mathematical theory of general equations with symmetry as developed by Golubitsky, Stewart and Schaeffer [61] and in particular for equations on the circle by Dangelmayr [45]. Various mathematical methods have been used to analyse orientational models. These methods have included linear stability analysis near the trivial homogeneous distribution ([76]), non-linear bifurcation theory ([44]), analysis of special stationary solutions usually for some very small parameter ([77]) and numerical simulations ([57]). The first two of these methods and the last rely on a spectral decomposition of the solutions which is possible because orientational equations are invariant under rotations ([38]). For the orientation aggregation system of the form

$$c_t(\theta, t) = -c(\theta, t)\int_{S^1} W[c](\theta, \psi, \Lambda)\mathrm{d}\psi + \int_{S^1} W[c](\psi, \theta, \Lambda)c(\psi, t)\mathrm{d}\psi, \tag{5.11}$$

Geigant [56] carried out bifurcation analysis near the homogenous solution, based on the invariance to turning, $\mathbb{O}(2)$-symmetry. Bifurcation equations are derived using Lyapunov-Schmidt reduction and the theory set out by Dangelmayr [45] is used to determine which coefficients are important in the equations corresponding to the Lyapunov-Schmidt reduction. Coefficients were calculated numerically where it was not possible to do so analytically. In this way generic bifurcations and the emergence of aggregates such as non-homogenous solutions are analysed and interpreted; hysteresis is found and various time-periodic solutions are constructed.

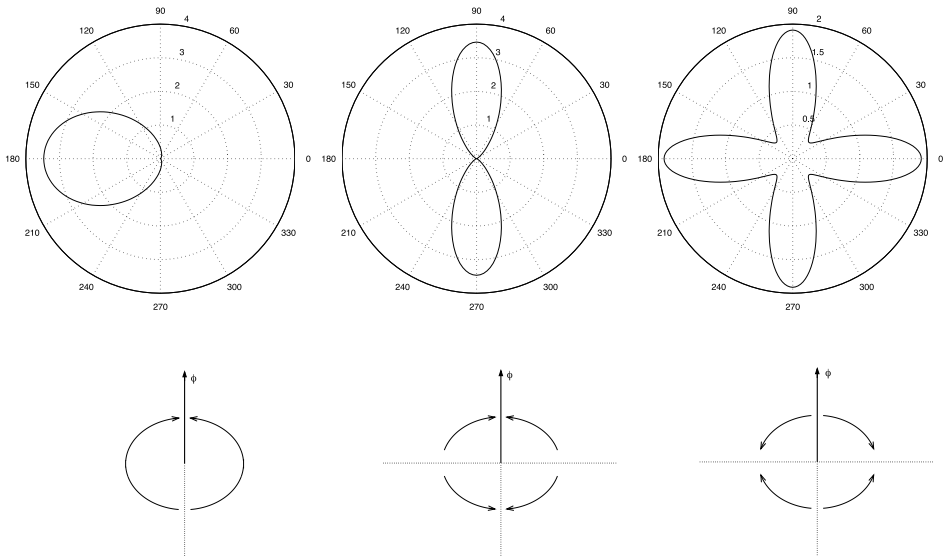

Figure 5.2: The formation of bundles and networks is associated with stationary solutions ([60]).

5.2.1 Stationary solutions - Bundles and networks

Stationary solutions are associated with the orientation of filaments into bundles and networks. Basic stationary aggregation types are unidirectional bundles where the density has a single maximum; bidirectional bundles where the density has two maxima of equal height at opposite 180 degrees orientations and orthogonal networks where the density has four equal maxima at orthogonal 90 degrees orientations. In the case of bidirectional bundles the solution satisfies $c(\theta+\frac{1}{2}) = c(\theta)$, $c_k = 0$ for odd k. The solution is invariant under reflection and the Fourier coefficients are real. Stationary solutions are observed when the first eigenvalues λ_1 and λ_{-1}, second eigenvalues λ_2 and λ_{-2} and fourth eigenvalues λ_4 and λ_{-4} of the linearisation are respectively unstable. In general a unidirectional bundle manifests when only the first mode eigenvalues, λ_1 and λ_{-1}, are positive and thus the trivial solution is unstable. A bidirectional bundle or a network manifests when only the second or fourth mode eigenvalues are positive respectively. λ_1 becomes positive for sufficiently small inaccuracy in the Gaussian g_σ if the optimal turning is attracting $0 < v(\psi) < \psi$ for $0 < \psi < \frac{1}{2}$ and the interaction rate is homogenous, $h = 1$.

Figure 5.2 shows from left to right unidirectional bundling, bidirectional bundling and an orthogonal arrangement. Beneath each type of bundle is the polar plot of the underlying optimal turning angle. The radius of the plot represents density $c(\theta)$. In this instance unidirectional bundles are observed for $v(\psi) = \frac{1}{2}\psi$, $h = 1$. Bidirectional bundles are observed for $v(\psi) = \frac{1}{2}\psi$ on $]-\frac{1}{4}, \frac{1}{4}[$ continued $\frac{1}{2}$ periodically, $h = 1$. Orthogonal arrangements are observed for $v(\psi) = -\frac{1}{8\pi}\sin(4\pi\psi)$ which is also $\frac{1}{2}$ periodic, $h(\psi) = \frac{1}{2}\left(G_\tau(\psi - \frac{1}{4}) + (G_\tau(\psi + \frac{1}{4}), \tau = 0.06\right)$.

How they are obtained mathematically?

Recall that time has been re-scaled and c, h average 1. The equation (5.11) with (5.7) and (5.8) is Fourier transformed to an infinite system of ODEs of the form

$$\dot{c}_l = \sum_{k\in\mathbb{Z}} w_{l,k}\ c_k\ c_{l-k} \tag{5.12}$$

where

$$w_{l,k} = -h_k + e^{-2\pi^2 l^2\sigma^2} \int_{S_1} h(\psi)\cos(2\pi(k\psi - lv(\psi)))\,\mathrm{d}\psi.$$

A numerical algorithm is used to find solutions wherein the Fourier transformed system (5.12) is restricted to some fixed bound N for the Fourier indices:

$$\dot{c}_l = \sum_{\max(0,l)-N\le k\le N+\min(0,l)} w_{l,k}\ c_k\ c_{l-k}, \quad -N \le l \le N. \tag{5.13}$$

The bound N is increased if for the higher Fourier coefficients c_l with $N < |l| \le 2N$ the growth of (5.13) is larger than some small error. The homogenous distribution $c = 1$, $c_0 = 1$, $c_k = 0$ for $k \neq 0$ is a trivial stationary solution of (5.11). The OAP is linearised at the homogenous solution $c = 1$. From the linearisation, eigenvalues are identified,

$$\lambda_l = w_{l,0} + w_{0,l} = -1 - h_l + 2e^{-2\pi^2 l^2\sigma^2} \int h(\psi)\cos(\pi l\psi)\cos(2\pi l(v(\psi) - \frac{1}{2}\psi))\,\mathrm{d}\psi.$$

As in the limiting case when $\sigma = 0$, only finitely many eigenvalues can become unstable if v is continuously differentiable and the points $\psi \ni\ v'(\psi) = 0$ or $v'(\psi) = 1$ are isolated since $c_l \mapsto -1$ for $l \mapsto \infty$ and the integral tends to 0 for $l \mapsto \infty$. Subject to an explicit Lyapunov-Schmidt reduction with formal power series of the form

$$c_{ml} = c_l^m \sum_{k\ge 0} \alpha_{m,k}|c_l|^{2k}. \tag{5.14}$$

with real coefficients $\alpha_{m,k}$ it is noted that the stationary solutions of (5.12) are convergent power series where both $c_l \ge 0$ and the bifurcation parameter are small enough ([56]).

Implication for system behaviour

Stationary solutions represent constant distribution of filament density. For the trivial solution $c = 1$, there is homogenous density. In the formation of unidirectional bundles, filaments try to meet in the middle and v is the most attracting possible. All these patterns are relevant to actin dynamics if the actin filaments interact via different kinds of actin binding proteins ([56]). The kinds of patterns that will be formed will be determined by the different kinds of actin binding proteins by which the filaments interact.

5.2.2 Stationary solutions - Peak solutions

Note again the form of the periodic gaussian

$$g_\sigma(\theta) = \frac{1}{\sigma\sqrt{(2\pi)}} \sum_{n\in\mathbb{Z}} e^{(-\frac{1}{2}(\frac{\theta+2\pi n}{\sigma})^2)}$$

where the parameter σ is called the **uncertainty of turning** and the smaller the value of σ, the stricter the alignment.

The orientation aggregation system also manifests stable, unipolar, stationary solutions that can be observed among other stationary solutions. When σ tends to zero, the peaks become narrower and, in the limiting case $\sigma = 0$, there is a delta peak solution which is stable. The turning angle v is described as attracting if after turning the angle between two filaments is narrower.

Theorem 5.2 ([59]) *If the interaction is attracting , i.e.* $0 < v(\psi) < \psi$ *for* $0 < \psi < \frac{1}{2}$*, then the delta peak is a stationary solution of the limiting equation of (5.6)-(5.8) as* $\sigma \to 0$ *and it is stable under perturbation by measures* $\widetilde{c}$*,* $\ni$

i $\tilde{c}$ *has compact support in* $]-\frac{1}{2}, \frac{1}{2}[$*, (where the reversed square bracket notation [open interval notation] indicates the exclusion of the end points from the interval),*

ii $\tilde{c}$ *has zero mass,* $\int_{-\frac{1}{2}}^{\frac{1}{2}} \tilde{c}(\psi)\, \mathrm{d}\psi = 0$*,*

iii $\tilde{c}$ *has vanishing barycenter,* $\int_{-\frac{1}{2}}^{\frac{1}{2}} \psi\, \tilde{c}(\psi)\, \mathrm{d}\psi = 0$*.*

The result is independent of the stability of subsequent higher modes ([59]). Peak solutions arise if the turning angle v is attracting and the first eigenvalue becomes positive for decreasing inaccuracy σ.

How they are obtained mathematically?

Linear stability analysis is used to study the behaviour of peak solutions. When σ is small, (5.11) and the state space representing the filaments is approximated on the real line instead of S^1, an exact Gaussian peak solution can be found ([60]). The stability of the solution is established by analysis of (5.11) on S^1 as σ tends to zero. Substitute

$$K(x, y, c) = h_\rho(y) w(x, y) p_\beta(c), \quad w(x, y) = g_\sigma(x - v_{k,\mu}(y)),$$

into

$$W[c](\theta, \psi, \Lambda) = \int_{S^1} K(\theta - \psi, \theta - \phi, c(\phi, t), \Lambda) \mathrm{d}\phi$$

to re-write (5.11) as

$$\dot{c}(\theta) = -(h * c)(\theta)c(\theta) + G_\sigma * \int_{S^1} h(\psi)c(\theta - v(\psi))\, c(\theta + \psi - v(\psi))\, \mathrm{d}\psi. \tag{5.15}$$

Then G_σ is replaced by the delta distribution, $\sigma \to 0$, to obtain the limiting equation

$$\dot{c}(\theta) = -(h * c)(\theta)c(\theta) + \int_{S^1} h(\psi)\, c(\theta - v(\psi))\, c(\theta + \psi - v(\psi))\, \mathrm{d}\psi. \tag{5.16}$$

The right hand side is then considered to comprise measures (distributions) $c \in D^{'}$ instead of functions. The integral is then applied to a test function ϕ and after some substitutions and a two-fold integration of c against some modified test function it is noted that:

$$\langle \dot{c}, \phi \rangle = -\langle c, (h * c)\varphi \rangle + \langle c(\theta), \langle c(\psi), h(\psi - \theta)\varphi(\theta + v(\psi - \theta)) \rangle_\psi \rangle_\theta \tag{5.17}$$

From (5.17) it is shown that σ is a stationary solution of the limiting equation (5.16) and any delta peak $\sigma_\theta = \sigma(. - \theta)$ is stationary since (5.16) is equivariant under rotations. By perturbing c the linearisation of (5.16) around the steady state solution σ can be analysed and the behaviour of the peak solutions can be explored.

Implication for system behaviour - actual behaviour of filaments and the physical system

When there are peak solutions filaments orient in the same direction, the turning angle is attracting and as the variation σ is reduced the filaments tend to maintain orientation in the same direction. There are stable unipolar stationary solutions and these peaks become narrower as $\sigma \to 0$.

5.2.3 Bifurcations and Time Dependent Solutions

What solutions (nature of solutions)?

The codimension of a bifurcation is the number of parameters which must be varied for the bifurcation to occur ([71]). The orientation aggregation system demonstrates codimension 1 and codimension 2 bifurcations. When a **single** eigenvalue becomes unstable and where σ the inaccuracy decreases and becomes small **codimension 1** bifurcation arise. **Codimension** 2 bifurcations occur when **two** eigenvalues change sign at the same parameter combination.

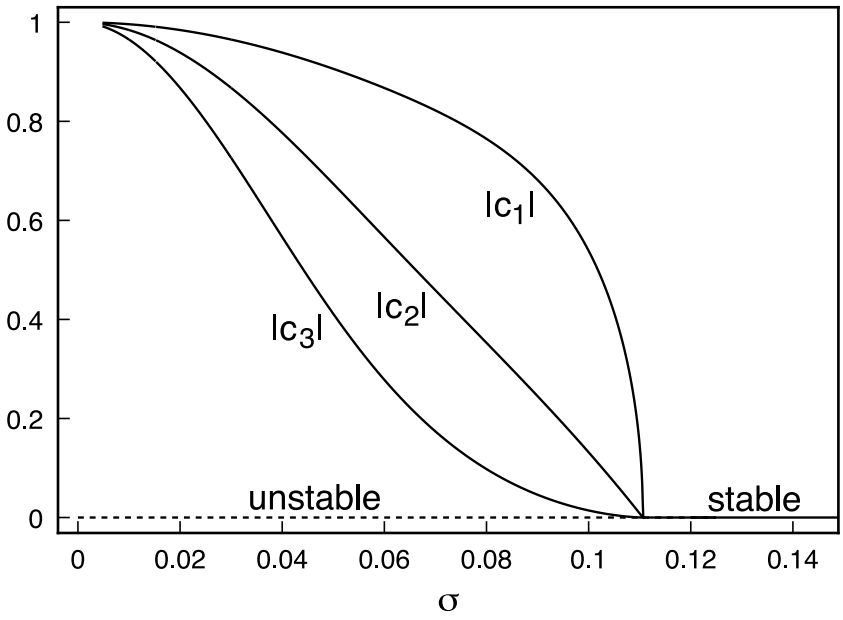

Figure 5.3: Codimension 1 forward bifurcation ([60]).

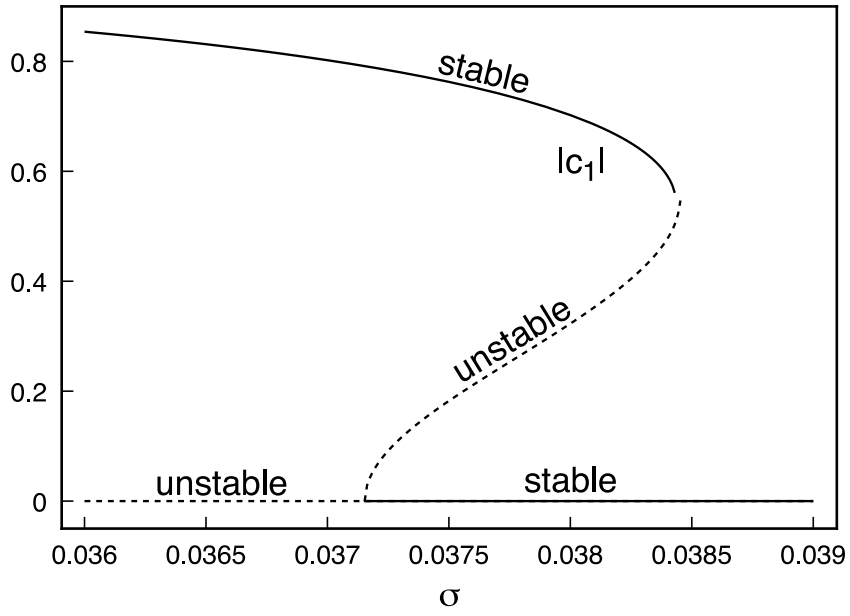

Figure 5.4: Codimension 1 periodic solution showing hysteresis ([60])

Recall that the orientation aggregation system is Fourier transformed to an infinite system of ODEs of the form in (5.12). Figure (5.3) shows the absolute values of the first three Fourier coefficients of the stable solution that branches off when the inaccuracy σ is decreased below

about 0.11.

Figure (5.4) shows a resulting unstable system orientation as σ is increased. The absolute value of the first Fourier coefficient of the stable solution is shown. The unstable branch bifurcates off the trivial solution; it then undergoes a saddle-node bifurcation and becomes stable. For these values of σ higher eigenvalues than the first are unstable.

Under what conditions they arise?

When the inaccuracy (σ) is large any solution (any starting arrangement where filaments are in attracting alignment) converges to the constant solution $c = 1$ in L^2 norm ([58]). That is to say with large values of σ there is greater dispersion of filaments (a diffusion like process away from the starting alignment) to a steady (dispersed) state. However when σ is small, both codimension 1 and codimension 2 bifurcations are observed. When a single eigenvalue becomes unstable and where σ the inaccuracy decreases and becomes small codimension 1 bifurcation arise. It is further noted that when eigenmodes that are nearby each other become unstable both bifurcations will interact resulting in an increased variety of solution branches.

How they are obtained mathematically?

The bifurcation equation derived - when a single eigenvalue changes sign - using a Lyapunov-Schmidt reduction can be used to study the behaviour of the codimension 1 bifurcation. The stable branch of the pitchfork bifurcation can be computed numerically using the algorithm (5.13) and the unstable branch in Figure (5.4) comes from a power series expansion based on a Lyapunov-Schmidt reduction, namely $c_l = \sum_{k\geq l} a_{l,k} c_1^k$ and $|c_1|^2 = \sum_{m\geq 1} b_m \lambda^m$, where $\lambda = \sigma - \sigma_{\text{crit}}$ is the bifurcation parameter.

Likewise a Lyapunov-Schmidt reduction where first and second eigenmodes become unstable is used to study the behaviour of codimension 2 bifurcations ([60]). For $l > 3$, c_l is expanded as a power series in $c_1, \bar{c_1}, c_2, \bar{c_2}$ and the bifurcation parameters near the point where both eigenvalues vanish.

$$c_m = \sum_{j_1 - k_1 + 2j_2 - 2k_2 = m} \alpha_{j_1,k_1,j_2,k_2} c_1^{j_1} \bar{c_1}^{k_1} c_2^{j_2} \bar{c_2}^{k_2}$$

giving

$$\begin{aligned} c_3 &= \alpha_{31} c_1 c_2 + \alpha_{32} \bar{c}_1 c_2^2 + \alpha_{33} c_1^3 + O(4), \\ c_4 &= \alpha_{41} c_2^2 + \alpha_{42} c_1^2 c_2 + O(4), \end{aligned} \tag{5.18}$$

where $O(n)$ denotes terms of total degree n or higher in the variables $c_1, \bar{c}_1, c_2, \bar{c}_2$ (the α values which are to be determined are the coefficients of the power series). Substituting (5.18) into (5.12) and calculating few α coefficients of c_3, c_4 leads to power series that can be used to obtain the reduced, complex two-dimensional system of ODEs corresponding to the Lyapunov-Schmidt reduction. From this reduced system the bifurcating branches are obtained as convergent power series in the bifurcation parameter.

Implication for system behaviour

Actin binding proteins influence how filaments interact and transition between orientational patterns. The transitional modes often interact. Actin binding proteins can compete for filaments leading to unidirectional and bidirectional bundling. When the first and second modes become unstable unidirectional and bidirectional bundling forces are active ([56]). If the first two coefficients in the expansion of the reduced complex two-dimensional system of ODEs corresponding to the Lyapunov-Schmidt reduction do not have opposite signs then transitions between unipolar and bipolar bundles are either via the homogeneous state i.e. bundles dissolve and then aggregate anew or via a mixed mode state which is neither unipolar nor bipolar. High competition

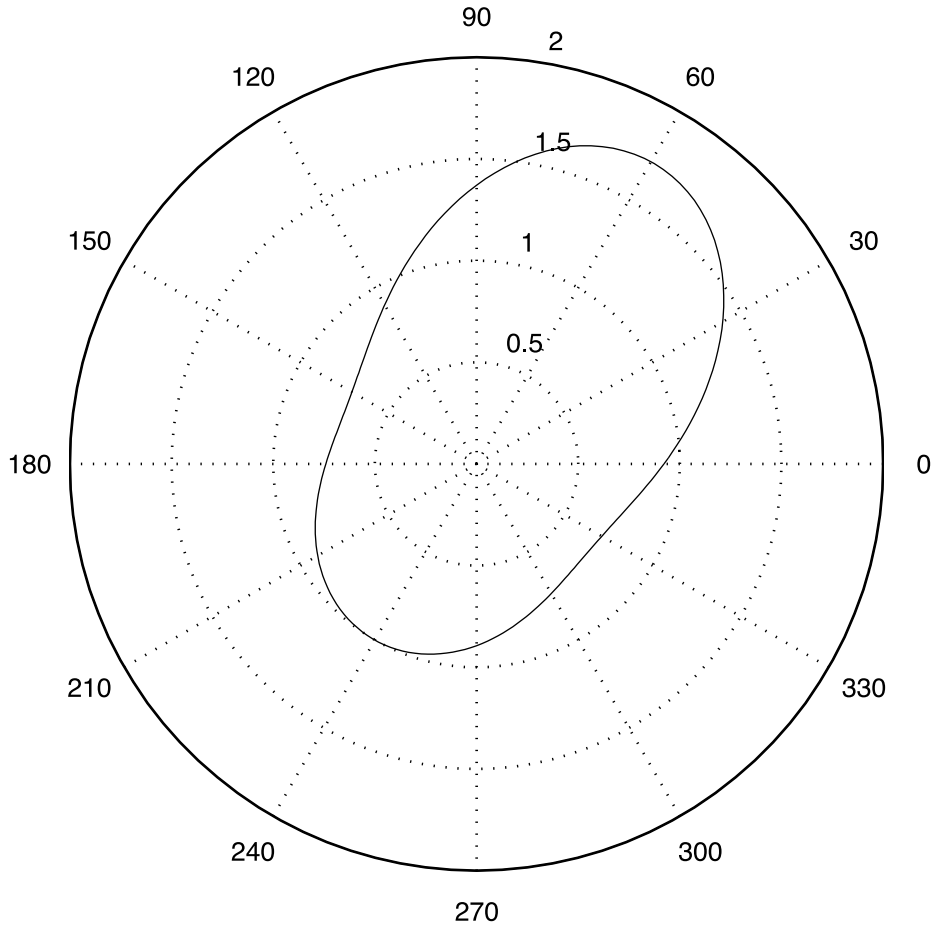

Figure 5.5: An example of a mixed mode transitional state ([60]).

for filaments by the actin binding proteins prevents the formation of bundles. When α increases, unidirectional bundles dissolve and when α decreases bidirectional bundles form. Competition can also lead to a high density bundle and a low density bundle in opposite orientation. In the case of codimension 1 bifurcation there is either a forward or backward pitchfork bifurcation. In general there are forward bifurcations while backward bifurcations are rare. In instances where backward bifurcations arise a single unstable stationary solution branches off and in a

secondary saddle-node bifurcation a stable stationary solution appears ([60]). For an existing unidirectional bundle formed for $\alpha = 0$ as competition increases the bundle transforms into a mixed mode solution (Figure (5.5)) comprising a strong bundle with a weak opposite bundle then a sudden transition into a bidirectional bundle. As α is decreased filaments disperse and the bidirectional bundle disappears. A mixed mode solution then suddenly forms. In other instances as α decreases the filaments do not disperse rather the bidirectional bundle suddenly loses stability and a mixed mode solution forms. The thicker bundle becomes the unidirectional bundle. In all observed instances a unidirectional bundle transforms into a bidirectional bundle via a mixed mode state. In general, when mixed mode solutions arise it is in the form of a bipolar bundle consisting of a high-density and a low-density arm in opposite orientation. The solution branches off the homogenous density and is symmetric under reflection. When the coefficients have opposite signs, in addition to unipolar and bipolar bundles and mixed mode solutions, traveling waves, modulated waves, oscillating bundles, and standing waves are observed.

Since the equation representing the system is mirror symmetric, waves can move both counter clockwise and clockwise. Oscillating bundles and traveling waves are the most common types of periodic solutions and some solution patterns are only seen clearly for very large times ([56]). In the case of travelling waves the solution consists of a high-density and a low-density bundle which rotate either clock or counter-clockwise; the two bundles are not opposite each other. The solution satisfies $c(\theta, t) = c(\theta - ct, 0)$.

Modulated wave solutions are like travelling wave solutions but the high-density bundle shrinks and grows periodically and the low-density bundle grows, although not to the thickness of the high-density bundle and then shrinks. The solution branches off a travelling wave solution via a Hopf bifurcation. While it looks similar to a travelling wave solution, the wave changes its shape periodically. It satisfies $c(\theta, t + \tau) = c(\theta - c\tau, t)$, $\forall \theta \in S^1,\ t \in \mathbb{R}$, with some constants c, τ ([56]). An oscillating bundle solution is like a bidirectional bundle which periodically almost dissolves looking like a not very distinct unidirectional bundle and forms again but rotated by about 90 degrees. The bundles exist for a relatively long period of time while transitions between the bundling phases are quick. The solution satisfies $c(\theta, t + \delta) = c(\theta + \lambda, t)$ with $\lambda \sim \frac{1}{4}$ with some $\delta \neq 0$.

Standing wave solutions are observed to be very similar to bipolar bundles which shrink and grow periodically in density but the two arms change their relative angle slightly. The solution represents a periodic orbit within the space of reflection-symmetric functions. It branches off a mixed mode solution via a hopf bifurcation. It satisfies $c(\theta, t + \tau) = c(\theta, t)$ for some $\tau > 0$.

Backward bifurcation leads to hysteresis. It is noticeable that when there is hysteresis the inaccuracy at which a bundle forms is larger than the inaccuracy at which an existing bundle dissolves. Moreover, this bundle does not form gradually, from a slight thickening to a bundle but very suddenly. In the case of a codimension 1 bifurcation as σ is decreased there is a time lag in the system reorienting back to its previously stable state. This behaviour is depicted as a pitchfork bifurcation in (5.4) of an unstable branch from the constant solution and the secondary saddle-node-bifurcation where the modulus of the first Fourier mode is shown. Here $v(\psi) = \frac{1}{2}\psi$ for $|\psi| < \frac{1}{6}$, $v(\psi) = 0$ otherwise and $h(\psi) = 1$. Hysteresis is also observed for a non-constant interaction rate h and in the transition between unidirectional and bidirectional bundles ([56]).

5.2.4 Higher nonlinearities

What solutions?

Recall the form of the sigmoid function given by (5.10). Consideration of the system behaviour when the filament interaction is non-symmetric has shown step function-like solutions in a particular instance where a jump process with a sigmoid jump rate was introduced.

Theorem 5.3 ([56]) *Let $\sigma = 0$, i.e. $G_\sigma = \sigma$. The stationary solutions of (5.11) with (5.19),*

$$\dot{c} = -\int_{-\frac{1}{2}}^{\frac{1}{2}} p(c(\phi))\,\mathrm{d}\phi\, c + M\, p(c)$$

are exactly the step functions

$$c = 0 \cdot x_0 + c_1 \cdot V_1 + c_2 \cdot x_2$$

where x_j are characteristic functions with volumes V_j, $V_0 + V_1 + V_2 = 1$, $c_1V_1 + c_2V_2 = M$ and $\dfrac{p(c_1)}{c_1} = \dfrac{p(c_2)}{c_2}$. Stationary solutions are unstable if $0 < c_1 < c_2$ or $c_1 = 0$, $c_2 = \frac{M}{V_2} < 1$. Stationary solutions are unstable in the space of step functions if $c_1 = 0$ and $c_2 = \frac{M}{V_2} > 1$.

Under what conditions they arise?

The interaction rate is homogenous ($h = 1$) and there is very small inaccuracy (small σ) where the number of unstable eigenvalues becomes large. For $\sigma = 0$ and $M < 1$, all eigenvalues are positive ($\lambda_l > 0$ for $|l| \neq 0$). See equation (5.20) for the eigenvalues of the linearisation.

How they are obtained mathematically?

By introducing non-symmetric interaction of the form

$$W[c](\theta, \psi) = \alpha \int_{S^1} g_\sigma(\psi - \phi) p(c(\phi))\,\mathrm{d}\phi \tag{5.19}$$

where $p : \mathbb{R}_+ \mapsto \mathbb{R}_+$,

$$p(c) = \frac{c^2}{(1 + \beta c^2)}$$

is a typical sigmoid function describing some non-proportional interaction of the filament at orientation θ with filaments at orientation ϕ and $\alpha > 0$ is the rate constant. Then analysing the eigenvalues of the linearisation near the homogenous distribution, $c = M > 0$ which are

$$\lambda_l = -p(M) + Mp^{'}(M)e^{(-2\pi^2 l^2 \sigma^2)} = \frac{M^2}{1 + M^2}\left(-1 + \frac{2}{1 + M^2}e^{-2\pi^2 l^2 \sigma^2}\right), \quad l = 0, 1, 2, \cdots . \tag{5.20}$$

The step function-like solutions can be approximated by reducing the integro-differential equation (5.11) to a partial differential equation. Methods applicable to ordinary and partial differential equations can also be used to study (5.11).

Implication for system behaviour

For non-symmetric interaction where there is higher nonlinearity the aggregation becomes mass dependent and for sufficiently small mass, namely $M < 1$ (for $M = 1$, $-p + Mp'$ vanishes) and decreasing inaccuracy σ lead to instability. For p at low filament density, a single filament that turns must interact with two filaments, because $p(c) \approx c^2$. At high density, differences in filament distribution at different orientations cannot be sensed by the filament, because $p(c) \approx \frac{1}{\beta}$ is constant. For small inaccuracy σ stationary solutions in numerical simulations consist of areas with equal density which are bounded by steep continuous descents to 0 ([60]). Thus, for small inaccuracy the integro-differential equation is basically a reaction-diffusion- system in which the diffusion term comes from the deviation from the optimal orientation v and the reaction term is due to interaction and turning ([56]). The diffusion not only smoothes the boundaries of homogeneous aggregates but also determines their density. For (5.11) numerical simulations lead to several peak-like aggregation centers when turnings take a filament almost to the interaction partner. For example, $v(\psi) = (1 - k)\psi$ with $0 < k \ll 1$ and $\sigma \ll 1$. Similarly, non-symmetric and non-saturating interaction, $p(f) = f^2$, leads to peak formation at small inaccuracy. With saturation, these peaks are flattened out to aggregation areas with homogeneous density in the interior. The basic reason is that the turning rate $W[c](\theta, .)$ is more or less constant toward all orientations where filament density is high enough ([56]).

5.2.5 Summary

Overview of system dynamics

The OAP exhibits varied and complicated behaviour. This behaviour includes backward bifurcations and hysteresis, peak solutions, the formation of bundles and networks, step function like solutions in instances of higher nonlinearity, unstable trivial solutions and a diversity of time periodic solutions. In general global forward bifurcation is the rule given an attracting optimal turning and homogeneous interaction rate. However, in particular where filaments do not turn when the interaction angle is too large - a cutting of the effective interaction rate - hysteresis is observed in the system. The type of aggregate for example uni-directional, bi-directional or mixed mode bundling may depend on the initial filament distribution or the history of the experiment. When the inaccuracy decreases, $\alpha = 0$, a single peak, i.e. a very tight unidirectional bundle is a stable solution. This behaviour indicates that travelling waves, oscillating bundles and bidirectional bundles might lose their stability. Changes in the concentration of actin binding proteins may lead to changes in the bundling patterns of the actin proteins and these filaments will orient into uni and bi-directional bundles via transitional mixed mode states. Transitions from bundles to networks is through a mixed mode solution state or the homogenous solution or both. For instance with regard to stable solutions with increasing proportion of network forming proteins i.e. with increasing α a unidirectional bundle may spread out and split into two neighbouring bundles while at the same time two additional bundles appear, usually nearby and out of these four unequal bundles a network gradually develops. Transitions from bidirectional bundles to networks are completely analogous to those of uni to bidirectional bundles, but with doubled periodicity i.e., there are two and four bundles instead of one and two ([56]). Simulations of transitions between different orientation structures model slow and

gradual changes in the mixture of actin binding proteins. Sudden changes in the composition, namely from one type of actin binding protein to another - either by setting α from 0 to 1 or by using a pre-structured initial condition will lead to different types of transitions. If the aggregate has fewer bundles than required by the dynamics of the system, then the requisite bundles gradually form in between the existing ones. If, on the other hand, the existing structure has more bundles, i.e., has higher symmetry, then the aggregate dissolves and the necessary number of bundles grow from an almost homogeneous distribution. In the latter case the orientation of the new bundle is rarely related to the orientation of its predecessor ([56]).

5.2.6 Limitations of the approaches to solving the OAP

The varied approaches to analysing the orientation aggregation model have all returned approximate solutions to the orientation aggregation model (5.11). This is because it is not possible to evaluate the complicated nonlinear expressions appearing in the orientation equation. As a consequence the approach to understanding the system behaviour has been numerical in nature. Further the numerical procedures employed to date are limited in scope, computationally demanding and have returned limited information. For instance, in exploring how non trivial solutions branch off of the trivial solutions, unstable branches could not be obtained numerically ([60]). Reversing time did not help since there are infinitely many other directions in which these branches are stable (5.4). To further the understanding of the system behaviour, a variety of methods numerical and otherwise must be incorporated. The required additional approaches such as Lyapunov Schmidt reduction and any needed change in analysis parameters lend further computational work to the study of the system. As a consequence an understanding of global system behaviour is limited and must be diligently built up. In carrying out numerical analysis assumptions are made about parameter functions and the bifurcation parameters. For example, in carrying out a Lyapunov Schmidt reduction with regard to codimension 1 bifurcations it is assumed that parameter functions such as h,v and σ depend analytically on a bifurcation parameter. This assumption led to a system of fixed point equations. An Ansatz for solutions of this system of equations led not to solutions but to a second system of inequalities ([60]). Additional assumptions about the nature of the nonlinear behaviour and the implementation of the Fourier transformation are also necessarily made but the extent to which the obtained solutions conform to the physical reality remain unclear ([56]). Through linearisation the orientation aggregation model is transformed into a mathematical one which deviates in degree in its representation of the actual real world system dynamics. So the assumptions and the associated mathematical approach will influence the types of solutions generated and the extent to which the solutions adequately represent actual system behaviour. Numerical analysis allows the calculation of approximate solutions for some values of time and space. The overall picture of system behaviour is therefore difficult to ascertain and other important, delicate, system behaviour may be overlooked, especially for very small time and space values. For instance in ([56]) the most frequent transitions between uni and bidirectional bundles when parameters vary were explored but there remained the possibility of more complicated ways of transition. For example, higher mode instabilities, appearing at small turnings $k \ll 1$ and small inaccuracy $\sigma \ll 1$, was observed to lead to behaviour that is difficult to analyse numerically. The possibility remains that the coefficients in the Lyapunov Schmidt reduction may have different signs to those assumed leading to other periodic solutions. Since Fourier transformation has been a basic

means of analysis the method will not be applicable to similar integro-differential equations in the presence of non-periodic boundary conditions. Models where there is a higher dimension involving an interaction between space and orientation would prove much more challenging to analyse numerically ([56]).

5.3 Suitability of the ADM for solving the OAP

Closed form solutions to the orientation aggregation model (5.11) have never been found because to date it has not been possible to treat the intricate nonlinearity arising in the orientation equation. Further still, theory governing the search of solutions to nonlinear models of this type is still being developed ([9]). The ADM successfully treats nonlinearity of the kind found in the OAP analytically. However, it has been shown that the ADM is only likely to generate closed form solutions in special cases (cf. proposition 6.6) as although it enables, in theory, more and more terms to be generated these in turn require more and more work (cf. proposition 6.7). The method can be implemented in a straight forward manner to the orientation aggregation problem irrespective of the initial, boundary conditions and as such it does not change the nature of the orientation aggregation model. There is no need to linearise, to parameterise, to make assumptions regarding the nature of the nonlinearity or the form of the solution. Therefore solutions obtained through the use of the ADM conform to the physical reality. These closed form solutions will more effectively facilitate a better real world understanding of the system behaviour.

Chapter 6

General formulation of the ADM for the OAP

Recall the details of the OAP as described in (5.6-5.8). The integro-differential equation representing the temporal development of the mean density distribution of filaments is

$$c_t(\theta, t) = F(c)(\theta, t) \tag{6.1}$$

with initial distribution

$$c(\theta, 0) = f(\theta), \tag{6.2}$$

where f is a periodic function $f : S^1 \to \mathbb{R}$ with $\int_{-\pi}^{\pi} f(\theta)\,\mathrm{d}\theta = 1$. The expression $F(c)$ means that F is a functional of c and specifically the nonlinearity of F in (6.1) is given by

$$F(c)(\theta, t) = \int_{-\pi}^{\pi} W[c](\psi, \theta)\, c(\psi, t)\,\mathrm{d}\psi - c(\theta, t) \int_{-\pi}^{\pi} W[c](\theta, \psi)\,\mathrm{d}\psi \tag{6.3}$$

where

$$\begin{aligned} W[c](\theta, \psi) &= \int_{-\pi}^{\pi} K(\theta - \psi, \theta - \phi, c(\theta, t))\,\mathrm{d}\phi \\ &= \int_{-\pi}^{\pi} h_\rho(\theta - \phi)\, w(\theta - \psi, \theta - \phi)\, p_\beta(c(\phi, t))\,\mathrm{d}\phi. \end{aligned}$$

Integrating in time, using the initial condition f, (6.1) is transformed into the integral equation

$$c(\theta, t) = f(\theta) + \int_0^t F(c)(\theta, s)\,\mathrm{d}s. \tag{6.4}$$

To apply the Adomian method to (6.4), the unknown function c is decomposed into an infinite series of components

$$c(\theta, t) = \sum_{n=0}^{\infty} c_n(\theta, t) = f(\theta) + \sum_{n=1}^{\infty} c_n(\theta, t),$$

where $c_0(\theta, t) = f(\theta)$. The nonlinear terms in (6.4) are basically represented from the integration of the Adomian polynomials obtained from p_β. This is explored in more detail in the next section.

6.1 Rationale for the calculation of the Adomian polynomials

$$\begin{aligned} F(c)(\theta,t) &= \int_{-\pi}^{\pi}\int_{-\pi}^{\pi} h_\rho(\theta-\phi)\, w(\psi-\theta,\theta-\phi)\, p_\beta(c(\phi,t))\,\mathrm{d}\phi\, c(\psi,t)\,\mathrm{d}\psi \\ &- c(\theta,t)\int_{-\pi}^{\pi}\int_{-\pi}^{\pi} h_\rho(\theta-\phi)\, w(\theta-\psi,\theta-\phi)\, p_\beta(c(\phi,t))\,\mathrm{d}\phi\,\mathrm{d}\psi \end{aligned} \tag{6.5}$$

A careful examination of the structure of F in (6.3) and (6.5) indicates that the nonlinear behaviour of F depends on products of the type

$$g_\beta(c)(\phi,\psi,t) = p_\beta(c(\phi,t))\, c(\psi,t). \tag{6.6}$$

From Lemma A.6, the Adomian polynomials of the function g_β at c_0 are given by

$$A_n[g_\beta,c_0](c)(\phi,\psi,t) = \sum_{k=0}^{n} A_k[p_\beta,c_0](c)(\phi,t)\, c_{n-k}(\psi,t),\ n\geq 0.$$

The explicit calculation of the Adomian series for (6.4) can now be made.

Theorem 6.1 *1. Let $f : S^1\times\mathbb{R}\to\mathbb{R}$ be an analytic function. For $n\geq 0$, the Adomian polynomials for F at f are equal to*

$$\begin{aligned} A_n[F,f](c)(\theta,t) &= \sum_{k=0}^{n}\int_{-\pi}^{\pi}\int_{-\pi}^{\pi} A_k[p_\beta,f](c)(\phi,t)\,[h_\rho(\psi-\phi)\, w(\psi-\theta,\psi-\phi)\, c_{n-k}(\psi,t) \\ &\qquad -h_\rho(\theta-\phi)\, w(\theta-\psi,\theta-\phi)\ c_{n-k}(\theta,t)]\ \mathrm{d}\phi\mathrm{d}\psi. \end{aligned}$$

2. The Adomian recursive formula for the solution of (6.4) is then given as

$$c_0(\theta,t) = f(\theta), \tag{6.7}$$

$$c_{n+1}(\theta,t) = \int_0^t A_n[F,f](c)(\theta,s)\,\mathrm{d}s,\ n\geq 0. \tag{6.8}$$

Proof. Because the integrals and the multiplication by h_ρ and w are linear operations, independent of c, the result follows from the definition and results of Appendix A. □

6.1.1 Examples

We consider two cases for p_β, the quadratic and sigmoid form nonlinearities. Set $c(\phi,t) = \sum_{n=0}^{\infty} c_n(\phi,t)$. Following Proposition A.5, when $p_\beta(c) = c$ in (6.6), the Adomian polynomials corresponding to g_β are

$$A_n[g_\beta,c_0](\phi,\psi,t) = \sum_{i=0}^{n} c_i(\phi,t)c_{n-i}(\psi,t), n\geq 0. \tag{6.9}$$

For the sigmoid form nonlinearity, when p_β is of the form

$$p_\beta(c) = \frac{c^2}{1+\beta^2 c^2}, \tag{6.10}$$

the calculations are more complicated. The first three Adomian polynomials are the following.

Proposition 6.2 *Given g_β in (6.6) with p_β in (6.10), the Adomian polynomials $A_i[g_\beta, c_0]$, $i = 0, 1, 2$, are the following.*

$$\begin{aligned}
A_0[g_\beta, c_0](\phi,\psi,t) &= \frac{c_0^2(\phi,t)\, c_0(\psi,t)}{1+\beta^2 c_0^2(\phi,t)}, &(6.11)\\
A_1[g_\beta, c_0](\phi,\psi,t) &= \frac{2c_0(\phi,t)c_1(\phi,t)c_0(\psi,t)}{(1+\beta^2 c_0^2(\phi,t))^2} + \frac{c_0^2(\phi,t)c_1(\psi,t)}{1+\beta^2 c_0^2(\phi,t)}, &(6.12)\\
A_2[g_\beta, c_0](\phi,\psi,t) &= \frac{c_0^2(\phi,t)c_2(\psi,t)}{1+\beta^2 c_0^2(\phi,t)} + \frac{2c_0(\phi,t)}{(1+\beta^2 c_0^2(\phi,t))^2}\big(c_0(\psi,t)c_2(\phi,t) + c_1(\phi,t)c_1(\psi,t)\big)\\
&\quad + \frac{(1-3\beta^2 c_0^2(\phi,t))}{(1+\beta^2 c_0^2(\phi,t))^3}\, c_1^2(\phi,t)c_0(\psi,t). &(6.13)
\end{aligned}$$

Proof. By definition $A_0[g_\beta, c_0](\phi,\psi,t) = g_\beta\left(c_0(\phi,t), c_0(\psi,t)\right)$. The two other results follow from (A.18) and (A.19) because $p'_\beta(c) = \dfrac{2c}{(1+\beta^2c^2)^2}$ and $p''_\beta(c) = \dfrac{2(1-3\beta^2c^2)}{(1+\beta^2c^2)^3}$. □

6.2 Solutions with zero turning functions

Given a bounded function $c : S^1 \times \mathbb{R} \to \mathbb{R}$, periodic in its first variable, and a continuous function $p_\beta : \mathbb{R} \to \mathbb{R}$, we define the functional term

$$P_\beta(c)(t) = \frac{1}{2\pi}\int_{-\pi}^{\pi} p_\beta(c(\phi,t))\,\mathrm{d}\phi. \tag{6.14}$$

Lemma 6.3 *When h_ρ is a constant, $h_\rho(x) = \frac{1}{2\pi}$, and the turning function $v_{k,\mu}$ is zero in (5.9), (6.1) simplifies to*

$$c_t(\theta,t) = P_\beta(c)(t)\left[\left(\int_{-\pi}^{\pi} g_\sigma(\psi-\theta)\, c(\psi,t)\,\mathrm{d}\psi\right) - c(\theta,t)\right]. \tag{6.15}$$

Proof. Under our hypotheses, (6.1) simplifies to

$$\begin{aligned}
c_t(\theta,t) &= \frac{1}{2\pi}\int_{-\pi}^{\pi}\int_{-\pi}^{\pi} p_\beta(c(\phi,t))\left[g_\sigma(\psi-\theta)\, c(\psi,t) - g_\sigma(\theta-\psi)\, c(\theta,t)\right]\,\mathrm{d}\phi\mathrm{d}\psi\\
&= \frac{1}{2\pi}\left(\int_{-\pi}^{\pi} p_\beta(c(\phi,t))\,\mathrm{d}\phi\right)\left[\left(\int_{-\pi}^{\pi} g_\sigma(\psi-\theta)\, c(\psi,t)\,\mathrm{d}\psi\right) - \int_{-\pi}^{\pi} g_\sigma(\theta-\psi)\, c(\theta,t)\mathrm{d}\psi\right]\\
&= P_\beta(c)(t)\left[\left(\int_{-\pi}^{\pi} g_\sigma(\psi-\theta)\, c(\psi,t)\,\mathrm{d}\psi\right) - c(\theta,t)\right],
\end{aligned}$$

because g_σ is a probability distribution and the $p_\beta(c)$ term is the only function of ϕ. $\square$

When g_σ is the periodic Gaussian,

$$g_\sigma(x) = \frac{1}{\sigma\sqrt{2\pi}} \sum_{n\in\mathbb{Z}} e^{-\frac{1}{2}(\frac{x+2\pi n}{\sigma})^2},$$

the dynamics of (6.15) is simplified further. Before we look into it, we need the following properties of integration of g_σ.

Lemma 6.4 *1. Let $f : S^1 \to \mathbb{R}$ be a bounded periodic function, then*

$$\sigma\sqrt{2\pi} \int_{-\pi}^{\pi} g_\sigma(\theta)\, f(\theta)\, \mathrm{d}\theta = \sum_{n\in\mathbb{Z}} \int_{-\pi}^{\pi} e^{-\frac{1}{2}(\frac{\theta+2\pi n}{\sigma})^2} f(\theta)\, \mathrm{d}\theta = \int_{\mathbb{R}} e^{-\frac{1}{2}(\frac{\theta}{\sigma})^2} f(\theta)\, \mathrm{d}\theta. \tag{6.16}$$

2. For every $k \in \mathbb{Z}$,

$$\int_{-\pi}^{\pi} g_\sigma(\psi-\theta)\, e^{ik\psi} \mathrm{d}\psi = e^{-\frac{k^2\sigma^2}{2}} e^{ik\theta}. \tag{6.17}$$

In particular (6.17) is also true for the integrals of the real and imaginary parts of $e^{ik\theta}$, namely $\cos(k\theta)$ and $\sin(k\theta)$.

3. Let $c : \mathbb{R} \to \mathbb{R}$ be a bounded 2π-periodic function, of Fourier series

$$c(\theta) = \frac{1}{2\pi} + \sum_{k=1}^{\infty} \left(a_k \cos k\theta + b_k \sin k\theta\right).$$

Then,

$$\int_{-\pi}^{\pi} g_\sigma(\psi-\theta)\, c(\psi)\, \mathrm{d}\psi = \frac{1}{2\pi} + \sum_{k=1}^{\infty} e^{-\frac{k^2\sigma^2}{2}} \left(a_k \cos k\theta + b_k \sin k\theta\right).$$

Proof.

1. It is a straightforward calculation for the first part because the series of integrals converge (f is bounded) and the 2π-periodic property of f implies that

$$\begin{aligned} \int_{-\pi}^{\pi} e^{-\frac{1}{2}(\frac{\theta+2\pi n}{\sigma})^2} f(\theta)\, \mathrm{d}\theta &= \int_{-\pi+2\pi n}^{\pi+2\pi n} e^{-\frac{1}{2}(\frac{\theta}{\sigma})^2} f(\theta-2\pi n)\, \mathrm{d}\theta \\ &= \int_{-\pi+2\pi n}^{\pi 2\pi n} e^{-\frac{1}{2}(\frac{\theta}{\sigma})^2} f(\theta)\, \mathrm{d}\theta. \end{aligned} \tag{6.18}$$

2. Using the first part with $f(\psi-\theta) = e^{ik(\psi-\theta)}$ leads to,

$$\int_{-\pi}^{\pi} g_\sigma(\psi-\theta)\, e^{ik\psi} \mathrm{d}\psi = \frac{1}{\sigma\sqrt{2\pi}} \int_{\mathbb{R}} e^{-\frac{1}{2}\frac{(\psi-\theta)^2}{\sigma^2}} e^{ik\psi} \mathrm{d}\psi.$$

Therefore, we can conclude because

$$\begin{aligned}\int_{\mathbb{R}} e^{-\frac{1}{2}\frac{(\psi-\theta)^2}{\sigma^2}} e^{ik\psi}\mathrm{d}\psi &= \int_{\mathbb{R}} e^{-\frac{1}{2}\frac{x^2}{\sigma^2}}\, e^{ik(x+\theta)}\mathrm{d}x = \int_{\mathbb{R}} e^{-\frac{1}{2}\left(\frac{x^2}{\sigma^2}\right)+ik(x+\theta)}\mathrm{d}x \\ &= e^{ik\theta}\int_{\mathbb{R}} e^{-\frac{1}{2}\left(\frac{x}{\sigma}-ik\sigma\right)^2+\frac{1}{2}(ik\sigma)^2}\mathrm{d}x = e^{ik\theta}e^{-\frac{1}{2}(k\sigma)^2}\int_{\mathbb{R}} e^{-\frac{1}{2}\left(\frac{x}{\sigma}\right)^2}\mathrm{d}x \\ &= \sigma\sqrt{2\pi}\, e^{-\frac{k^2\sigma^2}{2}} e^{ik\theta}.\end{aligned}$$

3. Evaluate,

$$\begin{aligned}\int_{-\pi}^{\pi} g_\sigma(\psi-\theta)\, c(\psi)\,\mathrm{d}\psi &= \int_{-\pi}^{\pi} g_\sigma(\psi-\theta)\left[\frac{1}{2\pi}+\sum_{k=1}^{\infty}\left(a_k\cos k\theta + b_k\sin k\theta\right)\right]\mathrm{d}\psi \\ &= \frac{1}{2\pi}\int_{-\pi}^{\pi} g_\sigma(\psi-\theta)\,\mathrm{d}\psi \\ &\quad +\sum_{k=1}^{\infty}\left[a_k\int_{-\pi}^{\pi} g_\sigma(\psi-\theta)\cos(k\psi)\,\mathrm{d}\psi + b_k\int_{-\pi}^{\pi} g_\sigma(\psi-\theta)\sin(k\psi)\,\mathrm{d}\psi\right] \\ &= \frac{1}{2\pi}+\sum_{k=1}^{\infty} e^{-\frac{k^2\sigma^2}{2}}\left(a_k\cos k\theta + b_k\sin k\theta\right).\end{aligned}$$

□

We can now show the following results about the solution of (6.15) in terms of the Fourier coefficients of the initial distribution. It says that, under the current hypotheses of this section, no Fourier mode will be activated because of the dynamics of (6.1).

Proposition 6.5 *When h_ρ is a constant, the turning function $v_{k,\mu}$ is zero and the variation function g_σ is a periodic Gaussian, solutions $c(\theta,t)$ of (6.15) with $c(\theta,0)=f(\theta)$, where*

$$f(\theta)=\frac{1}{2\pi}+\sum_{k=1}^{\infty} a_k(0)\cos(k\theta)+\sum_{k=1}^{\infty} b_k(0)\sin(k\theta),$$

satisfy the following: if any Fourier series coefficient of the initial distribution f is equal to 0, it will remain equal zero for all time.

Proof. Substitute

$$c(\theta,t)=\frac{1}{2\pi}+\sum_{k=1}^{\infty}\left(a_k(t)\cos k\theta + b_k(t)\sin k\theta\right) \tag{6.19}$$

into (6.15), we get

$$c_t(\theta,t)=\sum_{k=1}^{\infty}\left(\dot{a}_k(t)\cos k\theta+\dot{b}_k(t)\sin k\theta\right)=P_\beta(c)(t)\left[\left(\int_{-\pi}^{\pi} g_\sigma(\psi-\theta)\, c(\psi,t)\,\mathrm{d}\psi\right)-c(\theta,t)\right].$$

Use (6.17) to evaluate

$$\int_{-\pi}^{\pi} g_\sigma(\psi-\theta)\, c(\psi,t)\, \mathrm{d}\psi = \frac{1}{2\pi} + \sum_{k=1}^{\infty} e^{-\frac{k^2\sigma^2}{2}} \big(a_k(t)\cos k\theta + b_k(t)\sin k\theta\big).$$

Combined with $c(\theta,t)$, we get

$$\sum_{k=1}^{\infty} \left(e^{-\frac{k^2\sigma^2}{2}} - 1\right) \big(a_k(t)\cos k\theta + b_k(t)\sin k\theta\big),$$

and, with (6.14), we get the following infinite system of ODEs for the Fourier coefficients of c:

$$\dot{a}_k(t) = \left(e^{-\frac{k^2\sigma^2}{2}} - 1\right) P_\beta(c)(t)\, a_k(t),\ k \geq 1, \tag{6.20}$$

$$\dot{b}_k(t) = \left(e^{-\frac{k^2\sigma^2}{2}} - 1\right) P_\beta(c)(t)\, b_k(t),\ k \geq 1. \tag{6.21}$$

When $a_k(0)$, resp. $b_k(0)$, equal 0 for some k, we claim that a_k, resp. b_k, is identically 0. This is a direct consequence of the following general result about ODEs. Let $g : [a,b] \to \mathbb{R}$ be a continuous function. Via straightforward differentiation, the solution of the initial value problem

$$\dot{x} = g(t)x(t), \quad x(a) = x_0,$$

is $x(t) = x_0 \exp\left(\int_a^t g(s)ds\right)$. Clearly, if $x_0 = 0$, then $x(t) = 0,\ \forall t \in [a,b]$. □

6.3 Analytical solutions with proportional nonlinear interaction

When $p_\beta(c) = c$, corresponding to a quadratic interaction, we have an explicit solution.

Proposition 6.6 *Under the hypotheses of Proposition 6.5, when the nonlinear interaction is the quadratic case $p_\beta(c) = c$, the solution of (6.1) is*

$$c(\theta,t) = \frac{1}{2\pi} + \sum_{k=1}^{\infty} e^{\frac{(e^{-\frac{1}{2}k^2\sigma^2}-1)t}{2\pi}} \Big(\hat{a}_k \cos k\theta + \hat{b}_k \sin k\theta\Big), \tag{6.22}$$

where the initial distribution in (6.2) is

$$f(\theta) = \frac{1}{2\pi} + \sum_{k=1}^{\infty} \Big(\hat{a}_k \cos k\theta + \hat{b}_k \sin k\theta\Big).$$

Proof. Under the hypotheses (6.14) and (6.19) lead to ,

$$P_\beta(c)(t) = \frac{1}{2\pi}\int_{-\pi}^{\pi} c(\phi,t)\, \mathrm{d}\phi = \frac{1}{2\pi},$$

and so (6.20,6.21) become

$$\dot{a}_k = \frac{1}{2\pi}\left(e^{-\frac{k^2\sigma^2}{2}} - 1\right) a_k,\ k \geq 1, \tag{6.23}$$

$$\dot{b}_k = \frac{1}{2\pi}\left(e^{-\frac{k^2\sigma^2}{2}} - 1\right) b_k,\ k \geq 1, \tag{6.24}$$

with the initial conditions $a_k(0) = \hat{a}_k$ and $b_k(0) = \hat{b}_k$. A simple integration gives the result. □

Implementing the ADM led to the discovery of the ODEs (6.23,6.24). The reduction of the OAP to those ODEs indicates a constant geometry of the OAP in θ in the sense that the ratio of the filament distributions at two different times only depends on those times, not on the orientation of the filaments. Essentially similar behaviour in the pattern of solution terms and resulting ODEs are to be observed when the ADM is implemented for higher nonlinearities such as ρ_β being a sigmoid function.

6.4 Sigmoid function, nonproportional nonlinear interaction

In this section we consider the analytical solution with the nonlinear interaction given by the sigmoid function

$$p_\beta(c) = \frac{c^2}{1 + \beta^2 c^2}, \tag{6.25}$$

while keeping the same hypotheses as in Section 6.3, namely h_ρ is a constant, $h_\rho(x) = \frac{1}{2\pi}$, the turning function $v_{k,\mu}$ is zero in (5.9), and the probability distribution g_σ is the periodic Gaussian. The integral equation (6.4) transforms into a coupled system of integral equations.

Proposition 6.7 *Under the hypotheses of this section, let*

$$c(\theta, t) = \frac{1}{2\pi} + \sum_{k=1}^{\infty} (a_k(t)\cos k\theta + b_k(t)\sin k\theta), \tag{6.26}$$

be the Fourier decomposition of the solution c of (6.4), then its Fourier coefficients satisfy the following nonlinear system of integral equations

$$a_k(t) = a_k(0) + \left(e^{-\frac{k^2\sigma^2}{2}} - 1\right) \int_0^t P_\beta(c)(s)\, a_k(s)\, \mathrm{d}s,\ k \geq 1, \tag{6.27}$$

$$b_k(t) = b_k(0) + \left(e^{-\frac{k^2\sigma^2}{2}} - 1\right) \int_0^t P_\beta(c)(s)\, b_k(s)\, \mathrm{d}s,\ k \geq 1, \tag{6.28}$$

where P_β is given in (6.14) and c in (6.19).

Proof. The results follows from the integration of (6.20) and (6.21). □

Using the information of Theorem 6.1, we get the Adomian polynomials of the right hand side of (6.15) using the Adomian polynomials of P_β. We seek solutions in the form of a series

$$c(\theta, t) = f(\theta) + \sum_{n=1}^{\infty} c_n(\theta, t)$$

using the Adomian method.

Proposition 6.8 *When $c_0(\theta,t) = f(\theta) = \frac{1}{2\pi} + Q\cos k\theta$, with $k \in \mathbb{Z}$, the next two terms of the series solution of c given by the Adomian decomposition method are*

$$c_1(\theta,t) = \frac{HQ}{2\pi}\left[e^{-\frac{1}{2}k^2\sigma^2} - 1\right] t\cos k\theta, \tag{6.29}$$

where H is given in (E.18), and

$$c_2(\theta,t) = \left(e^{-\frac{k^2\sigma^2}{2}} - 1\right)^2 \frac{H}{8\pi^2}\left(HQ - \frac{\pi}{4\beta^3}\sqrt{\frac{d}{L}}\,\widehat{H}\right) t^2\cos k\theta. \tag{6.30}$$

with (cf. (E.19), (E.20) and (E.21))

$$\begin{aligned} d &= \frac{\beta Q}{1+\beta^2(Q-\frac{1}{2\pi})^2} && (6.31)\\ \xi &= \frac{\beta}{2Q}\left(Q^2 - \frac{1}{4\pi^2} - \frac{1}{\beta^2}\right) && (6.32)\\ L &= \xi + \sqrt{1+\xi^2} && (6.33) \end{aligned}$$

$$\widehat{H} = d\left(3-(L)^2\right)\left(1+\frac{(L)^3}{d^3\left(1+(L)^2\right)^3}\right) - 3L\left(1+\frac{L}{d\left(1+(L)^2\right)}\right).$$

Proof. For such c_0, the terms c_n in the decomposition of c are of the form $c_n(\phi,t) = a_k(t)\cos(k\theta)$. The term c_1 is given by

$$\begin{aligned} c_1(\theta,t) &= \int_0^t P_\beta(f)\left[\left(\int_{-\pi}^{\pi} g_\sigma(\psi-\theta)\,f(\psi)\,\mathrm{d}\psi\right) - f(\theta)\right]\mathrm{d}s \\ &= P_\beta(f)\int_0^t Q[e^{-\frac{k^2\sigma^2}{2}} - 1](\cos k\theta)\,\mathrm{d}s = P_\beta(f)Q[e^{-\frac{k^2\sigma^2}{2}} - 1]\; t\cos k\theta. \end{aligned}$$

In Lemma E.5 we calculate $P_\beta(f)$ as $\dfrac{H}{2\pi}$, and so we get (6.29).

For c_2, we have

$$\begin{aligned} c_2(\theta,t) &= \int_0^t \left(P'_\beta(f)c_1\right)(s)\left(e^{-\frac{k^2\sigma^2}{2}} - 1\right)Q\cos(k\theta)\,\mathrm{d}s + \int_0^t P_\beta(f)\left(e^{-\frac{k^2\sigma^2}{2}} - 1\right)c_1(\theta,s)\,\mathrm{d}s \\ &= \left(e^{-\frac{k^2\sigma^2}{2}} - 1\right)\left[Q\cos(k\theta)\int_0^t \left(P'_\beta(f)c_1\right)(s)\,\mathrm{d}s + P_\beta(f)\int_0^t c_1(\theta,s)\,\mathrm{d}s\right], \\ &= \left(e^{-\frac{k^2\sigma^2}{2}} - 1\right)Q\cos(k\theta)\int_0^t \left(P'_\beta(f)c_1\right)(s)\,\mathrm{d}s + \left(e^{-\frac{k^2\sigma^2}{2}} - 1\right)^2\frac{H^2}{4\pi^2}\,Q\,\frac{t^2}{2}\cos(k\theta). \end{aligned}$$

where the Fréchet derivative of P_β is given by

$$\begin{aligned}\left(P'_\beta(f)c_1\right)(t) &= \frac{1}{2\pi}\int_{-\pi}^{\pi} p'_\beta(f(\phi))\, c_1(\phi,t)\,\mathrm{d}\phi \\ &= \frac{1}{2\pi}\int_{-\pi}^{\pi} p'_\beta(f(\phi))\, P_\beta(f) Qt[e^{-\frac{k^2\sigma^2}{2}}-1]\cos(k\phi)\,\mathrm{d}\phi \\ &= \frac{H}{4\pi^2}[e^{-\frac{k^2\sigma^2}{2}}-1]\,Qt\int_{-\pi}^{\pi} p'_\beta(f(\phi))\,\cos(k\phi)\,\mathrm{d}\phi. \qquad (6.34)\end{aligned}$$

The integral $\int_{-\pi}^{\pi} p'_\beta(f(\phi))\,\cos(k\phi)\,\mathrm{d}\phi$ is evaluated in (E.47).

$$\frac{-\pi}{4Q^2\beta^3}\sqrt{\frac{d}{L}}\left[d\left(3-(L)^2\right)\left(1+\frac{(L)^3}{d^3\left(1+(L)^2\right)^3}\right)-3L\left(1+\frac{L}{d\left(1+(L)^2\right)}\right)\right].$$

Integrating in t the first term of (6.34), and re-arranging the whole expression, we get (6.30). □

Chapter 7

Computer generated solutions to the OAP using the ADM

Using Maple 15 software two computer programs have been developed. Each solves a different form of the OAP of Sections 6.3 and 6.4 by implementing the ADM. Initial conditions and combinations of the form below should be used with the programs:

$$\frac{1}{2\pi} + Q\cos k\theta + P\cos m\theta, \quad \frac{1}{2\pi} + Q\cos k\theta + P\sin m\theta, \quad \frac{1}{2\pi} + Q\sin k\theta + P\sin m\theta,$$

where k and m are integers. The values for P and Q, and β for (6.25), will need to be specified at the start of the program.

For (6.22), the computations such as the evaluation of integrals are done directly using Maple's built in capabilities. However, Maple's built in integration procedure is unable to return a value for expressions such as (E.17) or (E.6). So to programmatically return a solution to (6.25), separate procedures that apply the residue theorem have been written to implement the integration of terms in ϕ appearing in the Adomian polynomials. These procedures also incorporate rules for selecting the correct poles prior to applying the residue theorem.

Once these values are specified, each program returns the corresponding term of the solution up to the fourth recursion of the ADM; finally summing the first four terms of the solution; plotting and animating the sum of the first four terms of the solution for specified values of the parameters m, k, σ and β and the constants P and Q. These parameter and constant values can also be adjusted in order to further explore the solution and system behaviour. The code may also be replicated and modified to generate more terms of the Adomian solution if desired.

With regard to the calculations executed by the programs to generate the ADM solution, when the equation is of the form (6.22), upon specifying the initial condition, it is then substituted into the quadratic form nonlinearity to generate the A_0 polynomial. The integrals appearing in (6.22) are then all evaluated separately. The first inner integral is evaluated with respect to ϕ, then the second also with respect to ϕ, the difference obtained is then evaluated with respect to ψ then finally with respect to time to return the second term of the series solution of the ADM. This overall process is repeated with some variation until the fourth term of the Adomian solution is calculated. The terms are then summed to give the Adomian solution to the fourth

term and the solution is then plotted and animated for specified values of the parameters and constants. In the process of calculating the third and fourth terms of the solution, the initial condition and the previously generated solution terms are programmatically substituted into the general Fréchet derivative form of the Adomian polynomials which have been originally calculated by hand. The successive operations of the program then matches that as described above when A_0 is initially used. Segmenting the program and the calculation of the Adomian polynomials in this manner is advantageous in that it enables the examination of the result of the individual calculations and facilitates the isolation of errors during development.

When the model is (6.25) the program works in a similar manner to that detailed above for (6.22). With the initial conditions used and the sigmoid nonlinearity, integrals involving expressions of the form

$$\frac{\left(\frac{1}{2\pi} + Q\cos k\phi\right)^2}{1 + \beta^2\left(\frac{1}{2\pi} + Q\cos k\phi\right)^2} \tag{7.1}$$

and

$$\frac{\left(\frac{1}{2\pi} + Q\sin k\phi\right)^2}{1 + \beta^2\left(\frac{1}{2\pi} + Q\sin k\phi\right)^2} \tag{7.2}$$

need to be evaluated.

Since they are rational expressions of trigonometric functions the integral identities

$$\int_{-\pi}^{\pi} F(\sin x, \cos x)\,\mathrm{d}x = 2\int_{\infty}^{\infty} F\left(\frac{2u}{1+u^2}, \frac{1-u^2}{1+u^2}\right)\frac{\mathrm{d}u}{1+u^2}, \qquad \text{where} \quad u = \tan\frac{x}{2}, \tag{7.3}$$

with

$$\int_{\infty}^{\infty} F(\sin x, \cos x)\,\mathrm{d}x = \lim_{R\to\infty}\int_{-R}^{R} F\left(\frac{2u}{1+u^2}, \frac{1-u^2}{1+u^2}\right)\frac{\mathrm{d}u}{1+u^2} \tag{7.4}$$

are used. The residue theorem is used with the usual contour of a semicircular arc of radius R above the real interval $[-R, R]$.

But due to the Adomian polynomials corresponding to the nonlinearity (A.14) being in themselves large expressions, the residue theorem cannot be directly applied to the whole Adomian polynomials since Maple may not return a value for the singularities or the residues. Instead, Maple code that evaluates the integral by calculating the integral of each operand in turn by implementing the residue theorem has been written. So, for each term in ϕ composing the Adomian polynomials, the singularities are found, the poles with positive imaginary parts are selected and placed in a list. For each pole in this list, the residue is calculated and, then, these residues are summed and the final sum is multiplied by $2\pi i$ to give the value of the integral. Selection of the poles with positive imaginary parts is done via a function which notes the specified values of β, P, Q and then evaluates the sign of the imaginary part of the pole. The result of evaluating the integral of each term composing the polynomial is then added to a list from

which the value can be called. The result is then recombined using arrays with its corresponding term in ψ making up the Adomian polynomial. Specifically, at this stage the evaluated integral of each operand in ϕ exists in a list. Its correspondent term in ψ is likewise placed in a list, both lists are converted to vectors and recombined by taking the dot product. The result of this are evaluated integrals in ϕ and terms in ψ for which the integrals are unevaluated. From this stage the program then proceeds to evaluate the terms in ψ and t in the same manner as that detailed above for (6.22).

Since convergence of the ADM is rapid, in general the first few terms of the solution gives good accuracy and will be close to the exact solution ([21, 100]). A closed form solution may be deduced by examination of the terms of the series solution generated by the programs. The greater demand of integrating the terms in ϕ for (6.25) illustrates that, while it is possible to calculate the Adomian polynomials for all forms of nonlinearity ([101]), the difficulty in doing so is not uniform for all forms of nonlinearities. Furthermore, it may be progressively more computationally demanding, along with a greater calculating or processing time requirement, to evaluate the resulting terms of the Adomian polynomials for each recursion of the ADM.

Other challenges associated with evaluating the terms of the Adomian polynomials when implementing the ADM programmatically for the OAP may arise. For instance, the associated residues and sum of residues for expressions such as (E.17) or (E.6) are also large expressions and this could lead to progressive expression swell and consequent increasing demand for computer processing memory while calculating the terms of the Adomian solution. Built in Maple simplification at each calculation stage along with the application of simplification rules that have been developed and implemented throughout the program helps to curtail the size of the expressions. A natural consequence of the greater computational demand in calculating the terms of the Adomian solution for (6.25) is that returning the solution has a greater time requirement than its simpler form (6.22).

The singularities of expressions (7.1) and (7.2) themselves are large expressions as are their residues. This means that successive calculations tend to increase in expression size and also increase the processing time required to carry out evaluations. To control this, where expressions become huge numerical evaluation of the large expression is undertaken in order to shrink the expression size, free up memory and accelerate the calculations. The singularities of the expression resulting (from using (7.4)) in u are then calculated but, according to the manner in which Maple finds singularities and calculates residues, expressions of the form (7.2) cannot be calculated using the standard built in residue package while those of the form (7.1) can. Manual calculation of the singularities and residues of (7.1) that had already been carried out prior to the program's development are presented in Appendix E while calculations of the singularities and residues of (7.2) are done exclusively by the Maple program.

To address the difficulty of calculating expressions such as (7.2) the Maple MultiSeries package is utilised instead to evaluate the residues and consequently the integrals of those expressions containing sine. The package overrides the standard calculations of limits and instead performs asymptotic and series expansions in general asymptotic scales. The corresponding MultiSeries functions are more powerful than the default ones, but require more computational time. As a consequence, while initial conditions involving cosine evidently pose no challenge when initial conditions containing sine are given, the program will take longer to compute the terms of the Adomian series. For some initial conditions involving sine and, depending on the values of the

parameters Q, P or β that are given, the program might take a long time or it might not be able to calculate the intended four terms of the Adomian solution. If this happens the user should allow first sufficient time for the computations to complete and then could accept those terms of the series that have been calculated (or change the parameters or initial conditions). At this point the program could be stopped and the user could then proceed to plot and investigate the series solution that has been calculated so far. Bearing in mind that the first few terms of the Adomian series solution provide the greater accuracy.

In spite of these challenges, on the whole, as compared to manual calculation, many solutions to (6.15) can now be quickly and more easily generated by using these programs. The required initial condition is easily specified. Closed form solutions may be deduced. The graphical animation and animation code further facilitates study of the generated solutions and corresponding system behaviour and can be adjusted for different parameter values and graphical views. Compared to traditional linearisation methods used to obtain solutions to the OAP, the computer generated terms of the solution are likely to be to a higher degree of accuracy and to be returned in a shorter or comparable space of time ([27, 46, 47, 56, 57, 83, 99, 101]).

The following sections detail the programmatic instructions for implementing both programs and provide examples of solutions found. Both programs are provided on the enclosed disc.

7.1 Algorithm: Calculate $\sum_{n=0}^{3} c_n(\theta, t)$ with $p_\beta(c) = c$

Input: $\frac{1}{2\pi} + Q\cos(k\theta) + P\cos(m\theta)$, $\frac{1}{2\pi} + Q\sin(k\theta) + P\sin(m\theta)$; $k, m \in \mathbb{Z}$; $P, Q \in \mathbb{R}$.
Output: $\sum_{n=0}^{3} c_n(\theta, t)$.

Begin
define $c(\phi, t)c(\psi, t)$, $c(\phi, t)c(\theta, t)$
write kernel of $c(\theta, t)$
print $c(\theta, t)$ {confirm the form of the orientation problem}
substitute c_0 into $c(\phi, t)c(\psi, t)$, $c(\phi, t)c(\theta, t)$
return A_0, B_0
evaluate first inner integral with respect to ϕ with A_0
evaluate second inner integral with respect to ϕ with B_0
subtract evaluated first inner integral in ϕ from evaluated second inner integral in ϕ
evaluate the remaining integral in ψ
evaluate the remaining integral in t
return $c_1(\theta, t)$
substitute c_0 and c_1 into general Fréchet form of A_1, B_1
return A_1, B_1
evaluate first inner integral with respect to ϕ with A_1
evaluate second inner integral with respect to ϕ with B_1
subtract evaluated first inner integral in ϕ from evaluated second inner integral in ϕ
evaluate the remaining integral in ψ
evaluate the remaining integral in t
return $c_2(\theta, t)$
substitute c_0, c_1, c_2 into general Fréchet form of A_2,B_2
return A_2, B_2
evaluate first inner integral with respect to ϕ with A_2
evaluate second inner integral with respect to ϕ with B_2
subtract evaluated first inner integral in ϕ from evaluated second inner integral in ϕ
evaluate the remaining integral in ψ
evaluate the remaining integral in t
return $\sum_{n=0}^{3} c_n(\theta, t)$
plot $\sum_{n=0}^{3} c_n(\theta, t)$
plot $\sum_{n=0}^{3} c_n(\theta, t)$ for specified parameter values
End.

7.2 Algorithm: Calculate $\sum_{n=0}^{3} c_n(\theta,t)$ with a general $p_\beta(c)$

Input: β, Q, P,$\frac{1}{2\pi}+Q\cos(k\theta)+P\cos(m\theta)$, $\frac{1}{2\pi}+Q\sin(k\theta)+P\sin(m\theta)$; $k,m\in\mathbb{Z}$; $P,Q,\beta\in\mathbb{R}$
Output: $\sum_{n=0}^{3} c_n(\theta,t)$.

Begin
define $c^2(\phi,t)c(\psi,t)$, $c^2(\phi,t)c(\theta,t)$
write kernel of $c(\theta,t)$
print $c(\theta,t)$ {confirm the form of the orientation problem}
substitute u_0 into $c^2(\phi,t)c(\psi,t)$, $c^2(\phi,t)c(\theta,t)$
return A_0,B_0
Begin procedure f() to evaluate integral in ϕ using the residue theorem
if initial condition has cos **then**
  s1:= remove(has,A_0,ψ)
  $s2$:= subs($cos(k\phi)=\left(\frac{(1-u^2)}{(1+u^2)}\right),\cos(m\phi)=\left(\frac{(1-u^2)}{(1+u^2)}\right),\sin(k\phi)=\left(\frac{(2u)}{(1+u^2)}\right),\sin(m\phi)=\left(\frac{(2u)}{(1+u^2)}\right),s1)1/(1+u^2)$
  find the singularities in $s2$
  select poles with positive imaginary parts
  for each pole with positive imaginary part **do**
    calculate the residue of $s2$
    return $2\pi i$ (sum of residues)
  end for
else
  execute f() with(MultiSeries)
end if
end f()
CALL f() with respect to A_0
CALL f() with respect to B_0
subtract evaluated first inner integral in ϕ with A_0 from evaluated second inner integral in ϕ with B_0
evaluate the remaining integral in ψ
evaluate the remaining integral in t
return $c_1(\theta,t)$
substitute c_0 and c_1 into general Fréchet form of A_1, B_1
return A_1, B_1
Begin procedure f1() to evaluate integral in ϕ using the residue theorem
if initial condition has cos **then**
  h:=[];
  for each operand in A_1 **do**
    s1:= select(has,z,ϕ);
    $s2$:= subs($cos(k\phi)=\left(\frac{(1-u^2)}{(1+u^2)}\right),\cos(m\phi)=\left(\frac{(1-u^2)}{(1+u^2)}\right),\sin(k\phi)=\left(\frac{(2u)}{(1+u^2)}\right),\sin(m\phi)=\left(\frac{(2u)}{(1+u^2)}\right),s1)1/(1+u^2)$
    find the singularities in $s2$
    select poles with positive imaginary parts
    for each pole with positive imaginary part **do**

38: calculate the residue of $s2$
return result:= $2\pi i$ (sum of residues)
40: h:=[op(h),result]
end for
42: **end for**
else
44: execute f1() with(MultiSeries)
end if
46: End f1()
CALL f1() with respect to A_1
48: CALL f1() with respect to B_1
subtract evaluated first inner integral in ϕ for A_1 from evaluated second inner integral in ϕ for B_1
50: evaluate the remaining integral in ψ
evaluate the remaining integral in t
52: **return** $c_2(\theta, t)$
substitute c_0, c_1, c_2 into general Fréchet form of A_2, B_2
54: **return** A_2, B_2
simplify A_2, B_2 for large expressions
56: Begin procedure f2() to evaluate integral in ϕ using the residue theorem
if initial condition has cos **then**
58: h:=[];
for each operand in A_2 **do**
60: s1:= select(has,z,ϕ);
$s2$:= subs$(cos(k\phi) = \left(\frac{(1-u^2)}{(1+u^2)}\right), \cos(m\phi) = \left(\frac{(1-u^2)}{(1+u^2)}\right), \sin(k\phi) = \left(\frac{(2u)}{(1+u^2)}\right), \sin(m\phi) = \left(\frac{(2u)}{(1+u^2)}\right), s1)1/(1+u^2)$
62: find the singularities in $s2$
select poles with positive imaginary parts
64: **for** each pole with positive imaginary part **do**
calculate the residue of $s2$
66: **return** result:= $2\pi i$ (sum of residues)
h:=[op(h),result]
68: **end for**
end for
70: **else**
execute f2() with(MultiSeries)
72: **end if**
End f2()
74: CALL f2() with respect to A_2
CALL f2() with respect to B_2
76: subtract evaluated first inner integral in ϕ for A_2 from evaluated second inner integral in ϕ for B_2
evaluate the remaining integral in ψ
78: evaluate the remaining integral in t
return $c_3(\theta, t)$

80: **return** $\sum_{n=0}^{3} c_n(\theta, t)$
plot $\sum_{n=0}^{3} c_n(\theta, t)$
82: plot $\sum_{n=0}^{3} c_n(\theta, t)$ for specified parameter values
End.

7.3 Computer generated solutions

The following sections present graphical displays of the first four terms of the computer generated Adomian solution

$$C_3(\theta, t) = \sum_{n=0}^{3} c_n(\theta, t)$$

and of the closed form solution $c(\theta, t)$ deduced from (6.22) for the quadratic and sigmoid nonlinearities. Recall that the dynamics of (5.6) preserves the positivity of its solutions. For their interpretation in the context of the OAP, solutions must be positive, but, for convenience, we have displayed solutions that change sign.

7.3.1 Plots of solutions where the nonlinearity is $p_\beta(c) = c$

We concentrate on single or bimodal modes initial conditions of the type $c_0(\theta) = \frac{1}{2\pi} + \hat{c}(\theta)$ where $\hat{c}(\theta) = Q\cos k\theta + P\cos m\theta$ or similar linear combinations with sine functions. Let

$$H_3^k(t) = \left[1 - \frac{t}{2\pi}\left(1 - e^{-\frac{k^2\sigma^2}{2}}\right) + \frac{t^2}{8\pi^2}\left(1 - e^{-\frac{k^2\sigma^2}{2}}\right)^2 - \frac{t^3}{48\pi^3}\left(1 - e^{-\frac{k^2\sigma^2}{2}}\right)^3\right] \tag{7.5}$$

represent the Taylor series expansion up to order 3 of

$$\exp\left(\frac{-(1 - e^{-\frac{k^2\sigma^2}{2}})t}{2\pi}\right).$$

For $c_0(\theta) = \frac{1}{2\pi} + \hat{c}(\theta) = \frac{1}{2\pi} + Q\cos k\theta + P\cos m\theta$, we get

$$C_3(\theta, t) = \frac{1}{2\pi} + Q\, H_3^k(t)\cdot\cos k\theta + P\, H_3^m(t)\cdot\cos m\theta. \tag{7.6}$$

The terms of the ADM solution are plotted below along with any corresponding closed form solutions. In our case each solution tends uniformly to the uniform distribution $\frac{1}{2\pi}$ as t tends to infinity.

We consider first single mode solutions. In Figures 7.1, respectively 7.2, we represent, on the left, the ADM solution $C_3(\theta, t)$ and, on the right, the closed form solution $c(\theta, t)$ for $c_0(\theta) = \frac{1}{2\pi} + \cos\theta$, respectively $c_0(\theta) = \frac{1}{2\pi} + \sin\theta$.

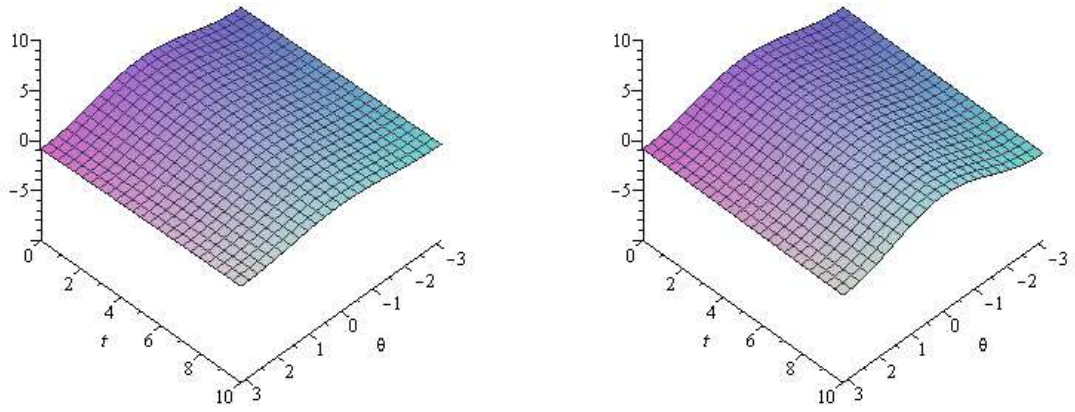

Figure 7.1: $C_3(\theta, t)$ and $c(\theta, t)$ with $c_0(\theta) = \frac{1}{2\pi} + \cos\theta$ and $\sigma = 1$.

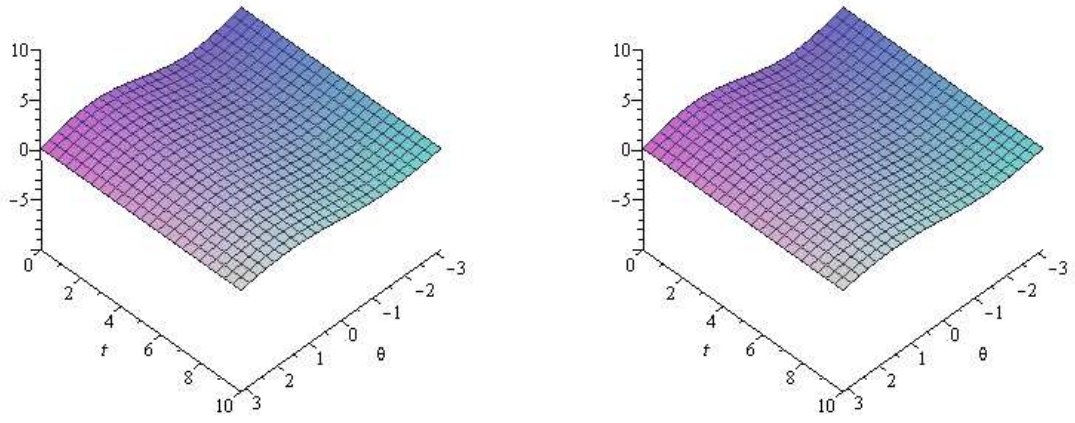

Figure 7.2: $C_3(\theta, t)$ and $c(\theta, t)$ with $c_0(\theta) = \frac{1}{2\pi} + \sin\theta$ and $\sigma = 1$.

Next, we consider two modes solutions.

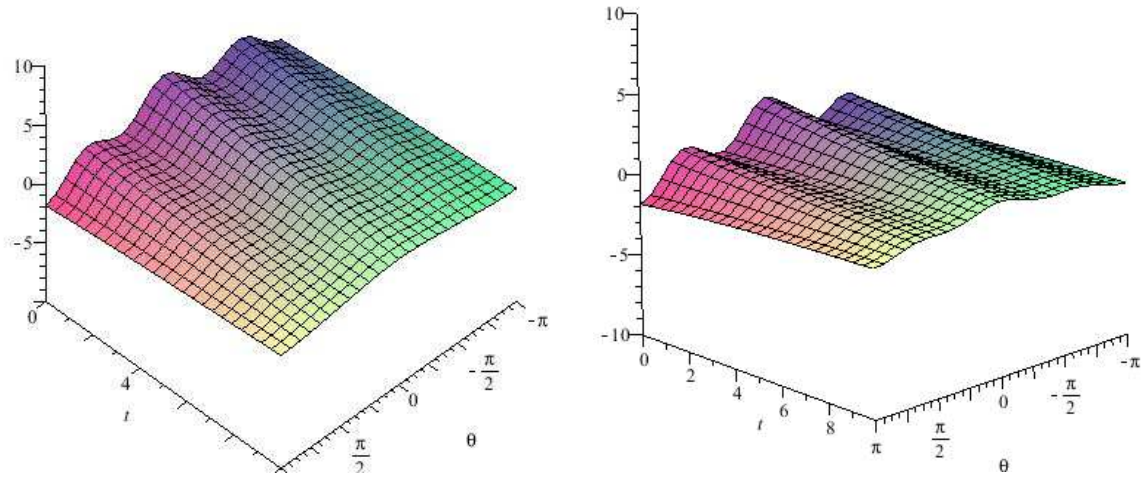

Figure 7.3: $C_3(\theta, t)$ and $c(\theta, t)$ with $c_0(\theta) = \frac{1}{2\pi} + \cos\theta + \cos 3\theta$ and $\sigma = 1$.

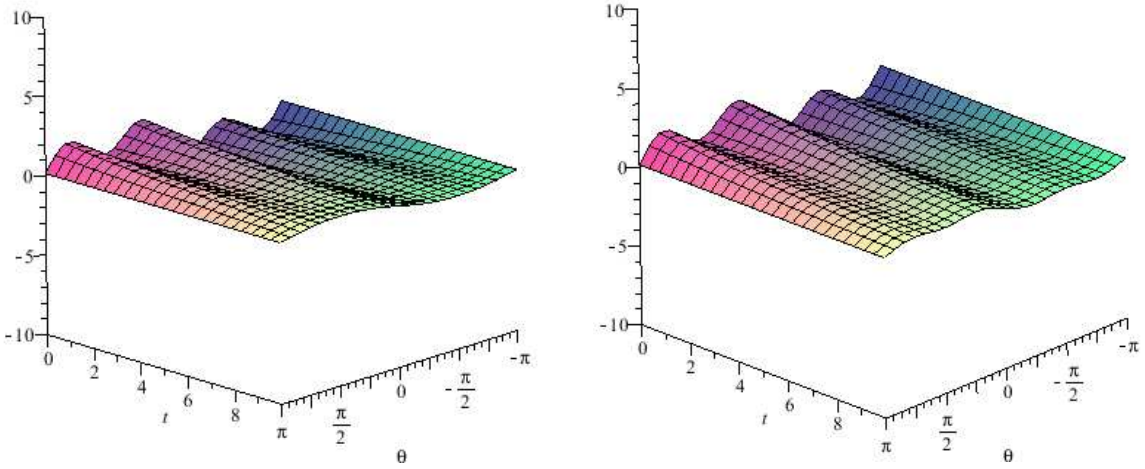

Figure 7.4: $C_3(\theta, t)$ and $c(\theta, t)$ with $c_0(\theta) = \frac{1}{2\pi} + \sin\theta + \sin 3\theta$ and $\sigma = 1$.

Finally, we illustrate the combination of a sine with a cosine mode.

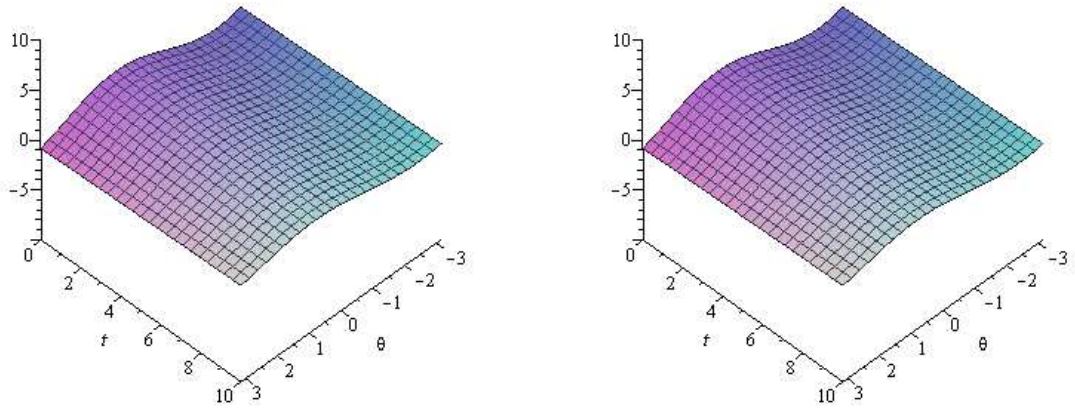

Figure 7.5: $C_3(\theta, t)$ and $c(\theta, t)$ with $c_0(\theta) = \frac{1}{2\pi} + \cos\theta + \sin\theta$ and $\sigma = 1$.

7.3.2 Effect of the different parameters on the solution

The following graphs show the effect of the different parameters k, m, P, Q, σ on the solution for different forms of initial conditions. The graphs show a stricter alignment of filaments for σ small. The graphs show that as σ increases the spread of filaments increase and they become less closely aligned.

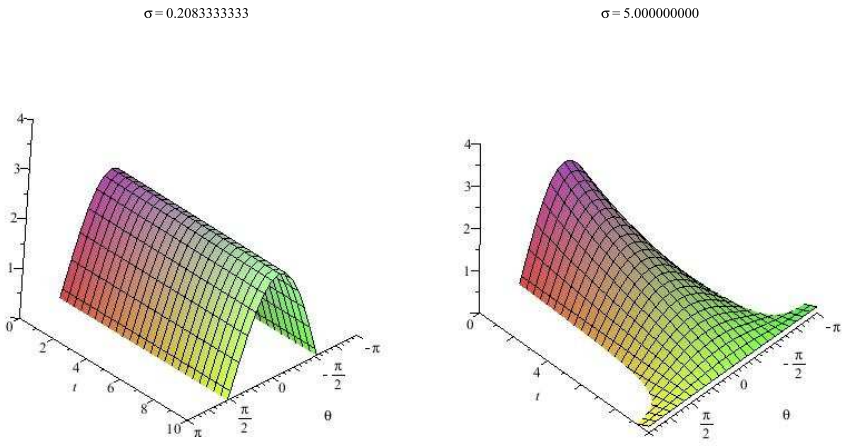

Figure 7.6: $C_3(\theta, t)$ with $c_0(\theta) = \frac{1}{2\pi} + 2\cos\theta$ and $\sigma = 0.2083$, $\sigma = 5$.

On the mixed mode solution, when $\sigma = 0.20833333$, the graph peaks at $\frac{\pi}{4}$.

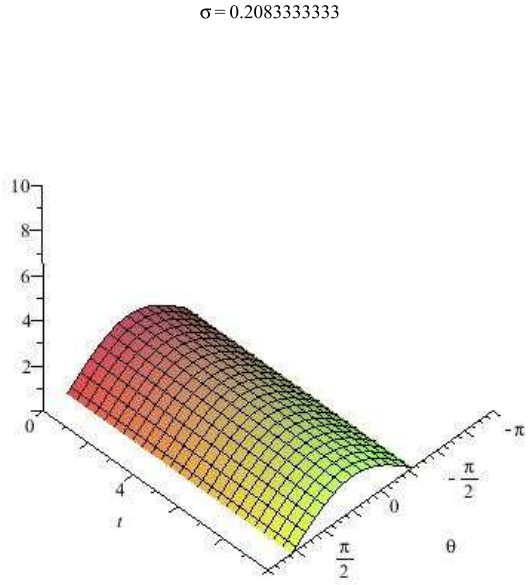

Figure 7.7: $c(\theta, t)$ with $c_0(\theta) = \frac{1}{2\pi} + \cos\theta + \sin\theta$ with $\sigma = 0.2083333$.

Both P and Q affect the amplitude of the solution. The greater the value of P or Q the greater the amplitude. While solutions containing $\cos\theta$ will manifest peaks at zero, solutions containing $\sin\theta$ will manifest peaks at $\frac{\pi}{2}$. In general the peak of plots of solutions for different parameters will shift depending on whether sine or cosine is present in the solution.

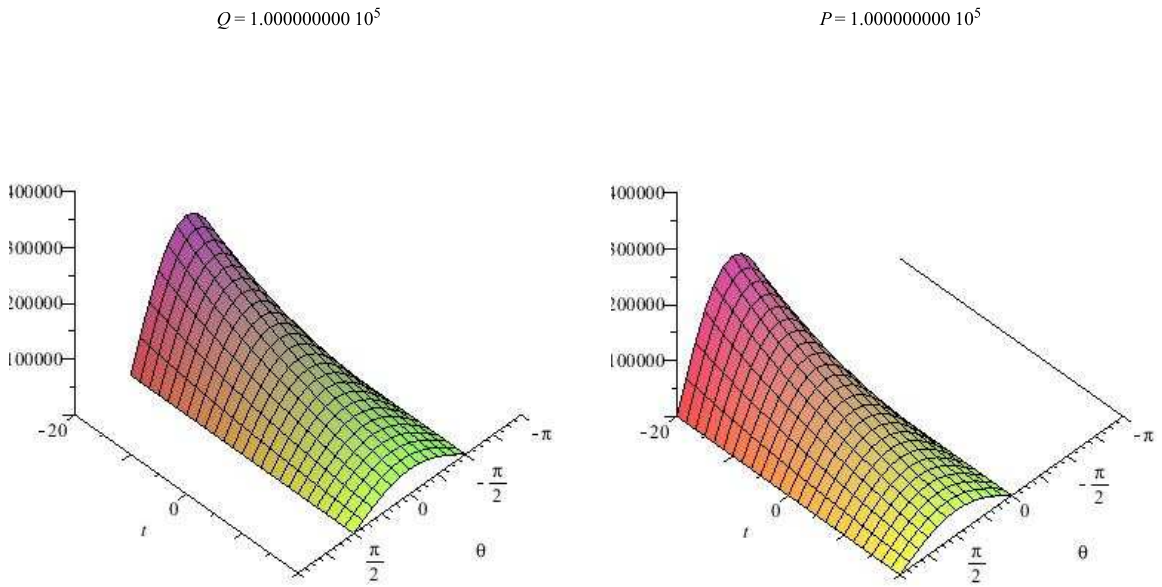

Figure 7.8: $c(\theta, t)$ with $c_0(\theta) = \frac{1}{2\pi} + Q\cos\theta + P\sin\theta$ with $\sigma = 0.75$.

7.3.3 Solution plots where the nonlinearity is of the sigmoid form

We now turn our attention to the graphs of the solutions when the nonlinearity is of the form (6.25). First, a single mode with $k = 1$ and increasing amplitude $P = 10$, on the left, or $P = 20$, on the right.

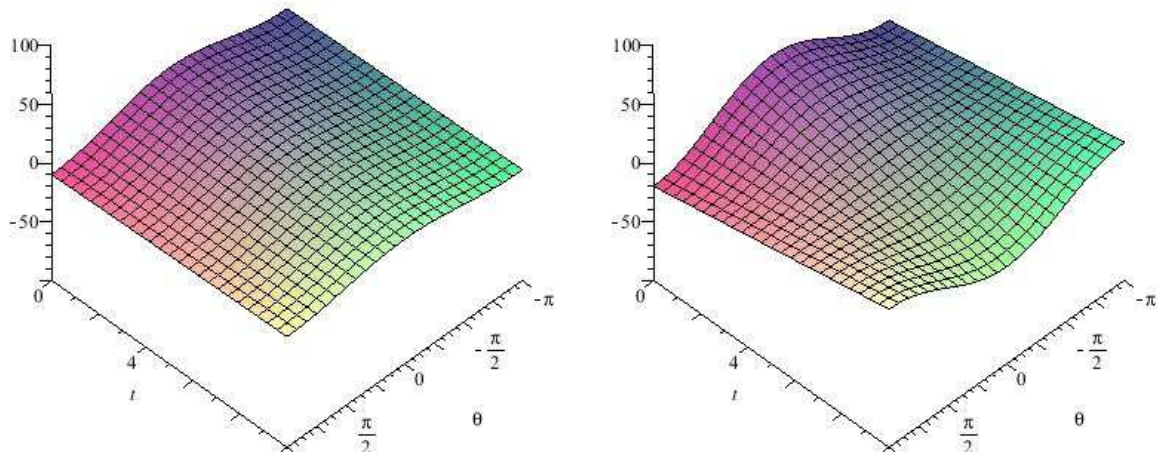

Figure 7.9: $C_3(\theta, t)$ with $c_0(\theta) = \frac{1}{2\pi} + P\cos\theta$ and $\sigma = 1$.

With a single mode of sine form, $c_0(\theta) = \frac{1}{2\pi} + 20\sin\theta$, or a double mode of sine form, $c_0(\theta) = \frac{1}{2\pi} + 15\sin\theta + 5\sin 3\theta$.

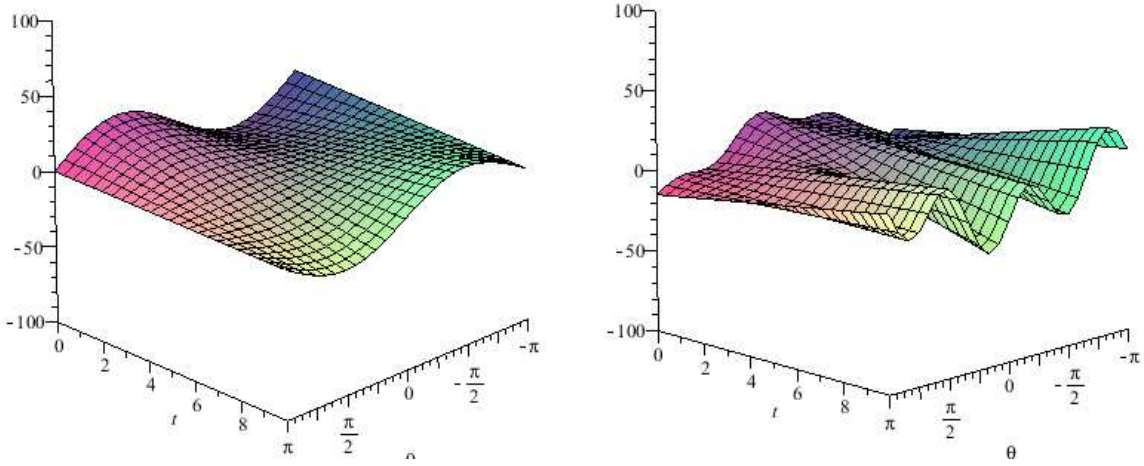

Figure 7.10: $C_1(\theta, t)$ with $c_0(\theta) = \frac{1}{2\pi} + P\sin\theta + Q\sin 3\theta$ and $\sigma = 1$.

Effect of the parameters on the solution for the sigmoid nonlinearity

Tighter alignment of filaments is associated with σ small. We illustrate here several examples with different values of σ and different initial conditions.

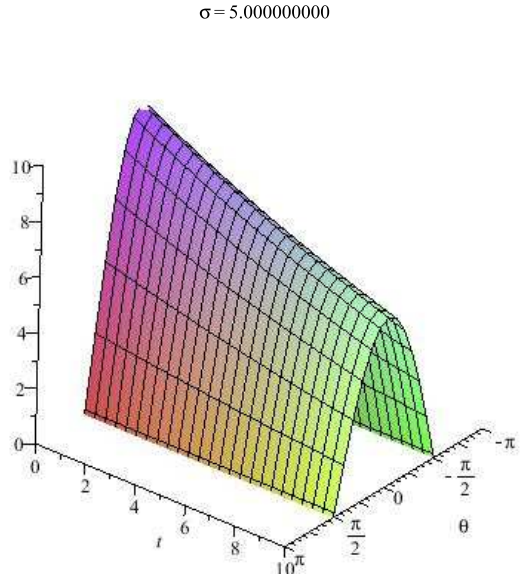

Figure 7.11: $C_3(\theta, t)$ with $c_0(\theta) = \frac{1}{2\pi} + 10\cos\theta$.

With $c_0(\theta) = \dfrac{1}{2\pi} + 20\cos\theta$ and $\sigma = 0.25$ or $\sigma = 6$.

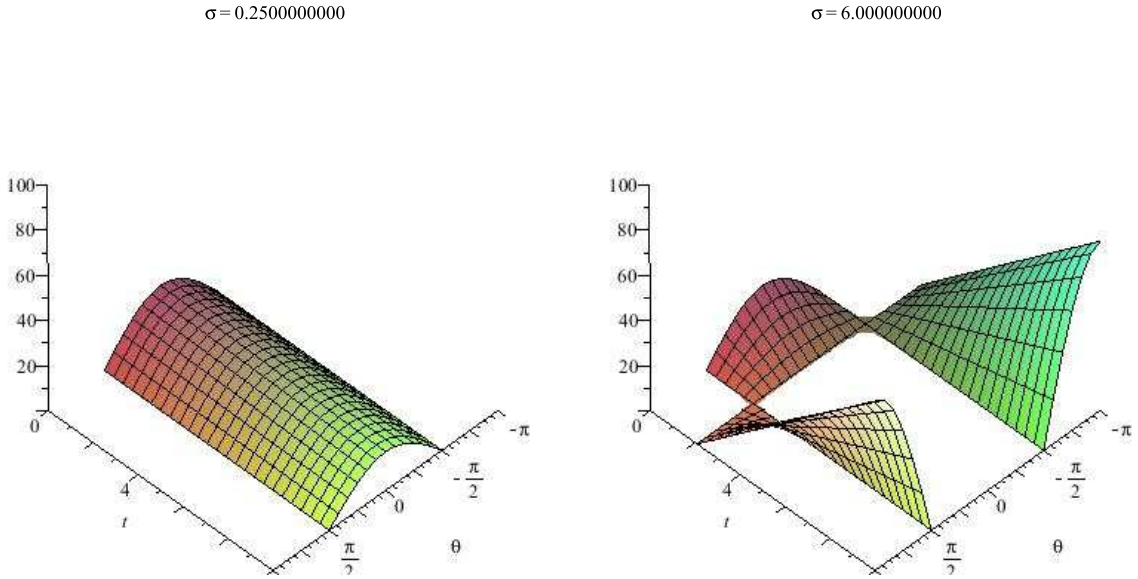

Figure 7.12: $C_3(\theta, t)$ with $c_0(\theta) = \frac{1}{2\pi} + 20\cos\theta$ with $\sigma = 0.25$ and $\sigma = 6$.

With $c_0(\theta) = \dfrac{1}{2\pi} + 15\sin\theta$ and $\sigma = 4.75$.

$\sigma = 4.750000000$

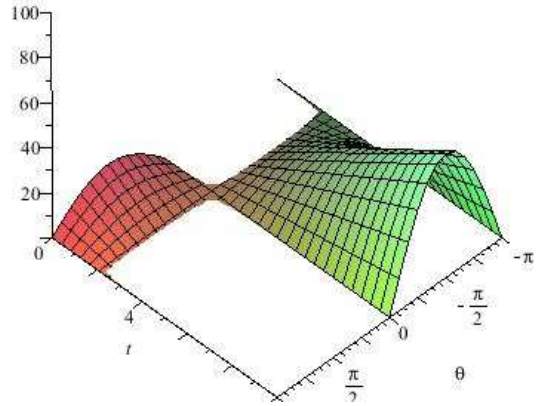

Figure 7.13: $C_1(\theta, t)$ with $c_0(\theta) = \frac{1}{2\pi} + 15\sin\theta$ and σ large.

With $c_0(\theta) = \dfrac{1}{2\pi} + 15\sin 4\theta$.

$k = 3.666666667$

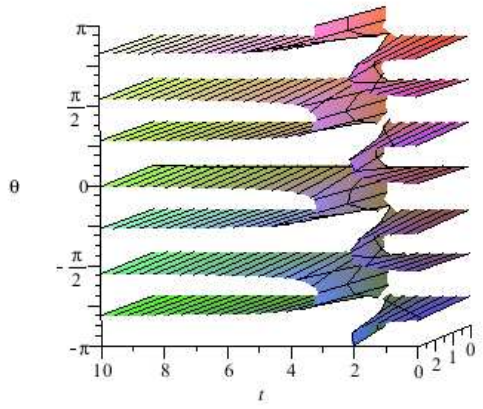

Figure 7.14: $C_1(\theta, t)$ with $c_0(\theta) = \frac{1}{2\pi} + 15\sin 4\theta$.

Further animation and investigation of solutions can be carried out using the enclosed programs.

Chapter 8

Conclusion

8.1 Concluding remarks

The main objectives of this thesis have been to seek to extend the utility of the ADM so that it would be able to converge to multiple solutions of a nonlinear problem and to apply the ADM to solve the OAP analytically. In this work, through applying the ADM to the OAP, a formula (6.22) which gives the exact solution of a special case of the orientation aggregation problem under specified conditions resulted. The programmatic implementation of the ADM in Maple 15 for solving the OAP helped to lead to this discovery. With regard to finding multiple solutions of nonlinear problems, the mathematical theory that enables the application of the ADM in such a way as to allow it to converge to more than one solution of a nonlinear problem has been developed and presented. That the ADM is an effective tool for path following bifurcation problems has been demonstrated and the corresponding theory developed. This thesis confirms the effectiveness of the ADM as a tool for solving the OAP and for finding multiple solutions to nonlinear problems and for use in the path following of bifurcation problems.

It was formally proven and demonstrated with specific examples that by varying the locality and strength of the contraction through the α parameter the root to which the ADM converges could be controlled. The novel application of the RADM to accelerate the speed of convergence to a choice of root from multiple was shown to be a useful tool when used in conjunction with the theory that enabled the convergence to more than one root. The ADM which is already applicable to a wide class of equations can now be implemented in such a manner so as to enable it to converge to more than one solution in practical applications. This powerfully extends the general utility of the method to enable it to find multiple solutions to a wide class of nonlinear problems. This in turn increases the number of tools available that can facilitate a more thorough examination of nonlinear systems and their solutions.

In this regard the original contribution herein is the development of the theoretical framework that enables the ADM to be used to find multiple solutions of a nonlinear problem and to be used as a corrector in path following procedures. Traditionally, other methods have been shown to be effective and efficient in numerical applications ([19]). For example, Newton's method is known to work well when solving a nonlinear equation and can be used in path following

procedures. What remains to be seen is the relative efficiency and effectiveness of the ADM for solving nonlinear problems and for use in path following applications.

A general formulation of the ADM for the OAP was developed and presented along with a rationale for the calculation of the Adomian polynomials corresponding to the nonlinearity found in the OAP. Two programs are provided for generating solutions by implementing the ADM to corresponding variants of the OAP. These programs also facilitate the graphical display and animation of the solutions to the OAP. The programs which can be extended and developed further for different forms of nonlinearity and for more terms of the Adomian solution are useful time saving tools that enable the study of solutions and the system behaviour.

8.2 Further work

A general theorem (6.22) giving the exact solution of the OAP under specified conditions was discovered and this confirmed the ADM as a fruitful method for studying the OAP. Further work can be done using the ADM to look for interesting solutions and system behaviour. In [56] and [60] authors explored various types of solutions that were of interest such as peak solutions, bifurcation solutions and periodic solutions. In a similar manner such like solutions could be explored using the ADM. Based on the linearisation of the OAP authors in [56] and [60] explored the solutions for certain parametric values. It would be of interest to see the results of a similar analytical approach using the ADM. What's more there are many variants of the OAP and there are corresponding forms of nonlinearities. How the ADM deals with more complicated forms of nonlinearity could be examined. In the thesis, Proposition 6.6 was introduced for constant interaction terms and periodic Gaussian. How the general formula would apply to the OAP with periodic Gaussian that are difficult to evaluate analytically such as $\sum_{n\in\mathbb{Z}} e^{(-\frac{1}{2}(\frac{(\psi-\theta)-k\sin(\theta-\phi)+2\pi n}{\sigma})^2)}$ could be examined. Behaviour associated with nonconstant interaction terms could also be further scrutinised. Since the ADM's utility has been extended to enable it to find multiple solutions of nonlinear problems, an obvious application would be to use the method to derive multiple solutions of the OAP. In addition the application of the ADM to generating multiple solutions of nonlinear problems in Chapter 3 led to interesting behaviour which led to the need to more carefully analyse the behaviour of the ADM for a range of starting values of u_0. Since the OAP manifests bifurcating solutions, the mathematical theory presented within this thesis relating to path following bifurcating branches using the ADM could be explored by making application of such theory to the OAP. This would prove useful in extending the understanding of how the orientation aggregation system works. The numerical stability of the ADM as a corrector could be compared to other commonly used corrector methods in order to judge the relative performances and ascertain its relative suitability for use in numerical analysis. In addition the ADM could be used as a corrector when conducting numerical analysis in a general sense on other forms of nonlinear mathematical equations.

In this thesis computer generated solutions proved useful. Solving the equation by implementing the ADM in Maple 15 enabled the problem to be solved quickly in turn saving time and enabling patterns in the solution to be easily spotted. The OAP could be further studied using Maple software. The areas that could be explored are more graphical, visual representation of other calculated Adomian solutions and animations of how the system works. Solutions that are of

interest such as bifurcating solutions, periodic solutions could be displayed graphically in order to better see how the dynamical system works. More complicated nonlinearities could also be solved using Maple software to implement the ADM. Here the Adomian polynomials were programmatically calculated according to the type of nonlinearity given in the OAP but an approach that would calculate the Adomian polynomials for any form of nonlinearity could be programmed and would prove useful for easily solving and studying more variants of the OAP with the ADM.

Bibliography

[1] Abbaoui K. and Cherruault Y., New ideas for proving convergence of decomposition methods, Computers Math. Applic. 29(7), 103-108, 1995.

[2] Abdelrazec A. and Pelinovsky D., Convergence of the Adomian Decomposition Method for Initial-Value Problems, Published online 3 November 2009 in Wiley Online Library (wileyonlinelibrary.com). DOI 10.1002/num.20549, 2011.

[3] Adomian G. and Rach R., A further consideration of partial solutions in the decomposition method, Computers Math. Applic. 23(1), 51-64, 1992.

[4] Adomian G. and Rach R., Analytic solution of nonlinear boundary value problems in several dimensions by decomposition, J. of Math. Anal. and Applic., 174, 118-137, 1993.

[5] Adomian G., Linear Stochastic Operators, Ph.D. Thesis, University of California, Los Angeles, CA, 1961.

[6] Adomian G., Solving Frontier Problems of Physics: The decomposition method, Kluwer, Boston, 1994.

[7] Adomian G., Nonlinear Stochastic Operator Equations, Academic Press, San Diego, CA, 1986.

[8] Adomian G., A review of the decomposition method and some recent results for nonlinear equation, Math. Comput. Modelling, 13(7), 17-43, 1992.

[9] Adomian G., Stochastic systems, Academic Press, London, 1983. 82,152,257

[10] Adomian G., Nonlinear stochastic operator equations, Academic Press, 1986.

[11] Adomian G., A new approach to nonlinear partial differential equations, J. of Math. Anal. and Applic. 102, 420-434, 1984.

[12] Adomian G. and Rach R., Equality of partial solutions in the decomposition method for linear or nonlinear partial differential equations, Computers Math. Applic. 19(12), 9-12, 1990.

[13] Adomian G., Solution of coupled nonlinear partial differential equations by decomposition, Computers Math. Applic. 31(6), 117-120, 1996.

[14] Adomian G. and DuBois D.F., Angular tracking noise in a randomized sequential lobing system, Hughes Aircraft Co., Rep. TM 414, 1956.

[15] Adomian G., Stochastic Green's functions, in Proc. of Annual Symposia in Applied Mathematics Vol.XVI, AMS, 1964.

[16] Adomian G. and Rach R., Noise terms in decomposition series solution, Computers Math. Applic. 24(11), 61-64, 1992.

[17] Adomian G. and Malakian K., Closure Approximation Error in the Mean Solution of Stochastic Differential Equations by the Hierarchy Method, Journal of Statistical Physics 21(2), 1979.

[18] Alberts B. et al., Molecular biology of the cell (3rd edition), Garland Publishing, New York and London, 1994.

[19] Allgower E.L. and Georg K., Numerical continuation methods: an introduction, Springer Verlag, Berlin, 1990.

[20] Astrom K.J., On a first order stochastic differential equation, Intern. J. Control 1, 301-326, 1965.

[21] Babolian E. and Biazar J., Solving concrete examples by Adomian method, Applied Mathematics and Computation 135, 161-167, 2003.

[22] Babolian E. and Javadi S., Restarted Adomian method for algebraic equations, Applied Mathematics and Computation 146, 533-541, 2003.

[23] Baker G.A. Jr., Essentials of Padé Approximants, Academic Press, 1975.

[24] Balakrishnan A.V., A Note on the Sampling Principle for Continuous Signals, Ire Transactions On Information Theory, 1957.

[25] Bellman R.E. and Kalaba R., Invariant imbedding and wave propagation in stochastic media, J. Math. Mech., 1959.

[26] Bellman R.E. and Kalaba R., Functional equations in adaptive processes and random transmission, Trans. Intern. Symp. Circuit Inform. Theory, 1959.

[27] Bellomo N. and Monaco R., A comparison between Adomian's decomposition methods and perturbation techniques for nonlinear random differential equations, J. of Math. Anal. and Applic. 110, 495-502, 1985.

[28] Bergen A.R., Random linear systems-a special case, AIEE Trans. (Applications and Industry), 1961.

[29] Bergen A.R., Stability of systems with randomly time-varying parameters, IRE Trans. on Automatic Control AC-5(1.01), 265-269, 1960.

[30] Bershad N., On the Stability of Randomly Time-Varying Linear Systems, IEEE Trans. Automatic Control AC-9(3), 391, 1964.

[31] Bharucha-Reid A.T., On the theory of random equations, in Annual Symposia in Applied Mathematics, Vol. XVI, 40-69, AMS, 1964.

[32] Bogdanoff J.L. and Kozin F., Moments of the output of linear random systems, J. Acous. Soc. Am. 34, I063, 1962.

[33] Boyd J., Padé approximant algorithm for solving nonlinear ordinary differential equation boundary value problems on an unbounded domain, Computers in physics 11(3), 299-303, 1997.

[34] Buffoni B. and Toland J., Analytic Theory of Global Bifurcation: An Introduction, Princeton Series in Applied Mathematics, Princeton University Press, Princeton NJ, 2003.

[35] Cartan H., Théorie Elémentaire des Fonctions Analytiques, Hermann, Paris, 1985.

[36] Casasus L. and Al-Hayani W., The decomposition method for ordinary differential equations with discontinuities, Appl. Math. Comput., 2001.

[37] Caughey T.K. and Dienes J.K., The behavior of linear systems with random parametric excitation, J. of Math. and Physics 41(4), 300-318, 1962.

[38] Chaplain M.A.J., Ganesh M. and Graham I.G., Spatio-temporal pattern formation on spherical surfaces: Numerical simulation and application to solid tumour growth, to appear in J. Math. Biol.

[39] Chernov L.A., Wave propagation in random medium, McGraw Hill, New York, 1960.

[40] Cherruault Y., Saccomandi G. and Some B., New results for convergence of Adomian's method applied to integral equations, Math. Comput. Modelling 16(2), 85-93, 1992.

[41] Cherruault Y., Convergence of Adomian's method, Kybernetes 18, 31-38, 1989.

[42] Civelekoglu G. and Edelstein-Keshet L., Modelling the dynamics of F-actin in the cell, Bull. Math. Biol. 56(4), 587616, 1994.

[43] Cooper J. and Pollard T., Actin and actin-binding proteins. A critical evaluation of mechanisms and functions, Annual Reviews Inc, 1986.

[44] Dallon J.C. and Sherrat J.A., A mathematical model for fibroblast and collagen orientation, Bull. Math. Biol. 60, 101-112, 1998.

[45] Dangelmayr G., Steady-state mode interactions in the presence of O(2)-symmetry, Dyn. Stab. Sys. 1, 159185, 1986.

[46] Datta B.K., A new approach to the wave equation - an application of the decomposition method, J. of Math. Anal. and Applic. 142, 6-12, 1989.

[47] Datta B.K,, Introduction to Partial Differential Equations, New Central Book Agency, Calcutta, 1993.

[48] Deeba E. and Khuri S., A decomposition method for solving the nonlinear Klein-Gordon equation, J. Computational Physics 124, 442-448, 1996.

[49] Deeba E. and Khuri S., The deccomposition method applied to Chandrasekhar H-equation, Appl. Math. Comput. 77, 67-78, 1996.

[50] Deimling K., Nonlinear Functional Analysis, Springer-Verlag, Berlin, 1985.

[51] Dvoretzky A. and Rogers C.A., Absolute and Unconditional Convergence in Normed Linear Spaces, Proc. Natl. Acad. Sci. USA, 36(4), 292-297, 1950.

[52] Edelstein-Keshet L. and Ermentrout G.B., Models for contact-mediated pattern formation, J. Math. Biol. 29, 3358, 1990.

[53] Edwards J.T, Roberts J.A. and Ford N.J., A comparison of Adomian's decomposition method and Runge Kutta methods for approximate solution of some predator prey model equations, University College Chester, 1997.

[54] Elrod M., Numerical Methods for Stochastic Differential Equations, PhD. Thesis, Univ. of Georgia, 1973.

[55] Gabet L., The theoretical foundation of the Adomian method, Computers Math. Applic. 27(12), 41-52, 1994.

[56] Geigant E. and Stoll M., Bifurcation analysis of an orientational aggregation model, Springer-Verlag, 2002.

[57] Geigant E., Ladizhansky K. and Mogilner A., An integrodifferential model for orientational distributions of F-actin in cells, SIAM J. Appl. Math. 59, 787809, 1999.

[58] Geigant E., Nichtlineare IntegroDifferentialGleichungen zur Modellierung interaktiver Musterbildungsprozesse auf S^1, PhD Thesis, Rheinische Friedrich-Wilhelms-Universität, Bonn, 1999.

[59] Geigant E., Stability of a peak solution to an orientational aggregation model, in Fiedler B., Gröger K. and Sprekels J. (eds), Differential Equations, World Scientific, Singapore, 2000.

[60] Geigant E., On Peak and Periodic Solutions of an Integro-Differential Equation on S^1, Abteilung Theoretische Biologie, Universität Bonn, Germany, 2002.

[61] Golubitsky M., Stewart I.N. and Schaeffer D., Singularities and groups in bifurcation theory, Vols. I and II, Springer Verlag, 1985 and 1988.

[62] Govaerts W.J.F., Numerical Methods for Bifurcation of Dynamical Equilibria, SIAM Publications, Philadelphia, 2000.

[63] Hadeler K.P., Reaction Transport Systems in Biological Modelling, in: Capasso V. and Diekmann O. (eds.), Mathematics inspired by Biology, CIME Lectures 1997, Lecture Notes in Mathematics, Springer Verlag, 1998.

[64] Heil C., A Basis Theory Primer, Birkhaüser, Boston, 2010.

[65] Himoun N., Abbaoui K., Cherruault, New results on Adomian method, Kybernetes 32(4), 2003.

[66] Jäger E. and Segel L., On the distribution of dominance in populations of social organisms, SIAM J. Appl. Math. 29, 3358, 1992.

[67] Jiao Y.C., Yamamoto Y., Dang C. and Hao Y., An after treatment technique for improving the accuracy of Adomian's Decomposition Method, Computers and Mathematics with Applications, 2002.

[68] Jiao Y.C., Hao Y. and Yamamoto Y., An extension of the decomposition method for solving nonlinear equations and its convergence, In Discussion Paper series 677, Institute of Policy and Planning Sciences, University of Tsukuba, 1996.

[69] Keller J.B., Stochastic equations and wave propagation in random media, in Stochastic Processes in Mathematical Physics and Engineering, AMS, Providence, Rhode Island, 1964.

[70] Keller E.F. and Segel L.A., Initiation of slime mold aggregation viewed as an instability, J. Theor. Biol. 26, 399.

[71] Kuznetsov Y.A., Elements of Applied bifurcation theory, Springer, 2010.

[72] Machado J.M and Tsuchieda M., Solutions for a Class of Integro-differential Equations with Time Periodic Coefficients, Applied Mathematics 2, 66-71, 2002.

[73] Maleknejad K. and Hadizadeh M., A new computational method for volterra-Fredholm Integral equations, Computers and Mathematics with Applications 37, 1-8, 1999.

[74] Mavoungou T and Cherruault Y., Numerical study of Fisher's equation by Adomian's method, Math. Comput. Modelling 19(1), 89-95, 1994.

[75] Mei Z., Numerical Bifurcation Analysis for Reaction-Diffusion Equations, Springer Verlag, Berlin, 2000.

[76] Mogilner A. and Edelstein-Keshet L., Selecting a common direction I: How orientational order can arise from simple contact responses between interacting cells, J Math. Biol. 33, 619660, 1995.

[77] Mogilner A., Edelstein-Keshet L. and Ermentrout G.B., Selecting a common direction II: Peak-like solutions representing total alignment of cell clusters, J. Math. Biol. 34, 811842, 1996.

[78] Olek S., An accurate solution to the multispecies Lotka-Volterra equations, SIAM Review 36(3), 480-488, 1994.

[79] Olivares A.G, Analytic solution of partial differential equations with Adomian's decomposition, Kybernetes 32(3), 2003.

[80] Othmer H., Dunbar S. and Alt W., Models of dispersal in biological systems, J. Math. Biol. 26, 263298, 1988.

[81] Pfistner B., Simulation of the dynamics of myxobacteria swarms based on a onedimensional interaction model, J. Biol. Sys. 3(2), 579588, 1995.

[82] Rach R., Baghdasarian A. and Adomian G., Differential Equations with Singular Coefficients, Appl. Math. Lett. 47(2/3), 179-184, 1992.

[83] Rach R., On the Adomian decomposition method and comparisons with Picards method, J.Mathl. Anal. and Applic. 128, 480-483, 1987.

[84] Verma R.U., Stochastic approximation-solvability of linear random equations involving numerical ranges, Journal of Applied Mathematics and Stochastic Analysis 10:1, 47-55, 1997.

[85] Ramis E., Deschamps C. and Odoux J., Cours de Mathtématiques Spéciales (volume 4), Masson, Paris, 1977.

[86] Re'paci A., Nonlinear dynamical systems: on the accuracy of Adomian's decomposition method, Appl. Math. Lett. 3, 35-39, 1990.

[87] Richardson J.M., The application of truncated hierarchy techniques in the solution of a stochastic linear differential equation, Annual Symposia in Applied Mathematics, Vol. XVI, Amer. Math. Soc., 1964.

[88] Rosenbloom A., Analysis of Randomly Time Varying Linear Systems, Ph.D. Thesis, University of California, L.A., 1954.

[89] Samels J.C. and Eringen A.C., On Stochastic Linear Systems, Technical Report Number 11, ONR, Division of Engineering Sciences, Purdue University, August, 1957.

[90] Samuelson P.A., Conditions that a root of a polynomial be less than unity in absolute value, Ann. Math. Stat. 12, 360-364, 1941.

[91] Seydel R., From equilibrium to chaos: practical bifurcation and stability analysis, Elsevier, New York, 1988.

[92] Shawagfeh N.T., Nonperturbative approximate solution for lane-Emden equation, J. math. Phys. 34(9), 4364-4369, 1993.

[93] Sibul L.H., Application of linear stochastic operator theory, Ph.D. Dissertation, Pennsylvania State University, 1968.

[94] Tikhonov A.N., Systems of differential equations containing small parameters in the derivatives, Mat.Sb.(N.S.) 31(73):3, 575586, 1952.

[95] Tatarski V.I., Wave Propagation in a Turbulent Medium, 1961.

[96] Vargas R.M.F, Cardona A.V. and De Vilhena M.T.M.B., An analytical solution for the multgroup slab geometry discrete ordinates problem by the decomposition method, International Conference on Computational Heat and Mass Transfer, 22-26, 2001.

[97] Venkatarangan S.N and Rajalakshmi K., A modification of Adomian's solution for nonlinear oscillatory systems, Computers Math. Applic. 29(6), 67-73, 1995.

[98] Wazwaz A.M., A new algorithm for solving differential equations of the Lane-Emden type, Appl. Math. Comput., 118(2/3), 287-310, 2001.

[99] Wazwaz. A.M., A computational approach to soliton solutions of the Kadomtsev-Petviashvili equation, Appl. Math. and Comput. 123(2), 205-217, 2001.

[100] Wazwaz A.M., A first course in integral equations, World Scientific, 1997.

[101] Wazwaz A.M., Partial differential equations methods and applications, A.A. Balkema, 2002.

Appendix A

Adomian polynomials

Let X be a Banach space and $F : X \to X$ be an analytic map. The classical Adomian polynomials of F at u_0 are given by the following formulas:

$$A_0(u_0) = F(u_0), \tag{A.1}$$

$$A_1(u_0, u_1) = F'(u_0)u_1, \tag{A.2}$$

$$A_2(u_0, \ldots, u_2) = \frac{1}{2}F''(u_0)u_1^2 + F'(u_0)u_2, \tag{A.3}$$

$$A_3(u_0, \ldots, u_3) = \frac{1}{6}F'''(u_0)u_1^3 + F''(u_0)u_1u_2 + F'(u_0)u_3, \tag{A.4}$$

$$A_4(u_0, \ldots, u_4) = \frac{1}{24}F^{(4)}(u_0)u_1^4 + \frac{1}{2}F'''(u_0)u_1^2u_2 + \frac{1}{2}F''(u_0)u_2^2 + F''(u_0)u_1u_3 + F'(u_0)u_4, \tag{A.5}$$

$$A_5(u_0, \ldots, u_5) = \frac{1}{120}F^{(5)}(u_0)u_1^5 + \frac{1}{6}F^{(4)}(u_0)u_1^3u_2 + \frac{1}{2}F'''(u_0)u_1u_2^2 + \frac{1}{2}F'''(u_0)u_1^2u_3 + F''(u_0)u_2u_3 + F''(u_0)u_1u_4 + F'(u_0)u_5, \tag{A.6}$$

$$A_6(u_0, \ldots, u_6) = \frac{1}{720}F^{(6)}(u_0)u_1^6 + \frac{1}{24}F^{(5)}(u_0)u_1^4u_2 + \frac{1}{4}F^{(4)}(u_0)u_1^2u_2^2 + \frac{1}{6}F^{(4)}(u_0)u_1^3u_3 + \frac{1}{6}F'''(u_0)u_2^3 + F'''(u_0)u_1u_2u_3 + \frac{1}{2}F'''(u_0)u_1^2u_4 + \frac{1}{2}F''(u_0)u_3^2 + F''(u_0)u_2u_4 + F''(u_0)u_1u_5 + F'(u_0)u_6. \tag{A.7}$$

A.1 Practical calculus of the Adomian polynomials

Formula (2.2) for the Adomian polynomials $A_n[F, u_0]$ indicates that they are the Taylor-Maclaurin coefficients of the function $G(\lambda) = F(u^+(\lambda))$. Explicitly, we have

$$\sum_{n=0}^{\infty} A_n[F, u_0]\lambda^n = \sum_{n=0}^{\infty} \frac{1}{n!}\, G^{(n)}(0)\, \lambda^n = \sum_{n=0}^{\infty} \frac{1}{n!}\, F^{(n)}(u_0)(u^+(\lambda) - u_0)^n.$$

There are other explicit or recurrence formula in the literature ([1],[65]). We state them here and sketch how they are established in a Banach space setting. Let $\underline{p} = (p_1, \ldots, p_n) \in \mathbb{N}_0^n$, define $|\underline{p}| = \sum_{i=1}^n p_i$ and $|i\underline{p}| = \sum_{i=1}^n i p_i$.

Theorem A.1 (Practical formulae for the Adomian polynomials) *1. Rach's Rule for the Adomian's polynomials is given by $A_0[F, u_0](u) = F(u_0)$ and, for all $n \geq 1$,*

$$A_n[F, u_0](u) = \sum_{k=1}^{n} F^{(k)}(u_0) \left(\sum_{|\underline{p}|=k,\, |i\underline{p}|=n} \prod_{i=1}^{n-k+1} \frac{u_i^{p_i}}{p_i!} \right) \tag{A.8}$$

$$= \sum_{|i\underline{p}|=n} F^{(|\underline{p}|)}(u_0) \left(\prod_{i=1}^{n-k+1} \frac{u_i^{p_i}}{p_i!} \right). \tag{A.9}$$

2. As recurrence formulae, we have two useful possibilities

$$A_n[F, u_0](u) = \sum_{k=0}^{n-2} \frac{(k+1)}{n} \frac{\partial A_{n-1-k}[F, u_0](u)}{\partial u_0} u_{k+1} + F'(u_0) u_n \tag{A.10}$$

$$= \frac{1}{n} \frac{\partial A_{n-1}[F, u_0](u)}{\partial u_0} u_1 + \sum_{k=1}^{n-1} \frac{(k+1)}{n} \frac{\partial A_{n-1}[F, u_0](u)}{\partial u_k} u_{k+1}. \tag{A.11}$$

Proof. Note that if $|\underline{p}| = k$ and $|i\underline{p}| = n$, the last $k-1$ entries of $\underline{p} \in \mathbb{N}_0^n$ are therefore 0. This follows because, if $k = 1$, then $p_n = 1 \neq 0$, and, if $k \geq 2$ and $p_{n+2-k} = 1 \neq 0$, then $p_1 = k-1$ so $p_1 + p_{n+2-k} = k$ and $p_1 + (n+2-k)p_{n+2-k} = n+1$. Hence, in reality, $\underline{p} \in \mathbb{N}_0^{n-k+1}$ for $1 \leq k \leq n$.

1. Formula (A.8) is shown in [6] following the definition in (2.2). Formula (A.9) follows from (A.8) observing that the union over $k = 1$ to n of the n-tuples $\underline{p}$ such that $|\underline{p}| = k$ and $|i\underline{p}| = n$ is simply the set of all $\underline{p}$ such that $|i\underline{p}| = n$.

2. First we show (A.11). To simplify notations, for $u = (u_1, \ldots, u_n)$, let

$$\Phi_n^k(u) = \sum_{|\underline{p}|=k,\, |i\underline{p}|=n} \prod_{i=1}^{n} \left(\frac{u_i^{p_i}}{p_i!} \right) = \sum_{|\underline{p}|=k,\, |i\underline{p}|=n} \prod_{i=1}^{n-k+1} \left(\frac{u_i^{p_i}}{p_i!} \right),$$

because $\underline{p} \in \mathbb{N}_0^{n-k+1}$. We have

$$\frac{1}{n} \frac{\partial A_{n-1}[F, u_0](u)}{\partial u_0} u_1 + \sum_{k=1}^{n-1} \frac{(k+1)}{n} \frac{\partial A_{n-1}[F, u_0](u)}{\partial u_k} u_{k+1} =$$

$$\frac{1}{n} \frac{\partial}{\partial u_0} \left(\sum_{k=1}^{n-1} F^{(k)}(u_0) \Phi_{n-1}^k(u) \right) u_1 + \sum_{k=1}^{n-1} \frac{(k+1)}{n} \frac{\partial}{\partial u_k} \left(\sum_{j=1}^{n-1} F^{(j)}(u_0) \Phi_{n-1}^j(u) \right) u_{k+1} =$$

$$\frac{1}{n} \left(\sum_{k=1}^{n-1} F^{(k+1)}(u_0) u_1 \, \Phi_{n-1}^k(u) \right) + \sum_{k=1}^{n-1} \frac{(k+1)}{n} \left(\sum_{j=1}^{n-1} F^{(j)}(u_0) \frac{\partial \Phi_{n-1}^j(u)}{\partial u_k} u_{k+1} \right).$$

Continuing, we have

$$\begin{aligned}
\frac{1}{n}\left(\sum_{l=2}^{n} F^{(l)}(u_0)u_1\,\Phi_{n-1}^{l-1}(u)\right) + \sum_{j=1}^{n-1} F^{(j)}(u_0)\left(\sum_{k=1}^{n-1}\frac{(k+1)}{n}\frac{\partial\Phi_{n-1}^{j}(u)}{\partial u_k}u_{k+1}\right) &= \\
F^{(n)}(u_0)\frac{u_1}{n}\Phi_{n-1}^{n-1}(u) + F'(u_0)u_n & \\
+\sum_{j=2}^{n-1} F^{(j)}(u_0)\left[\frac{u_1}{n}\,\Phi_{n-1}^{j-1}(u) + \sum_{k=1}^{n-j}\frac{(k+1)}{n}\,u_{k+1}\Phi_{n-1-k}^{j-1}(u)\right] &= \\
F^{(n)}(u_0)\Phi_n^n(u) + \sum_{j=2}^{n-1} F^{(j)}(u_0)\Phi_n^j(u) + F'(u_0)\Phi_n^1(u) &= A_n[F,u_0](u).
\end{aligned}$$

Second we show that $\dfrac{\partial A_n[F,u_0]}{\partial u_j}(u)w = \dfrac{\partial A_{n-j}[F,u_0]}{\partial u_0}(u)w$, $0 \le j \le n$, therefore (A.10) and (A.11) are equivalent. When $j = 0$ the result is obvious. When $j = n$,

$$\frac{\partial A_n[F,u_0]}{\partial u_n}(u)w = F'(u_0)w = \frac{\partial A_0[F,u_0]}{\partial u_0}(u)w.$$

For $1 \le j \le n-1$, we evaluate

$$\begin{aligned}
\frac{\partial A_n[F,u_0]}{\partial u_j}(u)w &= \frac{\partial}{\partial u_j}\left(\sum_{k=1}^{n} F^{(k)}(u_0)\left(\sum_{|\underline{p}|=k,\,|i\underline{p}|=n}\prod_{i=1}^{n-k+1}\frac{u_i^{p_i}}{p_i!}\right)\right)w \\
&= \sum_{k=2}^{n} F^{(k)}(u_0)\frac{\partial}{\partial u_j}\left(\sum_{|\underline{p}|=k,\,|i\underline{p}|=n}\prod_{i=1}^{n-k+1}\frac{u_i^{p_i}}{p_i!}\right)w \\
&= \sum_{k=2}^{n-j+1} F^{(k)}(u_0)\left(\sum_{|\underline{p}|=k-1,\,|i\underline{p}|=n-j}\prod_{i=1}^{n-k+1}\frac{u_i^{p_i}}{p_i!}\right)w \\
&= \sum_{l=1}^{n-j} F^{(l+1)}(u_0)\,w\left(\sum_{|\underline{p}|=l,\,|i\underline{p}|=n-j}\prod_{i=1}^{n-j-l+1}\frac{u_i^{p_i}}{p_i!}\right) \\
&= \frac{\partial A_{n-j}[F,u_0]}{\partial u_0}(u)w.
\end{aligned}$$

□

As an example of use of the recurrence formulas, we calculate $A_3[F,u_0]$. For (A.10),

$$\begin{aligned}
A_3[F,u_0]u &= \sum_{k=0}^{1} \frac{k+1}{3} \frac{\partial A_{2-k}[F,u_0]}{\partial u_0}(u)u_{k+1} + F'(u_0)u_3 \\
&= F'(u_0)u_3 + \frac{1}{3}\frac{\partial A_2[F,u_0]}{\partial u_0}(u)u_1 + \frac{2}{3}\frac{\partial A_1[F,u_0]}{\partial u_0}(u)u_2 \\
&= F'(u_0)u_3 + \frac{1}{3}\left[\frac{1}{2}F''(u_0)u_1^2 + F'(u_0)u_2\right]_{u_0}(u_1) + \frac{2}{3}F''(u_0)u_2u_1 \\
&= F'(u_0)u_3 + F''(u_0)u_2u_1 + \frac{1}{6}F'''(u_0)u_1^3.
\end{aligned}$$

and, for (A.11),

$$\begin{aligned}
A_3[F,u_0]u &= \frac{1}{3}\frac{\partial A_2[F,u_0]}{\partial u_0}u_1 + \sum_{k=1}^{2}\frac{k+1}{3}\frac{\partial A_2[F,u_0]}{\partial u_k}u_{k+1} \\
&= \frac{1}{3}\left[\frac{1}{2}F''(u_0)u_1^2 + F'(u_0)u_2\right]_{u_0}(u_1) + \frac{2}{3}\left[\frac{1}{2}F''(u_0)u_1^2 + F'(u_0)u_2\right]_{u_1}(u_2) \\
&\qquad + \left[\frac{1}{2}F''(u_0)u_1^2 + F'(u_0)u_2\right]_{u_2}(u_3) \\
&= \frac{1}{6}F'''(u_0)u_1^3 + \frac{1}{3}F''(u_0)u_1u_2 + \frac{2}{3}F''(u_0)u_1u_2 + F'(u_0)u_3 \\
&= F'(u_0)u_3 + F''(u_0)u_1u_2 + \frac{1}{6}F'''(u_0)u_1^3.
\end{aligned}$$

A.1.1 Solution of composed operator equations

In this thesis we have many instances where the equation to solve is the result of the composition of operators, linear or nonlinear. For instance, in a Volterra integral equation, we integrate in time (a linear operator) some nonlinear term. When the composed functions are nonlinear we need to use extensions of the Chain Rule, like in Lemma A.6. When one of the operator is linear, then the amendments are much simpler. We state here some results, extended from [55].

Theorem A.2 (Solution of LN composed operator equations) *In order to solve an equation $u = LN(u) + c$, where L is a continuous linear operator and N is an analytical nonlinear operator, the following decomposition scheme can be applied:*

$$u_0 = c, \quad u_{n+1} = LA_n[N,c](u),$$

where the A_n are the Adomian polynomials associated with N.

Proof. We need to show that the decomposition series $\sum_{n=0}^{\infty} LA_n[N,c](u)$ is strongly convergent and that its degenerated sum is $G(u) = LN(u)$. The decomposition series is weakly convergent because L is a linear operator, and continuous, so $\sum_{n=0}^{k} LA_n[N,c](u) = L\left(\sum_{n=0}^{k} A_n[N,c](u)\right)$. Let $u = \sum_{k=0}^{\infty} u_k$ be a convergent series. The sequence $s_n = \sum_{k=0}^{n} A_k[N,c](u)$ converges towards $N(u)$ because of the convergence of the ADM decomposition series of N. So, the sequence

$t_n = Ls_n$ converges towards $LN(u)$ because of the continuity of L. The convergence is strong because the limit $N(u)$ depends only on the sum u of the series in X, not on its terms. □

Theorem A.3 (Solution of *NL* composed operator equations, [55]) *In order to solve an equation $u = N(Lu)+c$, where L is a continuous linear operator and N is an analytical nonlinear operator, the following decomposition scheme can be applied:*

$$u_0 = c, \quad u_{n+1} = A_n[N, c](Lu),$$

where the A_n are the Adomian polynomials associated with N.

Proof. Consider the decomposition series $\sum_{n=0}^{\infty} A_n[N, c](Lu)$. Let $u = \sum_{n=0}^{\infty} u_n$ be a convergent series. The series $Lu = \sum_{n=0}^{\infty} Lu_n$ is also convergent because of the linearity and the continuity of L. So, the series $\sum_{n=0}^{\infty} A_n[N, c](Lu)$ converges because of the weak convergence of the ADM series. It converges strongly because, if $u = \sum_{n=0}^{\infty} u_n = \sum_{n=0}^{\infty} v_n$ are convergent series, then the series $\sum_{n=0}^{\infty} A_n[N, c](Lu)$ and $\sum_{n=0}^{\infty} A_n[N, c](Lv)$ both converge towards $N(Lu)$. □

Finally, if we have a sum of operators, then we can sum the Adomian polynomials.

Theorem A.4 (Sum of operators) *In order to solve an equation $u = N(u)+c$ where $N(u) = \sum_{i=0}^{p} N_i(u)$, the following decomposition scheme can be applied:*

$$u_0 = c, \quad u_{n+1} = \sum_{i=0}^{p} A_n^i[N_i, c](u),$$

where the A_n^i are the Adomian polynomials associated with each N_i.

Proof. It is a direct application of the vector space structure of the set of the strongly convergent decomposition series. □

A.2 Calculating some Adomian polynomials

A.2.1 Quadratic form nonlinearity

Given $c : \mathbb{R} \to \mathbb{R}$, consider the following nonlinearity

$$F(c)(\phi, \psi) = c(\phi)c(\psi). \tag{A.12}$$

Set $c(x) = \sum_{n=0}^{\infty} c_n(x)$.

Proposition A.5 *For F in (A.12), its Adomian polynomials A_n at c_0, $n \geq 0$, are the following*

$$A_n[F, c_0](c)(\phi, \psi) = \sum_{k=0}^{n} c_k(\phi)c_{n-k}(\psi). \tag{A.13}$$

Proof. Multiplying the expansions of $c(\phi)$ and $c(\psi)$, grouping terms where the sum of the subscripts are the same, leads to the formula (6.9) for the Adomian polynomials. □

A.2.2 A more general nonlinearity

Given an analytic $f : \mathbb{R} \to \mathbb{R}$, we consider the following nonlinearity

$$F(c)(\phi, \psi) = f(c(\phi))\, c(\psi). \tag{A.14}$$

We can give a simple recursive formula for the Adomian polynomials of F.

Lemma A.6 *Let $c_0 : \mathbb{R} \to \mathbb{R}$ be an analytic function, the Adomian polynomials of the function F at c_0 are given by*

$$A_n[F, c_0](c)(\phi, \psi) = \sum_{k=0}^{n} A_k[f, c_0](c)(\phi)\, c_{n-k}(\psi),\ n \geq 0.$$

Proof.

Recall that if we have $\sum_{k=0}^{n} a_k \lambda^k$ and $\sum_{k=0}^{n} b_j \lambda^j$ then

$$\begin{aligned} \frac{1}{n!}\frac{\mathrm{d}}{\mathrm{d}\lambda^n}\bigg|_{\lambda=0} \left(\sum_{k=0}^{n} a_k \lambda^k\right)\left(\sum_{j=0}^{n} b_j \lambda^j\right) &= \frac{1}{n!}\frac{\mathrm{d}}{\mathrm{d}\lambda^n}\bigg|_{\lambda=0} \left(\sum_{k+j=0}^{n} (a_k b_j)\lambda^{k+j}\right) \\ &= \sum_{\substack{k,j=0,\\ k+j=n}} a_k b_j = \sum_{k=0} a_k b_{n-k}. \end{aligned}$$

From the definition of the Adomian polynomials,

$$A_n[F, c_0](c)(\phi, \psi) = \frac{1}{n!}\ \frac{d}{d\lambda^n}\bigg|_{\lambda=0} f\big(\sum_{n=0}^{n} c_n(\phi)\lambda^n\big)\big(\sum_{n=0}^{n} c_n(\psi)\lambda^n\big).$$

Furthermore

$$f\left(\sum_{n=0}^{n} c_n(\phi)\lambda^n\right) = \sum_{n=0}^{n} A_k[f, c_0](c)(\phi)\lambda^k + \lambda^{n+1} R_{n+1}(\phi, \lambda)$$

where $\lambda^{n+1} R_{n+1}$ is the remainder of the terms of degree at least $n+1$ in λ. Then setting $a_k = A_k[f, c_0](c)(\phi)$ and $b_k = c_k(\psi)$ we conclude.

□

We could also use (A.2,A.3) to calculate the A_1 and A_2 polynomials of F. The following result is needed.

Lemma A.7 *Given F in (A.14),*

1. *The first derivative of F at c in the direction of u is*

$$(F'(c)u)(\phi, \psi) = f'(c(\phi))\, c(\psi)u(\phi) + f(c(\phi))\, u(\psi). \tag{A.15}$$

2. The second derivative of F at c in the directions of (u, v) is

$$(F''(c)uv)(\phi,\psi) = f''(c(\phi))\,c(\psi)u(\phi)v(\phi) + f'(c(\phi))\,(v(\psi)u(\phi) + v(\phi)u(\psi))\,. \qquad \text{(A.16)}$$

Proof. In both cases the directional derivative formulation of the Fréchet derivatives of a function F is used.

1. For the first derivative at c in the direction of u, there results

$$\begin{aligned}
(F'(c)u)(\phi,\psi) &= \lim_{s\to 0} \frac{F(c+su)(\phi,\psi) - F(c)(\phi,\psi)}{s} \\
&= \lim_{s\to 0} \frac{f((c+su)(\phi))\,(c+su)(\psi) - f(c(\phi))\,c(\psi)}{s} \\
&= \lim_{s\to 0} \frac{f((c+su)(\phi,t))\,(c+su)(\psi,t) - f(c(\phi,t))\,(c+su)(\psi,t)}{s} \\
&\qquad + \lim_{s\to 0} \frac{f(c(\phi))\,(c+su)(\psi) - f(c(\phi))\,c(\psi)}{s} \\
&= \lim_{s\to 0} \frac{f((c+su)(\phi)) - f(c(\phi))}{s} \cdot \lim_{s\to 0}(c+su)(\psi) \\
&\qquad + f(c(\phi))\,\lim_{s\to 0} \frac{(c+su)(\psi) - c(\psi)}{s} \\
&= f'(c(\phi))\,c(\psi)u(\phi) + f(c(\phi))\,u(\psi).
\end{aligned}$$

2. Then, for the second Fréchet derivative,

$$F''(c)uv = \lim_{s\to 0} \frac{F'(c+sv)u - F'(c)u}{s}, \qquad \text{(A.17)}$$

on formula (A.15) for $(F'(c)u)(\phi,\psi)$, gives formula (A.16) for $(F''(c)uv)(\phi,\psi)$.

□

As a direct application of (A.2,A.3), using those derivatives of F, we find that

$$\begin{aligned}
A_1[F,c_0](c)(\phi,\psi) &= f'(c_0)c_0(\psi)c_1(\phi) + f(c_0)c_1(\psi), & \text{(A.18)}\\
A_2[F,c_0](c)(\phi,\psi) &= f'(c_0)c_0(\psi)c_2(\phi) + f(c_0)c_2(\psi) \\
&\qquad + \frac{1}{2}f''(c_0)c_0(\psi)c_1^2(\phi) + f'(c_0)c_1(\phi)c_1(\psi). & \text{(A.19)}
\end{aligned}$$

Appendix B

Definitions and results of nonlinear analysis

The material presented in this section supports mainly the ideas in chapters 1 and 2.

In this section we recall some important notions, definitions and notations about continuous, differentiable and analytic maps between Banach spaces (see [34, 50, 64]).

B.1 Analytic maps

B.1.1 Differentiable maps, Taylor series

Let X and Y be two Banach spaces, $U \subset X$ be a neighbourhood of $x_0 \in X$, the derivative $f'(x_0)$ at x_0 of a differentiable map $f : X \to Y$ is often calculated in practical terms using the **directional derivative**: for every $v \in X$, the value $f'(x_0)v \in Y$ is given by

$$f'(x_0)v = \lim_{t\to 0} \frac{f(x_0+tv)-f(x_0)}{t} = \frac{\mathrm{d}}{\mathrm{d}t} f(x_0+tv)\Big|_{t=0}. \tag{B.1}$$

We also denote derivatives using subscripts when we would like to emphasize the variable, that is, $f' = f_x$. When f has many distinguished variables, say $f : X_1 \times X_2 \to Y$, we use the notation f_{x_1} for the partial derivative $\dfrac{\partial f}{\partial x_1}$. Higher derivatives are defined iteratively and calculated from the iteration of the relevant directional derivatives. The k-th derivative $f^{(k)}(x_0)$ of f at $x_0 \in U$ is a symmetric k-multilinear map $X^k \to Y$. When $f \in C^k(U, Y)$, for all $x_0 \in U$, the derivatives $f^{(l)}(x_0)$ are bounded for $0 \le l \le k$, that is, the following quantity

$$\|f^{(l)}(x_0)\| = \sup\{\|f^{(l)}(x_0)(v_1,\dots,v_l)\| : \ \|v_i\| \le 1,\ 1 \le i \le l\ \} < \infty.$$

Given a sequence of bounded k-multilinear symmetric maps $\{m_k\}_{k=1}^{\infty}$, the expression

$$\sum_{k=0}^{\infty} m_k(x-x_0)^k$$

is a **power series** at x_0. Its **radius of convergence** is $R = \left(\limsup_{k\to\infty} \|m_k\|^{1/k}\right)^{-1}$. To compare $n!$ and n^n, recall the Stirling formula $\lim_{n\to\infty} \dfrac{n!}{\sqrt{n}\cdot(n/e)^n} = \sqrt{2\pi}$ ([34]). The radius of convergence of a Taylor series is

$$R = \left(\limsup_{k\to\infty} \frac{e}{k}\|f^{(k)}(x_0)\|^{1/k}\right)^{-1} = \left(\limsup_{k\to\infty} \left(\frac{\|f^{(k)}(x_0)\|}{k!}\right)^{1/k}\right)^{-1}.$$

In Section 2.3, we introduce two conditions on the behaviour of the norms of the derivatives of $f^{(k)}(x_0)$. Let $M, \alpha > 0$. When $\|f^{(k)}(x_0)\| \leq M\alpha^k$, condition (H1), the radius of convergence is $R = \infty$. An an example, we can think of $f : \mathbb{R} \to \mathbb{R}$, $f(x) = Me^{\alpha x}$. When $\|f^{(k)}(x_0)\| \leq k!M\alpha^k$, condition (H2), the radius of convergence is $R = 1/\alpha$. For instance, $f : (-\infty, 1/\alpha) \to \mathbb{R}$, $f(x) = \dfrac{M}{1-\alpha x}$ is defined by its Taylor series at the origin on $(-1/\alpha, 1/\alpha)$.

An important and useful formula is the derivative of the composition of functions: the Faà de Bruno formula ([34]). Recall that for $\underline{p} = (p_1, \ldots, p_n) \in \mathbb{N}_0^n$, $|\underline{p}| = \sum_{i=1}^n p_i$ and $|i\underline{p}| = \sum_{i=1}^n ip_i$. Define $\underline{p}! = \Pi_{i=1}^n (p_i!)$. Let $h(x) = g(f(x))$ where f and g are at least n-times continuously differentiable functions such that h is defined on some neighbourhood of $x_0 \in X$. Then

$$h^{(n)}(x_0)v^n = \sum_{j=1}^{n} \left(\sum_{|\underline{p}|=j, |i\underline{p}|=n} \frac{n!}{\underline{p}!} g^{(j)}(f(x_0)) \left(\frac{f'(x_0)v}{1!}\right)^{p_1} \cdots \left(\frac{f^{(n)}(x_0)v^n}{n!}\right)^{p_n} \right).$$

B.1.2 Analytic maps

To apply the ADM, we need to deal with analytic functions. A map $f : U \subset X \to Y$ is **analytic at** $u_0 \in U$ if there exists $m_0 \in Y$ and a family of bounded k-multilinear symmetric maps $\{m_k\}_{k=1}^{\infty}$ with

$$f(x) = \sum_{k=0}^{\infty} m_k(x - x_0)^k$$

for every $x \in U$ such that $\|x - x_0\| < r$ is small enough and there exists $M, r > 0$ such that $\|m_k\| \leq \dfrac{M}{r^k}$ (or $\limsup_{k\to\infty} r^k\|m_k\| = M < \infty$). The map f is **analytic on** U if it is analytic at every point $x \in U$.

When f is analytic, its derivatives are also analytic and satisfy important estimates. Those estimates provide also a criterion to check if an infinitely differentiable function is actually analytic. The following result is a compilation of results proved in [34].

Proposition B.1 (Cauchy Estimates, [34]) *1. Let $U \subset X$ be open and $f : U \to Y$ be infinitively differentiable. Suppose that for each $x_0 \in U$ there exists $r, C, R > 0$, depending on x_0, such that*

$$\|F_{x^k}(x)\| \leq \frac{C \cdot k!}{R^k}, \quad \forall x \in B_{x_0}(r) \cap U,$$

then f is analytic on U with radius of convergence at least $\min\{r, R\}$.

2. Let $f : U \to Y$ be analytic on U, there exist $C > 1$, $R \in (0, 1)$ such that

$$\|F_{x^k}(x)\| \leq \frac{C \cdot k!}{R^k}, \quad \forall x \in B_{x_0}(r/2) \cap U.$$

B.2 The Contraction Mapping Theorem

Let X be a Banach space with norm $\|\,.\,\|$. Let $U \subset X$ and $g : U \to X$ be a continuous map. Consider the non linear equation in U

$$g(x) = x. \tag{B.2}$$

A solution of (B.2) is called a **fixed point** of g. When $g(U) \subset U$ and g is a continuous function, it is an idea to solve (B.2) by constructing a sequence

$$x_n = g(x_{n-1}), \;\; n \geq 1,$$

for some initial data x_0. If $\{x_n\}_{n=0}^{\infty}$ converges to some $\bar{x}$ then, by continuity of g, $\bar{x} = g(\bar{x})$. To ensure that $\{x_n\}_{n=0}^{\infty}$ converges, the following theory is built.

The map $g : U \to U$ is a **contraction** if there exists $k < 1$ such that

$$\|g(x) - g(y)\| < k\|x - y\|, \quad \forall x, y \in U.$$

The following theorem, due to Banach-Caccioppoli, about the convergence of iterative processes is very useful.

Theorem B.2 (Contraction Mapping Theorem (CMT), [50]) *Let $U \subset X$ be closed and $g : U \to U$ be a contraction, then the iterative process*

$$x_n = g(x_{n-1})$$

converges to the unique fixed point $\bar{x}$ in U independently of the choice of the initial point $x_0 \in U$.

Moreover, the rate of convergence of the sequence $\{x_n\}_{n=0}^{\infty}$ depends on the following:

$$\|\bar{x} - x_n\| \leq \frac{k^n}{1-k}\|x_1 - x_0\|, \quad \forall n \geq 1.$$

Note that the estimate of the rate of convergence gives us an estimate on the domain for the solution once we have calculated the first iterate. In particular,

$$\|\bar{x} - x_1\| \leq \frac{k}{1-k}\|x_1 - x_0\| \leq \frac{1}{1-k}\|x_1 - x_0\|.$$

When g is continuously differentiable, a better criterion for convergence is to ask that the **spectral radius of** $g'(\bar{x})$, denoted by $\rho(g'(\bar{x}))$, is smaller than 1. If this is the case, we call g **contractive (at $\bar{x}$)**. Note that $\rho(g'(\bar{x}))$ is actually a lower bound for any norm of $g'(\bar{x})$, therefore $\|g'(\bar{x})\| < 1$ is a sufficient condition for the conclusion of the CMT to hold and $\|g'(\bar{x})\| > 1$ is a sufficient condition for the existence of initial points x_0 as close as we wish whose orbit by g

does not converge to the fixed point. In that context, the choice of norm can be important for g to be a contraction.

Lemma B.3 *Let $g : U \subset X \to X$ such that $\bar{x} \in U$ is a fixed point of g and g is contractive at $\bar{x}$. Then, there exists $\epsilon > 0$ such that g satisfies the hypotheses of the CMT on $B_{\bar{x}}[\epsilon]$.*

Proof. We need to show that there exists an $\epsilon > 0$ such that $g(B_{\bar{x}}[\epsilon]) \subset B_{\bar{x}}[\epsilon]$. Recall the Mean Value Theorem for Banach Spaces ([34]). Let $x, \bar{x} \in U$ and define $y(t) = tx + (1-t)\bar{x}$ for $t \in [0,1]$. Then there exists a $\bar{t}$ such that

$$g(x) - g(\bar{x}) = g'(y(\bar{t}))\,(x - \bar{x}).$$

Because $\bar{x}$ is a fixed point of g, choose $\epsilon > 0$ such that $B_{\bar{x}}[\epsilon] \subset U$. For any $x \in B_{\bar{x}}[\epsilon]$,

$$\|g(x) - \bar{x}\| \leq \|g(x) - g(\bar{x})\| \leq \|g'(y(\bar{t}))\| \cdot \|x - \bar{x}\| \leq k\epsilon < \epsilon.$$

□

B.3 The Implicit Function Theorem

The Implicit Function Theorem gives a useful criterion when we can solve implicitly equations of the type

$$F(x, \gamma) = 0$$

in terms of x as a function of γ.

Theorem B.4 (Implicit Function Theorem (IFT), [34]) *Let X, Y, Λ be Banach spaces, or subsets of them, and $F : X \times \Lambda \to Y$ be a k-times continuously differentiable map on $X \times \Lambda$ such that*

(i) $F(x_0, \gamma_0) = 0$,

(ii) $F_x(x_0, \gamma_0)$ is invertible.

Then, there exist neighbourhoods $\gamma_0 \in L \subset \Lambda$, $x_0 \in U \subset X$ and $\bar{x} : L \to X$ such that

$$F(\bar{x}(\gamma), \gamma) = 0, \quad \forall \gamma \in L,$$

and $\bar{x}(x_0) = y_0$. Moreover,

(a) all the solutions of $F = 0$ inside $U \times L$ belong to the curve parametrised by γ: $\gamma \mapsto (\bar{x}(\gamma, \lambda))$,

(b) the regularity of F determines the regularity of $\bar{x}$, more precisely, $\bar{x}$ has as many derivatives as F has.

In case F is analytic, an analytic $\bar{x}$ can be found.

Appendix C

Jury's conditions

The following gives more information about the spectral radius of 2×2 matrices and supports the ideas presented in Lemmas 3.1 and 3.2 when the space involved is $\mathbb{R}^2$.

Let M be a 2×2-matrix. Consider its characteristic polynomial

$$P(\lambda) = \lambda^2 - a_1\lambda + a_0, \tag{C.1}$$

where λ are the eigenvalues of M, $a_1 = \mathrm{tr}(M)$ and $a_0 = \det(M)$.

We are seeking conditions for the spectral radius $\rho(M)$ to be less than 1.

Lemma C.1 *Let $0 \leq \rho < 1$. The region of the $(\det(M), \mathrm{tr}(M))$-plane where M has spectral radius ρ is the triangle joining the vertices $(-\rho^2, 0)$, $(\rho^2, 2\rho)$ and $(\rho^2, -2\rho)$. In particular, $\rho(M) < 1$ if and only if*

$$-1 < \det(M) < 1$$

and

$$-1 - \det(M) < \mathrm{tr}(M) < 1 + \det(M).$$

Proof. The necessary and sufficient conditions for all roots of the polynomial P in (C.1) to be inside the unit disk are $P(1), P(-1) > 0$ and $|a_0| < 1$. They are known as the Jury's conditions ([90]). The first two conditions are $1 - a_1 + a_0 > 0$ and $1 + a_1 + a_0 > 0$. They are equivalent to $1 + a_0 > |a_1|$. Now, we consider the roots of P, namely

$$\lambda_\pm = \frac{a_1 \pm \sqrt{a_1^2 - 4a_0}}{2},$$

to understand better the structure of the spectral radius inside the triangle $\rho(M) < 1$. We have complex roots when $4a_0 > a_1^2$. In that case

$$\rho(M)^2 = |\lambda_+|^2 = |\lambda_+|^2 = \lambda_+ \cdot \lambda_- = a_0.$$

Complex conjugate eigenvalues have magnitude ρ, iff $a_0^2 = \rho^2$ and as this occurs iff $a_1^2 \geq 4a_0$ it follows that the set of points in the a_0, a_1 plane corresponding to this is the line segment joining $(\rho^2, -2\rho)$ and $(\rho^2, 2\rho)$.

For real roots, when $a_1^2 > 4a_0$,

$$\rho(M) = \begin{cases} \lambda_+, & \text{when } a_1 > 0; \\ \lambda_-, & \text{when } a_1 < 0, \end{cases}$$

meaning that

$$\rho(M) = \frac{|a_1| + \sqrt{a_1^2 - 4a_0}}{2}, \quad 4a_0 < a_1^2.$$

This last expression represents two lines

$$\rho^2 \mp \rho a_1 + a_0 = 0, \quad 4a_0 < a_1^2$$

that are the tangents to the parabola $4a_0 = a_1^2$ at the points $(\rho^2, \pm 2\rho)$. Joining together all the pieces of information we can conclude. □

The situation is represented thereafter in Figure C.1.

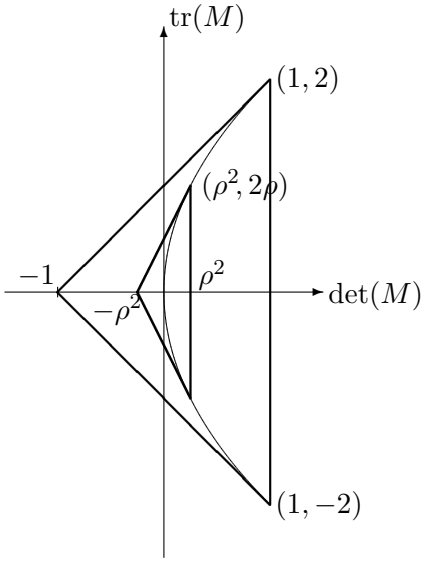

Figure C.1: Region of the (a_0, a_1)-plane where the spectral radius $\rho(M) < 1$ and the triangle $\rho(M) = \rho$.

C.1 Planar contractions

Consider the system

$$\begin{aligned} u &= u_0 + [u - u_0 + \alpha_1 f(u, \gamma)], \\ \gamma &= \gamma_0 + [\gamma - \gamma_0 + \alpha_2 g(u, \gamma)]. \end{aligned}$$

It is contractive if the matrix

$$
\begin{aligned}
M &= \begin{pmatrix} 1+\alpha_1 f_u(u,\gamma) & \alpha_1 f_\gamma(u,\gamma) \\ \alpha_2 g_u(u,\gamma) & 1+\alpha_2 g_\gamma(u,\gamma) \end{pmatrix} && \text{(C.2)} \\
&= I + \begin{pmatrix} \alpha_1 & 0 \\ 0 & \alpha_2 \end{pmatrix} \begin{pmatrix} f_u(u,\gamma) & f_\gamma(u,\gamma) \\ g_u(u,\gamma) & g_\gamma(u,\gamma) \end{pmatrix} && \text{(C.3)} \\
&= I + Kf'(u), \text{ where } K = \begin{pmatrix} \alpha_1 & 0 \\ 0 & \alpha_2 \end{pmatrix}. && \text{(C.4)}
\end{aligned}
$$

has spectral radius $\rho(M) < 1$.

We have

$$
\begin{aligned}
\mathrm{tr}(M) &= 2 + f_u\alpha_1 + g_\gamma\alpha_2, \\
\det(M) &= 1 + f_u\alpha_1 + g_\gamma\alpha_2 + c\alpha_1\alpha_2,
\end{aligned}
$$

where $c = f_u g_\gamma - f_\gamma g_u$. Note that

$$
\det(M) = -1 + \mathrm{tr}(M) + c\alpha_1\alpha_2.
$$

We can use those formula to study the influence of α_1 and α_2 on the contraction rate of $I + Kf'(u)$.

Appendix D

Path following

The material presented in this appendix mainly supports ideas presented in chapter 4.

Path following is about algorithm to construct numerically the zero-set of some non linear equation

$$F(x, \gamma) = 0$$

depending on a single parameter γ. Typically the solution set will consist of branches, which might bifurcate from each other, but which are essentially one dimensional objects in the space X. More complete and additional information can be found directly in [19, 62, 75, 91] and their references. We shall concentrate on the so called predictor-corrector methods, whose name indicate well their purpose. They attempt to follow the solution curve from one approximation to the next, first by predicting the new point then correcting the prediction to get a better approximation.

The set of all roots of $F(x, \gamma) = 0$ is called the **bifurcation diagram** of F. When the IFT applies, the bifurcation diagram of F consists locally of only one branch. We are going to describe numerical techniques to find branches of solutions. Because we focus on the numerical applications of the technique, we can assume that we work in finite dimension and thus in what follows $x \in \mathbb{R}, n \geq 1$.

D.1 Regular solutions

Let $F : U \subset \mathbb{R}^{n+1} \to \mathbb{R}^n$ be a smooth enough function, say C^k to fix the ideas, $k \geq 1$. We suppose that we know a solution (x_0, γ_0) of $F(x, \gamma) = 0$. Our objective is to get other solutions near (x_0, γ_0).

We say that (x_0, γ_0) is a **regular solution** if the total derivative $DF(x_0, \gamma_0)$ of F at (x_0, γ_0) is of maximal rank, that is, of rank n. The $n \times (n+1)$-matrix DF is formed of two blocks (F_x, F_γ) so, if (x_0, γ_0) is regular, this implies two possibilities. Either,

1. the rank of $F_x(x_0, \gamma_0)$ is n, or
2. the rank of $F_x(x_0, \gamma_0)$ is only $n - 1$ and $F_\gamma(x_0, \gamma_0) \in \mathbb{R}^n$ is not in the range of $F_x(x_0, \gamma_0)$.

In the first case, the IFT tells us that there is a unique curve parametrised by γ: $\gamma \mapsto (\bar{x}(\gamma), \gamma)$ of solutions of $F = 0$ near the regular point. In the second case, the γ-parametrisation fails. In the case, $x \in \mathbb{R}$ (i.e. $n = 1$) $F_x(x_0, \gamma_0) = 0$ and $F_\gamma(x_0, \gamma_0) \neq 0$ (the range of F_x is obviously 0 in this case) and so we have a point of 'vertical' tangent at (x_0, γ_0). In general the second derivative is not degenerate and (x_0, γ_0) will be called a **turning point**. From the plots shown in, for example, figure 4.1 one can see that even in this case we still have a unique curve (compared with the case of a bifurcation of two curves), it is simply the parametrisation in γ that fails. Therefore we will have to use a 'general' parametrisation $t \mapsto (\bar{x}(t), \bar{l}(t))$ to describe and follow the solution set around (x_0, γ_0). In the case $n = 1$, because $F_\gamma(x_0, \gamma_0) \neq 0$, we can use $t \mapsto (t, \bar{l}(t))$. This is a general occurrence because of the following result proved in [19]. As mentioned before, it is simple at a regular point of type (a) i.e. not a turning point (the IFT applies directly), but needs some work at a regular point of type (b) i.e. turning points.

Proposition D.1 ([19]) *Let $F : U \subset \mathbb{R}^{n+1} \to \mathbb{R}^n$ be a continuously differentiable map. If $(x_0, \gamma_0) \in U$ is a regular point of F, then the zero-set of F in a neighbourhood of (x_0, γ_0) is a smooth branch.*

The point is that, at a regular point, the bifurcation diagram, is always a single curve. In the next subsection we describe more fully and justify what happens at a regular point.

D.1.1 Branches of solutions

In the remainder of this section we analyse more precisely the bifurcating branch when F has a regular point at (x_0, γ_0). Suppose that we have a branch of solutions around some point (x_0, γ_0). That branch might or might not be parametrised by γ. We would like to find the Taylor series expansion of the branch of solution $s \mapsto (\bar{x}(s), \bar{l}(s))$ with $\bar{x}(s_0) = x_0$ and $\bar{l}(s_0) = \gamma_0$. If $\bar{l}(s) = s$, the branch is parametrised by γ.

By definition $F(\bar{x}(s), \bar{l}(s)) \equiv 0 \in \mathbb{R}^n$. In terms of components we have

$$F_i(\bar{x}(s), \bar{l}(s)) = 0, \quad i = 1, \cdots, n.$$

Taking the derivative in s, we get

$$\left(\sum_{j=1}^{n} \frac{\partial F_i}{\partial x_j}(\bar{x}(s), \bar{l}(s)\bar{x}_j'(s)) \right) + F_\gamma(\bar{x}(s), \bar{l}(s))\bar{l}'(s) = 0, \quad i = 1, \cdots, n.$$

In case the Jacobian matrix $(F_x)_{ij} = \left(\frac{\partial F_i}{\partial x_j}\right)$ is invertible we find an explicit formula for $\bar{x}'$, which can be rescaled using $\bar{l}'$. Actually, in that case the IFT applies and we can assume that $\bar{l}'(s) = 1$. There is, though, another possibility: $F_x(x_0, \gamma_0)$ is singular and $F_\gamma(x_0, \gamma_0) \in \mathbb{R}^n$ is not in the range of $F_x(x_0, \gamma_0)$. In that case we have to set $\bar{l}'(s_0) = 0$, consequently $\bar{x}'(s_0) \in \ker F_x(x_0, \gamma_0)$.

Taking the next derivative at $s = s_0$ (assuming that F is C^2 on U), using that $\bar{l}'(s_0) = 0$ and letting $x_0 = \bar{x}(s_0)$ and $l(s_0) = \gamma_0$ we get

$$\sum_{j=1}^{n}\sum_{k=1}^{n}\frac{\partial^2 F_i}{\partial x_j \partial x_k}(x_0,\gamma_0)\bar{x}_j'(s_0)\bar{x}_k'(s_0)$$
$$+\quad \sum_{j=1}^{n}\frac{\partial F_i}{\partial x_j}(x_0,\gamma_0)\bar{x}_j''(s_0)+\frac{\partial F_i}{\partial \gamma}(x_0,\gamma_0)\bar{l}''(s_0)=0,\quad i=1,\cdots,n.$$

If $\psi \in \mathbb{R}^n$ is a vector in $\ker(F_x)(x_0,\gamma_0)^T$, i.e. $<\ker(F_x)(x_0,\gamma_0)^T,\psi>=0$.

We denote by ϕ, resp. ψ the generators of $\ker F_x(x_0,\gamma_0)$, resp. $\ker F_x(x_0,\gamma_0)^T$. Because (x_0,γ_0) is regular, ϕ and ψ are unique up to rescaling. Recall that

$$\operatorname{im} F_x(x_0,\gamma_0)=\{\ x\in\mathbb{R}^n|\ \ <x,\psi>=0\ \}.$$

Take the scalar product of (D.1) with respect to ψ. We find that

$$<F_\gamma(x_0,\gamma_0),\psi>\bar{l}''(s_0)+<F_{xx}(x_0,\gamma_0)(\bar{x}'(s_0),\bar{x}'(s_0)),\psi>=0, \tag{D.1}$$

because $<F_x(\bar{x}(s),\bar{l}(s))\,\bar{x}'(s),\psi>=0$. Specifically,we get the following scalar equation which enables $\bar{l}''(s_0)$ to be determined.

$$\sum_{i=1}^{n}\sum_{j=1}^{n}\sum_{k=1}^{n}\frac{\partial^2 F_i}{\partial x_j\partial x_k}(x_0,\gamma_0)\bar{x}_j'(s_0)\bar{x}_k'(s_0)\psi_i+\left(\sum_{i=1}^{n}\frac{\partial F_i}{\partial\gamma}(x_0,\gamma_0)\psi_i\bar{l}''(s_0)\right)=0$$

From our assumptions, $<F_\gamma(x_0,\gamma_0),\psi>\neq 0$ and so

$$\bar{l}''(s_0)=-\frac{<F_{xx}(x_0,\gamma_0)(\bar{x}'(s_0),\bar{x}'(s_0)),\psi>}{<F_\gamma(x_0,\gamma_0),\psi>}.$$

The parametrisation of the branch is thus

$$\bar{l}(s)=\gamma_0+\frac{1}{2}\bar{l}''(s_0)(s-s_0)^2+\ \dots\ ,$$

which is one sided in γ so that, when $\bar{l}''(s_0)\neq 0$, we get a turning point looking like a parabola, a **quadratic turning point**, the direction of the parabola depending on the sign of $\bar{l}''(s_0)$ (obviously the branch is not symmetric, it is only quadratic at least order).

If $\bar{l}''(s_0)=0$, we have to go to the next derivatives and so on until some derivative $\bar{l}^{(m)}(s_0)\neq 0$ (a **simple limit point**).

D.2 Predictor-corrector methods

In this section we look at the easy situation when we have only regular points of type (a). We use the so called **predictor-corrector schemes**.

The broad idea in that case is the following. Let (x_0, γ_0) be some approximation to a solution of $F(x, \gamma) = 0$. To find the next point along the branch, we use a **prediction step** which gives a first approximation $(\hat{x}_1, \hat{\gamma}_1)$. Note that typically we take here a given step in γ, so $\hat{\gamma}_1 = \gamma_1 = \gamma_0 + \delta\gamma$. Then, we use that approximation as the starting point for the **correction step** which will be a fast converging method in x at γ constant to a better solution (x_1, γ_1) of $F = 0$. The correction step usually uses a non linear equation solver, typically of Newton's type.

This is the outline of the idea when we follow the curve in the parameter γ. We shall see later that this is restrictive because of the turning points. A somewhat more elegant, sometimes more efficient, tactic is to follow the curve along a well-chosen general parametrisation.

D.2.1 Predictor step

There are two simple predictor we could use, namely,

1. the **Trivial Predictor**.

   This is the simplest possible predictor. We take the next predicted value as the last calculated, without correction:

   $$\hat{x}_1 = x_0.$$

2. the **Second Interpolation Predictor**.

   We need two starting points, (x_{-1}, γ_{-1}) and (x_0, γ_0) say, then we interpolate linearly to get the next predicted value:

   $$\hat{x}_1 = x_0 + \frac{\gamma_1 - \gamma_0}{\gamma_0 - \gamma_{-1}} (x_0 - x_{-1}).$$

Here we shall concentrate on a widely used technique: the **Euler Predictor**.

Euler prediction

This is the most widely used technique. If we differentiate $F(\bar{x}(\gamma), \gamma) = 0$ with respect to γ, we find that

$$F_x(\bar{x}(\gamma), \gamma)\, \bar{x}'(\gamma) + F_\gamma(\bar{x}(\gamma), \gamma) \equiv 0. \tag{D.2}$$

We use Euler's method for this ODE and we get

$$\hat{x}_1 = x_0 + (\gamma_1 - \gamma_0)\, \bar{x}'(\gamma_0).$$

The error when F is at least C^2 on some interval containing γ_0 and γ_1, comes from the usual exact estimate for the Euler method. Because

$$\bar{x}(\gamma_1) - \hat{x}_1 = \frac{1}{2}\, \bar{x}''(\gamma_0)(\gamma_1 - \gamma_0, \gamma_1 - \gamma_0) + O(|\gamma_1 - \gamma_0|^3),$$

we can say that

$$\|\bar{x}(\gamma_1) - \hat{x}_1\| \leq \frac{1}{2} \|\bar{x}''\|\, \|\gamma_1 - \gamma_0\|^2,$$

that is, the predicted error depends quadratically on the step-size.

D.2.2 Corrector step

With the parametrisation in γ, we fix γ at γ_1 and solve $F(x, \gamma_1) = 0$ using the ADM specialising at the predicted point.

D.3 Turning points and extended systems

We have been able to tackle regular points of type (a). We turn now our attention to the regular points of type (b). This means that we need to take care of turning points.

Suppose $(x_0, \gamma_0) \in \mathbb{R}^{n+1}$ is regular. Then $\ker DF(x_0, \gamma_0)$ is of dimension 1, spanned by $\xi \in \mathbb{R}^{n+1}$ say. We suppose that ξ has been normalised, $\|\xi\| = 1$. Remark that if $s \mapsto (\bar{x}(s), \bar{l}(s))$ is a parametrisation of the zero-set of F near $(x_0, \gamma_0) = (\bar{x}(0), \bar{l}(0))$, then

$$\|(\bar{x}'(0), \bar{l}'(0))\|\xi = (\bar{x}'(0), \bar{l}'(0)),$$

and if s is the arc-length, then (by definition)

$$\xi = (\bar{x}'(0), \bar{l}'(0)).$$

Fix $u > 0$, the equation of the plane π perpendicular to ξ and at distance u from (x_0, γ_0) is

$$< \xi, (x - x_0, \gamma - \gamma_0) >= u.$$

If u is small enough, π will cut the curve $(\bar{x}, \bar{l})$ at a point $(\hat{x}(u), \hat{\gamma}(u))$. In some sense we have parametrised the curve by its projection onto the tangent at (x_0, γ_0) where the distance u is measured.

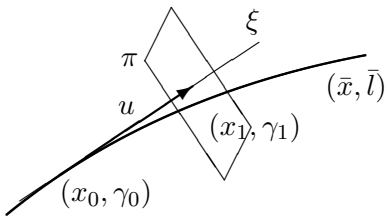

Figure D.1: Pseudo arc-length continuation.

It is clear from Figure D.1 that we also do not need to take exactly the tangent (that will vary at each step along the curve) but it is enough to take some ψ_0 such that $< \psi_0, \xi > \neq 0$. This type of parametrisation is called the **pseudo arc-length**.

We have thus enlarged the problem $F = 0$ to $G = 0$ where $G : \mathbb{R}^{n+2} \to \mathbb{R}^{n+1}$ is defined by

$$G(x, \gamma, u) = \begin{pmatrix} F(x, \gamma) \\ < \psi_0, (x - x_0, \gamma - \gamma_0) > -u \end{pmatrix}. \tag{D.3}$$

The value $u > 0$ determines the next point on the path from (x_0, γ_0).

The important point is that G is now regular of *type (a)* even if F is only regular of type (b). G is called an **extended system**.

The following result is proved in the very simple case of Section 4.2. The general result can be found in [19].

Lemma D.2 ([19]) *The function G, as previously defined, satisfies $G_{(x,\gamma)}(x_0, \gamma_0, 0) \in \mathrm{GL}(n+1, \mathbb{R})$ when F is regular at (x_0, γ_0). Where $\mathrm{GL}(n+1, \mathbb{R})$ denotes the space of invertible $(n+1) \times (n+1)$ real matrices.*

This shows that we can use the predictor-corrector technique, as previously described, on G even if F has a turning point at (x_0, γ_0).

To find the direction of the tangent we have to solve the system $DF(x_0, \gamma_0)\xi = 0$ with the normalising condition $<\xi, \psi>= 1$ and the Euler prediction is simply $(\hat{x}_2, \gamma_2) = (x_1, \gamma_1) + \delta u \cdot \xi$.

That is to say if we now consider $\bar{x} = \bar{x}(u)$ and $\bar{\gamma} = \bar{\gamma}(u)$ then

$$G(\bar{x}(u), \bar{\gamma}(u), u) = 0 \in \mathbb{R}^{n+1}$$

and differentiating w.r.t u and evaluating at $u = 0$ gives

$$G_x(x_0, \gamma_0, 0)x'(0) + G_\gamma(x_0, \gamma_0, 0)\gamma'(0) + G_u(x_0, \gamma_0, 0) = 0 \in \mathbb{R}^{n+1}.$$

In terms of F the structure of this system is

$$\begin{aligned} F_x(x_0, \gamma_0)\bar{x}'(0) + F_\gamma(x_0, \gamma_0)\bar{\gamma}'(0) &= 0 \in \mathbb{R}^n, \\ < \psi_0, (\bar{x}'(0), \bar{\gamma}'(0))^T > -1 &= 0. \end{aligned}$$

The solution of this system gives us the tangent $\xi = (\bar{x}'(0), \bar{\gamma}'(0))$ to the curve at (x_0, γ_0). The Euler prediction is then

$$(\hat{x_1}, \hat{\gamma_1}) = (x_0, \gamma_0) + (\delta u)\xi.$$

Sometimes one can simply interpolate between (x_0, γ_0) and (x_{-1}, γ_{-1}) to find good enough predictions before applying the correction techniques.

D.4 Final comments on path following algorithms

To construct an efficient and robust predictor-corrector method which can successfully approximate complicated or difficult curves, we need to look at several important points:

1. an effective step-size adaptation.

Obviously when the curve is behaving very predictably we do not need to compute many points of it, but when it is very 'wiggly' we will need many close points to be able to draw it accurately without missing some loops by jumping ahead of them with the predictor.

Therefore we need a strategy to adapt the step-size to the branch we want to follow. From our initial comments, the main factor is the curvature of the branch. This is usually quite complicated to estimate, so one uses approximation techniques of more or less sophistication (cf. [19, 91] for a deeper discussion of the issue).

2. an efficient implementation of the corrector, here the ADM.

3. the handling or approximation of points of special interest on the curve, like turning points, bifurcation points etc ...

   Those special points can be fundamental in a good numerical investigation of a problem. For instance, we often need to locate the bifurcation points so we could switch branches. Or start to draw (path follow branches of) the skeleton of special points in a multiparameter investigation.

4. two parameter continuation.

   In a multiparameter environment we need to be able to switch the parameters on and off so we could explore the whole range. Also the points of special interests are usually isolated on a branch (otherwise they are not of special interest). So they will come themselves as branches when we free a second parameter.

Appendix E

The Residue Theorem and applications

The results given here are used in chapters 6 and 7.

In this appendix we develop the techniques needed to calculate integrals of rational functions of trigonometric functions. They are based on residue theory. The main ingredients are now recalled.

Theorem E.1 (The Residue Theorem) *Let C be a simple closed curve in the complex plane, contained in a domain $\Omega \subset \mathbb{C}$, and $f : \Omega \to \mathbb{C}$ be a function analytic on Ω apart from a finite number of pole singularities $a_j \in \Omega$, $1 \leq j \leq k$. Denote by $(a_j)_{-1}$ the coefficient of $\dfrac{1}{(z-a_j)}$ of the Laurent series of f at $z = a_j$. Then,*

$$\oint_C f(z)\,\mathrm{d}z = 2\pi i \left(\sum_{j=1}^{k} (a_j)_{-1} \right). \tag{E.1}$$

The coefficient $(a_j)_{-1}$ is also called the residue of f at a_j. To calculate the residue of a function $f(z)$ at a pole $z = a$ of order k, we can use the following limit

$$a_{-1} = \lim_{z \to a} \frac{1}{(k-1)!} \frac{d^{k-1}}{dz^{k-1}} \Big((z-a)^k f(z) \Big). \tag{E.2}$$

When $k = 1$, it is

$$a_{-1} = \lim_{z \to a} (z-a) f(z). \tag{E.3}$$

Theorem E.1 can be used to evaluate integrals of the type

$$\int_{-\pi}^{\pi} F(\sin kx, \cos kx)\,\mathrm{d}x \tag{E.4}$$

where F is a rational function and $k \in \mathbb{N}$. We are going to deal with two types of such integrals, type I where

$$F(x, y) = \frac{q(y)}{1 + \beta^2 p(y)^2} \tag{E.5}$$

and type II where

$$F(x,y) = \frac{q(y)}{(1+\beta^2 p(y)^2)^2}, \tag{E.6}$$

for analytic functions p, q, typically polynomials.

In this appendix the calculations presented are those where $F(x,y)$ depends on the second argument in (E.4), $\cos kx$ but the techniques also apply to cases where the integrand (E.4) also depends on $\sin kx$. The latter cases are dealt with by the Maple program provided.

E.1 Preliminary results

Proposition E.2 *Let $F(x,y) = \dfrac{F_1(x,y)}{F_2(x,y)}$ be a rational function of denominator F_2 of larger or equal total degree than the numerator F_1 and such that F_2 has no zeroes on $[-1,1]^2$. Then, the integral (E.4) is equal to*

$$2\int_{-\infty}^{\infty} F\left(\frac{2u}{1+u^2}, \frac{1-u^2}{1+u^2}\right) \frac{\mathrm{d}u}{1+u^2}. \tag{E.7}$$

Proof. First, we claim that if f is a 2π-periodic function

$$\int_{-\pi}^{\pi} f(kx)\,\mathrm{d}x = \frac{1}{k}\int_{-k\pi}^{k\pi} f(y)\,\mathrm{d}y = \int_{-\pi}^{\pi} f(y)\,\mathrm{d}y,$$

so we can take $k = 1$ in (E.4). Then, the classical change of variable $u = \tan(x/2)$ is bijective from $(-\pi, \pi)$ to $(-\infty, \infty)$ and so transforms (E.4) into (E.7) because

$$\cos x = \frac{1-u^2}{1+u^2} \quad \text{and} \quad \sin x = \frac{2u}{1+u^2}.$$

□

To evaluate (E.7) we use Theorem E.1 in the usual way. We consider the path $\mathcal{C}$ formed of the real interval $[-R, R]$ and the semi-circle Re^{it}, $t \in [0, \pi]$. Letting R tend to infinity, our hypotheses on F implies that the integral on the semi-circle tends to 0 as R tends to infinity, and so (E.7) is equal to the integral

$$2\oint_{\mathcal{C}} F\left(\frac{2w}{1+w^2}, \frac{1-w^2}{1+w^2}\right) \frac{\mathrm{d}w}{1+w^2},$$

evaluated taking the residues of the integrand

$$f(w) = F\left(\frac{2w}{1+w^2}, \frac{1-w^2}{1+w^2}\right) \frac{1}{1+w^2}, \quad w \in \mathbb{C}, \tag{E.8}$$

at its complex poles with positive imaginary part.

When F is a rational function, $F(x,y) = \dfrac{F_1(x,y)}{F_2(x,y)}$ as in Proposition E.2 The following lemma describes the poles of f in (E.8) coming from F_2 when

$$F_2(x,y) = 1 + \beta^2 p(y)^2, \tag{E.9}$$

where p is a polynomial.

Lemma E.3 *Let p be a real polynomial, $\beta \neq 0$, the roots of*

$$1 + \beta^2 p\left(\frac{1-w^2}{1+w^2}\right)^2 = 0 \tag{E.10}$$

are quadruples

$$w_1, \quad w_2 = \overline{w_1}, \quad w_3 = -w_1 \quad \textit{and} \quad w_4 = -\overline{w_1}, \tag{E.11}$$

where $w_1^2 = \dfrac{1-z_0}{1+z_0}$, $1 \leq i \leq 4$, where z_0 is a root of $p(z) = \dfrac{i}{\beta}$.

Proof. Let $z = \dfrac{1-w^2}{1+w^2}$. Clearly the roots of (E.10) correspond to the roots of $1 + \beta^2 p(z)^2 = 0$, that is, the z_0's such that $p(z_0) = \pm\frac{i}{\beta}$. Note that, because p is real, z_0 is a root of $p(z) = \frac{i}{\beta}$ if and only if $\overline{z_0}$ is a root of $p(z) = -\frac{i}{\beta}$. In terms of z, $w^2 = \dfrac{1-z}{1+z}$. And so the roots have a structure of quadruples as represented in the following figure.

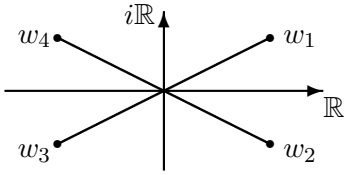

Figure E.1: Structure of quadruple (E.11) of the roots of (E.10).

□

Note that $w = \pm i$ cannot be a root for the F_2 contribution to f.

E.2 Type I integrals

We would like to evaluate integrals of the type

$$\int_{-\pi}^{\pi} \frac{q(\cos(k\phi))\,\mathrm{d}\phi}{1 + \beta^2 p(\cos(k\phi))^2}, \tag{E.12}$$

where p, q are polynomials such that $2\deg(p) \geq \deg(q)$. Using Proposition E.2, the integral (E.12) is equal to

$$2\int_{-\infty}^{\infty} \frac{q(z(u))\,\mathrm{d}u}{(1 + \beta^2 p(z(u))^2)(1+u^2)}, \tag{E.13}$$

where $z(u) = \dfrac{1-u^2}{1+u^2}$. To evaluate (E.13) we need the residues of the integrand with positive imaginary part. The following lemma provides us with the information.

Lemma E.4 *1. For each of the quadruples (E.11), the sum of the residues at the poles with positive imaginary parts for the integral (E.13) is*

$$\frac{i}{4\beta}\,\mathrm{re}\Big(\frac{q(z_1)(1+w_1^2)}{w_1 p'(z_1)}\Big), \tag{E.14}$$

where $w_1^2 = \frac{1-z_0}{1+z_0}$ and where z_0 satisfies $p(z_0) = \dfrac{i}{\beta}$. Further let z_1 satisfy $p(z_1) = \frac{i}{\beta}$ and let w_1 satisfy $z_1 = z(w_1)$ with $\mathrm{im}\, w_1 > 0$ as in Figure E.1.

2. When $2deg(p) = deg(q)$, the pole $w = i$ contributes a residue of

$$\frac{1}{2i}\lim_{z\to\infty}\frac{q(z)}{1+\beta^2(p(z))^2}.$$

Proof.

1. From Proposition E.2, we need to sum the residues of the poles with positive imaginary part corresponding to the integrand

$$\frac{q(z(w))}{((1+\beta^2)p(z(w))^2)(1+w^2)}, \tag{E.15}$$

where $z(w) = \dfrac{1-w^2}{1+w^2}$. From Lemma E.3, the poles of the integrand are single and the ones with positive imaginary part are w_1 and w_4 in the notation of the lemma, with $z(w_4) = \overline{z(w_1)}$ and opposite real parts. To simplify notations, let $z_i = z(w_i)$, $i = 1, 4$. Using (E.3), the value of the residue at a single pole $w = w_i$ is

$$\lim_{w\to w_i}\frac{(w-w_i)q(z(w))}{(1+\beta^2 p(z(w))^2)(1+w^2)} = \frac{q(z(w_i))}{2\beta^2 p(z(w_i))p'(z(w_i))z'(w_i)(1+w_i^2)}, \tag{E.16}$$

using l'Hôpital Rule. A straightforward calculation gives

$$z'(w) = \frac{-4w}{(1+w^2)^2},$$

and so (E.16) becomes

$$\frac{-(1+w_i^2)q(z_i)}{8\beta^2 w_i p(z_i)p'(z_i)}.$$

The sum for w_1 and w_4 gives

$$\frac{-1}{8\beta^2}\left(\frac{q(z_1)(1+w_1^2)}{w_1 p(z_1)p'(z_1)} + \frac{q(z_1)(1+w_4^2)}{w_4 p(z_4)p'(z_4)}\right).$$

Recalling that $p(z_1) = i/\beta$ and $w_4 = \overline{w_1}$, it simplifies to

$$\frac{i}{8\beta}\left(\frac{q(z_1)(1+w_1^2)}{w_1 p'(z_1)} + \overline{\frac{q(z_1)(1+w_1^2)}{w_1 p'(z_1)}}\right) = \frac{i}{4\beta}\,\mathrm{re}\Big(\frac{q(z_1)(1+w_1^2)}{w_1 p'(z_1)}\Big).$$

2. The residue of the integrand (E.15) when $w = i$ is

$$\lim_{w\to i} \frac{q(z(w))(w-i)}{(1+\beta^2 p(z(w))^2)(1+w^2)} = \frac{1}{2i} \lim_{z\to\infty} \frac{q(z)}{1+\beta^2(p(z))^2}$$

because $z \to \infty$ as $w \to i$.

□

E.2.1 Integral Ia

Our first integral is of the type I with $q(y) = p(y)^2$.

Lemma E.5 *The value of the definite integral*

$$\int_{-\pi}^{\pi} \frac{[\frac{1}{2\pi} + Q\cos k\phi]^2 \mathrm{d}\phi}{1+\beta^2[\frac{1}{2\pi} + Q\cos k\phi]^2} \tag{E.17}$$

is given as

$$H = \frac{\pi}{\beta^2}\left[2 - \frac{\sqrt{d(L)}}{\beta Q}\left(1 + \frac{L}{d\,(1+(L)^2)}\right)\right] \tag{E.18}$$

where

$$d = \frac{\beta Q}{1+\beta^2(Q-\frac{1}{2\pi})^2} \tag{E.19}$$

and

$$\xi = \frac{\beta}{2Q}\left(Q^2 - \frac{1}{4\pi^2} - \frac{1}{\beta^2}\right). \tag{E.20}$$

and

$$L = \xi + \sqrt{1+\xi^2}. \tag{E.21}$$

Proof. Because the integrand is of the type

$$\frac{p(z)^2}{1+\beta^2 p(z)^2} = \frac{1}{\beta^2} - \frac{1}{\beta^2}\frac{1}{1+\beta^2 p(z)^2},$$

the integral (E.17) is equal to

$$\frac{2\pi}{\beta^2} - \frac{1}{\beta^2}\int_{-\pi}^{\pi} \frac{\mathrm{d}\phi}{1+\beta^2[\frac{1}{2\pi} + Q\cos k\phi]^2}.$$

To evaluate that second integral

$$\int_{-\pi}^{\pi} \frac{\mathrm{d}\phi}{1+\beta^2[\frac{1}{2\pi} + Q\cos k\phi]^2}, \tag{E.22}$$

we use Lemma E.4 with $p(z) = \frac{1}{2\pi} + Qz$ and $q(z) = 1$. There is only one quadruple of poles to consider with $z_1 = \dfrac{1}{Q}\left(-\dfrac{1}{2\pi} + \dfrac{i}{\beta}\right)$. From (E.14), the residues from w_1 and w_4 is

$$\frac{i}{4\beta}\,\mathrm{re}\left(\frac{1+w_1^2}{Qw_1}\right) = \frac{i}{4\beta Q}\,\mathrm{re}\left(\frac{1+w_1^2}{w_1}\right).$$

The last expression, involving w_1, can be evaluated

$$2\,\mathrm{re}\left(\frac{1+w_1^2}{w_1}\right) = \frac{1+w_1^2}{w_1} + \frac{1+\overline{w_1}^2}{\overline{w_1}} = (w_1+\overline{w_1})\,\frac{(1+|w_1|^2)}{|w_1|^2}.$$

So, the sum of the residue is given by

$$\frac{i\,\mathrm{re}(w_1)}{4\beta Q}\,\frac{(1+|w_1|^2)}{|w_1|^2}.$$

Therefore, we look to evaluate the final value of the integral (E.22)

$$(2\pi i)(2)\left(\frac{i\,\mathrm{re}(w_1)}{4\beta Q}\,\frac{(1+|w_1|^2)}{|w_1|^2}\right) = \frac{-\pi\,\mathrm{re}(w_1)}{\beta Q}\,\frac{(1+|w_1|^2)}{|w_1|^2}. \tag{E.23}$$

We have

$$w_1^2 = \frac{1-z_1}{1+z_1} = \frac{1-|z_1|^2+(\overline{z_1}-z_1)}{|1+z_1|^2} = \frac{1-|z_1|^2}{|1+z_1|^2} - \frac{2i\,\mathrm{im}(z_1)}{|1+z_1|^2}.$$

Define $c = \dfrac{1-|z_1|^2}{|1+z_1|^2}$, $d = \dfrac{\mathrm{im}(z_1)}{|1+z_1|^2} > 0$ and $\xi = \dfrac{c}{2d} = \dfrac{1-|z_1|^2}{2\,\mathrm{im}(z_1)}$. Let $w_1 = a+ib$ with $b>0$. We have that $a^2-b^2 = c$ and $ab = -d$. Replacing b into the first equation, we find that a satisfies

$$a^4 - ca^2 - d^2 = 0,$$

that is,

$$a^2 = \frac{c+\sqrt{c^2+4d^2}}{2} = d\,(L).$$

Because $b>0$, we choose the negative root for a,

$$\mathrm{re}(w_1) = a = -\sqrt{d(L)}. \tag{E.24}$$

We get

$$\begin{aligned} |w_1|^2 &= a^2+b^2 = \frac{a^4+d^2}{a^2} = d\,\frac{\left(1+(L)^2\right)}{(L)}, \\ \frac{1+|w_1|^2}{|w_1|^2} &= 1 + \frac{(L)}{d\,(1+(L)^2)}. \end{aligned} \tag{E.25}$$

Putting things together, (E.23) becomes

$$\frac{\pi\sqrt{d(L)}}{\beta Q}\left(1+\frac{(L)}{d\,(1+(L)^2)}\right).$$

The final value of the integral (E.17) is thus

$$\frac{\pi}{\beta^2}\left[2 - \frac{\sqrt{d(L)}}{\beta Q}\left(1+\frac{(L)}{d\,(1+(L)^2)}\right)\right].$$

□

E.2.2 Integral Ib

Our second integral of type I has $q(y) = 2yp(y)$.

Lemma E.6 *The integral*

$$\int_{-\pi}^{\pi} \frac{2\left(\frac{1}{2\pi} + Q\cos k\phi\right)\cos k\phi}{1+\beta^2\left(\frac{1}{2\pi} + Q\cos k\phi\right)^2}\,\mathrm{d}\phi \tag{E.26}$$

is equal to

$$\frac{2\pi}{\beta^2 Q}\left(2 - \sqrt{\frac{d}{L}}\left(1 + \frac{L}{d\,(1+(L)^2)}\right)\right), \tag{E.27}$$

where d is given in (E.19), ξ in (E.20) and L in (E.21) .

Proof. We use Lemma E.4. For the contribution due to the pole at $w = i$ we have

$$\begin{aligned} q(c) &= 2\left(\frac{1}{2\pi} + Qc\right)c, \\ p(c) &= \frac{1}{2\pi} + Qc, \end{aligned}$$

and thus

$$\frac{1}{2i}\lim_{z\to\infty}\frac{q(z)}{1+\beta^2 p(z)^2} = \frac{1}{2i}\frac{2Q}{\beta^2 Q^2} = \frac{1}{i\beta^2 Q}.$$

When we multiply by $2\pi i$ we get the contribution

$$\frac{2\pi}{\beta^2 Q}$$

to the result.

To take account of the other poles we use formula (E.14) of Lemma E.4, the integral (E.26) is equal to

$$(2\pi i)(2)\,\frac{i}{4\beta}\,\mathrm{re}\left(\frac{q(z_1)(1+w_1^2)}{w_1 p'(z_1)}\right), \tag{E.28}$$

where $p(z) = \frac{1}{2\pi} + Qz$ and $q(z) = 2zp(z)$. We know that $p(z_1) = \frac{i}{\beta}$, and so (E.28) becomes

$$\begin{aligned} \frac{-\pi}{\beta}\,\mathrm{re}\left(\frac{q(z_1)(1+w_1^2)}{w_1 p'(z_1)}\right) &= \frac{-\pi}{\beta}\,\mathrm{re}\left(\frac{2iz_1}{\beta}\frac{(1+w_1^2)}{w_1 Q}\right) \\ &= \frac{-2\pi}{\beta^2 Q}\,\mathrm{re}\left(\frac{iz_1(1+w_1^2)}{w_1}\right) = \frac{-2\pi}{\beta^2 Q}\,\mathrm{re}\left(\frac{i(1-w_1^2)}{w_1}\right). \end{aligned}$$

Now, as in the proof of Lemma E.5,

$$\begin{aligned} 2\,\mathrm{re}\left(\frac{i(1-w_1^2)}{w_1}\right) &= \frac{i(1-w_1^2)}{w_1} - \frac{i(1-\overline{w_1}^2)}{\overline{w_1}} \\ &= i(\overline{w_1} - w_1)\,\frac{(1+|w_1|^2)}{|w_1|^2} = 2\,\mathrm{im}(w_1)\,\frac{(1+|w_1|^2)}{|w_1|^2}, \end{aligned}$$

so (E.28) becomes

$$\frac{-2\pi \operatorname{im}(w_1)}{\beta^2 Q} \frac{(1+|w_1|^2)}{|w_1|^2}.$$

Again, from the proof of Lemma E.5, we have

$$\operatorname{im}(w_1) = b = \frac{-d}{a} = \frac{d}{|a|} = \frac{d}{\sqrt{d(L)}} = \sqrt{\frac{d}{L}}. \tag{E.29}$$

Finally, the integral we seek is equal to (E.27). □

E.3 Type II integrals

For type II integrals, the integrand is of the form $\frac{q(y)}{(1+\beta^2 p(y)^2)^2}$. We need to evaluate integrals of the form

$$2\int_{-\infty}^{\infty} \frac{q(z(u))\,\mathrm{d}u}{(1+\beta^2 p(z(u))^2)^2(1+u^2)}, \tag{E.30}$$

where $z(u) = \frac{1-u^2}{1+u^2}$. For that we need the residues of the integrand with double poles. First we get from the following lemma the information we need.

Lemma E.7 *The residue of* $f(w) = \frac{Q(w)}{P(w)}$ *at* $w = w_i$ *where* $P(w_i) = P'(w_i) = 0$ *and* $P''(wi)Q(wi) \neq 0$, *is*

$$\frac{2\,(3Q'(w_i)P''(w_i) - Q(w_i)P'''(w_i))}{3P''(w_i)^2}. \tag{E.31}$$

Proof. Using (E.2), the value of the residue at a double pole $w = w_i$ is

$$\lim_{w\to w_i} \frac{\mathrm{d}}{\mathrm{d}w}\left[\frac{Q(w)}{P(w)}(w-w_i)^2\right]. \tag{E.32}$$

We have

$$\begin{aligned}\frac{\mathrm{d}}{\mathrm{d}w}\left[\frac{Q(w)}{P(w)}\,(w-w_i)^2\right] &= Q'(w)\,\frac{(w-w_i)^2}{P(w)} &\text{(E.33)}\\ &\quad +Q(w)\left[\frac{2P(w)(w-w_i) - P'(w)(w-w_i)^2}{P(w)^2}\right]. &\text{(E.34)}\end{aligned}$$

We apply now l'Hôpital's Rule to the singular elements of (E.33,E.34). The first fraction in (E.33) gives

$$\lim_{w\to w_i} \frac{(w-w_i)^2}{P(w)} = \lim_{w\to w_i} \frac{\left[(w-w_i)^2\right]''}{[P(w)]''} = \lim_{w\to w_i} \frac{2}{P''(w)} = \frac{2}{P''(w_i)}.$$

The second fraction in (E.34) needs derivatives up to the fourth order. For the numerator, we have

$$\begin{aligned}
[2P(w)(w-w_i) - P'(w)(w-w_i)^2]'''' &= [2P(w) - P''(w)(w-w_i)^2]'''' \\
&= [2P'(w) - 2P''(w)(w-w_i) - P'''(w)(w-w_i)^2]'' \\
&= [-4P'''(w)(w-w_i) - P''''(w)(w-w_i)^2]' \\
&= -4P'''(w) - 6P''''(w)(w-w_i) - P'''''(w)(w-w_i)^2.
\end{aligned}$$

At $w = w_i$, we get $-4P'''(w_i)$. The fourth derivative of the denominator is

$$6P''(w)^2 + 8P'(w)P'''(w) + 2P(w)P''''(w).$$

Taking the values at $w = w_i$, we get $6P''(w_i)^2$. Putting all together, we find the result we seek

$$\frac{2Q'(w_i)}{P''(w_i)} + Q(w_i)\,\frac{(-4P'''(w_i))}{6P''(w_i)^2} = \frac{2\,(3Q'(w_i)P''(w_i) - Q(w_i)P'''(w_i))}{3P''(w_i)^2}.$$

□

Now we turn our attention to the calculation of the residues for the integrand of type II. The following lemma provides us with the information.

Lemma E.8 *1. For each of the quadruples (E.11), the sum of the residues at the poles with positive imaginary parts for the integral (E.30) is*

$$\frac{i}{8\beta^2}\ \mathrm{im}\left(\frac{q'(z_1)(1+w_1^2)}{(p'(z_1))^2 w_1}\right), \tag{E.35}$$

$$\frac{i}{16\beta^2}\ \mathrm{im}\left(\frac{q(z_1)(1+w_1^2)^2}{(p'(z_1))^2 w_1}\right), \tag{E.36}$$

$$\frac{i}{8\beta}\ \mathrm{re}\left(\frac{q(z_1)(1+w_1^2)}{p'(z_1) w_1}\right), \tag{E.37}$$

$$-\frac{i}{8\beta^2}\ \mathrm{im}\left(\frac{q(z_1)p''(z_1)(1+w_1^2)}{(p'(z_1))^3 w_1}\right), \tag{E.38}$$

$$-\frac{i}{32\beta^2}\ \mathrm{im}\left(\frac{q(z_1)(3w_1^2-1)(1+w_1^2)^2}{(p'(z_1))^2 w_1^3}\right), \tag{E.39}$$

where $z_1 = z(w_1)$ is a root of $p(z) = \dfrac{i}{\beta}$.

2. When $deg(q) = 4deg(p)$, the pole $w = i$ contributes a residue of

$$\frac{1}{2i}\lim_{z\to\infty}\frac{q(z)}{(1+\beta^2 p(z)^2)^2}.$$

Proof.

1. From Proposition E.2, we need to sum the residues of the poles with positive imaginary part corresponding to the integrand

$$\frac{q(z(w))}{(1+\beta^2 p(z(w))^2)^2(1+w^2)},$$

where $z(w) = \dfrac{1-w^2}{1+w^2}$. From Lemma E.3, the poles of the integrand are now double and the ones with positive imaginary part are w_1 and w_4 in the notation of the lemma, with $z(w_4) = \overline{z(w_1)}$ and opposite real parts. To simplify notations, let $z_i = z(w_i)$, $i = 1, 4$. We can use (E.31) with

$$P(w) = \left((1+\beta^2 p(z(w))^2\right)^2 (1+w^2), \qquad Q(w) = q(z(w)).$$

We have

$$Q(w_i) = q(z_i), \quad Q'(w_i) = q'(z_i)z'(w_i).$$

For P, we have

$$P'(w) = 2w(1+\beta^2 p(z(w))^2)^2 + 4\beta^2(1+\beta^2 p(z(w)^2)(1+w^2)(p(z(w))p'(z(w))z'(w)),$$

and

$$\begin{aligned} P''(w) &= 2(1+\beta^2 p(z(w))^2)^2 + 8\beta^4(1+w^2)(p(z(w))p'(z(w))z'(w))^2 \\ &\quad +16\beta^2 w(1+\beta^2 p(z(w)^2)(p(z(w))p'(z(w))z'(w)) \\ &\quad 4\beta^2(1+\beta^2 p(z(w))^2)(1+w^2)(p(z(w))p'(z(w))z'(w))'. \end{aligned}$$

Hence, $P''(w_i) = 8\beta^4(1+w_i^2)(p(z_i)p'(z_i)z'(w_i))^2$. Finally,

$$\begin{aligned} P'''(w) &= 24\beta^2(1+\beta^2 p(z(w))^2)(p(z(w))p'(z(w))z'(w)) \\ &\quad +48\beta^4 w(p(z(w))p'(z(w))z'(w))^2 \\ &\quad +24\beta^2 w(1+\beta^2 p(z(w))^2)(p(z(w))p'(z(w))z'(w))' \\ &\quad +24\beta^4(1+w^2)(p(z(w))p'(z(w))z'(w))(p(z(w))p'(z(w))z'(w))' \\ &\quad +4\beta^2(1+w^2)(1+\beta^2 p(z(w))^2)(p(z(w))p'(z(w))z'(w))'', \end{aligned}$$

so

$$P'''(w_i) = 48\beta^4 w_i(p(z_i)p'(z_i)z'(w_i))^2 + 24\beta^4(1+w_i^2)(p(z_i)p'(z_i)z'(w_i))(p(z_i)p'(z_i)z'(w_i))'.$$

From (E.34), and simplifying, we get three parts

$$\begin{aligned} \frac{2\left(3Q'(w_i)P''(w_i) - Q(w_i)P'''(w_i)\right)}{3P''(w_i)^2} &= \frac{q'(z_i)}{4\beta^4(1+w_i^2)(p(z_i)p'(z_i))^2 z'(w_i)} && \text{(E.40)} \\ &\quad -\frac{w_i q(z_i)}{2\beta^4(1+w_i^2)^2(p(z_i)p'(z_i)z'(w_i))^2} && \text{(E.41)} \\ &\quad -\frac{q(z_i)(p\,p'\,z')'(w_i)}{4\beta^4(1+w_i^2)(p(z_i)p'(z_i)z'(w_i))^3}. && \text{(E.42)} \end{aligned}$$

Explicitly, $(pp'z')' = (p'z')^2 + pp''(z')^2 + pp'z''$. Replacing into (E.42), we find

$$\begin{aligned} -\frac{q(z_i)(p\,p'\,z')'(w_i)}{4\beta^4(1+w_i^2)(p(z_i)p'(z_i)z'(w_i))^3} &= -\frac{q(z_i)}{4\beta^4(1+w_i^2)p(z_i)^3 p'(z_i)z'(w_i)} && \text{(E.43)} \\ &\quad -\frac{q(z_i)p''(z_i)}{4\beta^4(1+w_i^2)p(z_i)^2 p'(z_i)^3 z'(w_i)} && \text{(E.44)} \\ &\quad -\frac{q(z_i)z''(w_i)}{4\beta^4(1+w_i^2)p(z_i)^2 p'(z_i)^2 z'(w_i)^3}. && \text{(E.45)} \end{aligned}$$

Recall that $z'(w) = \dfrac{-4w}{(1+w^2)^2}$, and so a straightforward calculation gives

$$z''(w) = \frac{4(3w^2-1)}{(1+w^2)^3}.$$

Each quadruple correspond to w_1 where $z_1 = z(w_1)$ and $p(z_1) = i/\beta$ and $w_4 = -\overline{w_1}$ with $z_4 = \overline{z_1}$ and $p(z_4) = -i/\beta$. Therefore, we can evaluate the five terms for the residues. First, (E.40) leads to

$$\frac{q'(z_1)(1+w_1^2)}{16\beta^2(p'(z_1))^2 w_1} - \overline{\frac{q'(z_1)(1+w_1^2)}{16\beta^2(p'(z_1))^2 w_1}}$$

that simplifies into (E.35), (E.41) gives

$$\frac{q(z_1)(1+w_1^2)^2}{32\beta^2(p'(z_1))^2 w_1} - \overline{\frac{q(z_1)(1+w_1^2)^2}{32\beta^2(p'(z_1))^2 w_1}},$$

simplifying into (E.36). Finally, (E.43), (E.44) and (E.45) give

$$\frac{iq(z_1)(1+w_1^2)}{16\beta p'(z_1) w_1} + \overline{\frac{iq(z_1)(1+w_1^2)}{16\beta p'(z_1) w_1}},$$

$$\frac{-q(z_1)p''(z_1)(1+w_1^2)}{16\beta^2(p'(z_1))^3 w_1} + \overline{\frac{q(z_1)p''(z_1)(1+w_1^2)}{16\beta^2(p'(z_1))^3 w_1}},$$

$$\frac{-q(z_1)(3w_1^2-1)(1+w_1^2)^2}{64\beta^2(p'(z_1))^2 w_1^3} + \overline{\frac{q(z_1)(3w_1^2-1)(1+w_1^2)^2}{64\beta^2(p'(z_1))^2 w_1^3}},$$

simplifying into (E.37), (E.38) and (E.39), respectively.

2. The residue of the integrand when $w = i$ is

$$\lim_{w\to i} \frac{q(z(w))(w-i)}{(1+\beta^2 p(z(w))^2)^2(1+w^2)} = \frac{1}{2i}\lim_{z\to\infty}\frac{q(z)}{(1+\beta^2 p(z)^2)^2}$$

because $z \to \infty$ as $w \to i$.

□

E.3.1 Integral IIa

We can turn our attention to the case where $q(z) = 2zp(z)$ where

$$p(z) = \frac{1}{2\pi} + Qz$$

for a constant $Q \in \mathbb{R}$.

Lemma E.9 *The integral*

$$\int_{-\pi}^{\pi} \frac{2\left(\frac{1}{2\pi} + Q\cos k\phi\right)(\cos k\phi)}{\left(1+\beta^2\left(\frac{1}{2\pi} + Q\cos k\phi\right)^2\right)^2}\,\mathrm{d}\phi \tag{E.46}$$

is equal to

$$\frac{-\pi}{4Q^2\beta^3}\sqrt{\frac{d}{L}}\left[d\left(3-L^2\right)\left(1+\frac{L^3}{d^3\left(1+L^2\right)^3}\right)\right.$$
$$\left.-3L\left(1+\frac{L}{d\left(1+L^2\right)}\right)\right], \tag{E.47}$$

where d is given in (E.19), ξ in (E.20) and L in (E.21).

Proof. Recall that $z(w)=\dfrac{(1-w^2)}{(1+w^2)}$. Note that $q'(z)=2p(z)+2zp'(z)$, and so $q'(z)=\dfrac{2i}{\beta}+2Q\dfrac{(1-w^2)}{(1+w^2)}$ and $q(z)=\dfrac{2i(1-w^2)}{\beta(1+w^2)}$. Replacing into (E.35), we get

$$\begin{aligned}\frac{i}{8\beta^2}\operatorname{im}\left(\frac{q'(z_1)(1+w_1^2)}{(p'(z_1))^2w_1}\right) &= \frac{i}{8\beta^2Q^2}\operatorname{im}\left(\left[\frac{2i}{\beta}+2Q\frac{(1-w_1^2)}{(1+w_1^2)}\right]\frac{(1-w_1^2)}{(1+w_1^2)}\right)\\ &= \frac{i}{4Q^2\beta^3}\operatorname{re}\left(\frac{1+w_1^2}{w_1}\right)+\frac{i}{4Q\beta^2}\operatorname{im}\left(\frac{1-w_1^2}{w_1}\right).\end{aligned}$$

For (E.36), after simplifications, we get

$$\frac{i}{16Q^2\beta^2}\operatorname{im}\left(\frac{2i}{\beta}\frac{(1-w_1^2)}{(1+w_1^2)}\frac{(1+w_1^2)^2}{w_1}\right)=\frac{i}{8Q^2\beta^2}\operatorname{im}\left(\frac{i(1-w_1^4)}{w_1}\right)=\frac{i}{8Q^2\beta^3}\operatorname{re}\left(\frac{1-w_1^4}{w_1}\right).$$

For (E.37), after simplifications, we get

$$\frac{i}{8Q\beta}\operatorname{re}\left(\frac{2i}{\beta}\frac{(1-w_1^2)}{(1+w_1^2)}\frac{(1+w_1^2)}{w_1}\right)=\frac{i}{4Q\beta^2}\operatorname{re}\left(\frac{i(1-w_1^2)}{w_1}\right)=\frac{-i}{4Q\beta^2}\operatorname{im}\left(\frac{1-w_1^2}{w_1}\right).$$

Because $p''(z)=0$, (E.38) gives no contribution, and, finally, (E.39) contributes

$$\begin{aligned}\frac{-i}{32Q^2\beta^2}\operatorname{im}\left(\frac{2i}{\beta}\frac{(1-w_1^2)}{(1+w_1^2)}\frac{(3w_1^2-1)(1+w_1^2)^2}{w_1^3}\right) &= \frac{-i}{16Q^2\beta^3}\operatorname{im}\left(\frac{i(3w_1^2-1)(1-w_1^4)}{w_1^3}\right)\\ &= \frac{-i}{16Q^2\beta^3}\operatorname{re}\left(\frac{(1-w_1^4)(3w_1^2-1)}{w_1^3}\right).\end{aligned}$$

Putting everything together we get the full residue

$$\frac{i}{4Q^2\beta^3}\operatorname{re}\left(\frac{(1+w_1^2)}{w_1}+\frac{(1-w_1^4)}{2w_1}-\frac{(1-w_1^4)(3w_1^2-1)}{4w_1^3}\right)=\frac{i}{16Q^2\beta^3}\operatorname{re}\left(\frac{(1+w_1^2)^3}{w_1^3}\right).$$

To evaluate this residue, recall that $w_1=a+ib$ where $b=-d/a$, a is given in (E.24) and d is given in (E.19).

Therefore,

$$\begin{aligned}
\mathrm{re}\left(\frac{(1+w_1^2)^3}{w_1^3}\right) &= \mathrm{re}(w_1^3)\,\frac{1+|w_1|^6}{|w_1|^6} + 3\mathrm{re}(w_1)\,\frac{1+|w_1|^2}{|w_1|^2} \\
&= \left(a^3 - 3\frac{d^2}{a}\right)(1+|w_1|^{-6}) + 3a\,(1+|w_1|^{-2}) \\
&= \sqrt{\frac{d^3}{L}}\,(3-L^2)\left(1+\frac{L^3}{d^3(1+L^2)^3}\right) - 3\sqrt{dL}\left(1+\frac{L}{d(1+L^2)}\right) \\
&= \sqrt{\frac{d}{L}}\left[d(3-L^2)\left(1+\frac{L^3}{d^3(1+L^2)^3}\right) - 3L\left(1+\frac{L}{d(1+L^2)}\right)\right]. \quad \text{(E.48)}
\end{aligned}$$

Multiplying the full residue by $4\pi i$, we get the final result (E.47). □

E.3.2 Integral IIb

We can turn our attention to the case where $q(z) = zp(z)^3$ where

$$p(z) = \frac{1}{2\pi} + Qz$$

for a constant $Q \in \mathbb{R}$.

Lemma E.10 *The integral*

$$\int_{-\pi}^{\pi} \frac{\left(\frac{1}{2\pi} + Q\cos k\phi\right)^3 (\cos k\phi)}{\left(1+\beta^2\left(\frac{1}{2\pi} + Q\cos k\phi\right)^2\right)^2}\,\mathrm{d}\phi \quad \text{(E.49)}$$

is equal to

$$\begin{aligned}
&\frac{\pi}{\beta^4 Q}\left[2 - \sqrt{\frac{d}{L}}\left(1+\frac{3L}{8\beta Q}\right)\left(1+\frac{L}{d(1+L^2)}\right)\right. \\
&\qquad \left. + \frac{d}{8\beta Q}\sqrt{\frac{d}{L}}(3-L^2)\left(1+\frac{L^3}{d^3(1+L^2)^3}\right)\right] \quad \text{(E.50)}
\end{aligned}$$

where d is given in (E.19), ξ in (E.20) and L in (E.21).

Proof. For the contribution due to the pole at $w = i$ we have

$$\begin{aligned}
q(c) &= \left(\frac{1}{2\pi} + Qc\right)^3 c, \\
p(c) &= \frac{1}{2\pi} + Qc,
\end{aligned}$$

and thus by Lemma E.8 we have

$$\frac{1}{2i}\lim_{z\to\infty}\frac{q(z)}{(1+\beta^2 p(z)^2)^2}=\frac{1}{2i}\frac{Q^3}{\beta^4Q^4}=\frac{1}{2i\beta^4Q}.$$

When we multiply by $4\pi i$ we get the contribution

$$\frac{2\pi}{\beta^4Q}$$

to the result.

Then note that $q'(z)=p(z)^3+3zp(z)^2p'(z)$, and so (E.35) becomes

$$\begin{aligned}\frac{i}{8\beta^2}\operatorname{im}\left(\frac{q'(z_1)(1+w_1^2)}{(p'(z_1))^2w_1}\right) &= \frac{i}{8\beta^2}\operatorname{im}\left(\frac{(p(z_1)^3+3z_1p(z_1)^2Q)(1+w_1^2)}{Q^2w_1}\right)\\ &= -\frac{i}{8Q^2\beta^5}\operatorname{re}\left(\frac{1+w_1^2}{w_1}\right)-\frac{3i}{8Q\beta^4}\operatorname{im}\left(\frac{1-w_1^2}{w_1}\right).\end{aligned}$$

For (E.36), after simplifications, we get

$$-\frac{i}{16Q^2\beta^5}\operatorname{re}\left(\frac{1-w_1^4}{w_1}\right).$$

For (E.37), after simplifications, we get

$$\frac{i}{8Q\beta^4}\operatorname{im}\left(\frac{1-w_1^2}{w_1}\right).$$

Because $p''(z)=0$, (E.38) gives no contribution, and, finally, (E.39) contributes

$$\frac{i}{32Q^2\beta^5}\operatorname{re}\left(\frac{(1-w_1^4)(3w_1^2-1)}{w_1^3}\right).$$

Putting everything together we get the residue

$$-\frac{i}{32Q^2\beta^5}\operatorname{re}\left(\frac{(1+w_1^2)^3}{w_1^3}\right)-\frac{i}{4Q\beta^4}\operatorname{im}\left(\frac{1-w_1^2}{w_1}\right). \tag{E.51}$$

To evaluate this residue, recall that $w_1=a+ib$ where $b=-d/a$, a is given in (E.24), d is given in (E.19) and to simplify notation, we define L in (E.21) from ξ in (E.20). Therefore, using (E.48) and

$$\operatorname{im}\left(\frac{(1-w_1^2)}{w_1}\right)=-\operatorname{im}(w_1)\,\frac{1+|w_1|^2}{|w_1|^2}=\frac{d}{a}\left(1+|w_1|^{-2}\right)=-\sqrt{\frac{d}{L}}\left(1+\frac{L}{d(1+L^2)}\right),$$

we get (E.51). Multiplying (E.51) by $4\pi i$, adding the contribution at $w=i$, we get the final result (E.50). □

Appendix F

Tables and graphs for Chapter 3

Table F.1: Adomian solutions for different values of α.

u_0	$\alpha = 1$	$\alpha = -0.1$	$\alpha = -0.2$	$\alpha = -0.4$	$\alpha = -0.6$
-1000	-2				
-10	-2				
-6	-1.892009647				
-5	-1.871033382				
-4	-1.855529089				
-3	-1.845588663	-3.800450527	-5.038813902	-9.589860378	-18.724808160
-2.8	-1.844264252	-3.454537843	-4.462592658	-8.146534651	-15.502571770
-2.6	-1.843177967	-3.110946956	-3.893385465	-6.731996662	-12.360305920
-2.4	-1.842343335	-2.770285437	-3.333266116	-5.356372380	-9.329801818
-2.2	-1.841773807	-2.433306948	-2.784834006	-4.032537110	-6.451894984
-2	-1.841472225	-2.100940413	-2.251307850	-2.776502273	-3.777459966
-1.8	-1.841408633	-1.774321883	-1.736614132	-1.607637740	-1.367491439
-1.6	-1.841489848	-1.454827402	-1.245453964	-0.548555182	0.708531554
-1.4	-1.841543331	-1.144103827	-0.783322479	0.375599665	2.377091881
-1.2	-1.841350607	-0.844092423	-0.356442507	1.138773814	3.569174001
-1	-1.840671715	-0.557037235	0.028439575	1.716917509	4.234015239
-0.8	-1.838698636	-0.285466647	0.364459924	2.092463913	4.358221383
-0.6	-1.830844423	-0.032132336	0.645311627	2.260343378	3.987998827
-0.4	-1.797712474	0.200113913	0.866232135	2.234768654	3.247830457
-0.2	-1.679093437	0.408526607	1.025281104	2.054760181	2.342719247
0	-1.341666667	0.590772908	1.124746133	1.784712533	1.526011200
0.2	-0.641699919	0.745339995	1.172286523	1.505122087	1.019038652
0.4	0.015612271	0.872010085	1.181146662	1.290184351	0.897115336
0.6	-2.295922865	0.972311149	1.168605436	1.176947977	1.018833025
0.8	-16.113223340	1.049772760	1.152150912	1.146338918	1.130455366
1	-42.398199661	1.109749871	1.144192455	1.145982646	1.144722811
1.2	80.233343340	1.158603625	1.148415330	1.146275307	1.149263911
1.4	1640.136368000	1.202278484	1.161868358	1.178726543	2.629738079
1.6	11929.861470000	1.244862131	1.182924303	2.429567439	39.2522609700
1.8	66300.877950000	1.288256891	1.246135673	20.890552990	443.628081000
2		1.288256891	1.852395767	187.343612792	3483.011263383
2.2		1.391561833	7.631154309	1315.389659000	21738.257440000
2.4		1.555442207	50.405422880	7685.970398000	
2.6		2.623377416	310.253167700	39451.411220000	
2.8		9.993591441	1680.617062000		
3		54.273272880	8202.818829016		

Table F.2: Seven terms sum of the RADM when $\alpha = -0.1$.

u_0	Value of the RADM	u_0	Value of the RADM
-3	-3.800450529	1.146193911	1.146193384
-2.100940414	-2.268044510	1.146194538	1.146193532
-2	-2.100940414	1.146194835	1.146193597
-1.936832652	-1.997101135	1.146196159	1.146193911
-1.9	-1.936832652	1.146198843	1.146194538
-1.8	-1.774321883	1.146200101	1.146194835
-1.774321883	-1.732871310	1.146205739	1.146196159
-1.732871310	-1.666215486	1.146217183	1.146198843
-1.666215486	-1.559720359	1.146222538	1.146200101
-1.559720359	-1.391484748	1.146246556	1.146205739
-1.5	-1.298255020	1.146295344	1.146217183
-1.298255020	-0.990007959	1.146318153	1.146222538
-0.990007959	-0.543079934	1.146420499	1.146246556
-0.543079934	0.036235695	1.146628440	1.146295344
0.036235695	0.620856679	1.146725663	1.146318153
0.620856679	0.981376983	1.147161986	1.146420499
0.981376983	1.104734561	1.148463766	1.146725663
1.104734561	1.136314962	1.150327086	1.147161986
1.136314962	1.143866904	1.154121992	1.146628440
1.143866904	1.145646830	1.155900383	1.148463766
1.145646830	1.146064969	1.163913954	1.150327086
1.146064969	1.146163121	1.180362806	1.154121992
1.146163121	1.146186156	1.188128469	1.155900383
1.146186156	1.146191564	1.223545566	1.163913954
1.146191564	1.146192830	1.298096019	1.180362806
1.146192830	1.146193130	1.333957323	1.188128469
1.146193130	1.146193198	1.5	1.223545566
1.146193198	1.146193216	1.844332777	1.298096019
1.146193220	1.146193220	2	1.333957323
1.146193223	1.146193221	2.5	1.844332777
1.146193226	1.146193224	2.6	2.623377416
1.146193236	1.146193226	2.623377416	2.945415079
1.146193256	1.146193231	2.7	4.691555094
1.146193294	1.146193236	2.945415079	34.036811650
1.146193532	1.146193294	3	54.27327288

Table F.3: Seven terms sum of the RADM when $\alpha = -0.2$.

u_0	Value of the RADM	u_0	Value of the RADM
-82.892521250	-243.543774100	1.146192755	1.146193204
-29.090741680	-82.892521250	1.146193194	1.146193221
-27.140095900	-77.067924110	1.146193204	1.146193219
-11.072642390	-29.090741680	1.146193219	1.146193220
-10.419381720	-27.140095900	1.146193222	1.146193220
-5.038813902	-11.072642390	1.146193226	1.146193221
-4.819849312	-10.419381720	1.146193231	1.146193221
-3	-5.038813902	1.146193244	1.146193221
-2.924247120	-4.819849312	1.146193260	1.146193221
-2.251307851	-2.924247120	1.146193282	1.146193221
-2	-2.251307851	1.146193313	1.146193226
-1.9	-1.991331811	1.146193560	1.146193233
-1.8	-1.736614132	1.146193907	1.146193244
-1.736614132	-1.578158327	1.146194351	1.146193260
-1.578158327	-1.193467179	1.146194953	1.146193282
-1.5	-1.010386192	1.146195900	1.146193313
-1.193467179	-0.3431695853	1.146203062	1.146193560
-1.010386192	0.009596787	1.146213092	1.146193907
-1	0.028439575	1.146233521	1.146194614
-0.343169586	0.917709974	1.146243304	1.146194953
0	1.124746133	1.146270686	1.146195900
0.009596787	1.128128573	1.146477607	1.146203062
0.028439575	1.134423332	1.146766786	1.146213092
0.1	1.154302481	1.147136128	1.146225936
0.5	1.176403427	1.147353866	1.146233521
0.917709974	1.145994708	1.148415330	1.146270686
1	1.144192455	1.154302481	1.146482091
1.124746133	1.145512631	1.161868358	1.146766786
1.128128573	1.145611775	1.171161330	1.147136128
1.134423332	1.145804515	1.176403427	1.147353866
1.144192455	1.146124571	1.182924303	1.147634023
1.145512631	1.146169751	1.2	1.148415330
1.145611775	1.146173164	1.299126335	1.154180117
1.145804515	1.146179802	1.4	1.161868358
1.145994708	1.146186363	1.5	1.171161330
1.146124571	1.146190847	1.6	1.182924303
1.146169751	1.146192409	1.852395767	1.299126335
1.146179802	1.146192755	2	1.852395767
1.146186363	1.146192983	2.1	3.319556323
1.146192409	1.146193194	3.319556323	88223.380600000

Table F.4: Seven terms sum of the RADM when $\alpha = -0.4$.

u_0	Value of the RADM	u_0	Value of the RADM
-6.038585043	-32.396746820	1.146193222	1.146193221
-3	-9.589860378	1.146193244	1.146193221
-2.776502273	-7.978677236	1.146193297	1.146193222
-2.5	-6.038585043	1.146193362	1.146193222
-2.179831789	-3.902508031	1.146193447	1.146193221
-2	-2.776502273	1.146204752	1.146193221
-1.9	-2.179831789	1.146233215	1.146193221
-1.8	-1.607637740	1.147228429	1.146193244
-1.7	-1.062847810	1.148249307	1.146193297
-1.6	-0.548555182	1.149069149	1.146193362
-1.5	-0.067977780	1.149892030	1.146193447
-1.4	0.375599665	1.170481765	1.146204752
-1.3	0.778903789	1.186982399	1.146233215
-1.062847810	1.556429801	1.290184351	1.148249307
-1	1.716917509	1.311194193	1.149892030
-0.586687614	2.264361104	1.386970299	1.170481765
-0.548555182	2.271146206	1.410338796	1.186982399
-0.5	2.269922667	1.5	1.386970299
-0.067977780	1.881747205	1.505122087	1.410338796
0	1.784712533	1.556429801	1.785857910
0.1	1.640975247	1.640975247	3.522297965
0.2	1.505122087	1.716917509	7.995862111
0.375599665	1.311194193	1.75	11.703867170
0.4	1.290184351	1.784712533	17.505432800
0.75	1.149069149	1.785857910	17.739211450
0.778903789	1.147228429	1.881747205	52.800298020
1	1.145982646	2	187
1.146193218	1.146193220	2.264361104	2361.271520000
1.146193220	1.146193220	2.269922667	2481.694262000
1.146193221	1.146193220	2.271146206	2508.958803000

Table F.5: Seven terms sum of the RADM when $\alpha = -0.6$.

u_0	Value of the RADM
-3	-18.724808166
-2	-3.777459966
-1.5	1.598297228
-1	4.234015242
0	1.526011200
0.1	1.224340953
0.5	0.943666036
0.943666036	1.144619591
1	1.144722812
1.144619591	1.146192860
1.144722812	1.146192851
1.146192851	1.146193220
1.146192860	1.146193220
1.146193220	1.146193221
1.146193221	1.146193221
1.146193222	1.146193221
1.146193245	1.146193221
1.146195460	1.146193222
1.146237188	1.146193245
1.148266416	1.14619546
1.156844477	1.146237188
1.193634481	1.148266416
1.224340953	1.156844477
1.263088358	1.193634481
1.292144062	1.263088358
1.3	1.292144062
1.4	2.629738079
1.5	9.855918207
1.526011200	14.223637040
1.598297228	38.372169640
2	3483.011263383

Table F.6: Three terms sum of the RADM when $\alpha = -0.1$.

u_0	Value of the RADM	u_0	Values of the RADM
-5.876836358	-6.691451987	-1.559934166	-1.512134990
-5.203188441	-5.876836358	-1.51213499	-1.456565006
-4.645807467	-5.203188441	-1.5	-1.442475114
-4.184250800	-4.645807467	-1.456565006	-1.392104428
-3.801626399	-4.184250800	-1.442475114	-1.375785810
-3.484006182	-3.801626399	-1.392104428	-1.317535369
-3.219932626	-3.484006182	-1.37578581	-1.298694184
-3	-3.219932626	-1.317535369	-1.231565106
-2.679319713	-2.835871759	-1.298694184	-1.209895522
-2.548251136	-2.679319713	-1.231565106	-1.132870114
-2.438326961	-2.548251136	-1.209895522	-1.108068467
-2.345984993	-2.438326961	-1.132870114	-1.020170958
-2.268295182	-2.345984993	-1.108068467	-0.991958862
-2.202841941	-2.268295182	-1.020170958	-0.892351610
-2.147628843	-2.202841941	-1	-0.869580124
-2.101001614	-2.147628843	-0.991958862	-0.860511647
-2.061585945	-2.101001614	-0.892351610	-0.748640076
-2.028237253	-2.061585945	-0.869580124	-0.723189946
-2	-2.028237253	-0.748640076	-0.588868132
-1.997139668	-2.024860491	-0.723189946	-0.560793157
-1.973650324	-1.997139668	-0.588868132	-0.413822400
-1.953735117	-1.973650324	-0.560793157	-0.383375254
-1.936841817	-1.953735117	-0.413822400	-0.225675695
-1.922505735	-1.922505735	-0.383375254	-0.193384067
-1.910335271	-1.922505735	-0.225675695	-0.02843375
-1.9	-1.910335271	-0.193384067	0.004833532
-1.8	-1.792770127	-0.028433756	0.171766379
-1.792770127	-1.784284317	0	0.2
-1.784284317	-1.774326896	0.004833532	0.204782740
-1.774326896	-1.762646137	0.171766379	0.366794869
-1.762646137	-1.748948615	0.2	0.393552807
-1.748948615	-1.732892850	0.204782740	0.398066102
-1.73289285	-1.714082217	0.366794869	0.547440569
-1.714082217	-1.692057122	0.398066102	0.575445741
-1.692057122	-1.666286558	0.547440569	0.705197900
-1.666286558	-1.636159223	0.575445741	0.728746208
-1.636159223	-1.600974537	0.728746208	0.852961024
-1.600974537	-1.559934166	0.834413413	0.933682855
0.852961024	0.947417470	1.146193099	1.146193146
0.933682855	1.005628991	1.146193146	1.146193175
0.947417470	1.015276023	1.146193175	1.146193191

Table F.6: (continued)

u_0	Value of the RADM	u_0	Values of the RADM
1	1.051502922	1.146193191	1.146193202
1.005628991	1.055314045	1.146193202	1.146193209
1.015276023	1.061815222	1.146193209	1.146193214
1.055314045	1.088384593	1.146193214	1.146193216
1.061815222	1.092635706	1.146193220	1.146193220
1.088384593	1.109824927	1.147053663	1.146723803
1.092635706	1.112547618	1.147588855	1.147053663
1.109824927	1.123478809	1.148049914	1.147337736
1.112547618	1.125198777	1.148457613	1.147588855
1.125198777	1.13314944	1.149868954	1.148457613
1.132072514	1.137440738	1.151086593	1.149206455
1.133149440	1.138111247	1.152164697	1.149868954
1.137440738	1.140778154	1.155906893	1.152164697
1.138111247	1.141194146	1.159148175	1.154148305
1.140778154	1.142846829	1.167350909	1.159148175
1.141194146	1.143104348	1.172096949	1.162027917
1.142846829	1.144126702	1.188818164	1.172096949
1.143104348	1.144285899	1.203622757	1.180911826
1.144285899	1.145015965	1.217037839	1.188818164
1.144917633	1.145406062	1.242518393	1.203622757
1.145015965	1.145466767	1.266032781	1.217037839
1.145466767	1.145745015	1.311889117	1.242518393
1.145745015	1.145916713	1.324678259	1.249464938
1.145916713	1.146088002	1.355711219	1.266032781
1.146088002	1.146153186	1.445870347	1.311889117
1.146153186	1.146168526	1.472244491	1.324678259
1.146168526	1.146177989	1.538717476	1.355711219
1.146177989	1.146183826	1.753793931	1.445870347
1.146183826	1.146187427	2	1.538717476
1.146189648	1.146191017	2.419476174	1.753793931
1.146191017	1.146191862	2.5	1.822595631
1.146191862	1.146192382	2.862048335	2.419476174
1.146192382	1.146192703	3	2.862048335
1.146192901	1.146193024	3.1	3.304825126
1.146193024	1.146193099	3.304825126	4.674644340

Table F.7: Three terms sum of the RADM when $\alpha = -0.2$.

u_0	Value of the RADM	u_0	Values of the RADM
-3.459815677	-4.114091086	1.143531280	1.145324453
-3	-3.459815677	1.144265001	1.145564232
-2.252000647	-2.407661012	1.145324453	1.145910035
-2.139888175	-2.252000647	1.145564232	1.145988226
-2.058814899	-2.139888175	1.145910035	1.146100950
-2	-2.058814899	1.145988226	1.146126430
-1.8	-1.784960953	1.146100950	1.146163159
-1.784960953	-1.764494414	1.146126430	1.146171462
-1.764494414	-1.736672285	1.146163159	1.146183428
-1.736672285	-1.698908903	1.146171462	1.146186131
-1.698908903	-1.647762053	1.146183428	1.146190031
-1.647762053	-1.578698647	1.146186131	1.146190911
-1.578698647	-1.485847283	1.146190031	1.146192181
-1.5	-1.380648391	1.146190911	1.146192468
-1.485847283	-1.361802382	1.146192181	1.146192882
-1.380648391	-1.22245669	1.146192882	1.146193110
-1.22245669	-1.015610466	1.14619311	1.146193184
-1.015610466	-0.750852913	1.146193184	1.146193209
-1	-0.73116872	1.146193209	1.146193217
-0.750852913	-0.42356438	1.146193217	1.146193219
-0.423564380	-0.042143187	1.146193219	1.146193220
-0.399837360	-0.015687408	1.147438108	1.146598420
-0.042143187	0.359155796	1.150024677	1.147438108
-0.015687408	0.384886153	1.158050349	1.150024677
0	0.4	1.183521245	1.158050349
0.359155796	0.713946527	1.246870534	1.176909269
0.4	0.745403599	1.270247158	1.183521245
0.713946527	0.954705187	1.510492342	1.246870534
0.745403599	0.972385294	1.591974499	1.270247158
0.954705187	1.074620098	2	1.510492342
1	1.093324420	2.067172964	1.591974499
1.074620098	1.121671531	2.3	2.067172964
1.093324421	1.128320266	2.4	2.406140050
1.128320266	1.140298244	2.406140050	2.430491222
1.138067651	1.143531280	2.5	2.863380109
1.140298244	1.144265001	2.863380109	6.164724157

Table F.8: Three terms sum of the RADM when $\alpha = -0.4$.

u_0	Value of the RADM	u_0	Values of the RADM
-3	-3.999433054	0.356562399	1.035462975
-2.358635549	-2.786837138	0.656314646	1.131075789
-2.126991370	-2.358635549	0.8	1.146923561
-2	-2.126991370	1	1.147923143
-1.946399649	-2.029981496	1.035462975	1.147043029
-1.9	-1.946399649	1.131075789	1.145969454
-1.8	-1.767604701	1.145969454	1.146188758
-1.767604701	-1.710101329	1.146188758	1.146193131
-1.710101329	-1.608567636	1.146193131	1.146193218
-1.608567636	-1.431085323	1.146193218	1.146193220
-1.5	-1.244089436	1.146193225	1.146193220
-1.431085323	-1.127031249	1.146193428	1.146193225
-1.244089436	-0.816657543	1.146203514	1.146193428
-1.127031249	-0.628473501	1.146702496	1.146203514
-1	-0.430371329	1.164918565	1.146702496
-0.816657543	-0.157302022	1.311312856	1.164918565
-0.628473501	0.104593400	1.550689655	1.311312856
-0.430371329	0.356562399	1.7	1.550689655
-0.157302022	0.656314646	1.8	1.817870287
0	0.8	1.817870287	1.877319893
0.104593400	0.882519347	1.877319893	2.105310043

Table F.9: Three terms sum of the RADM when $\alpha = -0.6$.

u_0	Value of the RADM	u_0	Values of the RADM
-3	-4.618852131	1.146200271	1.146193804
-2.204529412	-2.683165453	1.146207693	1.146194419
-2	-2.204529412	1.146215714	1.146195083
-1.8	-1.747931246	1.146221603	1.146195572
-1.747931246	-1.631238336	1.146278249	1.146200271
-1.631238336	-1.373434659	1.146367401	1.146207693
-1.5	-1.090323134	1.146463386	1.146215714
-1.373434659	-0.8250749373	1.146533618	1.146221603
-1.090323134	-0.264956676	1.147198861	1.146278249
-1	-0.097607825	1.147631108	1.146315894
-0.825074937	0.207992716	1.148210614	1.146367401
-0.264956676	0.977504362	1.149256554	1.146463386
-0.097607825	1.130181291	1.149996188	1.146533618
0	1.2	1.156186402	1.147198861
0.207992716	1.298837396	1.159639851	1.147631108
0.977504362	1.170336692	1.163796168	1.148210614
1	1.163796169	1.170336692	1.149256554
1.130181291	1.145307341	1.174428858	1.149996188
1.145307341	1.146121265	1.2	1.156186402
1.146193221	1.146193221	1.210735062	1.159639851
1.146193222	1.146193221	1.245058121	1.174428858
1.146193225	1.146193221	1.298837396	1.210735062
1.146193229	1.146193221	1.334396130	1.245058121
1.146193233	1.146193222	1.4	1.334396130
1.146193268	1.146193225	1.5	1.552430114
1.146193319	1.146193229	1.552430114	1.716600315
1.146193375	1.146193233	1.552430114	1.716600315
1.146193804	1.146193268	1.716600315	2.536818499
1.146194419	1.146193319	2	5.728165715
1.146195083	1.146193375	2.536818499	26.764996700

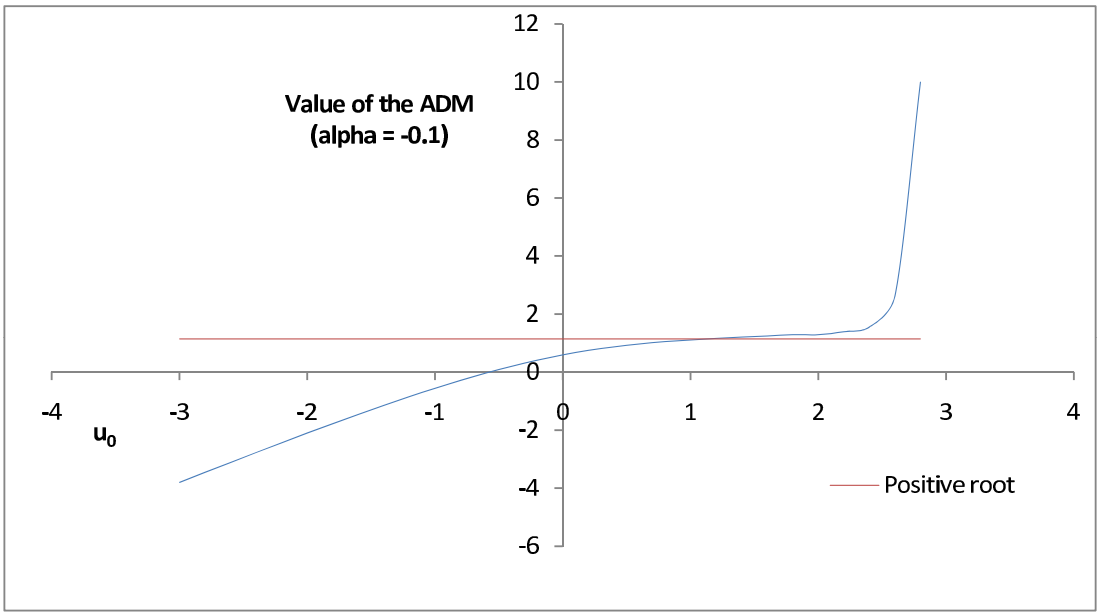

Figure F.1: Seven terms sum of the ADM for varying values of u_0 when $\alpha = -0.1$.

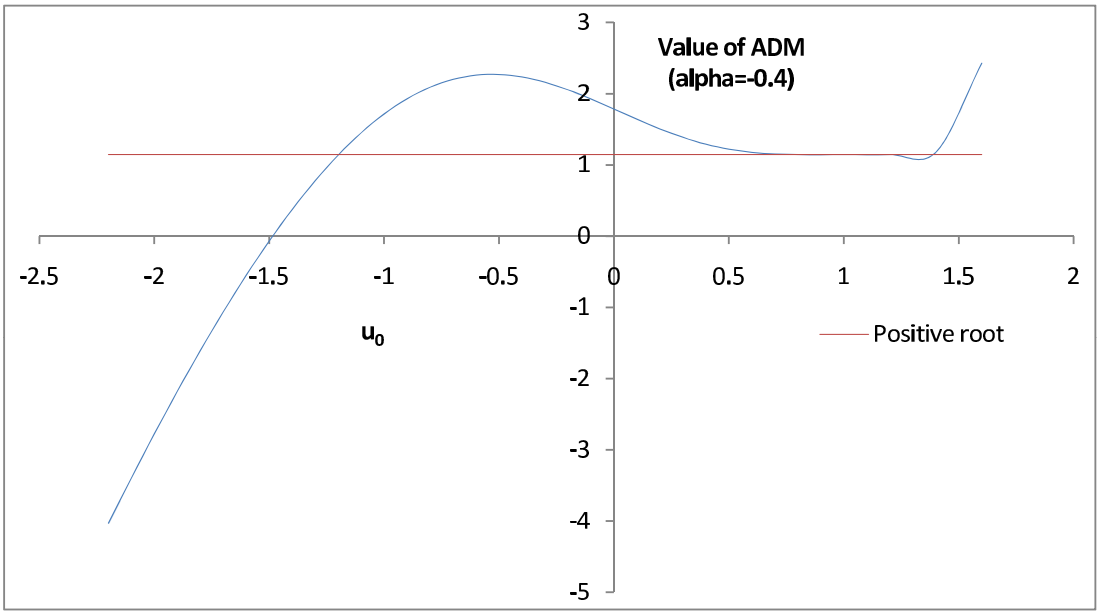

Figure F.2: Seven terms sum of the ADM for varying values of u_0 when $\alpha = -0.4$.

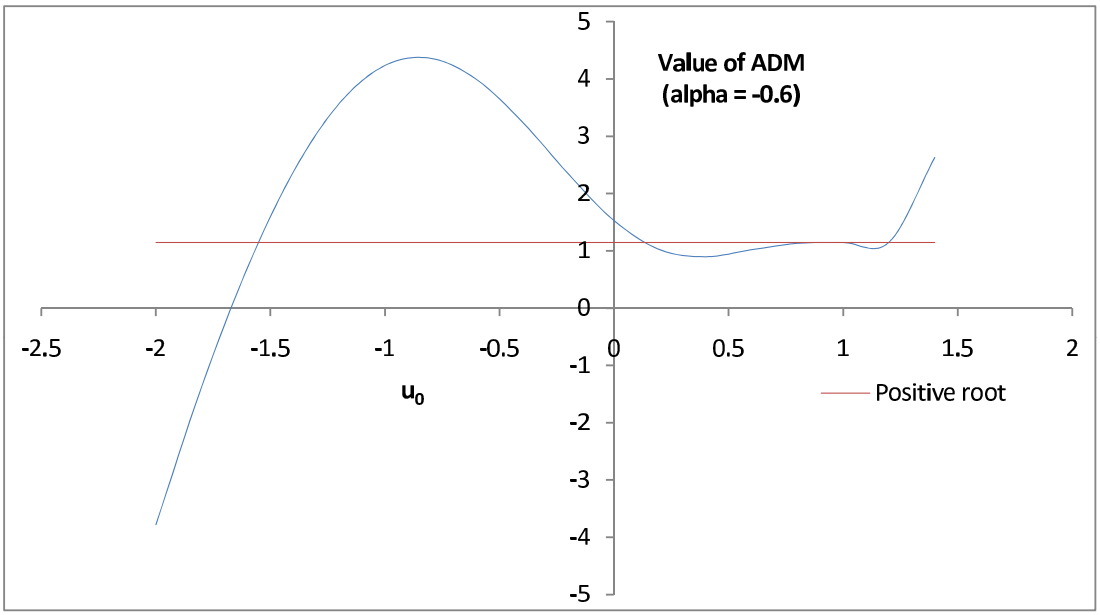

Figure F.3: Seven terms sum of the ADM for varying values of u_0 when $\alpha = -0.6$.

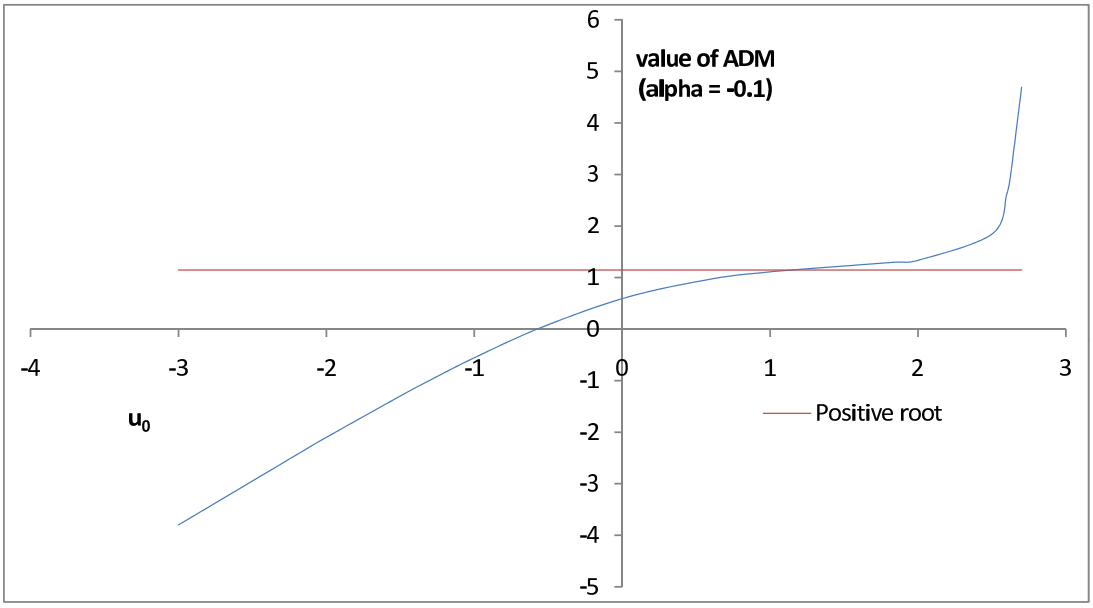

Figure F.4: Seven terms sum of the RADM for varying values of u_0 when $\alpha = -0.1$.

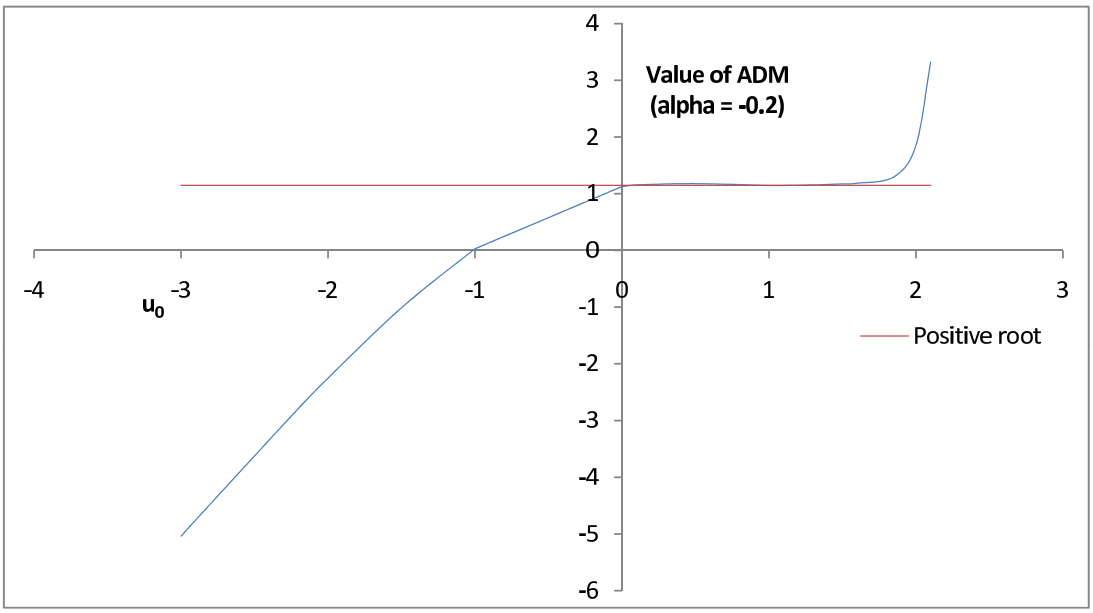

Figure F.5: Seven terms sum of the RADM for varying values of u_0 when $\alpha = -0.2$.

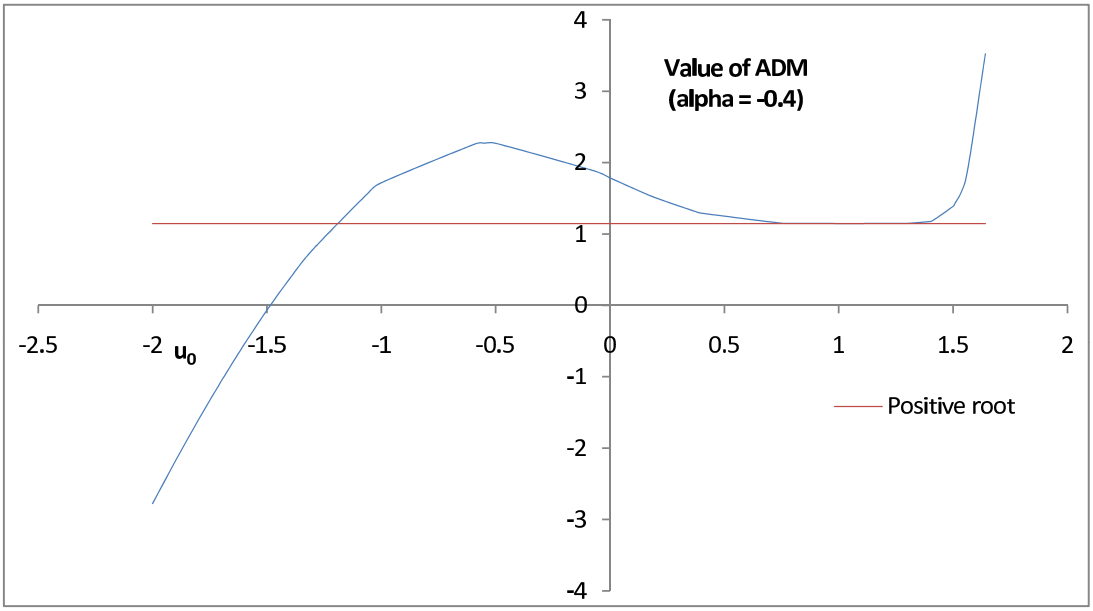

Figure F.6: Seven terms sum of the RADM for varying values of u_0 when $\alpha = -0.4$.

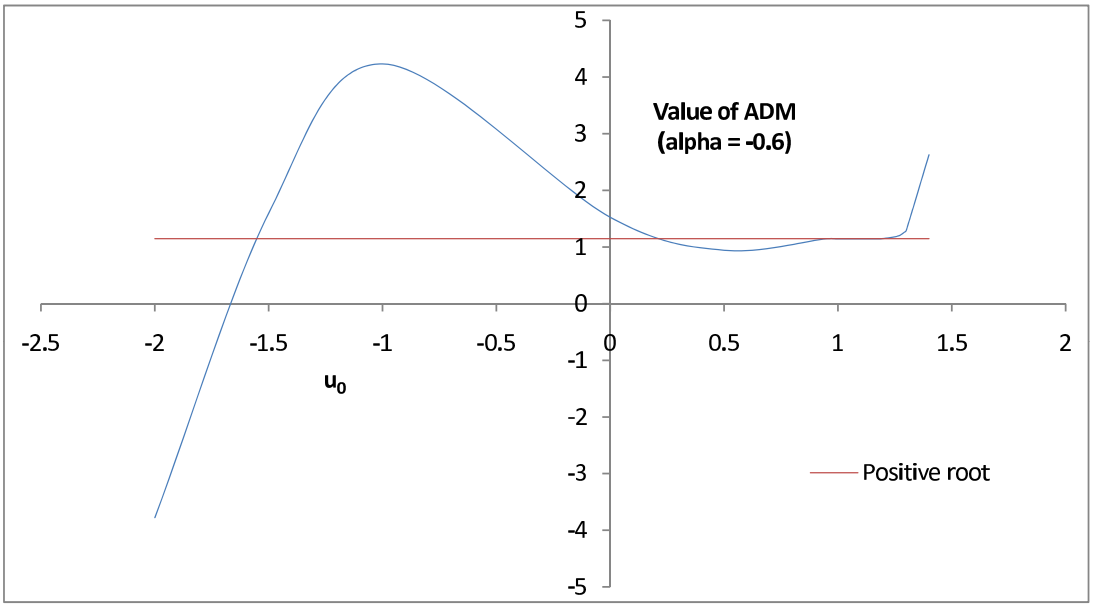

Figure F.7: Seven terms sum of the RADM for varying values of u_0 when $\alpha = -0.6$.

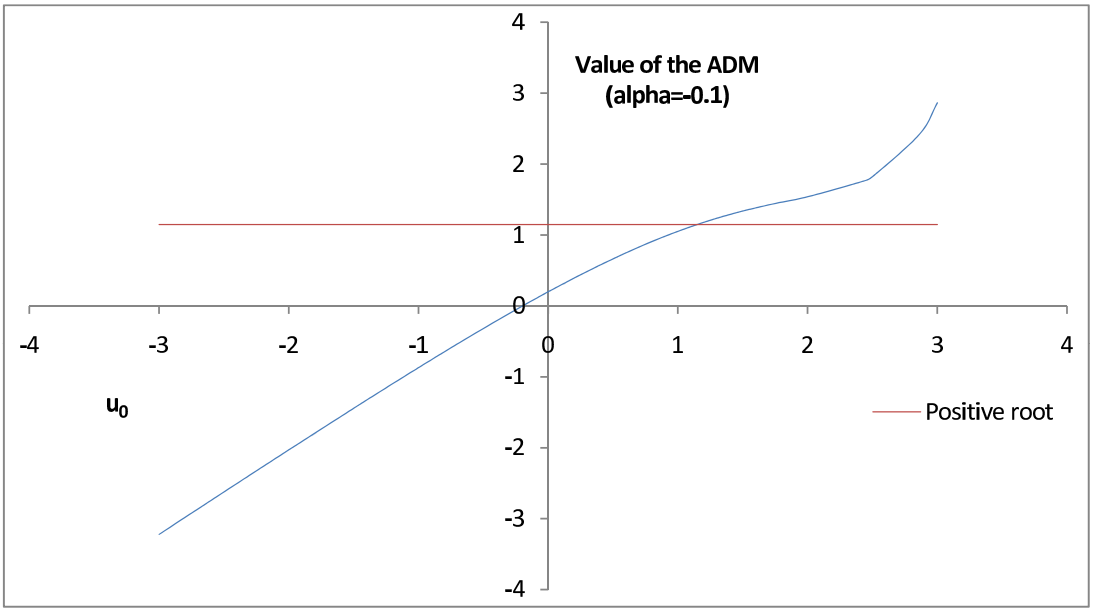

Figure F.8: Three terms sum of the RADM for varying values of u_0 when $\alpha = -0.1$.

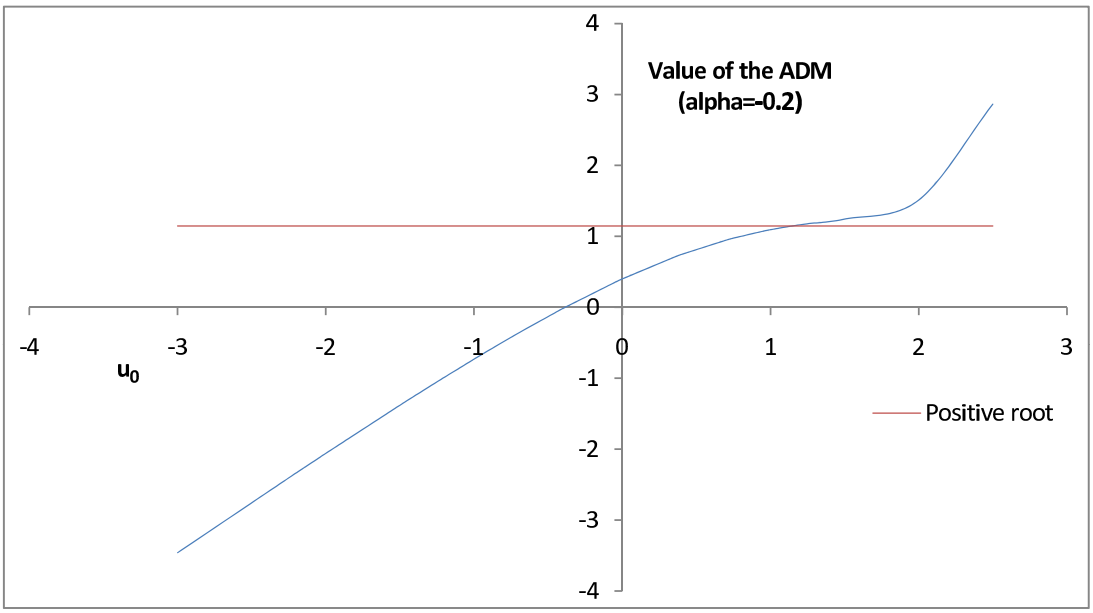

Figure F.9: Three terms sum of the RADM for varying values of u_0 when $\alpha = -0.2$.

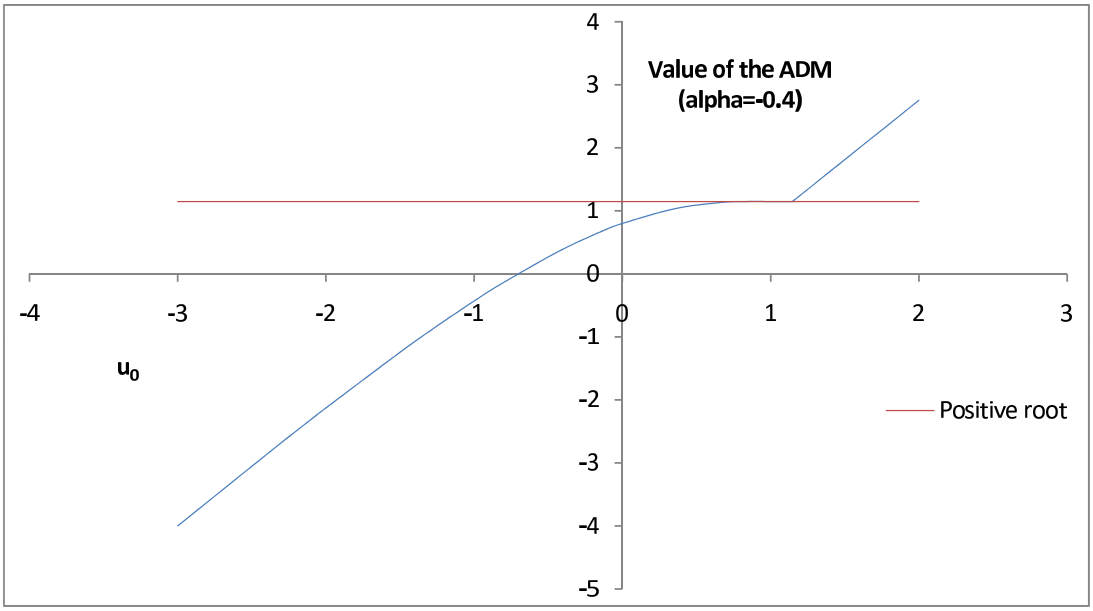

Figure F.10: Three terms sum of the RADM for varying values of u_0 when $\alpha = -0.4$.

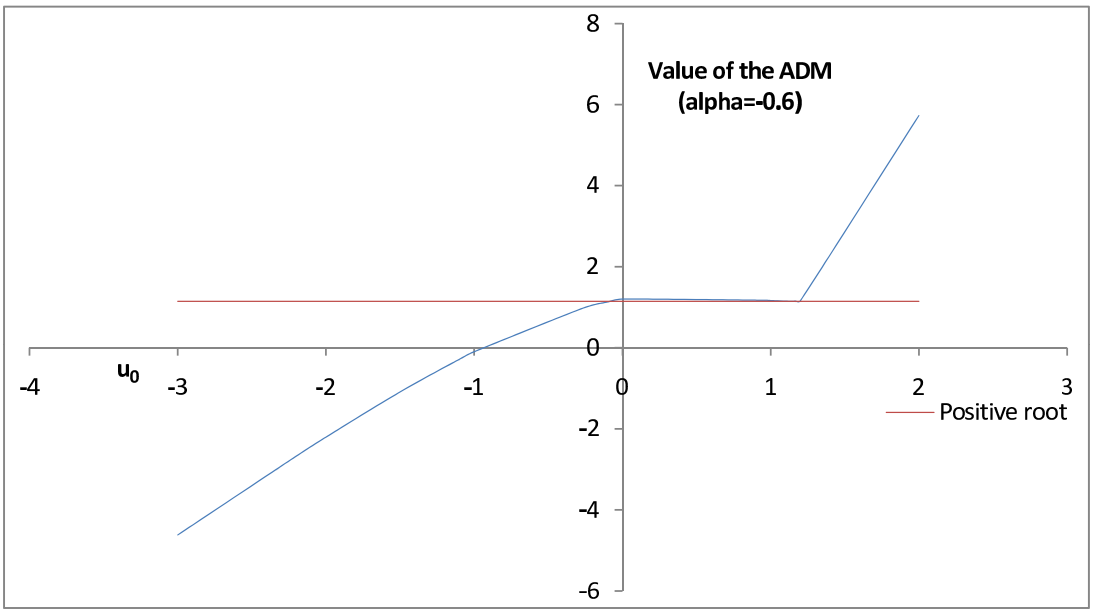

Figure F.11: Three terms sum of the RADM for varying values of u_0 when $\alpha = -0.6$.

Supplements to the thesis

Analytical solutions of orientation aggregation models, multiple solutions and path following with the Adomian decomposition method

A Thesis submitted for the degree of Doctor of Philosophy

By

Alex Clive Seymoore McKee

Department of Mathematical Sciences, School of Information Systems, Computing and Mathematics, Brunel University, London.

August 2011

The different maple codes for the programs developed as part of the thesis are presented for convenience in this supplement.

The following code works in Maple software version 15 to solve the OAP with a quadratic nonlinearity

The program calculates and sums the first four terms of the series solution given by the Adomian Decomposition Method to the orientation aggregation problem when the nonlinear term is of the form u(phi,t)u(psi,t).

Identify and specify u_0, the initial term below then execute command groups.

```
> restart:

> u_0:= 1/(2*Pi) + Q*cos(k*theta);# + P*cos(m*theta) ;
#test1:=simplify(u_0) assuming k::integer assuming sigma >0;
F(u):= u(phi,t)*u(psi,t):
F1 := u1*u2:
F(U):= unapply(F1,(u1,u2)):
F(v):= v(phi,t)*v(theta,t):
F2 := v1*v2:
F(V):= unapply(F2,(v1,v2)):


> kernel_1:=  '((1)/(2*pi)) * (1/(sigma * sqrt(2*pi))) *
Sum(exp(-1/2*(([psi-theta] + 2*pi*n)/(sigma))^2),n= 1..infinity)
' :
kernel_1a := exp(-1/2*((x) / sigma)^2):
kernel_2:=  ((1)/(2*pi)) * 1/(sigma * sqrt(2*pi)) * Sum(exp(-
1/2*(([theta - psi] + 2*pi*n)/(sigma))^2 ),n= 1..infinity):

> coefficient:= 1:

> before_summation := 1 / (2*Pi*sigma*sqrt(2*Pi)):

> u(theta, t) := u_0 + coefficient * Int(   Int(    Int(kernel_1
* F(u), phi = -Pi ..Pi) - Int (kernel_2 * F(v), phi = -Pi..Pi),
psi = -Pi..Pi), t=0..t );
```

Calculate the A_0 polynomial based on the form of u_0.

```
> u_0a := subs(theta=phi,u_0):
u_0b := subs(theta=psi,u_0):
```

```
A_0 := F(U)(u_0a,u_0b);
B_0 := F(V)(u_0a,u_0);
```

Calculate the second term of the Adomian solution.

```
> first_inner_wrt_phi_for_u1a:=
int((before_summation*kernel_1a) * A_0 , phi = -Pi ..Pi):
>
first_inner_wrt_phi_for_u1b:=value(first_inner_wrt_phi_for_u1a):
> first_inner_wrt_phi_for_u1:=
simplify(first_inner_wrt_phi_for_u1b) assuming k::integer
assuming m::integer:

> second_inner_wrt_phi_for_u1a:=
int((before_summation*kernel_1a)* B_0 , phi = -Pi ..Pi):
>
second_inner_wrt_phi_for_u1:=simplify(second_inner_wrt_phi_for_u
1a) assuming k::integer assuming m::integer:

> make_complex:=convert(cos(k*psi),exp):
make_complex1:=convert(cos(m*psi),exp):
make_complex2:=convert(sin(k*psi),exp):
make_complex3:=convert(sin(m*psi),exp):
> put_in_x:= subs(psi=x+theta, make_complex): put_in_x1:=
subs(psi=x+theta, make_complex1): put_in_x2:= subs(psi=x+theta,
make_complex2): put_in_x3:= subs(psi=x+theta, make_complex3):

> first_inner_wrt_psia:= int(expand(subs(cos(k*psi)=put_in_x,
cos(m*psi)=put_in_x1, sin(k*psi)=put_in_x2,sin(m*psi)=put_in_x3,
first_inner_wrt_phi_for_u1)), x=-infinity..infinity) assuming
sigma >= 0 :

exp2cos:=A::algebraic*exp(I*B::algebraic)+A::algebraic*1/exp(I*B
::algebraic)=2*A*cos(B):
exp2sinh:=conditional(A::algebraic*exp(a::algebraic)+B::algebrai
c*exp(b::algebraic)=
2*A*sinh((a-b)/2)*exp((a+b)/2),_verify(A+B,0,equal)):

>
first_inner_wrt_psi_for_u1_before:=applyrule(exp2cos,expand(firs
t_inner_wrt_psia)):
first_inner_wrt_psi_for_u1_after:=applyrule(exp2sinh,first_inner
_wrt_psi_for_u1_before):
first_inner_wrt_psi_for_u1:=first_inner_wrt_psi_for_u1_after:
```

```
> second_inner_wrt_psi_for_u1:=
int(second_inner_wrt_phi_for_u1,x=-infinity..infinity)assuming
sigma >=0:
>
> inner_integrals_wrt_psi_evaluated_for_u1a :=
first_inner_wrt_psi_for_u1 - second_inner_wrt_psi_for_u1:

>
inner_integrals_wrt_psi_evaluated_for_u1:=simplify(inner_integra
ls_wrt_psi_evaluated_for_u1a):

> u_1 :=
simplify(evalc(int(inner_integrals_wrt_psi_evaluated_for_u1,
t=0..t))) ;
```

Obtain the A_1 and B_1 polynomials.

```
> A_1:= (subs(theta=phi,u_0)* subs(theta=psi,u_1)) +
(subs(theta=phi,u_1)* subs(theta=psi,u_0));
> B_1:= (subs(theta=phi,u_0)* u_1) +  (subs(theta=phi,u_1)*u_0);
```

Calculate the third term of the Adomian solution.

```
> first_inner_wrt_phi_for_u2a:=  int((before_summation*
kernel_1a) * A_1 , phi = -Pi ..Pi):
>
first_inner_wrt_phi_for_u2b:=value(first_inner_wrt_phi_for_u2a):
> first_inner_wrt_phi_for_u2:=
simplify(first_inner_wrt_phi_for_u2b) assuming k::integer
assuming m::integer:
second_inner_wrt_phi_for_u2a :=  int((before_summation*
kernel_1a) * B_1 , phi = -Pi ..Pi):
>
second_inner_wrt_phi_for_u2b:=value(second_inner_wrt_phi_for_u2a
):
>
second_inner_wrt_phi_for_u2:=simplify(second_inner_wrt_phi_for_u
2b) assuming k::integer assuming m::integer:
>
> first_inner_wrt_psi_for_u2a:=
int(expand(subs(cos(k*psi)=put_in_x, cos(m*psi)=put_in_x1,
sin(k*psi)=put_in_x2, sin(m*psi)=put_in_x3,psi=x+theta,
first_inner_wrt_phi_for_u2)), x=-infinity..infinity) assuming
sigma>=0:
```

```
>
first_inner_wrt_psi_for_u2_before:=applyrule(exp2cos,expand(firs
t_inner_wrt_psi_for_u2a)):
first_inner_wrt_psi_for_u2_after:=applyrule(exp2sinh,first_inner
_wrt_psi_for_u2_before):
> first_inner_wrt_psi_for_u2b:=first_inner_wrt_psi_for_u2_after:
first_inner_wrt_psi_for_u2:=simplify(first_inner_wrt_psi_for_u2b
):
> second_inner_wrt_psi_for_u2:=
int(second_inner_wrt_phi_for_u2,x=-infinity..infinity)assuming
sigma>=0:
> inner_integrals_wrt_psi_evaluated_u2a:=
(first_inner_wrt_psi_for_u2) - (second_inner_wrt_psi_for_u2):
>
inner_integrals_wrt_psi_evaluated_u2:=simplify(inner_integrals_w
rt_psi_evaluated_u2a):

> u_2:=simplify(evalc(int(inner_integrals_wrt_psi_evaluated_u2,
t=0..t)));
```

Obtain the A_2 and B_2 polynomials.

```
> A_2:= simplify((subs(theta=phi,u_0)*subs(theta=psi,u_2)) +
(subs(theta=phi,u_1)* subs(theta=psi,u_1)) +
(subs(theta=phi,u_2)*subs(theta=psi,u_0)),size);

> B_2:= simplify((subs(theta=phi,u_0)*u_2) +
(subs(theta=phi,u_1)* u_1) + (subs(theta=phi,u_2)*u_0),size;
```

Calculate the fourth term of the Adomian solution.

```
> first_inner_wrt_phi_for_u3a:=  int((before_summation*
kernel_1a) * A_2 , phi = -Pi ..Pi):
> first_inner_wrt_phi_for_u3a:=  int((before_summation*
kernel_1a) * A_2 , phi = -Pi ..Pi):
>
first_inner_wrt_phi_for_u3b:=value(first_inner_wrt_phi_for_u3a):
> first_inner_wrt_phi_for_u3:=
simplify(first_inner_wrt_phi_for_u3b,size) assuming k::integer
assuming m::integer:
second_inner_wrt_phi_for_u3a :=  int((before_summation*
kernel_1a) * B_2 , phi = -Pi ..Pi):
>
second_inner_wrt_phi_for_u3b:=value(second_inner_wrt_phi_for_u3a
):
```

```
>
second_inner_wrt_phi_for_u3:=simplify(second_inner_wrt_phi_for_u
3b) assuming k::integer assuming m::integer:

> first_inner_wrt_psi_for_u3a:=
int(expand(subs(cos(k*psi)=put_in_x, cos(m*psi)=put_in_x1,
sin(k*psi)=put_in_x2,sin(m*psi)=put_in_x3,psi=x+theta,first_inne
r_wrt_phi_for_u3)), x=-infinity..infinity) assuming sigma>=0:
>
first_inner_wrt_psi_for_u3_before:=applyrule(exp2cos,expand(firs
t_inner_wrt_psi_for_u3a)):
first_inner_wrt_psi_for_u3_after:=applyrule(exp2sinh,first_inner
_wrt_psi_for_u3_before):
first_inner_wrt_psi_for_u3b:=first_inner_wrt_psi_for_u3_after:
first_inner_wrt_psi_for_u3:=simplify(first_inner_wrt_psi_for_u3b
):
> second_inner_wrt_psi_for_u3:=
int(second_inner_wrt_phi_for_u3,x=-infinity..infinity)assuming
sigma>=0:
> inner_integrals_wrt_psi_evaluated_u3a:=
(first_inner_wrt_psi_for_u3) - (second_inner_wrt_psi_for_u3):
>
inner_integrals_wrt_psi_evaluated_u3:=simplify(inner_integrals_w
rt_psi_evaluated_u3a):

> u_3:=simplify(evalc(int(inner_integrals_wrt_psi_evaluated_u3,
t=0..t)));
```

Sum the terms of the solution and plot the solution in 3 dimensions.

```
> U(theta,t):= evalc(u_0) +u_1+u_2+u_3;simplify(%);
>
> sigma:=1;
k:=1;
m:=1;
Q:=1;
P:=1;
> with(plots):
> plot3d(U(theta,t),theta=-Pi..Pi, t=0..10, view=-10..10,
axes=framed);
```

The following section plots and animates the solution calculated above.

Parameter values can be adjusted and user controls utilised to optimise graphical display. Certain parameter values and adjustments to the animation code below may not result in a plot.

Animate the solution for each parameter sigma,k,m,Q,P in turn.

Varying Sigma

```
> k:=1;
m:=1;
P:=1;
Q:=1;
sigma:='sigma';

eval(U(theta,t));
with(plots):
> animate(plot3d,[U(theta,t),theta=-Pi..Pi,t=0..10],sigma=0..5,
view= 0..10,axes=framed);


>
```

Varying k

```
> k:='k';
m:=1;
P:=1;
Q:=1;
sigma:=0.5;

> eval(U(theta,t));
> with(plots):
> animate(plot3d,[U(theta,t),theta=-Pi..Pi,t=0..10],k=0..1.75,
view= 0..3,axes=framed);
>
>
```

Varying m.

```
> k:=1;
m:='m';
P:=1;
Q:=1;
sigma:=0.5;

> eval(U(theta,t));
> with(plots):
> animate(plot3d,[U(theta,t),theta=-Pi..Pi,t=0..10],m=0..2,
view= 0..2.5,axes=framed);

>
```

Varying Q.

```
> k:=1;
```

```
m:=1;
P:=1;
Q:='Q';
sigma:=0.75;

> eval(U(theta,t));
>
> with(plots):

> animate(plot3d,[U(theta,t),theta=-Pi..Pi,t=-
20..20],Q=0..100000, view=-10..400000,axes=framed);
>
```

Varying P.

```
> k:=1;
m:=1;
P:='P';
Q:=1;
sigma:=0.75;

> eval(U(theta,t));
>
>
> with(plots):
> animate(plot3d,[U(theta,t),theta=-Pi..Pi,t=-
20..20],P=0..100000, view=-10..400000,axes=framed);


>
```

END CODE.

The following code works in Maple software version 15 to solve the OAP with a sigmoid nonlinearity

The program calculates and sums the first four terms of the series solution given by the Adomian Decomposition Method to the orientation aggregation problem when the nonlinear term is of the form $\frac{u^2(\phi,t)u(\psi,t)}{1+\beta^2 u^2(\phi,t)}$.

```
>
```

Enter the value for u_0, beta, Q and P below then execute command groups.

```
>
> restart:
> beta:=1;       Q:=10;         P:=8;
> printlevel:=3:
> readlib(residue):with(VectorCalculus):


> u_0:= 1/(2*Pi) + Q*cos(k*theta);# + P*cos(m*theta);
>

check:=has([u_0],sin):
>
> F(u):= u(phi,t)^2/ (1+beta^2*u(phi,t)^2)*u(psi,t):   #this is
the first form of the nonlinearity that
#appears in the equation

> F1 := u1^2/(1+beta^2*u1^2)*u2:
>
> F(U):= unapply(F1,(u1,u2)):
> F(v):= v(phi,t)^2/ (1+beta^2*(v(phi,t))^2)*v(theta,t): # this
is the second form of the nonlinearity
#that appears
> F2 := v1^2/(1+beta^2*v1^2)*v2:
> F(V):= unapply(F2,(v1,v2)):


>

kernel_1:=  '((1)/(2*pi)) * (1/(sigma * sqrt(2*pi))) * Sum(exp(-
1/2*(([psi-theta] + 2*pi*n)/(sigma))^2),n= 1..infinity)'   :
> kernel_1a := exp(-1/2*((x) / sigma)^2):
```

```
kernel_2:=  '((1)/(2*pi)) * 1/(sigma * sqrt(2*pi)) * Sum(exp(-
1/2*(([theta - psi] + 2*pi*n)/(sigma))^2 ),n= 1..infinity) '
:
> coefficient:= 1:
> before_summation := 1 / (2*Pi*sigma*sqrt(2*Pi)):
> u(theta, t) := u_0 + coefficient * Int(   Int(    Int(kernel_1
* F(u), phi = -Pi ..Pi) - Int (kernel_2 * F(v), phi = -Pi..Pi),
psi = -Pi..Pi), t=0..t );
```

Calculate the A_0 polynomial based on the form of u_0.

```
> u_0a := subs(theta=phi,u_0):

>
> u_0b := subs(theta=psi,u_0):
A_0 := F(U)(u_0a,u_0b):
> B_0 := F(V)(u_0a,u_0):


>
```

The procedure below uses the residue theorem to evaluate the integrals in phi.

```
>
# The integral is of the form
(1/2/Pi+Q*cos(k*phi))^2/(1+beta^2*(1/2/Pi+Q*cos(k*phi))^2)
>
f := proc() local
p1,s1,s2,s22,s,t,t1a,t1,res_count,i,u,res,poles,poles1,poles2,re
sidues1,residue_total1, result1, result:
if check = false then
 s1:= remove(has,A_0,psi);
s2:=subs(cos(k*phi)=((1-u^2) / (1+u^2)), cos(m*phi)=((1-u^2) /
(1+u^2)), sin(m*phi)=((2*u) / (1+u^2)),sin(k*phi)=((2*u) /
(1+u^2)), s1)*1/(1 + u^2);
s22 := unapply((eval(s1, [cos(k*phi) = (1-
u^2)/(1+u^2),cos(m*phi) = (1-u^2)/(1+u^2), sin(m*phi)=((2*u) /
(1+u^2)),sin(k*phi) = 2*u/(1+u^2)]))/(1+u^2), u);
  t:=singular(s2,u); t1a:=map(rhs@op,[t]);# puts elements of
call to singular in a list
p1:=(beta,Q,P)->select(x-
>Im(evalf(eval(x,[beta=beta,Q=Q,P=P])))>0,t1a):#evaluates sign
of imaginary #part
 t1:=p1(beta,Q,P); #selects the poles with positive imaginary
parts
# assign the poles to variables and calculate the residues -
another for loop within the global for #loop
```

```
res_count:=0;
for i from 1 to nops(t1) do
u[i]:=t1[i];
res[i]:=residue(s22(u),u=u[i]);# S22 is a mapping function
mapping u to s2;residue procedure needs a #mapping function.
res_count:= res_count + res[i];
end do; # this ends the residue calculations. It has summed the residues.
result:=  simplify((2*Pi*I)*(res_count),size); # result is the
value of the particular integral for #that particular loop.
else
s1:= remove(has,A_0,psi);
with(MultiSeries); _EnvExplicit := true;
s2:=subs(cos(k*phi)=((1-u^2) / (1+u^2)), cos(m*phi)=((1-u^2) /
(1+u^2)), sin(m*phi)=((2*u) / (1+u^2)),sin(k*phi)=((2*u) /
(1+u^2)), s1)*1/(1 + u^2); poles1 := singular(s2, u); t1a :=
map(`@`(rhs, op), [poles1]); p1 := proc (beta, Q, P) options
operator, arrow: select(proc (x) options operator, arrow; 0 <
Im(evalf(eval(x, [beta=beta, Q=Q, P=P])))) end proc, t1a) end
proc; t1 := p1(beta,Q,P); poles2 := []; for i to nops(t1) do u =
t1[i]; poles2 := [op(poles2), %] end do; poles := poles2;
residues1 := zip(proc (x, y) options operator, arrow;
simplify(x*(lhs-rhs)(y)) end proc,
`~`[convert](`~`[MultiSeries:-series](s2, poles, 1), polynom),
poles);
residue_total1 := 0;
for i to nops(residues1) do residue_total1 :=
simplify(residue_total1 + residues1[i], size) end do;
result1 := simplify(((2*Pi*I)*residue_total1),size);
end if;
end:   # procedure end
```

Calculate the second term of the Adomian solution.

```
>

> first_inner_wrt_phi_for_u1a:= (before_summation*kernel_1a) *
f() * u_0b: # where u_0b is the second # #argument of F(u)
>
>
first_inner_wrt_phi_for_u1b:=simplify(value(first_inner_wrt_phi_
for_u1a),size):
>
> first_inner_wrt_phi_for_u1:=
simplify(first_inner_wrt_phi_for_u1b,size) assuming k::integer
assuming m::integer:

>
```

```
> second_inner_wrt_phi_for_u1a:=  (before_summation*kernel_1a)*
f() * remove(has,B_0,phi):
>
second_inner_wrt_phi_for_u1:=simplify(second_inner_wrt_phi_for_u
1a,size) assuming k::integer assuming m::integer:
> make_complex:=convert(cos(k*psi),exp):
make_complex1:=convert(cos(m*psi),exp):
make_complex2:=convert(sin(k*psi),exp):
make_complex3:=convert(sin(m*psi),exp):

> put_in_x:= subs(psi=x+theta, make_complex): put_in_x1:=
subs(psi=x+theta, make_complex1): put_in_x2:= subs(psi=x+theta,
make_complex2): put_in_x3:= subs(psi=x+theta, make_complex3):


> # The rule below simplifies the exponential form into a cosine
form
> first_inner_wrt_psia:= int(expand(subs(cos(k*psi)=put_in_x,
cos(m*psi)=put_in_x1, sin(k*psi)=put_in_x2,sin(m*psi)=put_in_x3,
first_inner_wrt_phi_for_u1)), x=-infinity..infinity)assuming
sigma >0:

>
exp2cos:=A::algebraic*exp(I*B::algebraic)+A::algebraic*1/exp(I*B
::algebraic)=2*A*cos(B):
>
exp2sinh:=conditional(A::algebraic*exp(a::algebraic)+B::algebrai
c*exp(b::algebraic)=
2*A*sinh((a-b)/2)*exp((a+b)/2),_verify(A+B,0,equal)):
>
first_inner_wrt_psi_for_u1_before:=applyrule(exp2cos,expand(firs
t_inner_wrt_psia)):
>
first_inner_wrt_psi_for_u1_after:=applyrule(exp2sinh,first_inner
_wrt_psi_for_u1_before):
> first_inner_wrt_psi_for_u1:= first_inner_wrt_psi_for_u1_after:
> second_inner_wrt_psi_for_u1:=
int(second_inner_wrt_phi_for_u1,x=-infinity..infinity)assuming
sigma >0:
>
>
> inner_integrals_wrt_psi_evaluated_for_u1a :=
simplify(first_inner_wrt_psi_for_u1 -
second_inner_wrt_psi_for_u1,size):
```

```
>
inner_integrals_wrt_psi_evaluated_for_u1:=simplify(inner_integra
ls_wrt_psi_evaluated_for_u1a,size):
> u_1 :=
simplify(evalf(evalc(int(inner_integrals_wrt_psi_evaluated_for_u
1, t=0..t))),size);
>
```

Obtain the A_1 and B_1 polynomials.

```
>
> A_1:= (2* subs(theta=phi,u_0)* subs(theta=phi,u_1) *
subs(theta=psi,u_0))/ (1+beta^2*subs(theta=phi,u_0^2))  +
(subs(theta=phi,u_0^2) * subs(theta=psi,u_1)/ (
1+beta^2*subs(theta=phi,u_0^2) ) ) - (2*beta^2*
subs(theta=phi,u_0^3)* subs(theta=phi,u_1) *
subs(theta=psi,u_0)/ (1+beta^2*subs(theta=phi,u_0^2))^2):



> B_1:=(2* subs(theta=phi,u_0)* subs(theta=phi,u_1) * u_0)/
(1+beta^2*subs(theta=phi,u_0^2))  + (subs(theta=phi,u_0^2) * u_1
/ ( 1+beta^2*subs(theta=phi,u_0^2) ) ) - (2*beta^2*
subs(theta=phi,u_0^3)* subs(theta=phi,u_1) * u_0/
(1+beta^2*subs(theta=phi,u_0^2))^2) :
>
> # this will integrate using the residue theorem each of the
operands in phi in A_1.
> f1 := proc() local h, z, p1, s1,s1a, s2, s22,s,t,t1,
t1a,res_count,i,res,ord,p,poles,poles1,poles2,u,residues1,residu
e_total1,result1,result:
if check = false then
h:=[];# set up a list h to store the results of integrating the
terms in phi
for z in op(A_1) do
  s1:= select(has,z,phi);
s2:=subs(cos(k*phi)=((1-u^2) / (1+u^2)),cos(m*phi)=((1-u^2) /
(1+u^2)), sin(k*phi)=((2*u) / (1+u^2)), sin(m*phi)=((2*u) /
(1+u^2)),  s1) * 1/(1 + u^2);
s22 := unapply((eval(s1, [cos(k*phi) = (1-
u^2)/(1+u^2),cos(m*phi) = (1-u^2)/(1+u^2), sin(m*phi)=((2*u) /
(1+u^2)), sin(k*phi) = 2*u/(1+u^2)]))/(1+u^2), u);
 t:=singular(s2,u); t1a:=map(rhs@op,[t]); # puts elements of
call to singular in a list
p1:=(beta,Q,P)->select(x-
>Im(evalf(eval(x,[beta=beta,Q=Q,P=P])))>0,t1a): #evaluates sign
of imaginary #part
 t1:=p1(beta,Q,P); #selects the poles with positive imaginary
parts
```

```
# assign the poles to variables and calculate the residues -
another for loop within the global for #loop
res_count:=0;
for i from 1 to nops(t1) do
u[i]:=t1[i];
res[i]:=residue(s22(u),u=u[i]);# S22 is a mapping function
mapping u to s2;residue procedure needs a #mapping function.
res_count:= simplify(res_count + res[i]);
end do; # this ends the residue calculations. It has summed the residues.
result:=  simplify((2*Pi*I)*(res_count)); # result is the value
of the particular integral for that #particular loop.
h:=[op(h),result];
end do;
else  # For use with sine form initial condition
with(MultiSeries);
 _EnvExplicit := true;
ord:=4: #The order used in series
h:=[]:# set up a list h to store the results of integrating the
terms in phi
for z in op(A_1) do
s1a := expand(z):
s1 := simplify(remove(has, z, psi),size);
s2:=subs(cos(k*phi)=((1-u^2) / (1+u^2)),cos(m*phi)=((1-u^2) /
(1+u^2)), sin(k*phi)=((2*u) / (1+u^2)), sin(m*phi)=((2*u) /
(1+u^2)),  s1)*1/(1 + u^2);
poles1 := singular(s2, u);
t1a := map(rhs@op, [poles1]);
t1:=select(x->Im(evalf(x))>0,t1a);
poles2 := [];
for i to nops(t1) do poles2 := [op(poles2), u = t1[i]] end do;
poles := poles2;
s:=convert~(series~(s2,poles,ord),polynom);
p:=((lhs-rhs)~(poles))^~(-1);
residues1:=coeff~(s,p);
residue_total1 := 0;
for i to nops(residues1) do residue_total1 :=
simplify(residue_total1 + residues1[i], size) end do;result1 :=
simplify(((2*Pi*I)*residue_total1),size);
h:=[op(h),result1];
end do:
end if;
end:


>
> #Remove expressions in phi before passing on to be integrated
w.r.t psi
```

```
>
> grab1:=[]:
> for z in op(A_1) do
test1:= select(has,z,phi); # this is what was integrated in phi
test2:=remove(has,z,phi);
grab1:=[op(grab1),test2];verify(test1*test2,z);# test that what
was selected above is always the same #as what is removed
end do:
> remaining_terms_in_psi_from_A_1:=grab1:     #terms left after
the integration in phi is done
>
> grab2:=[]: # do same as above for B_1 polynomial
> for z in op(B_1) do
test3:= select(has,z,phi);
test4:=remove(has,z,phi);
grab2:=[op(grab2),test4];verify(test3*test4,z);# test that what
is selected is always the same as what #is removed
end do:
> remaining_terms_in_psi_from_B_1:=grab2:
>
>
> left_over_terms_in_psi_A1:= vector(grab1):
evaluated_terms_in_phi:= vector(f1()):
result_of_integrating_wrt_phi_A_1:=simplify(evalf(evalm(DotProdu
ct(left_over_terms_in_psi_A1,evaluated_terms_in_phi))),size):
> left_over_terms_in_psi_B1:= vector(grab2):
evaluated_terms_in_phi:= vector(f1()):
result_of_integrating_wrt_phi_B_1:=simplify(evalf(evalm(DotProdu
ct(left_over_terms_in_psi_B1,evaluated_terms_in_phi))),size):
```

Calculate the third term of the Adomian solution.

```
>
> first_inner_wrt_phi_for_u2a:=  simplify((before_summation *
kernel_1a) * result_of_integrating_wrt_phi_A_1,size):
>
first_inner_wrt_phi_for_u2b:=simplify(value(evalf(first_inner_wr
t_phi_for_u2a)),size):
> first_inner_wrt_phi_for_u2:=
simplify(evalf(first_inner_wrt_phi_for_u2b),size) assuming
k::integer assuming m::integer:


> second_inner_wrt_phi_for_u2a :=
simplify(evalf((before_summation * kernel_1a) *
result_of_integrating_wrt_phi_B_1),size) :
>
second_inner_wrt_phi_for_u2b:=evalf(value(second_inner_wrt_phi_f
or_u2a)):
```

```
>
second_inner_wrt_phi_for_u2:=simplify(second_inner_wrt_phi_for_u
2b,size) assuming k::integer assuming m::integer:
> first_inner_wrt_psi_for_u2aa:=
int(expand(subs(cos(k*psi)=put_in_x, cos(m*psi)=put_in_x1,
sin(k*psi)=put_in_x2, sin(m*psi)=put_in_x3,psi=x+theta,
first_inner_wrt_phi_for_u2)), x=-infinity..infinity) assuming
sigma>0:

first_inner_wrt_psi_for_u2a:=
simplify(evalf(first_inner_wrt_psi_for_u2aa),size):


>
first_inner_wrt_psi_for_u2_before:=simplify(applyrule(exp2cos,ex
pand(first_inner_wrt_psi_for_u2a)),size):
first_inner_wrt_psi_for_u2_after:=applyrule(exp2sinh,first_inner
_wrt_psi_for_u2_before):
> first_inner_wrt_psi_for_u2b:=
first_inner_wrt_psi_for_u2_after:

>
first_inner_wrt_psi_for_u2:=simplify(evalf(first_inner_wrt_psi_f
or_u2b),size):
> second_inner_wrt_psi_for_u2:=
simplify(evalf(int(second_inner_wrt_phi_for_u2,x=-
infinity..infinity)assuming sigma>0),size):
> inner_integrals_wrt_psi_evaluated_u2a:=
simplify(evalf(((first_inner_wrt_psi_for_u2) -
(second_inner_wrt_psi_for_u2))),size):
>
>
>
inner_integrals_wrt_psi_evaluated_u2:=simplify(evalf(inner_integ
rals_wrt_psi_evaluated_u2a),size):

>
u_2:=simplify(evalf[20](evalc(int(inner_integrals_wrt_psi_evalua
ted_u2, t=0..t))),size);
```

Obtain the A_2 and B_2 polynomials.

```
>


> A_2a:=simplify(evalf( 2*subs(theta=phi,u_0) * (
subs(theta=psi,u_0)* subs(theta=phi,u_2) +  subs(theta=phi,u_1)*
subs(theta=psi,u_1)) / (1 +
```

```
beta^2*subs(theta=phi,u_0^2))^2),size): A_2b:=
simplify(evalf(A_2a),size):
>
>
> A_2:=  simplify(evalf(((subs(theta=phi,u_0^2))*
(subs(theta=psi,u_2)))/ (1+ beta^2*subs(theta=phi,u_0^2)) +
(A_2b) + ((1-
(3*beta^2*subs(theta=phi,u_0^2)))/(1+(beta^2*subs(theta=phi,u_0^
2)))^3 )*(subs(theta=phi,u_1^2)* subs(theta=psi,u_0))),size):
>
>
> B_2a:=simplify(evalf((((2*subs(theta=phi,u_0))*((u_0)*
subs(theta=phi,u_2)) + (subs(theta=phi,u_1)*(u_1)) ))/(1 +
beta^2*subs(theta=phi,u_0^2))^2 )))):

> B_2b:= simplify(evalf(B_2a),size):

> B_2:=  ((subs(theta=phi,u_0^2))* (u_2))/ (1+
beta^2*subs(theta=phi,u_0^2)) + (B_2b) + ((1-
(3*beta^2*subs(theta=phi,u_0^2)))/(1+(beta^2*subs(theta=phi,u_0^
2)))^3 )*(subs(theta=phi,u_1^2)*(u_0)):
>
>
> f2 := proc() local h, z, ord,p,p1, poles, poles1,poles2,
residues1, residue_total1, result1,s1,s1a, s2, s22,s,t,t1,
t1a,res_count,i,u,res,result:
if check = false then
h:=[];# set up a list h to store the results of integrating the
terms in phi
for z in op(A_2) do #
 s1:= select(has,z,phi); # A_2a, A_2b simplifies the middle
operand of A_2 before passing to for loop
s2:=subs(cos(k*phi)=((1-u^2) / (1+u^2)), cos(m*phi)=((1-u^2) /
(1+u^2)), sin(m*phi)=((2*u) / (1+u^2)),sin(k*phi)=((2*u) /
(1+u^2)), s1)*1/(1 + u^2);
s22 := unapply((eval(s1, [cos(k*phi) = (1-
u^2)/(1+u^2),cos(m*phi) = (1-u^2)/(1+u^2), sin(m*phi)=((2*u) /
(1+u^2)),sin(k*phi) = (2*u)/(1+u^2)]))/(1+u^2), u);
 t:=singular(s2,u); t1a:=map(rhs@op,[t]); # puts elements of
call to singular in a list
p1:=(beta,Q,P)->select(x-
>Im(evalf(eval(x,[beta=beta,Q=Q,P=P])))>0,t1a): #evaluates sign
of imaginary #part
 t1:=p1(beta,Q,P); #selects the poles with positive imaginary
parts
# assign the poles to variables and calculate the residues -
another for loop within the global for #loop
```

```
res_count:=0;
for i from 1 to nops(t1) do
u[i]:=t1[i];
res[i]:=simplify(residue(s22(u),u=u[i]),size);# S22 is a mapping
function mapping u to s2;residue #procedure needs a mapping
function.
res_count:= simplify(res_count + res[i]);
end do; # this ends the residue calculations. It has summed the residues.
result:=  simplify((2*Pi*I)*(res_count)); # result is the value
of the particular integral for that #particular loop.
h:=[op(h),result];
end do;
else  # For use with sine form initial condition
with(MultiSeries);
 _EnvExplicit := true;
ord:=4: #The order used in series
h:=[]:# set up a list h to store the results of integrating the
terms in phi
for z in op(A_2) do
s1a := expand(z):
s1 := simplify(remove(has, z, psi),size);
s2:=subs(cos(k*phi)=((1-u^2) / (1+u^2)),cos(m*phi)=((1-u^2) /
(1+u^2)), sin(k*phi)=((2*u) / (1+u^2)), sin(m*phi)=((2*u) /
(1+u^2)),  s1)*1/(1 + u^2);
poles1 := singular(s2, u);
t1a := map(rhs@op, [poles1]);
t1:=select(x->Im(evalf(x))>0,t1a);
poles2 := [];
for i to nops(t1) do poles2 := [op(poles2), u = t1[i]] end do;
poles := poles2;
s:=convert~(series~(s2,poles,ord),polynom);
p:=((lhs-rhs)~(poles))^~(-1);
residues1:=coeff~(s,p);
residue_total1 := 0;
for i to nops(residues1) do residue_total1 :=
simplify(residue_total1 + residues1[i], size) end do;result1 :=
simplify(((2*Pi*I)*residue_total1),size);
h:=[op(h),result1];
end do:
end if;
end:
>
>
>
>
> #Remove expression in phi before passing on to be integrated
wrt psi for A2.
```

```
> #--------------------------
> grab3:=[]:
> for z in op(A_2) do
test4:= select(has,z,phi); # this is what was integrated in
w.r.t phi.
test5:=remove(has,z,phi);
grab3:=[op(grab3),test5];verify(test4*test5,z);# test that what
was selected above is always the same #as what is removed
end do:
> remaining_terms_in_psi_from_A_2:=grab3: #terms left after the
integration in phi is done
>
> grab4:=[]:# do same as above for B_1 polynomial
> for z in op(B_2) do
test6:= select(has,z,phi);
test7:=remove(has,z,phi);
grab4:=[op(grab4),test7];verify(test6*test7,z);# test that what
is selected is always the same as what #is removed
end do:
> remaining_terms_in_psi_from_B_2:=grab4:
>
> left_over_terms_in_psi_A2:= vector(grab3):
evaluated_terms_in_phiA2:= vector(f2()):
result_of_integrating_wrt_phi_A_2:=simplify(evalf(evalm(DotProdu
ct(left_over_terms_in_psi_A2,evaluated_terms_in_phiA2))),size):



> left_over_terms_in_psi_B2:= vector(grab4):
evaluated_terms_in_phiB2:= vector(f2()):
result_of_integrating_wrt_phi_B_2:=evalf(evalm(DotProduct(left_o
ver_terms_in_psi_B2,evaluated_terms_in_phiB2))):
>



>
```

Calculate the fourth term of the Adomian solution.

```
>
>
> first_inner_wrt_phi_for_u3a:=  (before_summation * kernel_1a)
* result_of_integrating_wrt_phi_A_2:
>
first_inner_wrt_phi_for_u3b:=evalf(value(first_inner_wrt_phi_for
_u3a)):
```

```
> first_inner_wrt_phi_for_u3c:=
simplify(evalf(first_inner_wrt_phi_for_u3b),size) assuming
k::integer assuming m::integer:

>
first_inner_wrt_phi_for_u3:=simplify(evalf(first_inner_wrt_phi_f
or_u3c)):
> second_inner_wrt_phi_for_u3a :=  (before_summation *
kernel_1a) * result_of_integrating_wrt_phi_B_2:
>
second_inner_wrt_phi_for_u3b:=value(second_inner_wrt_phi_for_u3a
):
>
second_inner_wrt_phi_for_u3:=simplify(second_inner_wrt_phi_for_u
3b,size) assuming k::integer assuming m::integer:
> first_inner_wrt_psi_for_u3a:=
int(expand(subs(cos(k*psi)=put_in_x, cos(m*psi)=put_in_x1,
sin(k*psi)=put_in_x2,sin(m*psi)=put_in_x3,psi=x+theta,first_inne
r_wrt_phi_for_u3)), x=-infinity..infinity) assuming sigma>0:

first_inner_wrt_psi_for_u3_before:=applyrule(exp2cos,expand(firs
t_inner_wrt_psi_for_u3a)):
first_inner_wrt_psi_for_u3_after:=applyrule(exp2sinh,first_inner
_wrt_psi_for_u3_before):
> first_inner_wrt_psi_for_u3b:=first_inner_wrt_psi_for_u3_after:
first_inner_wrt_psi_for_u3:=simplify(first_inner_wrt_psi_for_u3b
,size):
> second_inner_wrt_psi_for_u3:=
int(second_inner_wrt_phi_for_u3,x=-infinity..infinity)assuming
sigma>0:
> inner_integrals_wrt_psi_evaluated_u3a:=
(first_inner_wrt_psi_for_u3) - (second_inner_wrt_psi_for_u3):
>
inner_integrals_wrt_psi_evaluated_u3:=simplify(inner_integrals_w
rt_psi_evaluated_u3a,size):

>
u_3:=simplify(evalf(evalc(int(inner_integrals_wrt_psi_evaluated_
u3, t=0..t)))):
```

Sum the terms of the solution and plot the solution in 3 dimensions.

```
>
>
> U(theta,t):=   evalc(u_0) + u_1 + u_2+ u_3;
Compressed_U(theta,t):=collect(simplify(evalf[2](evalc(U(theta,t
))),size),t);
>
```

```
> sigma:=1;
k:=1;
Q:=Q;
m:=1;
P:=P;
>
>
> U(theta,t):
> with(plots):
> plot3d(U(theta,t),theta=-Pi..Pi, t=0..10, view=-100..100,
axes=framed);
>
```

The following section plots and animates the solution calculated above.

Parameter values can be adjusted and user controls utilised to optimise graphical display. Certain parameter values, large expression sizes and adjustments to the animation code below may not result in a plot.

Animate the solution for each parameter sigma,k,m in turn.

```
>
```

Varying Sigma

```
> k:=1;
m:=1;
P:=P;
Q:=Q;
sigma:='sigma';

eval(U(theta,t)):
with(plots):
> animate(plot3d,[U(theta,t),theta=-Pi..Pi,t=0..10],sigma=0..6,
view= 0..100,axes=framed);
>
```

Varying k.

```
> k:='k';
m:=1;
P:=P;
Q:=Q;
sigma:=0.5;

> eval(U(theta,t)):
> with(plots):
> animate(plot3d,[U(theta,t),theta=-Pi..Pi,t=0..10],k=0..4,
view= 0..3,axes=framed);
>
```

Varying m.

```
> k:=1;
m:='m';
```

```
P:=P;
Q:=Q;
sigma:=0.5;

> eval(U(theta,t)):
> with(plots):
> animate(plot3d,[U(theta,t),theta=-Pi..Pi,t=0..10],m=0..4,
view= 0..4,axes=framed);

>
>
>
>
```

The following code works in Maple software version 15 to help find multiple solutions to a one dimensional example.

This program solves the equation $f(u) = u_0 + \left(u - u_0 + \alpha\left(e^u - u - 2\right)\right)$ which is presented in chapter 3 as the one dimensional example. The program calculates and sums the first seven terms of the Adomian series solution according to the code below. It also indicates whether a contraction holds for the specified value of α . To proceed in using the program enter the value of u_0 and a value for α then execute all command groups . The default value for α is 1.

```
> restart:


u_0:= -2;                                                    # this is
the u_0 for the ADM
alpha:= 1;                                                # change value of
alpha to affect the contraction

u_hat:=1.146193221;                                          # u_hat is
the positive root of the equation
test_criterion:=2/ (1-exp(u_hat));
threshold:=evalf(test_criterion);
is(alpha > threshold);                                      # check
alpha is in right range
>
> f_u:= u_0 + ( u - u_0 + alpha*(exp(u)-u-2));              #
relevant equation
big_F:=  u - u_0 + alpha*(exp(u)-u-2);
                The Adomian polynomials for big_F are calculated below.
>


A_0:=subs(u=u_0, big_F);u_1:= A_0:
A_1:= subs(u=u_0,diff(big_F,u))*u_1: u_2:=A_1:
A_2:= subs(u=u_0,diff(big_F,u))*u_2 +
(1/2*u_1^2)*subs(u=u_0,diff(diff(big_F,u),u)):u_3:= A_2:
A_3 := subs(u=u_0,diff(big_F,u))*u_3 +
u_1*u_2*(subs(u=u_0,diff(diff(big_F,u),u))) +
(u_1^3/3!)*subs(u=u_0,diff(diff(diff(big_F,u),u),u)): u_4:=A_3:
A_4:= subs(u=u_0,diff(big_F,u))*u_4 +
(subs(u=u_0,diff(diff(big_F,u),u)))*((1/2)*(u_2^2 + u_1*u_3))+
subs(u=u_0,diff(diff(diff(big_F,u),u),u))*(1/2*u_1^2*u_2) +
subs(u=u_0,diff(diff(diff(diff(big_F,u),u),u),u))*(1/4!*u_1^4):
u_5:=A_4:
```

```
A_5:= subs(u=u_0,diff(big_F,u))*u_5+
subs(u=u_0,diff(diff(big_F,u),u))*(u_2*u_3+u_1*u_4)+
subs(u=u_0,diff(diff(diff(big_F,u),u),u))*(1/2*u_1*u_2^2+
1/2*(u_1^2*u_3)) +
subs(u=u_0,diff(diff(diff(diff(big_F,u),u),u),u))*(1/3!*u_1^3*u_
2)+
subs(u=u_0,diff(diff(diff(diff(diff(big_F,u),u),u),u),u))*(1/5!*
u_1^5): u_6:=A_5:


>
>
> u_0:=u_0; u_1:=A_0; u_2:=A_1; u_3:=
A_2;u_4:=A_3;u_5:=A_4;u_6:=A_5;
> soln:=u_0 + u_1 + u_2 + u_3 + u_4+u_5+u_6:

> answer:=evalf[20](soln);
> plot([f_u,soln], u = -3..3);
>
>
>
```

The roots of equation $f(u) = u_0 + \left(u - u_0 + \alpha\left(e^u - u - 2\right)\right)$ are calculated below for comparison.

```
> f:=exp(u)-u-2;
> solve(f=0,u);evalf[20](%);
>
```

The following code works in Maple software version 15 to help with path following a one dimensional bifurcation example.

This program solves the equation $f(u) = u_0 + \left(u - u_0 + \alpha\left(\Gamma u^2 - u + 2\right)\right)$ which is presented in chapter 4 as the path following bifurcation example.
The program calculates and sums the first seven terms of the Adomian series solution according to the code presented herein. It also indicates whether a contraction holds for the specified value of α and calculates the exact solution to $f(u)$ using the formula labelled 'specify_u' below. In order for this formula to calculate the solution the particular branch (+-) will need to be specified. Γ is the value on the Γ axis at the particular path following step (eg. with a step size 0.02 and initialising Γ at zero; Γ will increment from 0.02 to 0.04 etc.). To proceed in using the program enter values for u_0, Γ and α. The default value for α is 0.5.

```
>
restart:
u_0:= 2.08;                                  # this is the u_0 for
the ADM
alpha:= 0.5;                    # the value of alpha determines
whether a contraction holds change sign
#  of alpha when branch is changed
Gamma:= 0.02;                      # Gamma will change according to
the step size:corresponding value on
#the        gamma axis
specify_u:=(1-sqrt(1-8*(Gamma)))/(2*(Gamma)); # this is the u
value corresponding to Gamma that makes
#                                  the contraction hold

approximate_specify_u:=evalf(specify_u);
test_criterion:='1+alpha*((2*Gamma*specify_u)-1)'; #cf. lemma
3.2 and proposition 3.4. test_criterion
#is the criterion for a contraction to exist.
threshold:=evalf(test_criterion);
is(threshold > -1); is(threshold < 1);  # check alpha is in
right range both should be true; if not
#adjust alpha to make both true
>
> f_u:= 'u_0 + ( u - u_0 + alpha*(Gamma*u^2-u+2))'; # relevant
equation cf. lemma 3.1
big_F:=  'u - u_0 + alpha*(Gamma*u^2-u+2)';
```

The Adomian polynomials for big_F are calculated below.

```
> A_0:=subs(u=u_0, big_F):u_1:= A_0:
A_1:= subs(u=u_0,diff(big_F,u))*u_1: u_2:=A_1:
```

```
A_2:= subs(u=u_0,diff(big_F,u))*u_2 +
(1/2*u_1^2)*subs(u=u_0,diff(diff(big_F,u),u)):u_3:= A_2:
A_3 := subs(u=u_0,diff(big_F,u))*u_3 +
u_1*u_2*(subs(u=u_0,diff(diff(big_F,u),u))) +
(u_1^3/3!)*subs(u=u_0,diff(diff(diff(big_F,u),u),u)): u_4:=A_3:
A_4:= subs(u=u_0,diff(big_F,u))*u_4 +
(subs(u=u_0,diff(diff(big_F,u),u)))*((1/2)*(u_2^2 + u_1*u_3))+
subs(u=u_0,diff(diff(diff(big_F,u),u),u))*(1/2*u_1^2*u_2) +
subs(u=u_0,diff(diff(diff(diff(big_F,u),u),u),u))*(1/4!*u_1^4):
u_5:=A_4:
A_5:= subs(u=u_0,diff(big_F,u))*u_5+
subs(u=u_0,diff(diff(big_F,u),u))*(u_2*u_3+u_1*u_4)+
subs(u=u_0,diff(diff(diff(big_F,u),u),u))*(1/2*u_1*u_2^2+
1/2*(u_1^2*u_3)) +
subs(u=u_0,diff(diff(diff(diff(big_F,u),u),u),u))*(1/3!*u_1^3*u_
2)+
subs(u=u_0,diff(diff(diff(diff(diff(big_F,u),u),u),u),u))*(1/5!*
u_1^5): u_6:=A_5:


>
> u_0:=u_0; u_1:=A_0; u_2:=A_1; u_3:=
A_2;u_4:=A_3;u_5:=A_4;u_6:=A_5;
> soln:=u_0 + u_1 + u_2 + u_3 + u_4+u_5+u_6:

> answer:=evalf[20](soln);
>
```

A plot of $f(u)$.

```
gamm_a := (u-2)/u^2:
plot(gamm_a, u = 2 .. 18);
```